NOVEL METHODS OF MERIDIONAL AND CIRCUMFERENTIAL ANTERIOR CHAMBER ANGLE IMAGING

MANI BASKARAN

(DO, DNB)

A THESIS SUBMITTED

FOR THE DEGREE OF DOCTOR OF PHILOSOPHY

DEPARTMENT OF OPHTHALMOLOGY

NATIONAL UNIVERSITY OF SINGAPORE

2015

DECLARATION

I hereby declare that the thesis is my original work and it has been written by me in its entirety. I have duly acknowledged all the sources of information which have been used in the thesis.

This thesis also has not been submitted to any degree in any university previously.

Mani Baskaran

2015

THESIS COMMITTEE AND SUPERVISORS

Thesis Advisory Committee (TAC):

A/Prof Paul Chew Tec Kuan Paul MMed (Ophth), FRCSEd, FRCOphth, FAMS, Senior Consultant, Department of Ophthalmology, National University of Singapore

A/Prof Jodhbir Singh Mehta, FRCOphth, FRCSEd, Senior Consultant, Singapore National Eye Centre, Associate Professor, Office of Clinical Sciences, Duke-NUS, Singapore

Thesis Supervisors:

Aung Tin, Ph.D., PhD., MMed (Ophth), FRCSEd, FRCOphth, FAMS, Senior Consultant, Professor, Department of Ophthalmology, National University of Singapore (Main Supervisor)

Wong Tien Yin, Ph.D., MMed (Ophth), MPH, FRCSEd, FRANZCO, FAFPHM, Senior Consultant, Professor, Department of Ophthalmology, National University of Singapore (Co-Supervisor)

ACKNOWLEDGEMENTS

This dissertation was based on two clinical study programs and two collaborative research work undertaken in Singapore Eye Research Institute (SERI) over a period of nearly 8 years. This work would have been impossible without the contribution of many investigators, colleagues, coauthors, staff and participants in Singapore National Eye Centre and SERI. The various clinical studies have been supported by grants from SingHealth, Biomedical Research Council (BMRC) and National Medical Research Council (NMRC), Singapore, including a New Investigator Grant from NMRC awarded to me (NIG09nov001).

Foremost, I would like to acknowledge Dr Tin Aung, my mentor, for his generous, unwavering support and continued guidance as the main supervisor. I am thankful to Dr Tien Yin Wong, for his guidance as a co-supervisor. My gratitude goes to all my collaborators in this work, Dr Shamira Perera from SNEC, Dr Murukeshan VM from NTU, Dr Liu Jiang from I2R for allowing me to work in their studies and to the many valuable contributions in my publications.

I am eternally grateful to my research and clinical mentors from medical school A/Prof G Chandrasekaran, who encouraged the research attitude to begin with and Dr L Vijaya who continued to help through my clinical career.

Finally, thanks to my parents who always kept the faith in me; to my family for supporting me through out. I dedicate this dissertation to my lovely wife, Uma, for her many sacrifices and support that enabled me to achieve my goals.

TABLE OF CONTENTS

CHAPTERS

Summary

Background: One of the major concerns in the management of angle closure is detection of the disease in its early stages. Clinical gonioscopy, is a subjective assessment that has poor reproducibility and compliance**.** Most of the imaging techniques such as 2D ultrasound biomicroscopy (UBM), anterior segment optical coherence tomography (ASOCT) and Spectral Domain OCT that currently evaluate the angle, perform meridional or cross-sectional imaging and not the entire circumferential imaging. The **EyeCam^{TM} (**Clarity Medical Systems, Pleasanton, CA) wide-field photography anterior chamber angle and **Swept source OCT** (**Casia SS-1000**, Tomey Corp.) 3-dimensional angle imaging lack data in comparison to gonioscopy. There is also an unmet need for automatically deciphering the angle status from the images made available using these techniques, which will aid clinicians in decision-making for angle closure diagnosis.

Currently, there is no technology that combines digital photography of angle and infra-red imaging for irido-corneal angle assessment. Such a device will be very useful for clinicians to document the angle findings for better diagnosis and to follow up angle closure patients in the clinic.

Aims:

The aims of the PhD are to (a) evaluate the above novel angle assessment techniques (EyeCam and SSOCT) in comparison to gonioscopy for both meridional and circumferential imaging, (b) to develop and evaluate automated software solutions for diagnosis of angle closure and (c) To develop and evaluate a novel dual mode (circumferential angle photography and meridional angle imaging) device for angle imaging.

Methods:

Aim 1: In this hospital-based, prospective study, subjects underwent gonioscopy by a single observer, and EyeCam, Goniophotography and anterior segment optical coherence tomography (ASOCT) imaging by different operators. The anterior chamber angle in a quadrant was classified as closed if the posterior trabecular meshwork could not be seen by gonioscopy. An eye was classified as having angle closure if there were 2 or more quadrants of closure. Manual grading of images was performed using a standardized protocol. Automated grading of the angle images was performed using customized software. Any irido-corneal contact beyond the scleral spur (SS) was considered as angle closure on ASOCT. **Aim 2:** In this hospital-based, prospective study, subjects underwent SSOCT along with gonioscopy. Irido-trabecular index (ITC index) was derived from the machine's software tools, which is a surrogate for assessing the extent of angle closure. An automated grading of the 360° scan was done for the extent of angle closure. **Aim 3:** A dual mode probe with visible light and infrared light source was developed for angle photography with the collaboration of optical engineering team. The probe was tested in two species of animals (rabbits and primates) for utility in angle photography.

Statistical analysis: Agreement between the methods was ascertained by kappa statistic, first order co-efficient statistics and comparison of area under receiver operating characteristic curves (AUC) with the gold standard gonioscopy.

Results: Aim 1: EyeCam assessment of angle was not inferior to goniophotography and superior to ASOCT in the detection angle closure in comparison to gold standard, gonioscopy. EyeCam image grading was successfully automated successfully and was found to have excellent performance for angle closure detection in comparison to gonioscopy. **Aim 2:** Circumferential imaging with SSOCT using ITC index showed good repeatability and diagnostic performance for

detection of angle closure in comparison to reference standard gonioscopy. An automated analysis of 128 cross-sectional scans from SSOCT angle imaging was developed successfully. **Aim 3:** A dual mode probe (visible and infrared) for wide-field angle imaging was developed and successfully tested in primate eyes.

Summary - significance of the study: This study evaluated the current novel techniques in angle assessment and provided valuable input for routine clinical practice in angle closure detection. The automated methods and device developed in collaboration with engineering partners for circumferential angle imaging and evaluated will be of relevance to clinical practice and future continuum of work in this field.

List of Tables

List of Figures

Chapter 1:

Chapter 3:

Chapter 4:

Chapter 5:

List of Abbreviations

ACA:	Anterior Chamber Angle
ASOCT:	Anterior Segment Optical Coherence Tomography
ATM:	Anterior Trabecular Meshwork
CB:	Ciliary Body
CCD:	Charge-coupled device
CDR:	Cup: Disc Ratio
EP:	End Point (Iris trabecular contact end points in SSOCT scans)
GON:	Glaucomatous Optic Neuropathy
IACUC:	Institutional Animal Care and Use Committee
IRB:	Institutional Review Board
ITC:	Iris Trabecular Contact
LPI:	Laser Peripheral Iridotomy
LR+:	Positive Likelihood Ratio
LR-:	Negative Likelihood Ratio
MPE:	Maximum Permissible Emission
NIR:	Near Infrared

NPV:	Negative Predictive Value
PACS:	Primary Angle Closure Suspect
PAC:	Primary Angle Closure
PACG:	Primary Angle Closure Glaucoma
PAS:	Peripheral Anterior Synechiae
POAG:	Primary Open Angle Glaucoma
PPV:	Positive Predictive Value
PSD:	Pattern Standard Deviation
PTM:	Posterior Trabecular Meshwork
SS:	Scleral Spur
SDOCT:	Spectral Domain Optical Coherence Tomography
SSOCT:	Swept Source Optical Coherence Tomography
UBM:	Ultrasound Bio Microscopy
WHO:	World Health Organization

List of Publications from this research

First-authored publications:

1. **Baskaran M,** Perera SA, Nongpiur ME, Tun TA, Park J, Kumar RS, Friedman DS, Aung T. Angle assessment by EyeCam, goniophotography, and gonioscopy. J Glaucoma. 2012;21(7):493-7. (Aim 1)
2. **Baskaran M,** Aung T, Friedman DS, Tun TA, Perera SA. Comparison of EyeCam and anterior segment optical coherence tomography in detecting angle closure. Acta Ophthalmol. 2012 Dec;90(8):e621-5. (Aim 1)
3. **Baskaran M**, Cheng J, Perera SA, Tun TA, Liu J, Aung T. Automated analysis of angle closure from anterior chamber angle images. Invest Ophthalmol Vis Sci. 2014 Oct 21;55(11):7669-73. (Aim 1)
4. **Baskaran M,** Ho SW, Tun TA, How AC, Perera SA, Friedman DS, Aung T. Assessment of circumferential angle-closure by the iris-trabecular contact index with swept-source optical coherence tomography. Ophthalmology. 2013 Nov;120(11):2226-31. (Aim 2)

Publications as one of the authors (related to PhD):

5. Cheng J, Liu J, Lee BH, Wong DW, Yin F, Aung T, **Baskaran M**, Shamira P, Yin Wong T. Closed angle glaucoma detection in RetCam images. Conf Proc IEEE Eng Med Biol Soc. 2010;1:4096-9. (Aim 1)
6. Perera SA, Quek DT, **Baskaran M**, Tun TA, Kumar RS, Friedman DS, Aung T. Demonstration of angle widening using EyeCam after laser peripheral iridotomy in eyes with angle closure. Am J Ophthalmol. 2010 Jun;149(6):903-7. (Aim 1)

7. Perera SA, **Baskaran M**, Friedman DS, Tun TA, Htoon HM, Kumar RS, Aung T. Use of EyeCam for imaging the anterior chamber angle. Invest Ophthalmol Vis Sci. 2010 Jun;51(6):2993-7. (Aim 1)
8. Cheng J, Tao D, Liu J, Wong DW, Lee BH, **Baskaran M**, et al. Focal biologically inspired feature for glaucoma type classification. Med Image Comput Comput Assist Interv. 2011;14(Pt 3):91-8. (Cheng J, Liu J, Wong DW, Tan NM, Lee BH, Cheung C, **Baskaran M,** et al. Focal edge association to glaucoma diagnosis. Conf Proc IEEE Eng Med Biol Soc.2011;2011:4481-4.) (Aim 1)
9. Ho SW, **Baskaran M,** Zheng C, Tun TA, Perera SA, Narayanaswamy AK, Friedman DS, Aung T. Swept source optical coherence tomography measurement of the iris-trabecular contact (ITC) index: a new parameter for angle closure. Graefes Arch Clin Exp Ophthalmol. 2013 Apr;251(4):1205-11. (Aim 2)
10. Xu Y, Liu J, Tan NM, Lee BH, Wong DW, **Baskaran M,** Perera SA, Aung T. Anterior chamber angle classification using multiscale histograms of oriented gradients for glaucoma subtype identification. Conf Proc IEEE Eng Med Biol Soc. 2012 Aug;2012:3167-70. (Aim 2)
11. Xu Y, Liu J, Cheng J, Lee BH, Wong DW, **Baskaran M,** Perera S, Aung T. Automated anterior chamber angle localization and glaucoma type classification in OCT images. Conf Proc IEEE Eng Med Biol Soc. 2013;2013:7380-3. (Aim 2)
12. Shinoj VK, Murukeshan VM, **Baskaran M,** Aung T. Note: A gel based imaging technique of the iridocorneal angle for evaluation of angle-closure glaucoma. Rev Sci Instrum. 2014 Jun;85(6):066105. (Aim 3)
13. Shinoj VK, Murukeshan VM, **Baskaran M,** Aung T. Integrated flexible handheld probe for imaging and evaluation of iridocorneal angle. J Biomed Opt. 2015 Jan 1;20(1):16014.

Related publications to the research work (Anterior segment imaging in angle closure):

1. He Y, **Baskaran M**, Narayanaswamy AK, Sakata LM, Wu R, Liu D, Nongpiur ME, He M, Friedman DS, Aung T. Changes in anterior segment dimensions over 4 years in a cohort of Singaporean subjects with open angles. Br J Ophthalmol. 2015 Feb 13. pii: bjophthalmol-2014-305816.
2. Tun TA, **Baskaran M**, Perera SA, Htoon HM, Aung T, Husain R. Swept-source optical coherence tomography assessment of iris-trabecular contact after phacoemulsification with or without goniosynechialysis in eyes with primary angle closure glaucoma. Br J Ophthalmol. 2015 Jul;99(7):927-31.
3. Tun TA, **Baskaran M,** Perera SA, Chan AS, Cheng CY, Htoon HM, Sakata LM, Cheung CY, Aung T. Sectoral variations of iridocorneal angle width and iris volume in Chinese Singaporeans: a swept-source optical coherence tomography study. Graefes Arch Clin Exp Ophthalmol. 2014 Jul;252(7):1127-32.
4. Nongpiur ME, Haaland BA, Perera SA, Friedman DS, He M, Sakata LM, **Baskaran M,** Aung T. Development of a score and probability estimate for detecting angle closure based on anterior segment optical coherence tomography. Am J Ophthalmol. 2014 Jan;157(1):32-38.e1.
5. Guzman CP, Gong T, Nongpiur ME, Perera SA, How AC, Lee HK, Cheng L, He M, **Baskaran M,** Aung T. Anterior segment optical coherence tomography parameters in subtypes of primary angle closure. Invest Ophthalmol Vis Sci. 2013 Aug 7;54(8):5281-6.
6. Tun TA, **Baskaran M,** Zheng C, Sakata LM, Perera SA, Chan AS, Friedman DS,

Cheung CY, Aung T. Assessment of trabecular meshwork width using swept source optical coherence tomography. Graefes Arch Clin Exp Ophthalmol. 2013 Jun;251(6):1587-92.

7. Ku JY, Nongpiur ME, Park J, Narayanaswamy AK, Perera SA, Tun TA, Kumar RS, **Baskaran M,** Aung T. Qualitative evaluation of the iris and ciliary body by ultrasound biomicroscopy in subjects with angle closure. J Glaucoma. 2014 Dec;23(9):583-8.
8. Chong RS, Sakata LM, Narayanaswamy AK, Ho SW, He M, **Baskaran M,** Wong TY, Perera SA, Aung T. Relationship between intraocular pressure and angle configuration: an anterior segment OCT study. Invest Ophthalmol Vis Sci. 2013 Mar 5;54(3):1650-5.
9. Narayanaswamy A, Zheng C, Perera SA, Htoon HM, Friedman DS, Tun TA, He M, **Baskaran M,** Aung T. Variations in iris volume with physiologic mydriasis in subtypes of primary angle closure glaucoma. Invest Ophthalmol Vis Sci. 2013 Jan 23;54(1):708-13.
10. Nongpiur ME, Haaland BA, Friedman DS, Perera SA, He M, Foo LL, **Baskaran M,** Sakata LM, Wong TY, Aung T. Classification algorithms based on anterior segment optical coherence tomography measurements for detection of angle closure. Ophthalmology. 2013 Jan;120(1):48-54.
11. Zheng C, Cheung CY, Aung T, Narayanaswamy A, Ong SH, Friedman DS, Allen JC, **Baskaran M,** Chew PT, Perera SA. In vivo analysis of vectors involved in pupil constriction in Chinese subjects with angle closure. Invest Ophthalmol Vis Sci. 2012 Oct 1;53(11):6756-62.

12. Quek DT, Narayanaswamy AK, Tun TA, Htoon HM, **Baskaran M**, Perera SA, Aung T. Comparison of two spectral domain optical coherence tomography devices for angle-closure assessment. Invest Ophthalmol Vis Sci. 2012 Aug 3;53(9):5131-6.
13. How AC, **Baskaran M,** Kumar RS, He M, Foster PJ, Lavanya R, Wong HT, Chew PT, Friedman DS, Aung T. Changes in anterior segment morphology after laser peripheral iridotomy: an anterior segment optical coherence tomography study. Ophthalmology. 2012 Jul;119(7):1383-7.
14. Perera SA, Ho CL, Aung T, **Baskaran M,** Ho H, Tun TA, Lee TL, Kumar RS. Imaging of the iridocorneal angle with the RTVue spectral domain optical coherence tomography. Invest Ophthalmol Vis Sci. 2012 Apr 2;53(4):1710-3.
15. Zheng C, Cheung CY, Narayanaswamy A, Ong SH, Perera SA, **Baskaran M,** Chew PT, Friedman DS, Aung T. Pupil dynamics in Chinese subjects with angle closure. Graefes Arch Clin Exp Ophthalmol. 2012 Sep;250(9):1353-9.
16. Tian J, Marziliano P, **Baskaran M,** Wong HT, Aung T. Automatic anterior chamber angle assessment for HD-OCT images. IEEE Trans Biomed Eng. 2011 Nov;58(11):3242-9.
17. Nongpiur ME, He M, Amerasinghe N, Friedman DS, Tay WT, **Baskaran M,** Smith SD, Wong TY, Aung T. Lens vault, thickness, and position in Chinese subjects with angle closure. Ophthalmology. 2011 Mar;118(3):474-9.
18. Narayanaswamy A, Sakata LM, He MG, Friedman DS, Chan YH, Lavanya R, **Baskaran M,** Foster PJ, Aung T. Diagnostic performance of anterior chamber angle measurements for detecting eyes with narrow angles: an anterior segment OCT study. Arch Ophthalmol. 2010 Oct;128(10):1321-7.

19. Ulaganathan S, Ganeshrao SB, **Baskaran M,** Srinivasan S, Shantha B, Vijaya L. Plateau Iris Configuration and Dark-Light Changes in Anterior Segment Optical Coherence Tomography. Ophthalmic Surg Lasers Imaging. 2010 Mar 9:1-4.

Chapter 1: Background and Global literature review

1.1.Introduction to glaucoma and primary angle closure glaucoma

Glaucoma is a group of heterogeneous optic neuropathies characterized by progressive loss of axons in the optic nerve. Data from WHO show that glaucoma accounts for 5.1 million of blindness in the world and is the 2nd leading cause of blindness worldwide (behind cataract) as well as the foremost cause of irreversible blindness.[1] As the number of elderly in the world rapidly increases, glaucoma morbidity will rise, causing increased health care costs and economic burden. Since cataract is easily treated, glaucoma will become the **most common cause of blindness** in the world later this century with almost 70 million cases of glaucoma worldwide. Importantly, between 50-90% of people with glaucoma worldwide are unaware they have the disease.[2.3]

Glaucoma is classified according to the configuration of the **angle** (the part of the eye between the cornea and iris mainly responsible for drainage of aqueous humor) into open angle (Figure 1a, 2a) and angle closure (Figure 1b, 2b) glaucoma. **Primary angle closure glaucoma (PACG)** is a major form of glaucoma in Asia,[4,5] compared to primary open angle glaucoma (POAG), which is more common in Caucasians and Africans.[6,7] This is true especially in populations of Chinese and Mongoloid descent.[3,8,9] Recent glaucoma prevalence studies in southern India found that the prevalence of PACG in Indians is also high.[10,11] In China itself, it is estimated that PACG afflicts 3.5 million people and 28 million have a narrow drainage angle, which is the anatomical trait predisposing to PACG.[4] The disease is already responsible for the majority of bilateral glaucoma blindness in Mongolia,[8] Singapore,[9] China[3] and India.[10,11] It is estimated that PACG blinds more people than POAG in relative terms, although the numbers of those with

Figure 1 (a) Open angles; (b) Closed angles – Anterior Segment Optical Coherence Tomography (white arrows indicate angle area)

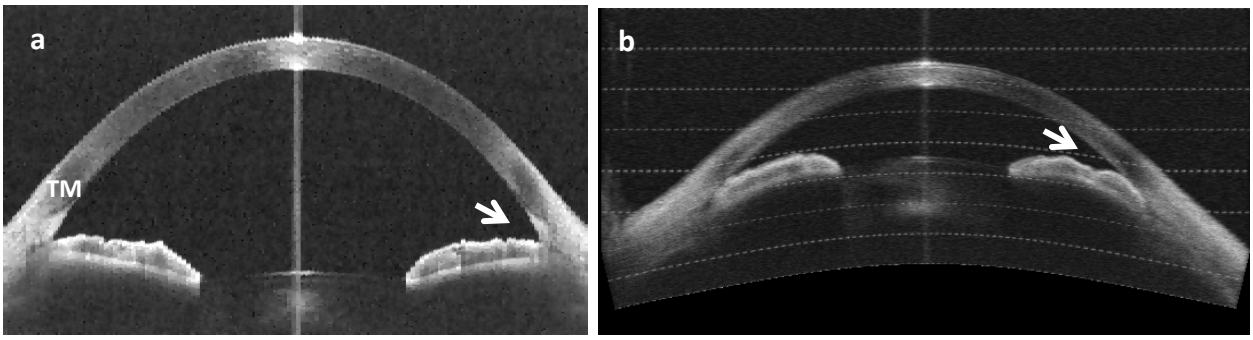

Figure 2 (a) Open angles showing trabecular meshwork (TM) - Gonioscopic view of the irido-corneal angle; (b) Closed angles (black arrows indicate angle area)

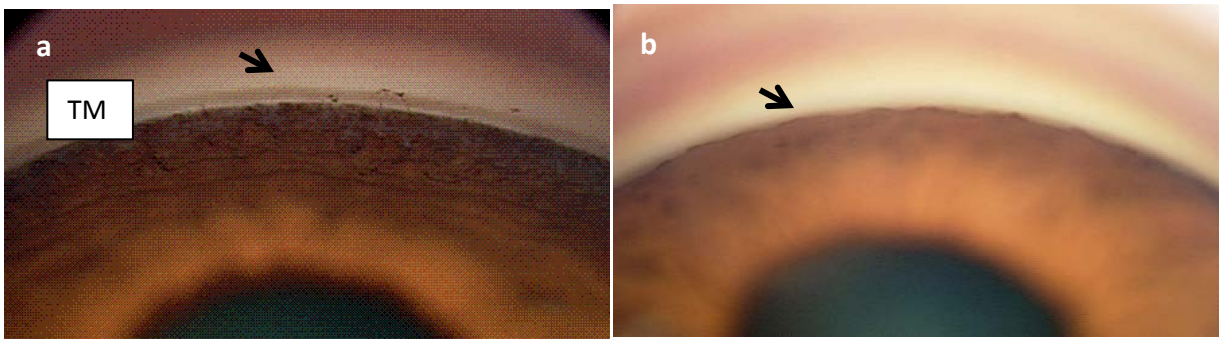

POAG worldwide is only 30% higher than PACG.[12] By 2020, PACG will affect 20 million people and 5.3 million will be blind.[13]

1.2 Diagnosis and screening of Angle Closure: Relevance of imaging methods

Anatomical landmarks of irido-corneal angle of the eye

Irido corneal angle of the eye is that is the specialized tissue at the junction of cornea and iris. The trabecular meshwork (TM, pigmented portion in the angle – Figure 2a) which forms the bridging tissue is an important landmark since it drains the aqueous humor of the eye. Mechanical or functional blockage of this portion may cause raise in intraocular pressure and subsequently glaucoma. The various other landmarks in the angle from anterior to posterior end include (see Figure 2, Chapter 3) – Schwalbe's line (SL is the termination of Descemet's membrane from the posterior layer of the cornea), anterior non-pigmented TM (ATM), posterior pigmented TM (PTM), Scleral spur (SS, the main landmark to which the ciliary muscles attach) and the ciliary body (CB), which is the anterior most portion of the ciliary musculature.[14]

Physiologically, the angle is wide open (Figure 2a). When the iris in the peripheral anterior chamber is convex and blocks the PTM, then it is considered closed (Figure 2b). There are several mechanisms involved in the occurrence of this closed angle. We do not elaborate on the mechanisms as it is beyond the scope of this dissertation. The main mechanism is called pupillary block, when the apposition between iris and lens become prominent at pupil margin with accumulation of fluid behind the iris. This pushes the iris forward and closed angle occurs.

Stages of primary angle closure glaucoma:

At the earliest or most basic stage of angle closure disease, eyes have **narrow angles** (NA) without any other abnormality. The term **primary angle-closure suspect (PACS)** is an

alternative term for this condition, as these eyes are at increased risk of developing disease. There is no established definition of what narrow angles are, and the term has been used when an observer cannot see the posterior pigmented trabecular meshwork for a certain extent of the angle on gonioscopy. This exact amount is arbitrary and has been quoted as 270 degrees, 180 degrees, or even 90 degrees. By consensus, no visible pigmented trabecular meshwork for 180 degrees or more of the angle is categorized as having NA. **Primary angle-closure (PAC)** is said to occur in eyes with NA that have peripheral anterior synechiae (PAS) and/or raised intraocular pressure (IOP) (defined as an IOP greater than two standard deviations above the norm for the population being studied) due to closure of the angle, but without glaucomatous optic neuropathy. Finally, **primary angle-closure glaucoma (PACG)** is reserved for cases of PAC with glaucomatous optic neuropathy. Symptomatic or acute primary angle closure (APAC) can occur at any stage of this spectrum of disease. Although acute episodes can cause severe visual loss, majority of PACG occurs without an episode of APAC.[1-13]

Preventive strategies and need for screening/case detection of angle closure:

Laser peripheral iridotomy (LPI), is a procedure that creates small hole in the iris thus removing the pupillary block. This can prevent APAC fully and probably may play a role in delaying or preventing PACG in susceptible individuals, if advocated in the earlier stages such as PACS or PAC.[5]

Problems related to current clinical evaluation methods:

One of the major concerns in the management of angle closure is detection of the disease in its early stages. At present, angle evaluation in the clinical setting is accomplished by gonioscopy, a process in which a simple hand-held instrument is placed on the patient's eye, and the physician then examines the angle of the eye using a slit-lamp biomicroscope. **Gonioscopy** is a subjective

assessment that has poor reproducibility, and the agreement between expert observers was found to be less than kappa = 0.5 in most studies.[14] The technique is difficult to learn and being a contact procedure, it is mostly disliked by patients. The type of lens used, the technique employed and the skill of the observer affect the variability of gonioscopy findings. Apart from this, there is limited quantitative assessment, and limited documentation is only available for future review. The main advantage of gonioscopy is that the treating physician can assess 360º of the angle circumferentially.

Although gonioscopy is an essential part of a glaucoma evaluation, a survey conducted in the USA on preferred practice patterns showed that only 50% of ophthalmologists use gonioscopy as part of their examination in subjects who require it.[15] This undermines the utility of the technique and raises the need for a reliable alternative.

In this context, the availability of simple photographic techniques to document angle findings is an appealing option in clinical practice, especially if imaging provided clinically useful information about the risk of angle closure and can be used for documentation of longitudinal changes. In particular, there is a need for an imaging method that documents the angle with less discomfort to the patient, in a shorter time-period and that is less dependent on the examiners' expertise.

Screening for angle closure is a desired objective in certain high-risk populations where ageing increases the number of people affected with angle closure disease, thus raising the overall prevalence of glaucoma. However, contact photographic procedures may not be suitable in this situation. Imaging techniques involving no expertise is the method of choice for screening angle closure. Further, screening strategies that are automated may enhance health care delivery, thus reducing the burden for ophthalmologists.

1.3 Meridional vs Circumferential angle evaluation

The visualisation capabilities of various ocular imaging techniques can be broadly classified into photographic (gonioscopic photography, EyeCam^{TM}, pentacam, etc.) and optical cross-sectional methods (optical coherence tomography (OCT), Ultrasound biomicroscopy (UBM), etc.). All these imaging modalities can contribute to the diagnosis and management of glaucoma by allowing visualization of the iridocorneal angle. However, each technique has benefits along with associated drawbacks in obtaining reliable and repeatable measurements to assist the clinician in evaluating the angle.

Most imaging techniques that currently evaluate the angle, perform meridional or cross-sectional (i.e. 1 or 2 transverse scans) imaging and not circumferential (i.e. 360°) imaging.

In photographic methods, the iridocorneal region is captured using a camera and images can be saved on a computer thus allowing comparisons to be made over time. This allows for monitoring of angle changes over time, tracking of angle changes with disease progression as well as treatment effects. Different type for photographic methods for evaluating angle-closure is discussed in the following subsections.

Goniophotography is a clinical photographic method of documenting gonioscopic findings using a slit-lamp mounted camera and indirect gonioscopic lens. This technique requires some expertise to discern the ocular structures with the gonioscopy lens and for obtaining clear images of the angle.

Pentacam (Oculus, Optikgerate GmbH, Wetzlar, Germany) is based on **Scheimpflug's photography** principle,[16,17] where the imaging of an obliquely tilted object can be accomplished with maximum depth of focus and least image distortion under given conditions. It explains the orientation of plane of focus of an optical system when the lens plane is not parallel with image

plane. If the object plane is not in parallel with the image plane, the lens focuses only along the line where it intersects plane of focus. The Scheimpflug principle is employed in Pentacam through a rotating camera to obtain optical sections of the entire anterior segment of eye. It images the anterior segment from the cornea to the posterior surface of the lens in three dimensions. A Pentacam image of a closed angle eye is shown in Figure 3.

This non-contact device offers rapid three-dimensional analysis of the anterior chamber and can be used to measure anterior chamber depth and volume, anterior chamber angle width, corneal pachymetry, corneal radius and diameter of curvature and lens position.[18] The imaging lasts less than 2 seconds and the centre of cornea; and its anterior and posterior surfaces can be measured accurately. It can be used as the primary assessment tool to evaluate angle-closure disease condition. However, the assessment of the iridocorneal angle cannot be done in detail using this method since direct visualization of the angle recess is not available. Furthermore, user definition of the iris plane necessarily uses a straight line to describe a curved plane, leading to inaccuracies in angle width measurement.

1.4 Angle closure evaluation: Current Imaging Technologies for Angle Closure

Imaging of the angle of the eye is gaining increasing importance for the diagnosis, management and follow-up of PACG. The main pathological area in this form of glaucoma is the **trabecular meshwork** (TM), which is the site for drainage of aqueous humor of the eye (TM in Fig 1a). Optical tomographic imaging techniques are non-invasive imaging techniques that allow visualization of the internal structures of an eye without the superposition of over- and under-lying structures. Currently,

(i) 2D ultrasound biomicroscopy imaging (UBM – Figure 4a),

(ii) anterior segment optical coherence tomography (OCT – Figure 4b e.g. Visante ASOCT) and

(iii) Spectral Domain Optical Coherence Tomography (Figure 4c)

are utilized for anterior segment imaging.

Ultrasound BioMicroscopy (UBM) images the anterior segment by utilizing a piezoelectric, manual scanning tool which is bulky and non-user friendly, and has a relatively poor angular resolution. In this method, the depth of ocular tissue structures is decided by measuring the time delay of returning ultrasound signal which the computer assembles to provide a magnified high resolution image. UBM requires the transducer in contact with the eye hence the scanning is generally performed through an immersion bath. UBM provides two-dimensional gray scale images of the various anterior segment structures and can be used to measure the anterior chamber angle in degrees as well as the depth of anterior and posterior chambers. UBM has been extensively used in various clinical and experimental applications on glaucoma for diagnostic purpose. Image acquisition time depends upon the cooperation of the patient and the experience of the examiner. Axial resolution of up to 20 μm is possible at operating frequency of 50 MHz.[17] Figure 4 shows the UBM image of the anterior chamber, chamber angle and angle parameters.[19]

With UBM it is easy to note and confirm a narrow angle. The angle can be assessed in bright light condition where the pupil constricts and in dark conditions where the angle tends to narrow because of pupil dilatation. The cornea, anterior chamber, posterior chamber, the angle, ciliary body and the anterior lens surface can be easily visualized.[20] Since this technique helps in evaluation of underlying mechanisms of angle-closure, it helps in deciding the appropriate form of treatment. It is also useful in evaluation of some forms of open angle glaucoma such as pigment dispersion syndrome. However, contact of transducer with eye is necessary which

Figure 3: Pentacam image of anterior chamber in open angle eye

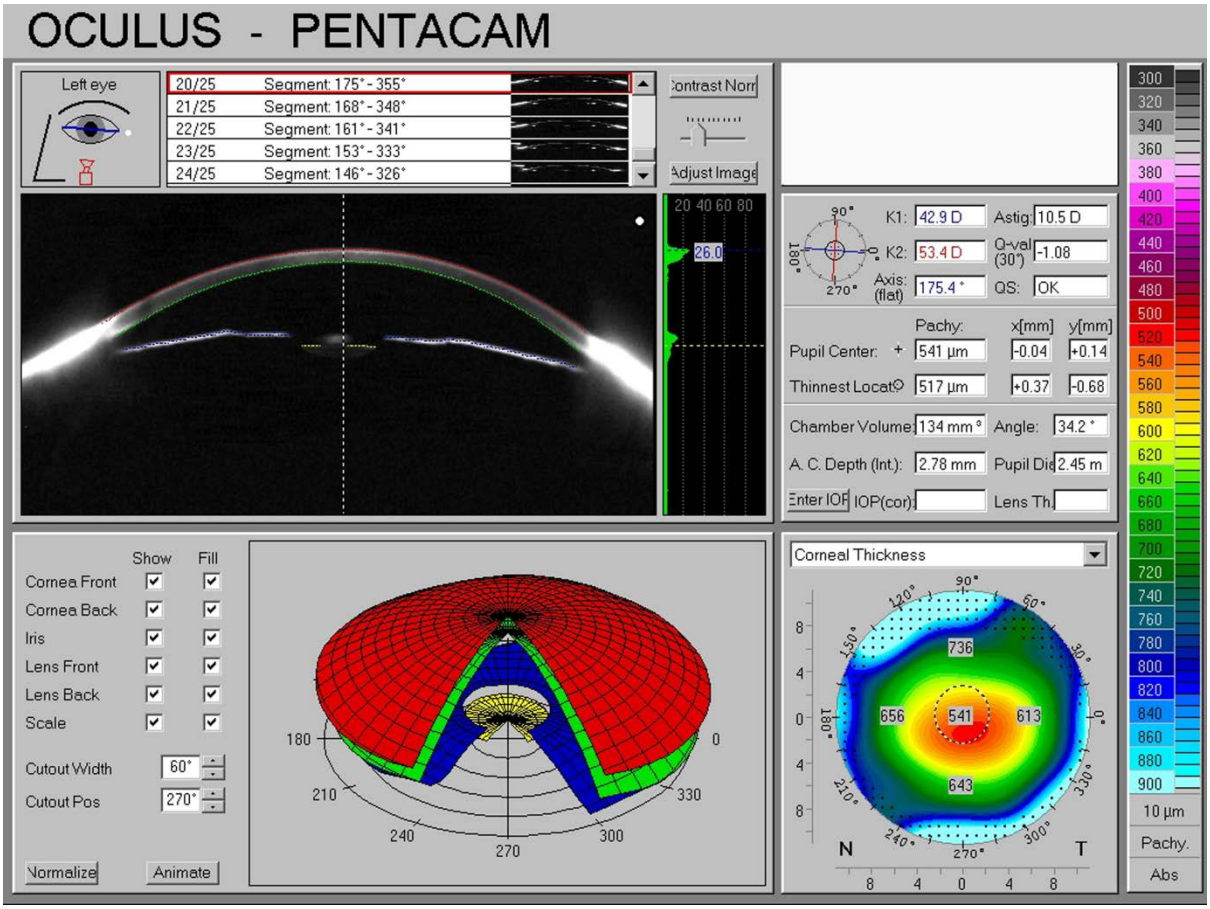

Figure 4a: Ultrasound biomicroscopy (2D) image of a closed angle in cross-section – Ciliary body seen (Arrow)

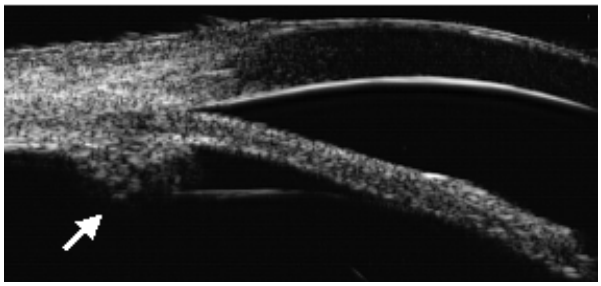

Figure 4b: Visante anterior segment optical coherence tomography image showing a partially closed angle in cross-section – Ciliary body not seen (Arrow)

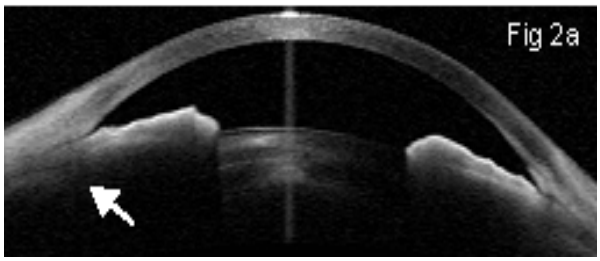

Figure 4c: Cirrus high definition anterior segment optical coherence tomography image showing an open angle in cross-section – Scleral spur (Top arrow); Ciliary body not seen (Bottom Arrow)

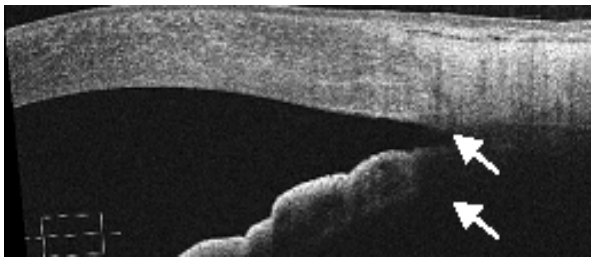

creates discomfort to the patient with risks of corneal abrasions and infections. A skilled and experienced operator is needed and the procedure is time-consuming. The requirement of the patient to be in a supine position may cause an artifactual widening of the anterior chamber angle.[21] Another disadvantage is the lack of standardization between UBM scans.

Optical coherence tomography (OCT) is analogous to UBM, but light is used instead of sound. The working mechanism of the OCT is based on low-coherence tomography and it uses the principle of a Michelson Interferometer to detect optical backscatter. The ability of the OCT to provide good repeatability and reproducibility for quantitative and qualitative analyses of the angle recess makes it an important diagnostic tool for disease documentation of PACG, disease progression, and therapeutic outcomes. Higher spatial resolution, high-speed image acquisition, ability for standardization of scans, its non-contact nature and minimal requirements for expertise make OCT advantageous over UBM. One of the anterior segment OCT (ASOCT) (Visante; Carl Zeiss Meditec, Dublin, CA) system uses a longer wavelength (1.3 μm), allowing deeper penetration and cross-sectional imaging of the anterior chamber (AC) and visualization of the angle.[22] Low-coherence light beam at 1310 nm in the near infrared (NIR) region is split, and simultaneously directed onto the tissue and the reference mirror. The relative location of the light backscattered from the image tissue can be obtained, based on the information from the internal reference mirror. Following data acquisition, the raw scanned images are processed by a geometric computational process that converts the optical distance to physical distance prior to scan review and analysis, taking into consideration the refraction index variations at the corneal air/ tissue interface and the tissue/ aqueous interface. Light at this wavelength (1.3 μm) has lower scattering loss and hence, greater penetration through the ocular structures. In addition, this wavelength is strongly absorbed by the vitreous humor, resulting in only an approximated 10%

of the incident light reaching the retina. The increase in retinal protection enables high power illumination which in turn results in high speed imaging. These two properties of the NIR light allow clinicians to obtain a more detailed morphology of the anterior segment and minimize image distortion and motion artifacts. Interference is measured by a photodetector when the backscattered light from both sources combined.

The Visante™ ASOCT is able to make 2000 A-scans per second, with a scan acquisition time of 0.125 second per line (8 frames per second) for the Anterior Segment Scans, and 0.25 second per line (4 frames per second) for High resolution Corneal Scans. The 6 mm deep scan range and 16 mm wide field scanning allow the entire anterior chamber to be imaged in a single frame. As in the case of conventional microscopy, the transverse resolution of 60 µm is determined by the spot size of the focusing beam, the focusing parameter, and the diffraction properties of light. Good axial resolution of 18 µm is possible due to the small numerical aperture focusing and a large depth of focus using low-coherence tomography. The quality of the images is also influenced by pixel intensity (analogous to pixel density in digital photography) and the speed of acquisition. Details on the basic principles of the Visante™ OCT have already been covered extensively in previous literature.[23-25] Since the posterior layer of the iris is not transparent for the infrared light, the area of the sulcus is not presentable. Also, the infrared light will be absorbed on its way through the sclera and hence, the area of the ciliary body is not entirely visible.[26,27] The location of the trabecular meshwork is also undetermined.

Angle closure with the Visante™ ASOCT is determined by any contact between the iris and the angle wall anterior to the scleral spur whereas for gonioscopy, the quadrant would still be considered open unless the apposition reached the posterior trabecular meshwork. The Visante™ OCT therefore overestimates the frequency of angle closure with respect to gonioscopy,[28] which

is the gold standard for angle evaluation. There are also no built-in analytical tools to detect an angle measurement and indicate "narrow angles" to the user. The scleral spur, which is the anatomical landmark for angle imaging, has to be determined manually and is not detectable in up to 28% of the patients in one study.[28]

The Spectral domain OCT (e.g. Cirrus, Zeiss meditech, USA) is another commercially available optical instrument that is non-invasive. Unlike the time-domain Visante™ OCT system, the Cirrus OCT is a spectral-domain instrument that uses NIR light of 840 nm wavelength. This system is designed primarily for retinal imaging but also supports several modes, including corneal and angle evaluation. Since the SDOCT obtains the detected interferometric signal as a function of optical frequencies, its imaging speed is 50-60 times faster than the Visante™ OCT[29] and it has an axial resolution of 5 μm, and a transverse resolution of 15 μm. The higher resolution SDOCT means improved visualization of the cornea and angle, as well as the ability to image ocular substructures such as the trabecular meshwork, the scleral spur, and the Schwalbe's line.[30-32]

Above modalities lack good angular resolution (except SDOCT), are bulky or lack real time 3-dimensional details, due to the limited data that can be collected and processed. These methods utilize meridional scanning which limit the angle evaluation and clinical utility. **For the diagnosis of angle closure, one looks for contact between the iris and the trabecular meshwork.** Unfortunately, the trabecular meshwork is not visible in most UBM or anterior segment OCT images, limiting its ability to define angle closure.

1.5 Novel methods of angle closure assessment

Recently there is interest in circumferential angle evaluation using some of the novel methods.

1.The **EyeCam™** (Clarity Medical Systems, Pleasanton, CA) is a camera capable of taking wide-field photographs of the fundus,[33] and has recently been assessed for its ability to image the optic disc[17] and the anterior chamber angle.[34] For angle imaging; patients are asked to be in supine position and coupling gel (e.g. vidisic gel), provides an optical interface between the camera's lens and the cornea. This eliminates the total internal reflection that naturally occurs at the corneal tear film-air interface, allowing rays of light coming from the iridocorneal angle region. The coupling gel is applied at the tip of EyeCam's lens and is placed at the opposite limbus to image the opposite angle. (EyeCam is the anterior segment version of RetCam meant for posterior segment photography).

The images produced by EyeCam™ are easy for clinicians to interpret as the angle appears similar to what is seen during gonioscopy (Figures 5a – 5d). However, imaging of angle using EyeCam™ takes longer than gonioscopy (about 5-10 min per eye). The device is more expensive than gonioscopy and additional space is required for supine examination. It is not known if supine positioning would widen the angle due to the effect of gravity on the lens-iris diaphragm. There is lack of data on the evaluation of this instrumentation in comparison to gonioscopy. There is also an unmet need for automatically deciphering the angle status from the images made available using these photographic techniques.

2. **Swept source OCT** system is based on the Fourier Domain system which employs a swept laser source at wavelength 1310 nm to capture high-resolution images of the anterior segment structures. High image acquisition speed reduces motion artifact thereby enhancing the quality of images produced. The **Casia SS-1000** (Tomey Corp., Nagoya, Japan) is based on this technology. One important feature of this instrument is the presence of a wide scanning range and depth of 16 mm and 6 mm which allows the entire cross-sectional image of the anterior

Figure 5: Image of an open angle obtained from human eye using EyeCam: (a) Inferior, (b) Superior, (c) Nasal and (d) Temporal

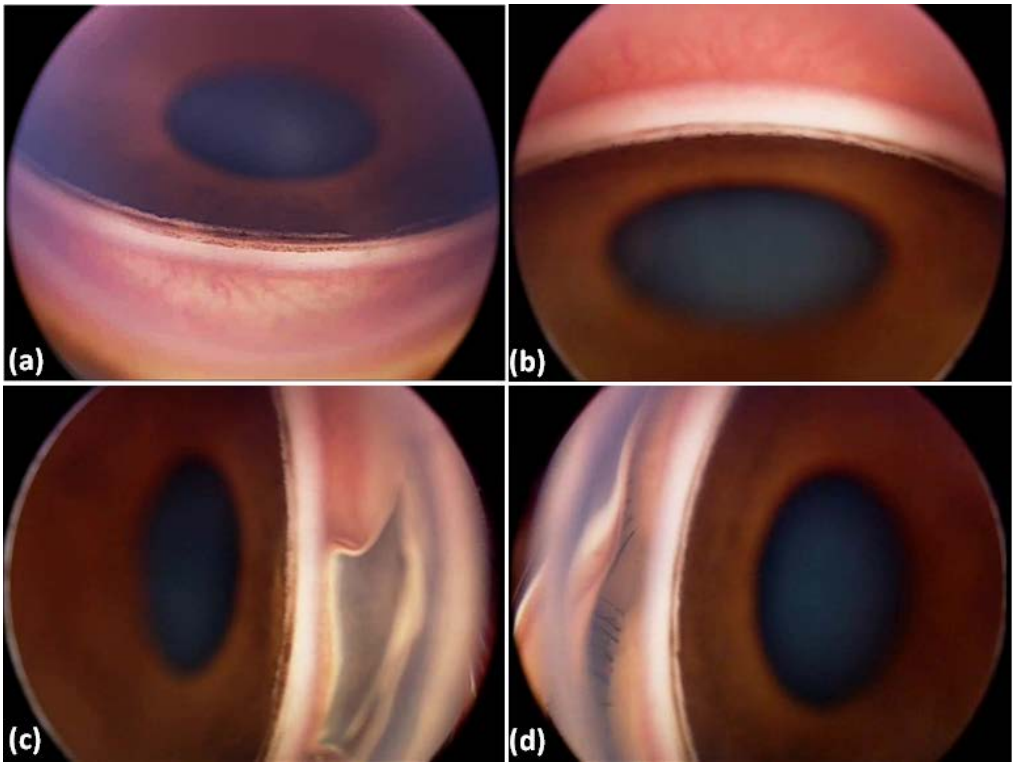

Figure 6: Swept Source Optical Coherence Tomography image in an angle closure eye (One of 128 scans). Inset shows the video image of the position of scan.

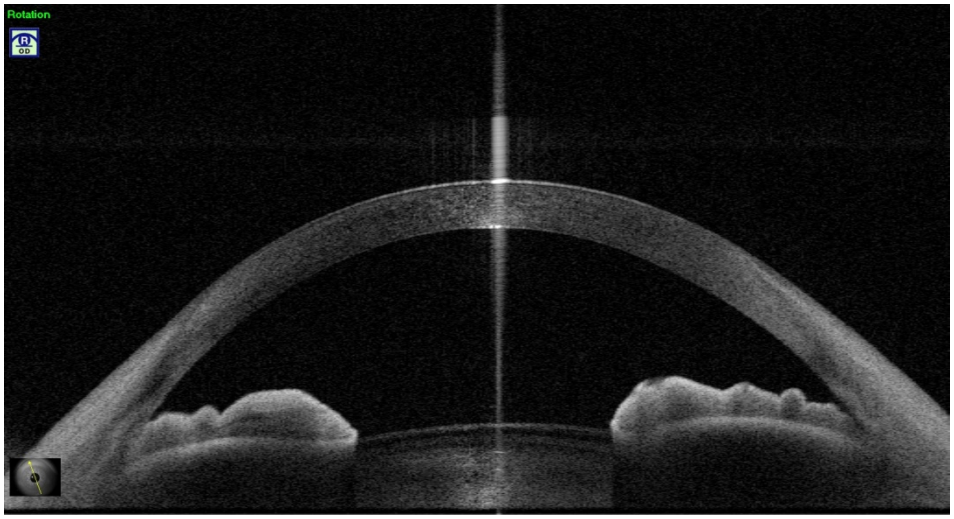

chamber to be captured and measured (Fig 6). The Casia SS-1000 OCT has A-scan frequency of 30,000 Hz, an axial resolution of 10 µm, and a transverse resolution of 30 µm. In addition, multiple radial scans of the entire circumference of the anterior chamber angle can be obtained using the low density 3-D angle analysis scan. Table 1 shows a comparison of the properties and differences between the Visante™ ASOCT, Cirrus ASOCT, Slit lamp ASOCT and the CASIA SS-1000 SSOCT. However, this technology is limited by a lack of application software to quantify the 3-D data.

Currently, there are no technology that combines digital photography of angle and infra red photography for irido-corneal angle assessment. Such a device will be very useful for clinicians to interpret circumferential angle data for a better diagnosis and to follow up angle closure patients in the clinic. A new investigator grant (NIG 09Nov001, National Medical Research Council, Singapore) awarded to the author, explored this possibility in collaboration with Nanyang Technological University, Singapore. While visible light documents the angle structures and pathology, it can interfere with the pupil and angle configuration is altered. Infrared light source can be useful combination with visible light to document closed angle status accurately. Thus, this study designed a dual mode probe with visible light source and infrared light source to document angle.

Summary of rationale for the PhD: Gonioscopy, the current clinical method for angle closure detection lacks objectivity and is not useful for screening or clinical documentation. Current cross-sectional (meridional) imaging method (ASOCT) for angle closure detection lacks information from 360° of the angle. This aspect is crucial to have a direct comparison to clinical method such as gonioscopy. Further, currently there is lack of automated tools for diagnosis of angle closure using imaging methods. This will largely remove the need for expertise in primary

and secondary eye care set up for screening or case detection of angle closure. Novel methods such as EyeCam and Casia SSOCT provide the platform for filling the above gaps including circumferential angle imaging, however, lack clinical data or automation to fulfil all of the unmet needs. Thus the current PhD work aims to bridge this gap in clinical need for angle closure detection in providing clinical data using these tools and explore opportunities to automate the process of angle closure detection. Further, we also aim to build a new device that can be economical for widespread clinical documentation of angle images in combination with infrared mode which does not affect the pupil dynamics and thus angle anatomy.

1.6 Summary of significance of the study:

This PhD program will evaluate current novel techniques in angle assessment (i.e. EyeCam and Casia SSOCT) and will provide valuable input for routine clinical practice in angle closure detection. The automated methods and device developed in collaboration with engineering partners for circumferential angle imaging and evaluated will be of relevance to clinical practice and future continuum of work in this field.

Table 1: Comparison of the properties and differences among the Visante™ ASOCT, Cirrus ASOCT and Slit Lamp ASOCT.

OCT Type	Manufacturer	Optical Source	Axial Resolution	Transverse Resolution	Scan Speed (A- Scans per second)	Scan Depth	Scan Width
Visante™ ASOCT	Carl Zeiss Meditec, Dublin, CA	SLD 1310 nm	18 µm	60 µm	2,000	6 mm	16 mm
Slit Lamp ASOCT	Heidelberg Engineering, Dossenheim, Germany	SLD 1310 nm	< 25 µm	20-100 µm	200	7 mm	15 mm
Cirrus ASOCT	Carl Zeiss Meditec, Dublin, CA	SLD 840 nm	5 µm	15 µm	27,000	2 mm	6 mm
CASIA SS-1000 OCT	Tomey Corporation, Nagoya, Japan	Swept source laser at 1310 nm	10 µm	30 µm	30,000	6 mm	16 mm

1.7 References: (Chapter 1)

1. Thylefors B, Negrel AD, Pararajasegaram R, Dadzie KY. Global data on blindness. Bull WHO 1995; 73(1): 115-21
2. Sathyamangalam RV, Paul PG, George R, et al. Determinants of glaucoma awareness and knowledge in urban Chennai.Indian J Ophthalmol. 2009t;57:355-60.
3. Foster PJ, Oen FT, Machin D, Ng TP, Devereux JG, Johnson GJ, Khaw PT, Seah SK. The prevalence of glaucoma in Chinese residents of Singapore: a cross-sectional population survey of the Tanjong Pagar district. **Arch Ophthalmol** 2000; 118:1105-11
4. Hu Z, Zhao ZL, Dong FT. An epidemiological investigation of glaucoma in Beijing and Shun-Yi county. Chin J Ophthalmol 1989; 25: 115-8
5. Foster PJ, Johnson GJ. Glaucoma in China: how big is the problem? Br J Ophthalmol 2001; 85: 1277-82
6. Tielsch JM, Sommer A, Katz J, Royall RM, Quigley HA, Javitt J. Racial variations in prevalence of primary open angle glaucoma. JAMA 1991; 266: 369-74
7. Klein BE, Klein R, Sponsel WE, Franke T, Cantor LB, Martone J, Menage MJ.Prevalence of glaucoma. The Beaver Dam Eye Study. **Ophthalmology** 1992; 99: 1499-1504
8. Congdon N, Wang F, Tielsch JM: Issues in the epidemiology and population based screening of primary angle-closure glaucoma. Surv Ophthalmol 1992; 36: 411-423
9. Foster PJ, Baasanhu J, Alsbirk PH, Munkhbayar D, Uranchimeg D, Johnson GJ. Glaucoma in Mongolia-a population-based survey in Hovsgol Province, Northern Mongolia. Arch Ophthalmol 1996; 114: 1235-41.

10. Dandona L, Dandona R, Mandal P, Srinivas M, John RK, McCarty CA, Rao GN. Angle closure glaucoma in an urban population in Southern India. The Andhra Pradesh Eye Disease Study. Ophthalmology 2000; 107: 1710-6
11. Jacob A, Thomas R, Koshi SP, Braganza A, Muliyil J. Prevalence of primary glaucoma in an urban south Indian population. Indian J Ophthalmol 1998; 46: 81-6
12. Quigley HA, Congdon NG, Friedman DG. Glaucoma in China (and worldwide): changes in established thinking will decrease preventable blindness. Br J Ophthalmol 2001;85:1271-1272.
13. Quigley HA, Broman AT. The number of people with glaucoma worldwide in 2010 and 2020. Br J Ophthalmol 2006; 90: 262-7.
14. Schirmer KE. Gonioscopy and artefacts. Br J Ophthalmol 1967; 51: 50-53.
15. Quigley HA, Friedman DS, Hahn SR. Evaluation of practice pattern for the care of open angle glaucoma compared with claims data: the Glaucoma Adherence and Persistence Study. Ophthalmology 2007 11(9):1599-606.
16. T. Scheimpflug, "Improved method and apparatus for the systematic alteration or distortion of plane pictures and images by means of lenses and mirrors for photography and for other purposes," *GB patent,* vol. 1196, 1904.
17. R. Jain and S. Grewal, "Pentacam: Principle and Clinical Applications," *Journal of Current Glaucoma Practice,* vol. 3, pp. 20-32, 2009.
18. J. L. S. See, "Imaging of the anterior segment in glaucoma," *Clinical & experimental ophthalmology,* vol. 37, pp. 506-513, 2009.
19. C. J. Pavlin and F. S. Foster. "Ultrasound biomicroscopy in glaucoma," *Acta Ophthalmologica,* vol. 70, pp. 7-9, 1992.

20. C. Pavlin, K. Harasiewicz, M. Sherar, and F. Foster. "Clinical use of ultrasound biomicroscopy," *Ophthalmology,* vol. 98, pp. 287-295, 1991.
21. H. Ishikawa, K. Inazumi, J. M. Liebmann, and R. Ritch, "Inadvertent corneal indentation can cause artifactitious widening of the iridocorneal angle on ultrasound biomicroscopy," *Ophthalmic surgery and lasers,* vol. 31, pp. 342-345, 1999.
22. S. Radhakrishnan, A. M. Rollins, J. E. Roth, S. Yazdanfar, V. Westphal, D. S. Bardenstein, and J. A. Izatt, "Real-time optical coherence tomography of the anterior segment at 1310 nm," *Archives of Ophthalmology,* vol. 119, p. 1179, 2001.
23. J. G. Fujimoto, C. Pitris, S. A. Boppart, and M. E. Brezinski, "Optical coherence tomography: an emerging technology for biomedical imaging and optical biopsy," *Neoplasia (New York, NY),* vol. 2, p. 9, 2000.
24. D. Huang, E. A. Swanson, C. P. Lin, J. S. Schuman, W. G. Stinson, W. Chang, M. R. Hee, T. Flotte, K. Gregory, and C. A. Puliafito, "Optical coherence tomography," *Science,* vol. 254, pp. 1178-1181, 1991.
25. I. I. K. Ahmed, "Anterior Segment Optical Coherence Tomography in Glaucoma," *Journal of Current Glaucoma Practice,* vol. 3, pp. 14-23, 2009.
26. W. P. Nolan, J. L. See, P. T. Chew, D. S. Friedman, S. D. Smith, S. Radhakrishnan, C. Zheng, P. J. Foster, and T. Aung, "Detection of primary angle closure using anterior segment optical coherence tomography in Asian eyes," *Ophthalmology,* vol. 114, pp. 33-39, 2007.
27. S. Dorairaj, J. M. Liebmann, and R. Ritch, "Quantitative evaluation of anterior segment parameters in the era of imaging," *Transactions of the American Ophthalmological Society,* vol. 105, p. 99, 2007.

28. L. M. Sakata, R. Lavanya, D. S. Friedman, H. T. Aung, H. Gao, R. S. Kumar, P. J. Foster, and T. Aung, "Comparison of gonioscopy and anterior segment ocular coherence tomography in detecting angle closure in different quadrants of the anterior chamber angle," *Ophthalmology*, vol. 115, pp. 769-774, 2008.
29. R. Forte, G. Cennamo, M. Finelli, and G. de Crecchio, "Comparison of time domain Stratus OCT and spectral domain SLO/OCT for assessment of macular thickness and volume," *Eye*, vol. 23, pp. 2071-2078, 2008.
30. E. B. Rodrigues, M. Johanson, and F. M. Penha, "Anterior segment tomography with the cirrus optical coherence tomography," *Journal of ophthalmology*, vol. 2012, 2012.
31. T. Jing, P. Marziliano, and H.-T. Wong, "Automatic detection of Schwalbe's line in the anterior chamber angle of the eye using HD-OCT images," in *Engineering in Medicine and Biology Society (EMBC), 2010 Annual International Conference of the IEEE*, 2010, pp. 3013-3016.
32. H.-T. Wong, M. C. Lim, L. M. Sakata, H. T. Aung, N. Amerasinghe, D. S. Friedman, and T. Aung, "High-definition optical coherence tomography imaging of the iridocorneal angle of the eye," *Archives of ophthalmology*, vol. 127, p. 256, 2009.
33. Erraguntla V, MacKeen LD, Atenafu E, et al. Assessment of change of optic nerve head cupping in pediatric glaucoma using the RetCam 120. J AAPOS. 2006;10:528-33.
34. Narayanaswamy A, Singh M. RetCam — a Useful Adjunctive Tool to Evaluate and Manage Paediatric Glaucomas. Asian J Ophthalmol. 2008;109:30-31.
35. Ahmed I, MacKeen L. A New Approach to Imaging the Angle. *Glaucoma Today*. 2007;4:1-3.

Chapter 2: Rationale, Overview and Methods

2.1 Statement of the problem and rationale

Recent meta-analysis estimates point to the global prevalence of glaucoma to be 3.44% (95% CI 2.32-5.08). Of note is the high primary angle closure glaucoma (PACG) prevalence in Asia (1.01%, 95% CI 0.43-2.32). The estimates for angle closure precursor stages such as primary angle closure suspects (PACS) and primary angle closure (PAC) are undetermined. These estimates maybe higher due to a rapidly ageing population, thus increasing future blindness rates due to PACG.

Established diagnostic techniques such as gonioscopy or meridional (cross-sectional) imaging techniques lack patient comfort, objectivity or the resolution/information needed to accurately diagnose, screen or document angle closure in high-risk populations. Thus there is a need for novel eye care approaches to rapidly diagnose or document angle closure disease.

Unmet clinical needs in Angle Closure Diagnostics:

The currently available anterior segment tools **lack** the following aspects:

1. Evaluation of the entire angle and automated assessment of angle status
2. Utilization of 3-dimensional cross-sectional imaging data in angle assessment
3. Combined digital photography (visible and infrared light based dual mode methods) and cross sectional imaging methods
4. Clear and direct delineation of trabecular meshwork with high resolution (TM);
5. The ability to explore dynamic features of aqueous humor (e.g. aqueous flow rate).

This thesis will be exploring the first three unmet clinical needs in terms of evaluation of EyeCam digital angle photography, assess 3D-data (circumferential imaging data) from SSOCT and then explore the possibilities of a combined technology (i.e. digital angle photography and infra-red angle imaging) in the form of a novel instrumentation.

2.2 Hypothesis and Specific aims

The aims of the thesis are to (a) evaluate the above novel angle assessment techniques (EyeCam and SSOCT) in comparison to gonioscopy for both meridional and circumferential imaging, (b) to develop and evaluate automated software solutions for diagnosis of angle closure and (c) To develop and evaluate a novel dual mode (circumferential angle photography and meridional angle imaging) device for angle imaging.

Hypothesis:

We hypothesize that the novel methods will be at least as sensitive in angle closure detection in comparison to one of the established meridional imaging method i.e. ASOCT, for which the sensitivity is reported to be 82% in comparison to gonioscopy in a clinical setting. Further the hypotheses can be summarised as:

- Novel circumferential angle imaging techniques (EyeCam and SSOCT) can be utilized for angle assessment (in comparison to gonioscopic reference standard) – Aims I and II
- Automated angle grading with the above methods will have comparable diagnostic performance as manual grading, to detect gonioscopic angle closure – Aims I and II
- Novel, dual mode (visible light wide-field photo + infra-red laser mode) device for angle evaluation can provide images of the angle – Aim III

Aims & Specific aims:

I. Development and evaluation of a manual and automated grading system for EyeCam angle digital photography

   a. Development of a manual grading system for EyeCam angle digital photography and comparing it with reference standard gonioscopy for angle closure diagnosis
   b. Comparison of EyeCam with goniophotography for angle closure
   c. Comparison of EyeCam with anterior segment optical coherence tomography (cross-sectional imaging) for angle closure
   d. Development of an automated grading software solution for angle closure using EyeCam images
   e. Comparison of manual vs automated grading software in EyeCam images for angle closure

II. Evaluation of 3-dimensional data from swept source optical coherence tomography for angle closure

   a. Iris trabecular contact (ITC) index – a novel biomarker for angle closure: inter and intra observer reproducibility
   b. Comparison of ITC index and gonioscopic angle closure
   c. Comparison of an automated software solution for evaluation of 3-D data from SSOCT to reference standard gonioscopy

III. Evaluation of a novel device combining angle digital photography and infra red imaging of the angle

   - Proof of concept study with preliminary results from rabbit eyes and primate experiments

2.3 Study population (Cases and Controls)

Aim I: One hundred and fifty two consecutive subjects who are above the age of 40 years were studied (out of 169 recruited) from a single glaucoma clinic at a Singapore hospital.

Aim II: One hundred and forty subjects who are above 40 years were studied (out of 152 recruited) from a single glaucoma clinic at a Singapore hospital.

Aim III: A novel device combining digital photography and infra-red angle imaging will be developed in collaboration with Nanyang Technological University, Singapore and the device will be evaluated in porcine eyes and primates to provide proof of concept regarding angle imaging.

Study Design: Prospective, non-randomized, diagnostic case-control study (Aims 1 and 2)

2.4 Recruitment

The recruitment was performed in a non-randomized, prospective, consecutive manner in a specialty glaucoma clinic at a tertiary care hospital. Subjects attending a general ophthalmology clinic in the same clinical setting, undergoing examination for refractive errors and common ocular ailments such as dry eyes, cataract etc., were included. Subjects with secondary glaucoma were excluded (details in individual chapters). The recruitment was performed according to the tenets of declaration of Helsinki after approval from the institutional review board (IRB), SingHealth. Written informed consents were obtained from patients before inclusion in the studies. The animal experiments had the approval of Institutional Animal Care and Use Committee (IACUC), SingHealth. Personnel handling the animals have been certified.

Recruitment Period: Between 2008 till 2012 (Aims 1 and 2)

2.5 Study procedures and definitions

Aim I: Subjects with prior intraocular surgery or penetrating eye injury, or corneal disorders such as corneal endothelial dystrophy, pterygium or corneal scars that may preclude satisfactory imaging, were excluded from the study. Poor quality images from EyeCam, goniophotography and subjects with poor landmark visibility on ASOCT with blurred angle details were excluded from the study. Patients who had previously undergone LPI were also included. After obtaining a detailed ophthalmic history, each subject underwent a standardized examination that included

1. Visual acuity assessment,
2. Slit-lamp biomicroscopy,
3. Goldmann applanation tonometry,
4. Gonioscopy,
5. Goniophotography and
6. Angle Imaging with EyeCam™

Manual grading method was developed and standardized by the examiner and used against a novel automated method of angle closure detection (developed in collaboration with Institute of Information technology Research, A-STAR). Subjects involved in the testing phase of the software tool have not been used in the validation phase.

Aim II: Patients had similar criteria as above for inclusion and exclusion. All of them underwent SSOCT imaging for 360 degrees of the angle. The 3-D data was assessed using manual and automated detection methods either inbuilt in the machine (ITC index) or

customized (automated software by I2R) in comparison with reference standard gonioscopy. Subjects involved in the testing phase of the software tool have not been used in the validation phase.

Statistical analysis One eye from each patient was randomly selected for analysis if both eyes were eligible for the study. The McNemar test was used to compare differences in the distribution of categorical variables between two related samples. Kappa statistic was used to assess the agreement between categorical variables and for reproducibility analysis. Receiver operating characteristic (ROC) curves, with calculations of area under the curve (AUC) and 95% confidence intervals (CI) were used as an index of each instrument's performance for identifying eyes with angle closure, using gonioscopy as the reference standard. A p value <0.05 was considered statistically significant. Statistical analysis was performed using SPSS version 18.0, and Med Calc version 8.1.0.0 (Mariakerke, Belgium).

Sample size calculation:

The sample size calculation was based on comparison of sensitivities for matched groups in a diagnostic study, as reported by Beam CA et al.[19] With an estimated sensitivity of 82% for the novel methods in comparison to reference standard (with sensitivity of 96% or more), the minimum numbers of subjects required was 78 in this study, with 80% power with an alpha error of 5%.

The clinical definitions of angle closure across the various methods are summarized in Table1, including the angle closure definition for reference standard gonioscopy.

Table 1: Definitions of angle closure for various techniques used in the study

Techniques	Gonioscopy	EyeCam	Goniophotography	ASOCT	SSOCT
Angle closure if	PTM not seen	PTM not seen	PTM not seen	Iris trabecular contact	Iris trabecular contact
Quadrants closed	1 or more	√	√	√	ITC index >35% ITC index ≥50% ITC index >75%
	2 or more *	√	√	√	
	3 or more	√	√	√	
	4	√	√	√	
	Superior	√	√	√	-
	Inferior	√	√	√	-
	Nasal	√	√	√	-
	Temporal	√	√	√	-

*Main definition of angle closure; ASOCT – Anterior Segment Optical Coherence Tomography; SSOCT – Swept source optical coherence tomography; PTM – Posterior trabecular meshwork; ITC index – Iris trabecular index, represents the ratio of iris trabecular contact beyond scleral spur with respect to overall frames marked in SSOCT

Definitions:

Primary angle closure suspect (PACS)[3] was diagnosed in patients with angle closure (defined as eyes in which at least 180° of the posterior pigmented trabecular meshwork was not visible on viewing with a gonioscopy lens in primary position of gaze without indentation) without peripheral anterior synechiae (PAS), IOP < 21mmHg and normal optic disc (See Table 1 for other definitions). PAS was defined as abnormal adhesions of the iris to the angle that were at least half a clock hour in width and were present to the level of the anterior trabecular meshwork or higher.

Primary angle closure (PAC) was diagnosed in eyes with angle closure, normal optic discs and visual fields, and elevated IOP (defined as an IOP > 21 mm Hg), and/or presence of PAS.

Primary angle closure glaucoma (PACG) was diagnosed on the basis of angle closure with glaucomatous optic neuropathy (GON), defined as vertical cup-to-disc ratio [CDR] ≥ 0.7, CDR asymmetry >0.2 and/or focal notching with compatible visual field loss on static automated perimetry (SITA Standard/Fast algorithm with a 24- 2 test pattern; Humphrey Visual Field Analyzer II, Carl Zeiss Meditec, Dublin, California, USA). This was defined as Glaucoma Hemifield Test outside normal limits; a cluster of 3 or more, non-edge, contiguous points on the pattern deviation plot, not crossing the horizontal meridian with a probability of <5% being present in age-matched normals (one of which was <1%); and an abnormal pattern standard deviation (PSD) with p<5% occurring in the normal population, and fulfilling the test reliability criteria (fixation losses <20%, false positives <33% and/or false negatives<33%).

Previous acute primary angle closure (APAC) was diagnosed in patients with the following criteria: presence of any 2 of the following symptoms: ocular or peri-ocular pain, nausea and/or vomiting, an antecedent history of intermittent blurring of vision with haloes, presenting IOP of

>21mmHg; and presence of at least 3 of the following signs: conjunctival injection, corneal epithelial edema, mid-dilated pupil, and shallow anterior chamber.

Meridional imaging: Cross-sectional imaging methods which scan the meridional sections of the angle are termed meridional imaging methods e.g. ASOCT by Visante.

Circumferential imaging: Imaging methods that capture 360° of the angle are termed circumferential imaging methods e.g. EyeCam and Casia SSOCT.

Iris Trabecular Contact index (ITC index)[4] represents the ratio of positive ITC (angle closure) in degrees to the total angle with visible scleral spur (SS) and ITC end points (EP) in degrees; this essentially represents the extent of angle closure as a percentage in SSOCT scans.

Invisible range represents the circumferential extent (in degrees) throughout which either the scleral spur SS or EP could not be determined in the meridional frames of SSOCT scans.

Sensitivity (Sens)[5] of a diagnostic test quantifies its ability to correctly identify subjects with the disease condition. It is the proportion of true positives that are correctly identified by the test. [Sens = True positives/(True positives + False Negatives)]

Specificity (Spec) is the ability of a test to correctly identify subjects without the condition. It is the proportion of true negatives that are correctly identified by the test. [Spec = True Negatives/(False positives + True Negatives)]

Positive Predictive Value or Precision (PPV) is the probability that the disease is present given a positive test result. It is dependent on the disease prevalence (π). (PPV = Sens* π /Sens* π + (1-Spec)*(1- π))

Negative Predictive Value (NPV) is the probability that the disease is absent given a negative test result. (NPV = Spec (1- π)/Spec*(1- π)+(1-sens)* π))

Positive Likelihood ratio (LR+) is the probability of a person who has the disease testing positive divided by the probability of a person who does not have the disease testing positive. (LR+ = Sens/(1-Spec)). LR of greater than 1 indicates that the test result is associated with the disease. The pretest odds (mostly prevalence) of a particular diagnosis, multiplied by likelihood ratio, determine the post-test odds.

Negative Likelihood ratio (LR-) is the probability of a person who has the disease testing negative divided by the probability of a person who does not have the disease testing negative. (LR- = (1-Sens)/Spec). LR less than 1 indicates that the result is associated with absence of the disease.

Receiver Operating Characteristic Curve (ROC curve) is a graphical plot representing the performance of a binary classifier system as the discrimination threshold is varied. It is a plot of true positive rate (sensitivity) against false positive rate (1-specificity).

Area under the ROC curve (AUROC) represents the probability that a classifier will rank a randomly chosen positive instance higher than a randomly chosen negative one (if positive ranks are higher than negative ranks).

Accuracy determines the predictiveness power of a given diagnostic test. It represents the proportion of true test results among the total number of cases examined.
(sensitivity*prevalence)+specificity*(1-prevalence)

2.6 Thesis structure

The thesis experiments were conducted as per the structure given below for the various aims:

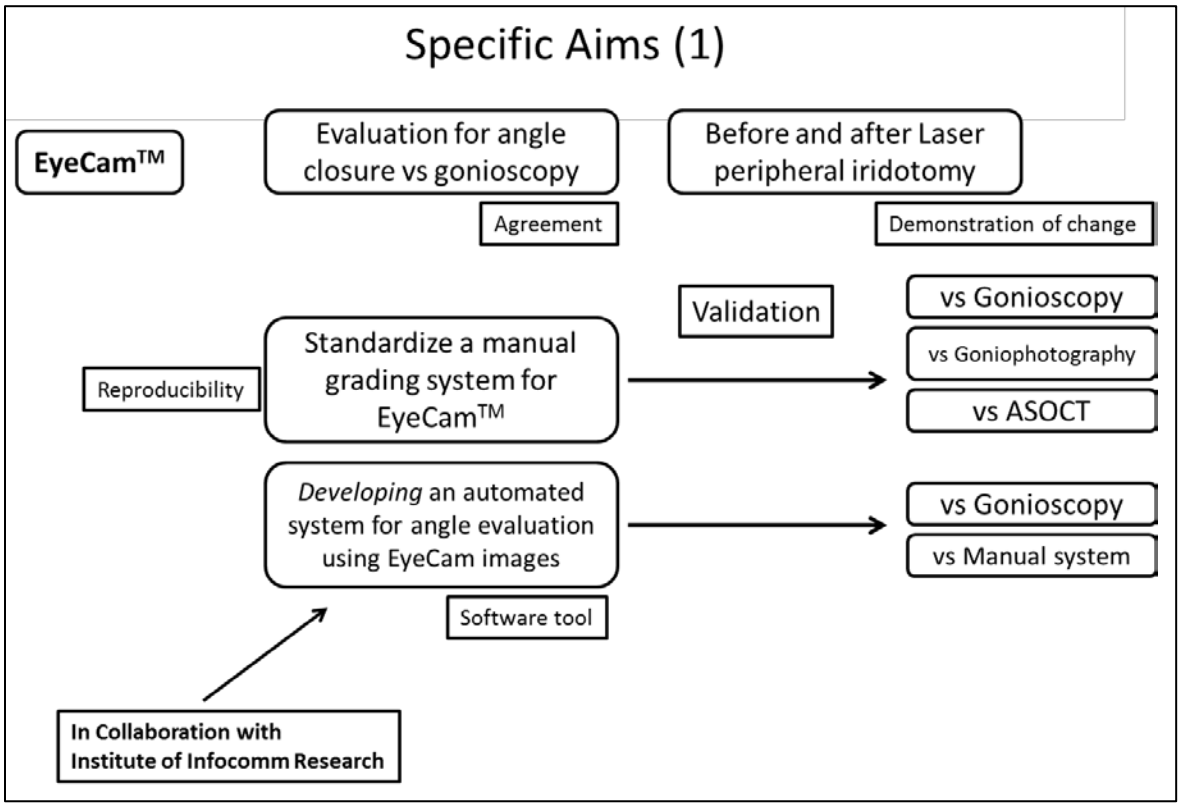

1. **Baskaran M** et al. Angle assessment by EyeCam, goniophotography and gonioscopy. J Glaucoma 2012:21(7):493-7.
2. **Baskaran M** et al. Comparison of EyeCan and ASOCT in detecting angle closure. Acta Ophthalmol. 2012;90(8):e621-5.
3. **Baskaran M** et al. Automated analysis of angle closure from anterior chamber angle images. IOVS. 2014;55(11):7669-73.

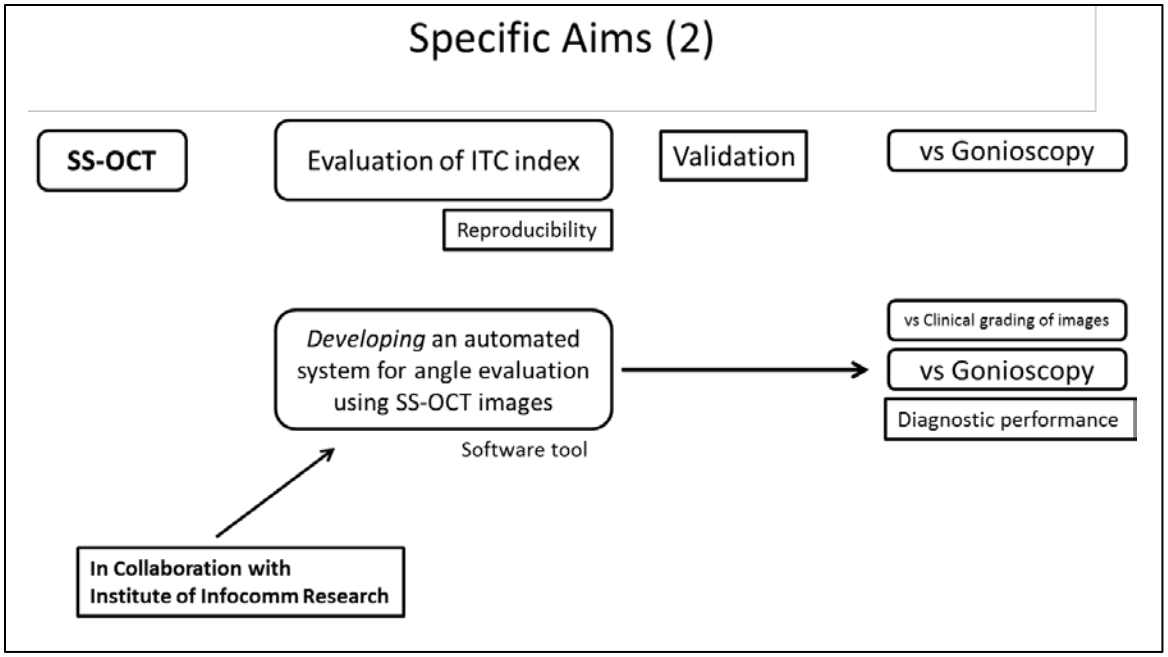

4. **Baskaran M** et al. Assessment of circumferential angle closure by the ITC index with SSOCT. Ophthalmology. 2013;120(11):2226-31.

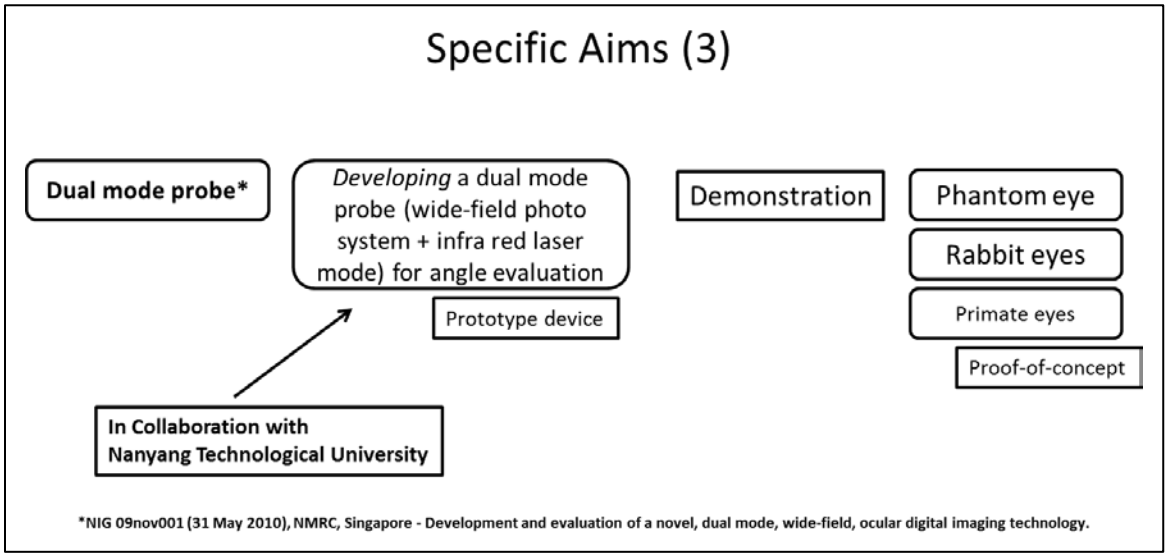

5. Shinoj VK, Murukeshan VM, **Baskaran M** et al. A gel based imaging technique of the iridocorneal angle for evaluation of angle closure glaucoma. Rev Sci Instrum. 2014:85(6):0666105.
6. Shinoj VK, Murukeshan VM, **Baskaran M** et al. Integrated flexible handheld probe for imaging and evaluation of iridocorneal angle. J Biomed Opt. 2015;20(1):16014.

2.7 References: (Chapter 2)

1. Tham YC, Li X, Wong TY, Quigley HA, Aung T, Cheng CY. Global prevalence of glaucoma and projections of glaucoma burden through 2040: a systematic review and meta-analysis. Ophthalmology. 2014 Nov;121(11):2081-90.
2. Beam CA. Strategies for Improving Power in Diagnostic Radiology Research. AJR 1992;159:631-637.
3. Guzman CP, Gong T, Nongpiur ME, Perera SA, How AC, Lee HK, Cheng L, He M, Baskaran M, Aung T. Anterior segment optical coherence tomography parameters in subtypes of primary angle closure. Invest Ophthalmol Vis Sci. 2013 Aug 7;54(8):5281-6.
4. Ho SW, Baskaran M, Zheng C, Tun TA, Perera SA, Narayanaswamy AK, Friedman DS, Aung T. Swept source optical coherence tomography measurement of the iris-trabecular contact (ITC) index: a new parameter for angle closure. Graefes Arch Clin Exp Ophthalmol. 2013 Apr;251(4):1205-11.
5. Altman DG, Bland JM. Diagnostic tests. 1: Sensitivity and specificity. BMJ. 1994 Jun 11;308(6943):1552.

Chapter 3: EyeCam™ - Manual and automated grading system for wide angle digital photography in angle closure detection (Aim 1)

3.1 *Manual grading system for EyeCam Vs. gonioscopy*

Abstract

Purpose: To compare EyeCam™ (Clarity Medical Systems, Pleasanton, CA) imaging with gonioscopy for detecting angle closure.

Methods: In this prospective hospital-based study, subjects underwent gonioscopy by a single observer, and EyeCam imaging by a different operator. EyeCam images were graded by 2 masked observers. The anterior chamber angle in a quadrant was classified as closed if the trabecular meshwork could not be seen; the eye was classified as having angle closure if ≥ 2 quadrants were closed. A subset (n=24) of PACG patients underwent imaging before and after laser peripheral iridotomy (LPI).

Results: 152 subjects were studied. The mean age was 57.4 years (SD 12.9 years) and there were 82 males (54%). The EyeCam was able to obtain clear images of the angles in 98.8% of subjects. The agreement between EyeCam and gonioscopy for detecting angle closure in the superior, inferior, nasal and temporal quadrants based on AC1 statistics was 0.73, 0.75, 0.76 and 0.72 respectively. With gonioscopy, 21/152 (13.8%) eyes were diagnosed as angle closure compared to 41/152 (27.0%) with EyeCam ($p<0.001$, McNemar Test), giving an overall sensitivity of 76.2% (95%CI: 54.9%-90.7%); specificity of 80.9% (95%CI: 73.5%-87.3%) and an area under curve receiver operating characteristic (AUC) of 0.79. The mean (± SD) number of clock-hours of angle closure decreased significantly from 8.15 ± 3.47 before LPI to 1.75 ± 2.27 after LPI ($p<0.0001$, Wilcoxon signed-ranked test).

Conclusions: EyeCam showed good agreement with gonioscopy for detecting quadrant wise angle closure. However, there was a higher rate of angle closure diagnosed by EyeCam compared to gonioscopy. EyeCam™ can demonstrate angle widening after LPI in serial documentation.

Introduction

Gonioscopy is the current reference standard for assessing the anterior chamber angle (ACA). Various grading schemes have been developed to categorize eyes on the basis of gonioscopic assessment of the ACA,[1-3] but such schemes are based upon subjective and at best semi-quantitative assessments. Gonioscopy utilises certain unique aspects such as use of corneal wedge to identify trabecular meshwork and indentation technique for peripheral anterior synechiae (PAS), which are not available in other tools. However, factors such as the type of lens used, the technique employed, and the skill of the observer affect the variability of gonioscopy findings.[4] Documentation of gonioscopic findings is often poor with most clinicians recording gonioscopic findings in charts without images or photographic records.

The EyeCam™ (Clarity Medical Systems, Pleasanton, CA) is an imaging modality that was originally designed to obtain wide-field photographs of the fundus. It has recently been used in glaucoma management to image the optic disc[5] and the anterior chamber angle.[6] With the use of 120° and 130° wide field lenses, high-resolution anterior segment images of the iris and ACA can be obtained (**Figure 1**). The hardware consists of a handheld digital video camera connected fibreoptically to a light-emitting control unit and computer assembly. The operator controls focus, illumination, and the acquisition of images with a foot switch. Images are automatically saved to a computer hard drive. Alternatively, a short video stream can be captured, with still frames

selected from the video and saved at the end of the imaging session. The EyeCam™ is an objective way of documenting angle configuration, using a photographic method. The images produced are easy for clinicians to interpret as the angle appears similar to what is seen during gonioscopy. Further, the documentation on digital media enables serial documentation and review of images as well. Subjects who undergo surgical interventions such as laser procedures need serial documentation to monitor changes to the angle configuration. Lack of prior evaluation prevents wide spread use of this technique in angle assessment.

The aim of this study was to evaluate the use of EyeCam for angle imaging and to assess its diagnostic performance in detecting angle closure using gonioscopy as the reference standard. Further, it explored serial documentation of angle configuration using EyeCam after laser peripheral iridotomy (LPI) in PACG patients.

Methods

Consecutive subjects were recruited from a glaucoma clinic at a Singapore hospital from July to October 2008. We recruited a subset of 24 consecutive PACG patients from glaucoma clinics of the Singapore National Eye Centre who were undergoing LPI. Written informed consent was obtained from all participants, and the study had the approval of the hospital's Institutional Review Board and adhered to the tenets of the Declaration of Helsinki.

After an interview about previous medical and ophthalmic history, each subject underwent the following examinations on the same day: visual acuity, gonioscopy and imaging with the EyeCam. Subjects were excluded if they were taking any topical medications which had an effect on the pupil size, secondary glaucoma, had a history of previous cataract surgery or any corneal opacity or abnormalities that precluded EyeCam imaging such as severe pterygium or corneal pathology. Previous LPI was not an exclusion criterion in this study.

Sequential argon-Yttrium Aluminium Garnet (YAG) LPI was performed in the subset of cases with standardized settings (argon laser 0.7–1.0 Watts, spot size 50 microns, duration 0.1 seconds, 10–30 shots followed by Nd-YAG laser 2–5 mJ, 3–5 shots).

Gonioscopy

Gonioscopy was performed in the dark in all cases by a single examiner with glaucoma fellowship training (SAP), who was masked to EyeCam findings. A 1-mm light beam was reduced to a narrow slit and the vertical beam was offset horizontally for assessing superior and inferior angles and offset vertically for nasal and temporal angles. Static gonioscopy was performed using a Goldmann 2-mirror lens at high magnification (x16), with the eye in the primary position of gaze. Care was taken to avoid light falling on the pupil and to avoid accidental indentation during examination. Gonioscopic lens was tilted only minimally just to permit view of the angle over the convexity of the iris, so as to avoid distortion of angle status. The angle in each quadrant was graded using the Scheie grading system/modified Schaffer system, according to the anatomical structures observed during non-indentation gonioscopy.[1] According to this, Grade 0 was absence of any angle structures, Grade 1 was presence of Schwalbe's line (SL), Grade 2 was presence of non-pigmented anterior trabecular meshwork 9ATM), Grade 3 was presence of pigmented posterior trabecular meshwork (PTM) or Scleral spur (SS) and Grade 4 was presence of Ciliary body band. The ACA was considered 'closed' in that quadrant if the posterior pigmented trabecular meshwork (TM) could not be seen in the primary position without indentation. The eye was classified as having angle closure if there were 2 or more quadrants of closure. If there was any doubt as to the state of the angle or any suspicion of peripheral anterior synechiae (PAS), this was confirmed on indentation gonioscopy with a Sussman lens. PAS were defined as abnormal adhesions of the iris to the angle that were

present to the level of the anterior trabecular meshwork or higher, and were deemed to be present if apposition between the peripheral iris and angle structures could not be broken despite indentation gonioscopy.

EyeCam™ imaging

EyeCam imaging was performed on subjects who lay supine on a couch in a darkened room. Images were captured by a single trained technician in all 4 quadrants of a randomised eye of all subjects, unless any exclusion criteria were present. The technician was trained to understand the basic angle structures as well as the technical details of EyeCam imaging. After applying topical anaesthetic eye drops (Proparacaine hydrochloride 0.5% ophthalmic solution, Alcon laboratories Inc., FortWorth, TX), coupling gel was applied to the anesthetised eye, before imaging proceeded with a 130° lens held next to the limbus. The probe was positioned at the opposite limbus to the angle being photographed and light from the fiber optic probe was directed toward the angle of interest and then tilted downward, to bring the angle structures into view while minimizing pupillary constriction. Care was taken to point the illumination light at the angle rather than the pupil. The probe was moved anteriorly within 10 degrees from limbus if the angle was not visible due to convexity of iris. The illumination was adjusted using the foot pedal to avoid overexposure. Clear still images were captured to the hard disk of the attached computer for subsequent grading. Imaging of all four quadrants of the eye was performed in less than 5 minutes. EyeCam imaging was performed before and approximately 2 weeks after LPI, where applicable.

Manual Grading of images

EyeCam images were graded in each quadrant by two fellowship trained glaucoma

specialists working together, who were masked to the gonioscopic data. Images were first graded for their quality as follows: grade 1 if the angle details were clear and well-focused in all quadrants; grade 2 if angle images were blurred in any quadrant but some details discerned; grade 3 if the angle structures were blurred in at least 1 quadrant such that no details can be discerned, and grade 4 if the structures were blurred in all 4 quadrants and no angle details were discerned. Images were excluded if they were assessed to be grade 3 or 4.

The angle-grading scheme for each quadrant was similar to that used for gonioscopy and was based on anatomical structures observed in the ACA **(Figure 2)**. Grade 0 represented completely closed angle, visibility of SL was noted as Grade 1, Non-pigmented area beyond SL in the absence of any pigmentation was noted as ATM and Grade 2, presence of pigmented PTM and Scleral spur (SS) was noted to be Grade 3 and the presence of CB was noted as Grade 4. The final grading of a quadrant was determined by the most prevalent grade seen in that quadrant. For EyeCam images, angle closure in any quadrant was defined as the inability to visualize the TM in that quadrant **(Figure 2 – Grade 2 and below)** and the eye was considered to have angle closure if the TM was not visible in at least two quadrants. Assessment of peripheral anterior synechiae (PAS) was very subjective with EyeCam images due to the inability to perform indentation; and so we have not graded PAS using EyeCam.

To examine for intra-observer reproducibility, the images from 40/152 (26.31%) randomly selected eyes were graded again at a different session by one of the examiners, masked to previous grading, for angle structures seen in each quadrant and for angle closure in the eye. For inter observer agreement, the images were also graded by a separate glaucoma fellowship trained examiner who was masked to previous grading results. EyeCam angle imaging was done in the same eye twice by the same technician after 30 minutes in 20 subjects separately. These

Figure 1: EyeCam™ imaging being performed on a supine subject.

Fig 2: Standard manual grading system used in EyeCam™ images showing Grade 0, Grade 1 (Schwalbe's line seen), Grade 2 (PTM not visible/ATM seen), Grade 3 (PTM/SS visible) and Grade 4 (CB seen) angle images similar to gonioscopic grading system used.

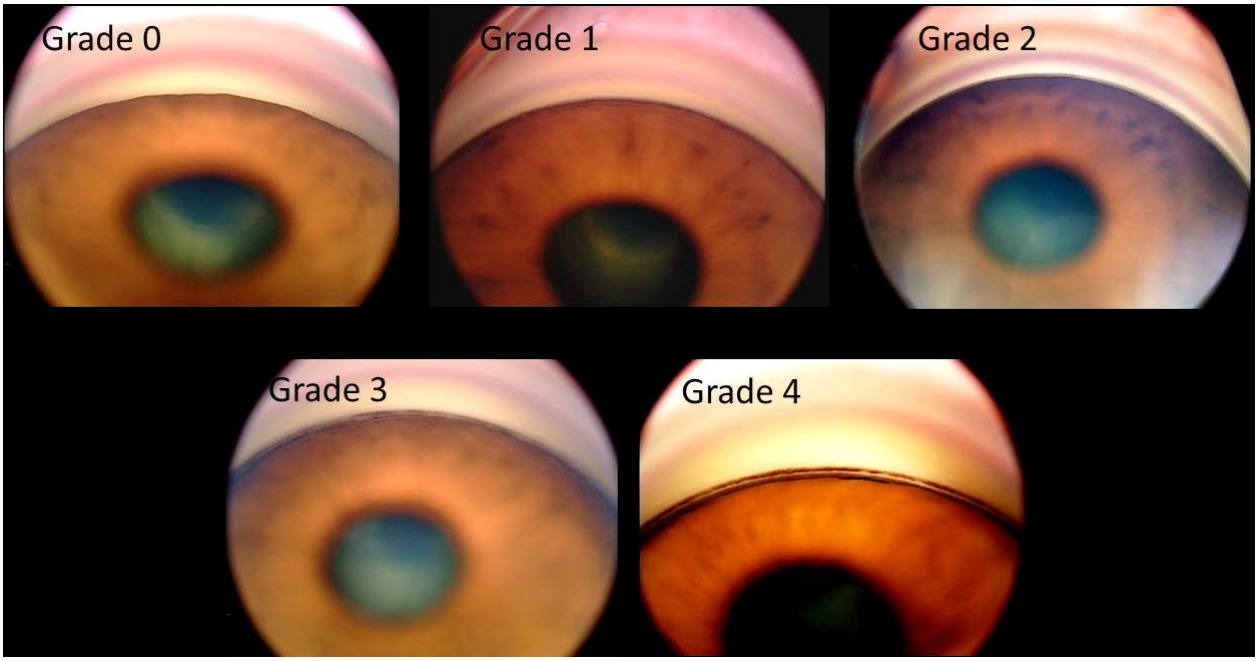

images were graded twice for intra-observer reproducibility in image acquisition.

Statistical Analysis

Only eyes, which had complete data for all 4 quadrants by both modalities, were included for statistical analysis. Parametric and non-parametric tests were used to compare continuous variables, according to data distribution. The Chi-square test was used to compare categorical data. The McNemar test was used to compare differences in distribution of a categorical variable between two related samples. Kappa statistic was used to assess the agreement between categorical variables. However, as the kappa statistic may be affected by trait prevalence (distribution) and base rates,[7,8] AC1 statistics were used to assess the agreement between graders in situations where the prevalence of positive classifications may lead to inconsistent results. A p value <0.05 was considered statistically significant. The extent of angle closure before and after LPI was compared using Wilcoxon signed rank nonparameteric test for paired samples. Extent of angle widening between quadrants was compared using Kruskal-Wallis test. Post LPI angle status for number of quadrants open with gonioscopy and EyeCam was compared using Mann Whitney test. Statistical analysis was performed using JMP 5 (SAS Institute, Inc., Cary, NC, USA), and MedCalc version 8.1.0.0 (Mariakerke, Belgium) software.

Results 1 – EyeCam grading agreement with gonioscopy

Of the 169 subjects recruited, 15 were excluded for incomplete or missing data. Two subjects (1.2%) were excluded due to poor quality (grade 3 or 4) of EyeCam images. A total of 152 eyes of 152 subjects were finally analyzed which included 15.1% (23/152) fair quality (grade 2) gradable images. The mean age was 57.4 years (SD 12.9 years) and there were 82 males (54%). The majority of subjects were Chinese (80.3%), the remainder comprised of Malay

(4.6%), Indian (7.9%) and other races (7.2%). Of the 21 eyes that had angle closure disease, 6 had primary angle closure suspect (PACS), 4 had primary angle cosure (PAC) and 11 had primary angle closure glaucoma (PACG). Among this, 15 eyes had previous laser iridotomy performed.

The agreement between EyeCam and gonioscopy in detecting a closed angle in the superior, inferior, nasal and temporal quadrants based on AC1 statistics was 0.73, 0.75, 0.76 and 0.72 respectively **(Table 1)**.

With gonioscopy, 21/152 (13.8%) eyes were diagnosed as angle closure compared to 41/152 (27.0%) with EyeCam ($p<0.001$, McNemar Test), giving an overall sensitivity of 76.2% (95%CI: 54.9%-90.7%); specificity of 80.9% (95%CI: 73.5%-87.3%) and an area under curve receiver operating characteristic (AUC) of 0.79. The agreement between the two modalities, using AC1 stats, varied depending on the definition of angle closure used (summarized in Table 1).

<u>Reproducibility analysis:</u> 1. Intra and inter-observer reproducibility:

The intra-observer reproducibility for detecting angle closure in two quadrants or more using EyeCam images was 0.57 (AC1) and 0.43 (Kappa; 95% CI 0.13–0.74); and that of inter-observer agreement was 0.64 (AC1) and 0.49 (Kappa; 95% CI 0.20–0.79) **(Table 2)** respectively.

2. Repeatability of tests – intra-observer reproducibility:

Further, EyeCam images acquired twice in 20 eyes of 20 subjects showed good intra-observer reproducibility for angle closure detection [0.84 (AC1) and 0.73 (Kappa; 95% CI 0.38 – 1.08)].

Table 1: Analysis of the eyes with closed quadrants detected by EyeCam and Gonioscopy (n=152)

	Quadrant	Gonioscopy N (%, 95% CI)	EyeCam N (%, 95% CI)	P value*	AC1†
Number of eyes with the following number of closed quadrants	1	15 (9.9%,5.9-15.4)	7 (4.6%, 2-8.89)	0.1	0.86
	2	8 (5.3%, 2.5-10.2)	11 (7.2%, 4-12.6)	0.63	0.73
	3	7 (4.6%, 2.1-9.4)	10 (6.6%, 3.5-11.8)	0.61	0.89
	4	6 (4%, 1.6-8.5)	20 (13.2%, 8.6-19.5)	<0.01	0.86
Number of eyes with closed quadrants by location	Superior	23 (15.1%, 10-21.5)	34 (22.5%, 16.4-29.7)	0.04	0.73
	Inferior	23 (15.1%, 10-21.5)	35 (23%, 16.9-30.2)	0.03	0.75
	Nasal	21 (13.8%, 8.9-20)	36 (23.8%, 17.6-31.1)	0.004	0.76
	Temporal	10 (6.6%, 3.4-11.4)	34 (22.4%, 16.3-29.5)	<0.001	0.72
Number of eyes with angle closure using different definitions	≥ 2 quadrants	21 (13.8%, 8.9-20)	41 (27%, 20.4-34.5)	<0.001	0.71
	≥ 3 quadrants	13 (8.6%, 5-14.2)	30 (19.7%, 14.2-26.8)	<0.001	0.78

* McNemar test

†Inter-instrument agreement based on AC1 statistics;

CI: confidence interval

Related publication: 1. Perera SA, **Baskaran M**, Friedman DS, Tun TA, Htoon HM, Kumar RS, Aung T. Use of EyeCam for imaging the anterior chamber angle. Invest Ophthalmol Vis Sci. 2010 Jun;51(6):2993-7.

2. Perera SA, Quek DT, **Baskaran M**, Tun TA, Kumar RS, Friedman DS, Aung T. Demonstration of angle widening using EyeCam after laser peripheral iridotomy in eyes with angle closure. Am J Ophthalmol. 2010 Jun;149(6):903-7.

Table 2: The inter and intraobserver agreement in detecting closed quadrants and detecting overall angle closure status using EyeCam and gonioscopy

	Interobserver agreement (n=40)		Intraobserver agreement (n=20)	
Quadrants	Kappa (95% CI)	AC1	Kappa (95% CI)	AC1
Superior	0.63 (0.38,0.88)	0.67	0.52 (0.23,0.82)	0.67
Inferior	0.59 (0.31,0.87)	0.70	0.65 (0.4,0.91)	0.74
Nasal	0.39 (0.06, 0.72)	0.58	0.57 (0.27,0.86)	0.71
Temporal	0.40 (0.06,0.75)	0.65	0.48 (0.16,0.80)	0.68
Angle closure[†]	0.49 (0.20,0.79)	0.64	0.43 (0.13,0.74)	0.57

[†]Defined as closure in two quadrants or more; CI: confidence interval

Table 3: Angle status before and after laser peripheral iridotomy as assessed by both gonioscopy and EyeCam (n=24)

	Closed before LPI			Closed after LPI			Widened from Closed to Open after LPI		
	Gonioscopy	**EyeCam**	**P Value***	**Gonioscopy**	**EyeCam**	**P Value***	**Goniosopcy**	**EyeCam**	**P Value***
Median (Range)	4 (2to 4)	3 (0 to 4)	0.0035	4 (0 to 4)	1 (0 to 4)	0.0002	0 (0 to 4)	2 (0 to 4)	0.005
Quadrants	**Number of eyes (n=24)**								
0	0	1	-	4	10	-	13	2	-
1	0	0	-	1	8	-	5	8	-
2	1	6	-	1	2	-	2	4	-
3	0	6	-	5	3	-	1	7	-
4	23	11	-	13	1	-	3	3	-

LPI – Laser peripheral iridotomy; *Mann-Whitney U test

Results 2 – Demonstration of angle widening after LPI

Twenty-four subjects (24 eyes) with PACG were recruited. There were 23 Chinese and 1 Indian subjects, with a mean age of 61.8 $\pm$ 7.9 years, and 62.5% were women.

The mean (± SD) number of clock-hours of angle closure decreased significantly from 8.15 ± 3.47 before LPI to 1.75 ± 2.27 after LPI ($p<0.0001$, Wilcoxon signed-ranked test). There was no significant difference in the change in clock-hours of angle closure between the superior, inferior, nasal and temporal quadrants after LPI ($p>0.5$; Kruskal-Wallis test).

While the pre LPI apposition in clock hours between quadrants was found to be similar ($p=0.5$; Kruskal Wallis test), post LPI apposition between the inferior compared to the rest of the quadrants showed a significant difference ($p=0.0006$; Kruskal Wallis test). This suggested maximum apposition in the inferior quadrant both before and after LPI.

Comparison of angle status after LPI by Gonioscopy vs EyeCam

Table 3 shows the number of eyes and quadrants which were open using EyeCam and gonioscopy. The angle status of 22 eyes was more open in at least one quadrant after LPI, and remained unchanged (and closed) in two eyes with gonioscopy; whereas with EyeCam, all angles opened up at least one quadrant.

Overall, gonioscopy showed 1.0 ± 1.41 (95% CI, 0.43 – 1.57) quadrants opening from closed to open after LPI compared to 2.0 ± 1.28 (95% CI, 1.49 – 2.51, $p = 0.009$) quadrants with EyeCam. Gonioscopy consistently revealed more closed quadrants than EyeCam, before and after LPI (Table 3).

Discussion

In this study, we found good agreement between EyeCam angle imaging and clinical gonioscopy for detecting quadrants with closed angles. However, for detecting eyes with angle closure, there was a higher rate of angle closure diagnosed by EyeCam compared to gonioscopy, with a sensitivity and specificity of 76.2% and 80.9% respectively (AUC 0.79), using the 2 quadrant definition of angle closure. The EyeCam was able to obtain clear images of the angles in 98.8% of studied individuals, with imaging performed by a technician.

We also found that changes in angle width after LPI could be documented with the EyeCam in eyes with angle closure. All eyes had at least 1 quadrant of angle widening, and there was a significant reduction in the mean number of clock-hours of angle closure from 8.15 ± 3.47 before LPI to 1.75 ± 2.27 after LPI.

This difference in findings between the EyeCam and gonioscopy could be due to numerous factors including patient positioning (the patient is supine for the EyeCam and seated for gonioscopy), different illumination (although light is needed for both assessments), and the optics used in the EyeCam to image the angle. Of note, the light used for EyeCam is quite bright although no flash is used. The probe is placed 180 degrees across from the angle being imaged and requires a direct line of sight to see angle structures. However, a convex iris profile can block the camera from angle structures. Interestingly, EyeCam imaging revealed a very uniform distribution of closed quadrants across all 4 quadrant locations of the eye, in contrast to gonioscopy which showed a trend towards more closure in the inferior and superior quadrants, supporting previous gonioscopic and anterior segment optical coherence tomography (AS-OCT) data.[9,10]

The EyeCam offers advantages over other angle imaging methods. It provides a direct, colour view of the angle with excellent optical quality, similar to what is seen when performing gonioscopy. The number of poor quality images is small (about 1% in our study) and a technician can perform EyeCam easily after a short period of training. In contrast, in a previously published large community based study of AS-OCT for the detection of angle closure, 16% (a significant proportion) of eyes could not be assessed for angle closure, mainly due to poor quality images or poor visibility of the scleral spur.[11] Goniophotography using a slit-lamp mounted camera is another method of angle imaging that is similar to EyeCam. However, slit lamp goniophotography is technically challenging and it is not easy to obtain good quality images with this method.

The EyeCam cannot be used to identify PAS during image capture. It is likely that this is a limitation of the device since indentation cannot be performed with the EyeCam and therefore iris processes can appear like PAS. Indentation gonioscopy is the reference standard approach to distinguish between appositional and synechial angle closure.[12] Furthermore, being unable to dynamically indent the eye made it difficult at times to distinguish TM pigment from pigment on Schwalbe's line. The interpretation of EyeCam images in eyes with lightly pigmented TM may be difficult while gonioscopy has the advantage of using the optical corneal wedge technique to identify the anterior edge of TM. These reasons may have contributed to the moderate intra- and inter-observer agreement found in the interpretation of EyeCam images. This level of agreement is lower than that seen when interpreting AS-OCT images.[13]

Current documentation of the angle in patient records is often subject to a variety of different classification systems and can be difficult to interpret. The EyeCam may potentially be used to document a 360° view of the angle, which could then be interpreted by any observer. The

EyeCam also delivers images which show more than simply the angle width, it can show pigment, and new vessels (although not evaluated in this study) which cannot be imaged by the cross sectional imaging modalities.

Our study has some limitations. The use of a single observer for gonioscopy could have led to a systematic bias. EyeCam was performed on supine patients while gonioscopy was performed on patients sitting at the slit lamp. As mentioned above, the lighting conditions for EyeCam and gonioscopy were different. While EyeCam uses coherent source of light, gonioscopy uses slit lamp light source. The images seen with the EyeCam gave a good 90º view or more of the angle, but there is some degradation of the images at the periphery that are related to optical aberrations and depth of field. Further, the moderate to poor reproducibility of EyeCam image grading seen in this study is a concern. The proportion of subjects with angle closure was lesser (13.8%), and this may affect the generalizability of the results as explained by the wider confidence intervals seen in reproducibility analyses for angle closure detection. The strengths of the study stem from the fact that standard definitions and grading system were used for angle closure and a large number of eyes have been imaged. Also, the assessment of EyeCam images was performed masked to the gonioscopic data.

In summary, this initial study showed a good degree of agreement between EyeCam angle imaging and clinical gonioscopy, with moderate sensitivity and specificity for detecting angle closure. The EyeCam has potential for use in anterior segment imaging, particularly in the clinical setting for documentation of angle findings, serial documentation after intervention such as LPI and as patient education tool to demonstrate angle widening after LPI.

3.2 EyeCam, Goniophotography Vs. Gonioscopy

Abstract

Purpose: To compare EyeCam™ (Clarity Medical Systems, Pleasanton, CA) and goniophotography in detecting angle closure, using gonioscopy as the reference standard.

Methods: In this hospital-based, prospective, cross sectional study, subjects underwent gonioscopy by a single observer, and EyeCam imaging and goniophotography by different operators. The anterior chamber angle in a quadrant was classified as closed if the posterior trabecular meshwork could not be seen. A masked observer categorised the eyes as per the number of closed quadrants, and an eye was classified as having angle closure if there were 2 or more quadrants of closure. Agreement between the methods was analyzed by kappa statistic and comparison of area under receiver operating characteristic curves (AUC).

Results: Eighty-five subjects (85 eyes) were included, the majority of whom were Chinese. Angle closure was detected in 38 eyes (45%) with gonioscopy, 40 eyes (47%) using EyeCam and 40 eyes (47%) with goniophotography (p=0.69 in both comparisons, McNemar Test). The agreement for angle closure diagnosis (by eye) between gonioscopy and the 2 imaging modalities was high (k=0.86; 95% Confidence Interval (CI), 0.75–0.97) while the agreement between EyeCam and goniophotography was not as good (k=0.72; 95%CI, 0.57–0.87); largely due to lack of agreement in the nasal and temporal quadrants (k=0.55– 0.67). The AUC for detecting eyes with gonioscopic angle closure was similar for goniophotography and EyeCam (AUC 0.93, sensitivity=94.7%, specificity=91.5%; p>0.95).

Conclusions: Eyecam and goniophotography have similarly high sensitivity and specificity for the detection of gonioscopic angle closure.

Introduction

Goniophotography is a clinical method of documenting gonioscopic findings using a slit-lamp mounted camera and indirect gonioscopic lens. This technique requires some expertise to discern the angle structures with the gonioscopy lens and for obtaining clear images of the angle. Further, no prior evaluation was performed on the diagnostic performance for angle assessment using this technique.

The aim of this study was to compare EyeCam images to those obtained with goniophotography for angle assessment and to assess their diagnostic performance in detecting angle closure, as identified with gonioscopy.

Methods (specific to this study)

Goniophotography was performed using the slitlamp with the MagnaView Goniolens (Ocular Instruments Inc, Bellevue, WA) by an ophthalmologist, masked to other findings. This is a single mirror goniolens with high magnification (x1.3). We used a thin film of goniogel when using this lens in order to capture images with better clarity. A slit beam of 1 mm width and lowest possible height was utilised to capture the angle structures in primary gaze. Images of all 4 quadrants of the study eye were documented, taking precautions to avoid pupil constriction during photography. In all images, the slit beam was rotated so as to be radial in each quadrant view. Care was taken to avoid distortion artifacts from cornea, which can decrease the quality of images.

The resulting EyeCam and goniophotograph images were randomly ordered and graded on separate occasions, by a glaucoma fellowship trained examiner (Author) who was masked to gonioscopic data. The methodology for grading the quality of EyeCam images and the method of grading the images has been described earlier in section 3.1.

Statistical Analysis (specific to this study)

One eye from each patient was randomly selected for analysis if both eyes were eligible for the study. Receiver operating characteristic (ROC) curves, with calculations of area under the curve (AUC) and 95% confidence intervals (CI) were used as an index of each instrument's performance for identifying eyes with angle closure, using gonioscopy as the reference standard. Statistical analysis was performed using STATA version 10 (Statacorp, College Station, TX), and Med Calc version 8.1.0.0 (Mariakerke, Belgium).

Results

Of the 90 subjects recruited, 5 were excluded due to incomplete, poor quality or missing goniophotography/EyeCam images in some quadrants. The mean age of the remaining 85 study subjects was 61.6 years (SD 12.1 years) and there were 44 females (52.9%). The majority of subjects were Chinese (74.1%), the rest comprised of Malay (8.2%) and Indian (17.6%) ethnic groups. All images were of gradable quality.

Of the 85 eyes analyzed, 38 eyes (44.7%) had angle closure (in 2 quadrants or more) by gonioscopy; while EyeCam and goniophotography each identified 40 eyes (47.1%) as having angle closure (p=0.69 in both comparisons, McNemar test). The agreement for angle closure diagnosis (by eye) between gonioscopy and the 2 imaging modalities was high (k = 0.86; 95% Confidence Interval (CI), 0.75 – 0.97) while the agreement between EyeCam and goniophotography was not as good (k = 0.72; 95% CI, 0.57 – 0.87). Figure 3a and 3b show an open angle seen in the inferior quadrant for the same subject using EyeCam and goniophotography. **Figures 3a and 3b** show the comparison of the above classification of angle closure between the three modalities. When defining angle closure as one, two or three

Figure 3: EyeCam (3a) and goniophotograph (3b) images showing open angle in the inferior quadrant of the same subject. (Arrow indicates angle area)

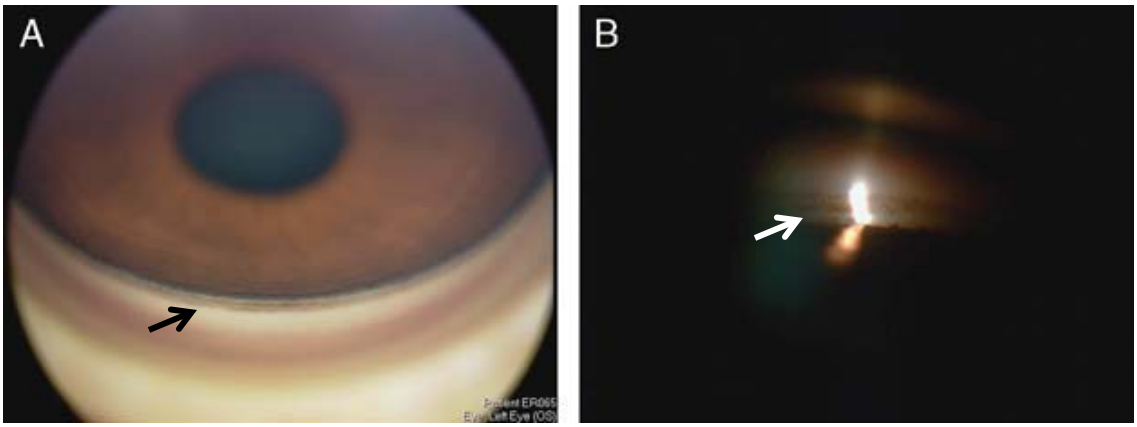

Figure 4: Venn diagram showing distribution of closed angles (2 quadrants or more) between gonioscopy (n=38); goniophotography (n=40) and EyeCam (n=40).

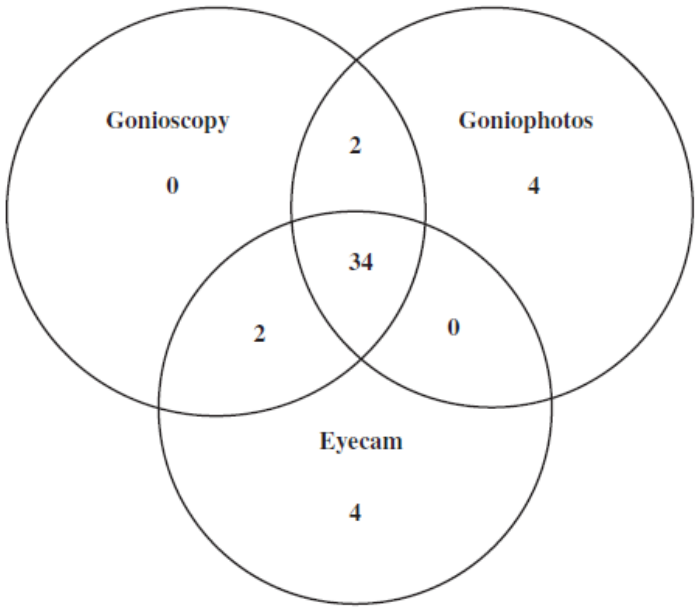

Related publication: Baskaran M, Perera SA, Nongpiur ME, et al. Angle assessment by EyeCam, goniophotography, and gonioscopy. J Glaucoma. 2012;21(7):493-7.

quadrants or more closed on gonioscopy, EyeCam and gonioscopy had good to excellent agreement (Table 4). Agreement was best when defining angle closure as two or more quadrants closed on gonioscopy. In a quadrant wise analysis of angle closure, goniophotography and Eye Cam imaging had poorer agreement in the nasal and temporal quadrants (k = 0.55 vs 0.67) as compared to the superior and inferior quadrants (k = 0.69 vs 0.76, Table 4). **Figure 4** shows a Venn diagram depicting the distribution of eyes with 2 quadrant closure between the three modalities.

The AUC was over 90% for each imaging modality when defining angle closure as having 2 or more quadrants closed on gonioscopy (Table 5). The AUC was lower when defining angle closure using more or fewer quadrants closed on gonioscopy.

The inter-observer agreement for EyeCam (using two or more quadrants closed to define angle closure) was 0.8 (95% CI kappa = 0.57 to 1) and for goniophotography was 0.67 (95% CI kappa = 0.40 to 0.93). The intra-observer agreement for the EyeCam was 0.73 (95% CI kappa = 0.38 to 1.1) and for goniophotography was 0.87 (95% CI kappa = 0.69 to 1).

Discussion

To the best of our knowledge, this is the first study comparing EyeCam and goniophotography with gonioscopy in a clinical setting. We found good diagnostic performance for both these modalities for detecting angle closure compared to gonioscopy, especially using the 2-quadrant definition of angle closure. Subjective grading of goniophotographs and EyeCam images was reproducible both within and between observers, and identified angle closure as defined by gonioscopy with high accuracy. Reproducibility of EyeCam images was found to be better compared to previous study. Our current EyeCam

Table 4: Summary statistics of agreement of EyeCam and goniophotography compared to gonioscopy for different definitions of angle closure (n=85)

	Agreement between methods - Kappa statistic (95% CI)		
Definition of closure	**EyeCam vs. Gonioscopy**	**Goniophotography vs. Gonioscopy**	**EyeCam vs Goniophotography**
1 or more quadrants closed	0.84 (0.62, 1.05)	0.77 (0.56, 0.98)	0.74 (0.60, 0.88)
2 or more quadrants closed	0.86 (0.65, 1.07)	0.86 (0.65, 1.07)	0.72 (0.57, 0.87)
3 or more quadrants closed	0.78 (0.57, 0.99)	0.70 (0.49, 0.91)	0.73 (0.59, 0.88)
Superior quadrant closed	0.83 (0.72, 0.95)	0.76 (0.63, 0.90)	0.69 (0.54, 0.85)
Inferior quadrant closed	0.93 (0.85, 1.01)	0.83 (0.71, 0.95)	0.76 (0.62, 0.90)
Nasal quadrant closed	0.64 (0.47, 0.81)	0.59 (0.41, 0.77)	0.55 (0.37, 0.74)
Temporal quadrant closed	0.68 (0.51, 0.84)	0.59 (0.41, 0.76)	0.67 (0.51, 0.83)

CI – Confidence Interval

Table 5: Receiver Operating Characteristic curve (ROC) analysis to compare EyeCam and Goniophotography with Gonioscopy for various definitions of angle closure (n=85)

	EyeCam vs. Gonioscopy			Goniophotography vs. Gonioscopy			
Definition of closure	**AUC (95% CI)**	**Sens.**	**Spec.**	**AUC (95% CI)**	**Sens.**	**Spec.**	***P*-value***
1 or more quadrants closed	0.92 (0.84, 0.97)	0.95	0.89	0.89 (0.79, 0.94)	0.95	0.82	0.38
2 or more quadrants closed	0.93 (0.85, 0.97)	0.95	0.92	0.93 (0.85, 0.97)	0.95	0.92	>0.95
3 or more quadrants closed	0.89 (0.79, 0.94)	0.94	0.87	0.85 (0.7, 0.92)	0.81	0.89	0.22

AUC=area under ROC curve; Sens – Sensitivity; Spec – Specificity; CI=confidence interval

**p*-value to test equality of the two ROC curves

technique is to lower the illumination once the EyeCam is focused on the pigmented TM. If the quadrant is closed and the posterior TM cannot be visualized, the technician should then focus on the peripheral iris or Schwalbe's line and once again decrease illumination prior to obtaining the image. A highly convex iris profile can block the camera from angle structures and this may be mistaken for angle closure. Gonioscopy could cause some indentation of the angle resulting in a wider angle appearance compared to the Eyecam, which is non-contact.

Only 5 eligible subjects (6%) were excluded due to incomplete or poor quality goniophotograph/EyeCam images. Almost all goniophotographs and EyeCam images were of good quality and could be evaluated in the study. In contrast, as many as 30% of anterior segment optical coherence tomography (AS-OCT) angle images could not be graded in previous studies, mainly due to poor visibility of the scleral spur.[13,14] The EyeCam and goniophotography may have an advantage over present AS-OCT technologies in that a wide field view and documentation of the angle is possible and these images can be easily interpreted by most ophthalmologists.

While goniophotography and EyeCam imaging performed equally well in the current study, they differ in important ways. Goniophotography is performed with the patient seated (as in gonioscopy), while EyeCam imaging is performed with the patient in the supine position. In theory, body positioning could lead to variation in angle findings and a supine position may be inconvenient for some subjects. Goniophotography samples a smaller segment of the angle quadrant. In order to minimize the impact of illumination on angle findings, the photographer must use a narrow slit of light, analogous to the cross-sectional scans attained by the ASOCT,[13] rather than the full quadrant view afforded by EyeCam. Goniophotography is also more cumbersome to obtain. Although we did not measure the time needed to obtain

goniophotographs, we found that the procedure was relatively time-consuming and more operator-dependent than image acquisition with the EyeCam. Goniophotography requires a technician familiar with gonioscopy (in this study, an ophthalmologist performed the goniophotography) to place the goniolens on the eye and to focus on the angle structures. In contrast, a less trained individual can perform EyeCam imaging. Goniophotography may have advantages over the EyeCam, including the ability to capture the corneal wedge to help identify Schwalbe's line, and the use of less light (32.28 lux compared to 129.12 lux with EyeCam). The agreement in identifying angle closure between EyeCam and goniophotography, while good, was lower than the agreement between each modality with the reference standard, gonioscopy. Agreement was lowest in the nasal quadrant, followed by the temporal quadrant. The latter may be due to difficulties in image capture due to the nasal bridge; however we are unable to explain the poor agreement in the nasal quadrant. The inability of both modalities to perform indentation and detect PAS, and the use of illumination (which may cause pupil constriction with widening of angle) are significant drawbacks.[15]

Our study had several limitations. This clinic-based population may not be representative of community-based populations since many had been examined with lenses touching the eye, and therefore may have been more cooperative with the examination. This could have led to better results than would be obtained in non-clinic settings. Second, the operators performing the tests were well-trained and experienced. Whether or not others could be trained to obtain such high-quality images is uncertain. Only one examiner performed gonioscopy, which is a potential limitation of the study. In addition, the difference in position adopted by the study subjects when undergoing gonioscopy (seated) and EyeCam (supine) may

have affected the results. The cost of EyeCam, being higher than either gonioscopy and goniophotography, may be a limitation to its routine use in clinical practice.

In summary, this study showed that both EyeCam and goniophotography can be utilised to document angle findings, and analysis of the images was consistent with findings on gonioscopy. Both modalities showed good diagnostic performance for detecting angle closure, with good agreement between each other, and with gonioscopy. EyeCam may have advantages over goniophotography such as easier image capture, a wider field of view of the angle, higher quality images and greater patient comfort. However as these techniques are technically demanding and time consuming, they are unlikely to replace gonioscopy but may be a useful adjunct to document gonioscopic findings in clinical practice.

3.3 EyeCam Vs. ASOCT (cross-sectional imaging) for angle closure

Abstract

Purpose: To compare the diagnostic performance of EyeCam (Clarity Medical Systems, Pleasanton, CA) and anterior segment optical coherence tomography (ASOCT, Visante, Carl-Zeiss Meditec, Dublin, CA) in detecting angle closure, using gonioscopy as the reference standard.

Methods: Ninety-eight phakic patients, recruited from a glaucoma clinic, underwent gonioscopy by a single examiner, and EyeCam and ASOCT imaging by another examiner. Another observer, masked to gonioscopy findings, graded EyeCam and ASOCT images. For both gonioscopy and EyeCam, a closed angle in a particular quadrant was defined if the posterior trabecular meshwork was not visible. For ASOCT, angle closure was defined by any contact between the iris and angle anterior to the scleral spur. An eye was diagnosed as having angle closure if ≥2 quadrants were closed. Agreement and area under the receiver operating characteristic curves (AUC) were evaluated.

Results: The majority of subjects were Chinese (69/98, 70.4%) with a mean age of 60.6 years. Angle closure was diagnosed in 39/98 (39.8%) eyes with gonioscopy, 40/98 (40.8%) with EyeCam and 56/97 (57.7%) with ASOCT. The agreement (kappa statistic) for angle closure diagnosis for gonioscopy vs EyeCam was 0.89; gonioscopy vs ASOCT and EyeCam vs ASOCT were both 0.56. The AUC for detecting eyes with gonioscopic angle closure with EyeCam was 0.978 (95%CI: 0.93-1.0) and 0.847 (95%CI: 0.76-0.92, $p< 0.01$) for ASOCT.

Conclusion: The diagnostic performance of EyeCam was better than ASOCT in detecting angle closure when gonioscopic grading was used as the reference standard. The agreement between the two imaging modalities was moderate.

Introduction

Anterior segment optical coherence tomography (ASOCT) on the other hand, offers a rapid, non-contact method of angle assessment which can be qualitative as well as quantitative. Its diagnostic capabilities have been described in detail and angle assessment using ASOCT has been documented to correlate moderately well with gonioscopy.[13]

The aim of this study was to compare the use of EyeCam and ASOCT for angle imaging and to assess their diagnostic performance in detecting angle closure using gonioscopy as the reference standard.

Methods (specific to this study)

After obtaining a detailed ophthalmic history, each subject underwent a standardized examination that included visual acuity assessment, slit-lamp biomicroscopy, Goldmann applanation tonometry, gonioscopy, ASOCT and imaging with the EyeCam.

Anterior segment imaging was obtained using a commercially available ASOCT device (Visante; Carl Zeiss Meditec, Dublin, CA, USA). The details of ASOCT imaging technology have been described previously.[16,17] Briefly, this technology permits image acquisition at a rate of 8 frames per second (2000 A scans per second) with a transverse and an axial resolutions of 60 microns and 10 to 20 microns respectively. The combination of wide-field scanning optics (16 mm) and a deep axial scan range (8 mm) allows ASOCT to image a cross section of the anterior chamber in 1 image frame. The scanned images are then processed by customized dewarping software, which compensates for index of refraction transitions to correct the physical dimensions of the images. Seated subjects were examined by a single examiner who was masked to gonioscopic findings. Three ASOCT images of each eye were obtained in dark conditions: 1 image scanning the angle at the 3- and 9-o'clock hour positions, one scanning the superior angle

at 12 o'clock, and one scanning the inferior angle at 6 o'clock. Because of interference from the eyelids with image acquisition of the ACA at 6 and 12 o'clock, the lower lid was pulled down gently by the operator to image the inferior angle, and the upper lid was elevated gently to image the superior angle, taking care to avoid inadvertent pressure on the globe. Imaging was repeated once if the scleral spur visibility was poor, to select the best set of images. The ASOCT image files were exported to a personal computer and were evaluated for the presence of a closed or open ACA by 2 examiners with glaucoma subspecialty training who were masked to other test results. A closed angle in a particular quadrant was defined as any contact between the iris and angle wall anterior to the scleral spur on the ASOCT images.

Statistical analysis was similar to the previous study described in 3.2.

Results

Of the 98 subjects recruited, all EyeCam images were gradable. Five subjects had poor scleral spur identification in atleast one quadrant in ASOCT images. All the remaining images were gradable in all four quadrants. The majority of study subjects were Chinese (69/98, 70%) with a mean age of 60.7 (SD - 12.6) years and there were an equal number of men and women. Of the 98 eyes analyzed, 39 (39.8%) had angle closure (in ≥2 quadrants) by gonioscopy.

Angle closure was present in 40/98 (40.8%) with EyeCam and 56/97 (57.7%) with ASOCT. Although 5 eyes had some incomplete/non-gradable quadrants, if an eye satisfied the criteria for a diagnosis of angle closure in the available two quadrants, they were graded as having angle closure instead of being totally excluded.

The kappa agreement between the two imaging modalities was moderate at 0.56. The kappa statistic for agreement varied between 0.62 and 0.89 for EyeCam against gonioscopy and

Table 6: Kappa values using EyeCam and ASOCT compared to gonioscopy (n=98)

	Agreement between methods - Kappa statistic (95% CI)		
Definition of closure	**EyeCam vs. Gonioscopy (n=98)**	**ASOCT vs. Gonioscopy (n=93)**	**EyeCam vs ASOCT (n=93)**
1 or more quadrants closed	0.86 (0.75, 0.96)	0.54 (0.38, 0.70)	0.54 (0.38, 0.70)
2 or more quadrants closed	0.89 (0.80, 0.99)	0.56 (0.41, 0.72)	0.56 (0.41, 0.72)
3 or more quadrants closed	0.80 (0.68, 0.92)	0.56 (0.39, 0.72)	0.65 (0.49, 0.80)
4 quadrants closed	0.62 (0.43, 0.80)	0.45 (0.26, 0.64)	0.46 (0.28, 0.65)
Superior quadrant closed	0.85 (0.74, 0.96)	0.46 (0.30, 0.62)*	0.42 (0.27, 0.58)*
Inferior quadrant closed	0.94 (0.87, 0.99)	0.57 (0.41, 0.73)*	0.55 (0.39, 0.71)*
Nasal quadrant closed	0.67 (0.51, 0.83)	0.53 (0.37, 0.70)*	0.63 (0.47, 0.79)*
Temporal quadrant closed	0.67 (0.52, 0.83)	0.52 (0.35, 0.68)*	0.57 (0.41, 0.74)*

* n=95 (Superior Quadrant); 96 (Inferior Quadrant); 98 (for nasal and temporal quadrants)

Table 7: Receiver Operating Characteristic curve (ROC) analysis to compare EyeCam and with Gonioscopy for various definitions of angle closure

	EyeCam vs. Gonioscopy			ASOCT vs. Gonioscopy			
Definition of closure	**AUC (95% CI)**	**Sens.**	**Spec.**	**AUC (95% CI)**	**Sens.**	**Spec.**	***P*-value***
1 or more quadrants closed	0.957 (0.896, 0.988)	0.93	0.93	0.884 (0.801, 0.941)	0.95	0.61	0.076
2 or more quadrants closed	0.978 (0.926, 0.997)	0.95	0.95	0.847 (0.758, 0.914)	0.92	0.65	0.002
3 or more quadrants closed	0.945 (0.879, 0.981)	0.94	0.89	0.877 (0.792, 0.936)	0.84	0.75	0.137
4 quadrants closed	0.891 (0.812, 0.945)	0.77	0.88	0.795 (0.699, 0.872)	0.77	0.76	0.102

AUC – Area under the ROC curve; Sens – Sensitivity; Spec – Specificity; CI – Confidence Interval

*Comparison of independent ROC curves between EyeCam and ASOCT

Related publication: Baskaran M, Aung T, Friedman DS, Tun TA, Perera SA. Comparison of EyeCam and ASOCT in detecting angle closure. Acta Ophthalmol. 2012 Dec;90(8):e621-5.

between 0.45 and 0.56 for ASOCT and gonioscopy, depending on the definition of angle closure by number of quadrants closed (**Table 6**). The highest agreement was seen with a definition of 2 or more quadrants closed for both devices. The inferior quadrant showed the highest agreement with gonioscopy using both devices. Using our definition of angle closure as 2 or more quadrants closed on gonioscopy, both sensitivity and specificity using the EyeCam was 95% while they were 92% and 65% respectively for ASOCT. The AUC for EyeCam was 0.978 (95% CI 0.926-0.997) and that for ASOCT was 0.847 (95%CI 0.758-0.914) (**Table 7**).

Discussion

The EyeCam accurately identified angle closure in this clinic-based mostly Chinese population and performed better than ASOCT when both were compared to gonioscopy.

The disagreement between EyeCam and ASOCT may be due to several technical and operational reasons. Firstly, ASOCT is performed in the dark and does not require contact with the eye; inadvertent indentation and excessive light during gonioscopy (or EyeCam) would open the ACA artificially.[13] On gonioscopy, non-visibility of the pigmented trabecular meshwork is used to define a closed angle. On ASOCT, the trabecular meshwork itself is rarely seen, and hence any contact anterior to the scleral spur (used as a surrogate marker) defines angle closure. As the scleral spur lies posterior to the pigmented trabecular meshwork, the ASOCT definition uses a more lenient definition of angle closure. Cumulatively, all these discrepancies would lead to a relative overestimation of angle closure by ASOCT.

Operationally, each modality has specific nuances in imaging particular quadrants. With gonioscopy, viewing the temporal and nasal angles can be difficult due to the horizontal positioning of the light beam. With EyeCam imaging, the temporal angle may be more

challenging in deep-set eyes, due to obtaining the correct angulation of the probe via a nasal approach. Imaging the superior and inferior quadrants with ASOCT can be difficult as manipulations to move the lids out of the way prior to ASOCT may alter the appearance of the angle[14] or due to variable identification of scleral spur during image analysis.[18]

This study has some limitations. The analysis of the ACA in each quadrant by ASOCT was based on only a cross-sectional image of the angle, and there may be variations throughout the quadrant that may be missed by this single meridional image. In contrast, both gonioscopy and EyeCam give wide field views of the whole quadrant from which an overall decision can be made. The number of images in which the ACA status cannot be determined may be higher in clinical practice, where technicians and observers may have less expertise in angle assessment. On the other hand, the use of a single gonioscopist in our study could result in a systematic bias for the gonioscopy findings and is a potential weakness, although it does reflect common medical practice. Another limitation relates to the fact that the reproducibility of detecting a closed ACA in ASOCT images was not assessed in this study. A previous study has reported the inter-observer variability as moderate with a kappa of 0.48 with respect to angle closure status.[13] Studies comparing ASOCT with a more comprehensive gonioscopic grading system such as the Spaeth system, or with other imaging methods of assessing the ACA such as ultrasound biomicroscopy, may provide further insights to the discrepancies between gonioscopy and ASOCT.

In conclusion, the EyeCam discriminated angle closure status better than ASOCT when gonioscopic grading was used as a reference standard. The agreement between the two imaging modalities was moderate.

3.4 Automated grading solution for angle closure detection using EyeCam images

Introduction

Closed/Open angle glaucoma classification is important for glaucoma diagnosis. EyeCam is a new imaging modality that captures the image of iridocorneal angle for the classification. However, manual grading and analysis of the EyeCam image is subjective and time consuming. We worked in collaboration with software engineers from Institute of Infocomm research, A-Star, Singapore to utilize intelligent analysis of irido-corneal angle images, which can differentiate closed angle from open angle automatically. Two approaches were used for the classification and their performances were compared.

Methods:

Subjects from study 3.1 have been utilised for this automated grading software testing. Consecutive 99 patients were included (1866 images), of which 54 were open angles (1083 images) and 45 were closed angles (783 images). These images were used to automatically grade the image nature by the following steps by the engineering team at Institute of Infocomm research, more details are found in the relevant research publications (List of publications – 1 &5, Figure 5):

1. **Edge detection:** This was performed using Canny edge method, to detect the region of interest.
2. **Arc detection (using circular Hough transform method):** The irido corneal angle is in an arc shape i.e. part of a circle. Thus arc detection algorithms were applied to detect true arcs, remove false arcs, and connect broken edges. Circular Hough transform method was used to achieve this goal.
3. **Identifying angle structures and grading** – this was accomplished by two methods initially (2010):

Figure 5: Automated grading of EyeCam images – Method overview

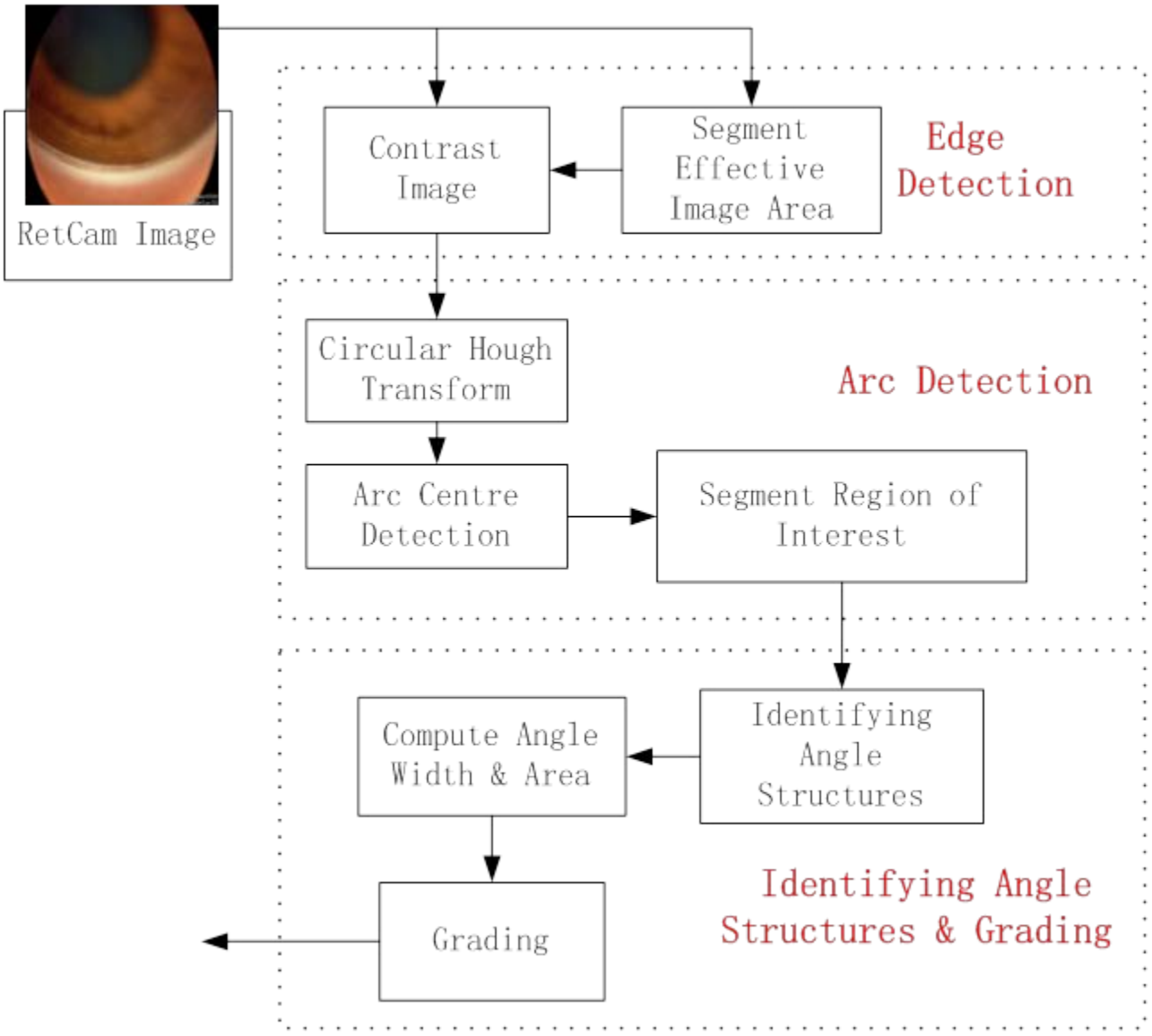

In collaboration with Institute of Infocomm research team, Singapore

Related publication: Cheng J, Tao D, Liu J, Wong DW, Lee BH, **Baskaran M**, et al. Focal biologically inspired feature for glaucoma type classification. Med Image Comput Comput Assist Interv. 2011;14(Pt 3):91-8.

a. **Arc amount based approach**: In a closed angle, the number of edges detected and the corresponding true arcs detected were single in most cases while that of closed angles were multiple. This finding was used in this approach.

b. Angle width based approach: This method considered the angle width at the region of interest by initially detecting the strongest arc; then closing process was applied on the angle recess to detect the surrounding edges. The mean width across the arc was taken for analysis. If the width was beyond a threshold level, then it was considered open; and vice versa.

4. Later a refinement using **focal edge detection method** for iris surface detection and angle grading was also tried (2011): Focal edge refers to the edge associated with certain objects or structures, in this case the angle structures. The region of interest, i.e. angle recess along with iris surface was taken into account for analysis here. The strongest arc apart from the true arc from angle, usually was the iris surface. The iris surface was taken into account in this method to detect the edges in angle, combining Canny edge and Circular Hough Transform methods. In this approach, the quadrant of interest was also automatically detected before focal edge detection.

Results and Discussion

Arc amount based approach yielded 83.3% sensitivity and 86.7% specificity, while angle width approach provided 92.6% sensitivity and 97.8% specificity compared to manual grading of images by a qualified ophthalmologist. Single arc specified closed angle and multiple arcs identified open angles (Figure 6)

Subsequent focal edge based method, also identified the quadrant automatically based on orientation of the image to superior or inferior, nasal or temporal quadrants. Compared to previous approach, the arc near iris is used to enhance accuracy. Using a machine learning approach, the accuracy of the classifier improved to 7%, 23.4% and 1.3% for open, Grade 1 and Grade 0 respectively.

A new automated grading software system was developed for EyeCam angle image classification (named AGATE) and quadrant identification from 4 images. It was validated with manual grading of the images by an expert.

In conclusion, this software can be useful in clinical application if a suitable hardware is aligned. The application can be useful in initial case detection in high risk population and it will be useful in high volume clinics where an initial screening is required. This software needs to be validated against gonioscopic findings and manual grading in a different set of patient images.

3.5 Manual grading, Automated grading of EyeCam images Vs. Gonioscopy

Abstract

Purpose: To evaluate a novel software capable of automatically grading angle closure on EyeCam™ (Clarity Medical Systems, Pleasanton, CA) angle images in comparison to manual grading of images, with gonioscopy as the reference standard.

Methods: In this hospital-based, prospective study, subjects underwent gonioscopy by a single observer, and EyeCam imaging by a different operator. The anterior chamber angle in a quadrant was classified as closed if the posterior trabecular meshwork could not be seen. An eye was classified as having angle closure if there were 2 or more quadrants of closure. Automated grading of the angle images was performed using customized software. Agreement between the methods was ascertained by kappa statistic and comparison of area under receiver operating characteristic curves (AUC).

Results: One hundred and forty subjects (140 eyes) were included, the majority of whom were Chinese (102/140, 72.9%) and females (72/140, 51.5%). Angle closure was detected in 61 eyes (43.6%) with gonioscopy in comparison to 59 eyes (42.1%, p=0.73) using manual grading and 67 eyes (47.9%, p=0.24) with automated grading of EyeCam images. The agreement for angle closure diagnosis between gonioscopy and both manual (k=0.88; 95% Confidence Interval (CI), 0.81–0.96) and automated grading of EyeCam images was good (k=0.74; 95% CI, 0.63–0.85). The AUC for detecting eyes with gonioscopic angle closure was comparable for manual and automated grading (AUC 0.974 vs 0.954, p = 0.31) of EyeCam image.

Conclusions: Customized software for automated grading of EyeCam angle images was found to have good agreement with gonioscopy. Human observation of the images may still be needed to avoid gross misclassification, especially in a few angle closure eyes.

Introduction

Currently grading of the documented angle images can only be done manually, but automated solutions are needed to enable clinician independent grading of these images. In the absence of routine gonioscopy in clinical practice, such automated angle image analysis potentially may serve as a surrogate for gonioscopy by a clinician.

This article aims to test this software by comparing automated grading of EyeCam^{TM} angle images with manual grading of images, with gonioscopy as the reference standard.

Methods (specific to this study)

Automated analysis of the images was performed by AGATE (Version 1.0, Institute of Infocomm Research & Singapore Eye Research Institute, Singapore), a software program to analyse the angle images by quadrants and assign the classification as “open” or “closed” based on a training data set. The methodology for the program evaluation and the basis for the program was described earlier in section 3.4.

In brief, the method first determined the quadrant information from the image. Then it detected focal edges associated with angle structures, especially the iris tissue. A circular Hough transform method was applied for arc detection to locate the iris surface and the strongest arc in the nearby angle recess. True arcs were separated from false arcs to avoid artifacts. From the iris surface and the quadrant information, a focal region was calculated. Edges within the focal region were extracted using Canny edge detection method and used to estimate the angle width profile. Mean angle width was considered for analysis. Finally, a classification between “open” and “closed” was given based on angle width profile, considering a threshold for mean angle width (Figures 5 - 7). Single arcs were graded as closed, while multiple arcs were labelled as open (Figure 6c, 7).

Figure 6: Automated software process of angle closure detection – illustrated example

6a. Region of interest detection

6b. Arc detection

6c. Grading of angle

Figure 7: Classification of open and closed angles by the automated software

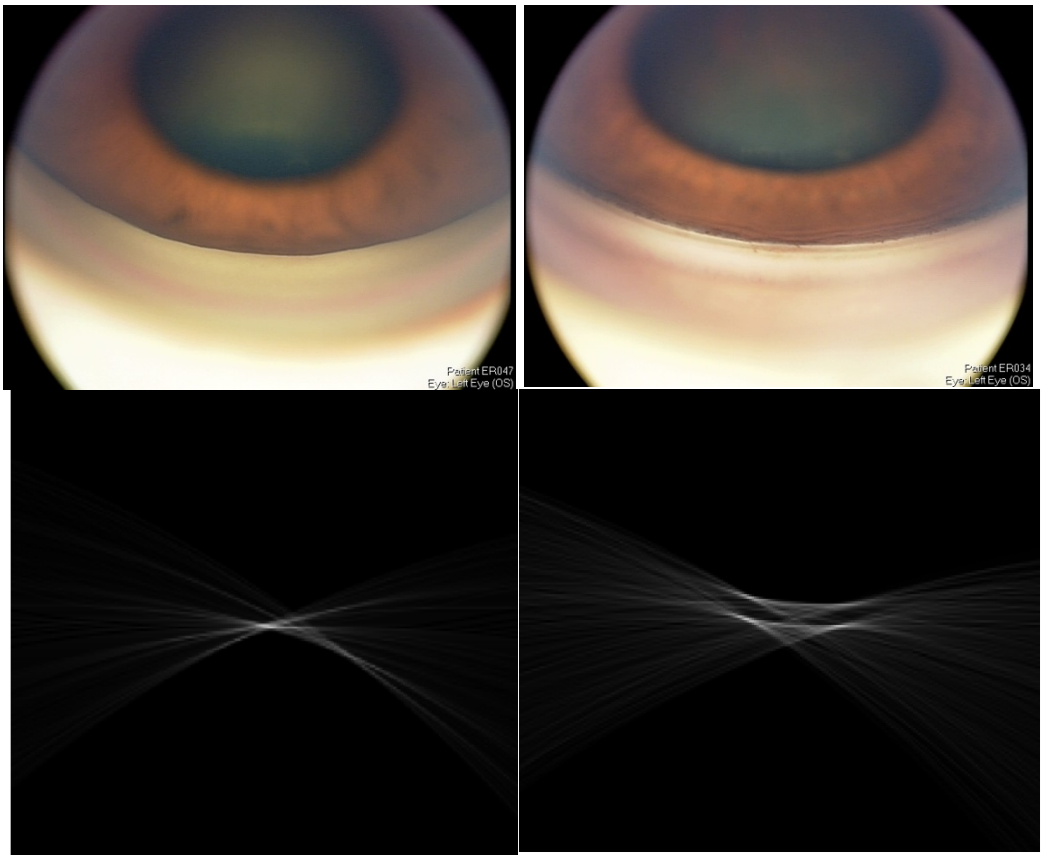

Single arc - Closed angle

Multiple arcs - Open angle

Reproducibility of grading methods

Intra and inter-observer reproducibility for EyeCam^{TM} manual grading was analysed in 40 randomly selected eyes by two observers masked to gonioscopic data and were found to be acceptable for two quadrants angle closure (First order Agreement Coefficient statistics between 0.57 and 0.63).

Automated software (AGATE) reproducibility was excellent (Kappa = 0.99) for a sample of 30 eyes (120 images).

Statistical analysis was similar to earlier described diagnostic performance studies. In addition, Cochran's Q test was performed to test differences in proportions of 2 or 3 quadrants of angle closure, between the three methods. Venn diagrams to scale were generated for either 2 or 3 quadrants of angle closure between the 3 methods.[19]

Results

Out of the145 consecutive eligible subjects, 5 were excluded due to missing/poor quality images. One hundred and forty eyes were included for analysis using the automated software. The mean age of included subjects was 60.5 (standard deviation 12.9) years with majority being Chinese (102/140, 72.9%) and females (72/140, 51.5%). Five subjects had prior LPI. Gonioscopic angle closure was noted in two quadrants or more among 61 eyes (43.6%) in comparison to 59 (42.1%, p=0.73) using manual grading of angle images. Automated grading of angle images graded more angle closure eyes but was statistically insignificant in comparison to gonioscopy (67/140, 47.9%, p=0.24).

Table 8 shows the agreement for various definitions of angle closure between the three methods. Generally, two or three quadrant closure definitions showed good agreement between methods. The temporal quadrant showed the least agreement with automated grading in

Table 8: Kappa agreement of manual and automated grading of EyeCam angle images compared to gonioscopy (n=140)

Agreement between methods						
Definition of closure	**Manual vs. Gonioscopy (n=140)**		**Automated vs. Gonioscopy (n=140)**		**Manual vs. Automated (n=140)**	
	k (95% CI)	**AC1**	**k (95% CI)**	**AC1**	**k (95% CI)**	**AC1**
1 or more quadrants closed	0.87 (0.79, 0.95)	0.87	0.50 (0.36, 0.64)	0.50	0.57 (0.44, 0.70)	0.57
2 or more quadrants closed	0.88 (0.81, 0.96)	0.89	0.74 (0.63, 0.85)	0.74	0.68 (0.56, 0.81)	0.69
3 or more quadrants closed	0.76 (0.64, 0.87)	0.79	0.78 (0.67, 0.89)	0.82	0.79 (0.68, 0.89)	0.81
4 quadrants closed	0.60 (0.44, 0.76)	0.76	0.46 (0.28, 0.65)	0.72	0.47 (0.29, 0.65)	0.70
Superior quadrant closed	0.81 (0.71, 0.91)	0.82	0.69 (0.57, 0.81)	0.69	0.73 (0.62, 0.84)	0.73
Inferior quadrant closed	0.88 (0.81, 0.96)	0.89	0.65 (0.52, 0.78)	0.67	0.58 (0.45, 0.72)	0.62
Nasal quadrant closed	0.65 (0.51, 0.79)	0.74	0.64 (0.50, 0.78)	0.72	0.61 (0.47, 0.75)	0.67
Temporal quadrant closed	0.67 (0.54, 0.80)	0.73	0.37 (0.21, 0.53)	0.41	0.48 (0.33, 0.62)	0.50

CI – Confidence Interval; k - Kappa statistic; AC1

Table 9: Receiver Operating Characteristic curve (ROC) analysis to compare Manual and with Gonioscopy for various definitions of angle closure (n=140)

	Manual vs. Gonioscopy (n=140)			**Automated vs. Gonioscopy (n=140)**			
Definition of closure	**AUC (95% CI)**	**Sens.**	**Spec.**	**AUC (95% CI)**	**Sens.**	**Spec.**	***P*-value***
1 or more quadrants closed	0.955 (0.906, 0.983)	0.92	0.95	0.923 (0.865, 0.961)	0.95	0.55	0.266
2 or more quadrants closed	0.974 (0.933, 0.994)	0.92	0.96	0.954 (0.905, 0.982)	0.90	0.85	0.306
3 or more quadrants closed	0.927 (0.87, 0.964)	0.88	0.89	0.94 (0.886, 0.973)	0.84	0.93	0.665
4 quadrants closed	0.891 (0.828, 0.938)	0.75	0.88	0.877 (0.811, 0.926)	0.56	0.89	0.728

AUC – Area under the ROC; Sens – Sensitivity; Spec – Specificity; CI – Confidence interval;

*Comparison of independent ROC curves between manual and automated grading of EyeCam images

Related publication: Baskaran M, Cheng J, Perera SA, Tun TA, Liu J, Aung T. Automated analysis of angle closure from anterior chamber angle images. Invest Ophthalmol Vis Sci. 2014 Oct 21;55(11):7669-73.

comparison to gonioscopy. Manual vs automated grading comparison showed moderate to good agreement. **Figure 8a** shows a Venn diagram depicting eyes identified by each method for two quadrant angle closure definition, with automated grading overestimating angle closure. **Figure 8b** shows similar diagram for three quadrant angle closure definition, suggesting slight overestimation by manual grading. However, this difference in agreement was not statistically significant for 2 (Cochran's Q test, Manual vs Automated, 0.88 vs 0.74, p = 0.12) or 3 quadrants (0.76 vs 0.78, p = 0.28) of angle closure between the 3 methods. The agreement statistics did not change when subjects with LPI were removed from the analysis (data not shown). **Table 9** shows that the AUC is similar and very high for both methods. AUC for 2 quadrants closure (Manual vs Automated = 0.974 vs 0.954, p=0.31) was slightly better than 3 quadrant closure definition (Manual vs Automated = 0.927 vs 0.94, p=0.67), but this was not statistically significant.

Figures 9 and 10 depict Eyecam^{TM} images showing discrepancy with gonioscopic diagnosis of open and closed angles respectively. **Figure 9a** image was graded as closed on both manual and automated grading possibly due to a convex iris configuration. **Figure 9b and 9c** images were graded as open on manual grading and gonioscopy but closed on automated grading, possibly due to the presence of a lightly pigmented TM or heavy TM pigmentation respectively, thus blurring the demarcation between TM and iris root. **Figure 10a** image was graded as open on both grading due to partial angle closure while **Figure 10b** was graded as open with automated grading owing to the presence of pigmented Schwalbe's line. **Figure 11** shows the ROC curve comparing manual and automated (Agate) grading system for detection of angle closure in comparison to gonioscopy.

Figure 8: Venn diagrams showing the number of (8a) two and (8b) three quadrants closed angle detection by gonioscopy (solid fill), Eyecam™ manual (stripes) and automated (empty) grading methods, suggesting overestimation by the latter two methods. (n=140)

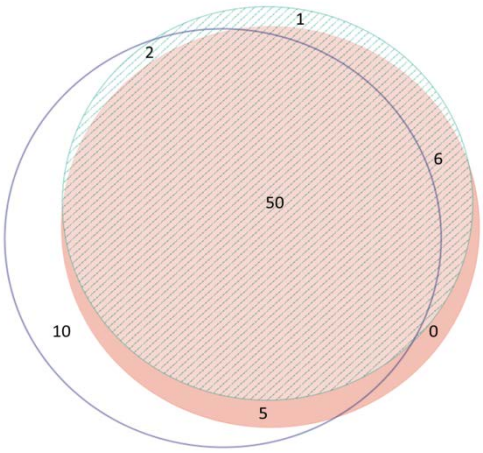

Figure 8a

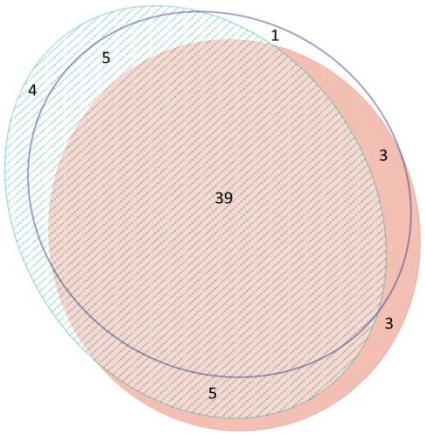

Figure 8b

Figure 9: EyeCam™ images – misclassification into closed angles by automated grading method due to (9a) Convex iris, (9b) Lightly pigmented trabecular meshwork (TM) and (9c) Heavy TM pigmentation.

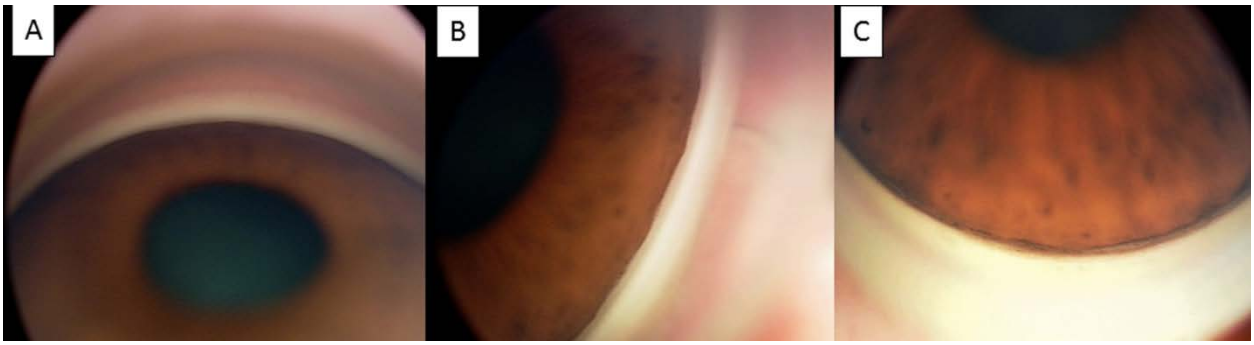

Figure 10: EyeCam™ images – misclassification into open angles by automated grading method due to (10a) Partial angle closure in that quadrant and (10b) Pigmented Schwalbe's line.

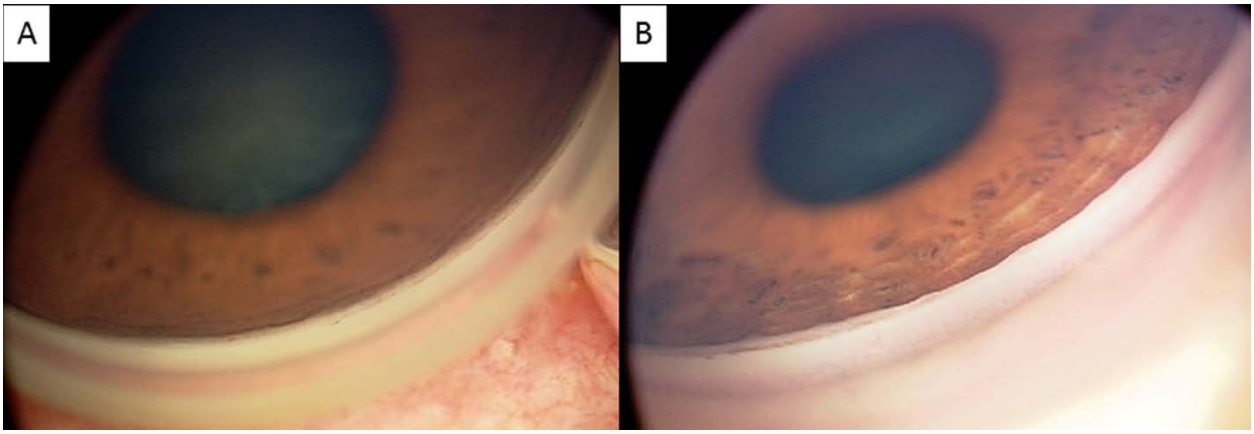

Figure 11: Receiver Operating Characteristic Curve comparing the diagnostic performance for angle closure: EyeCam manual Vs. automated Vs. Gonioscopic reference standard

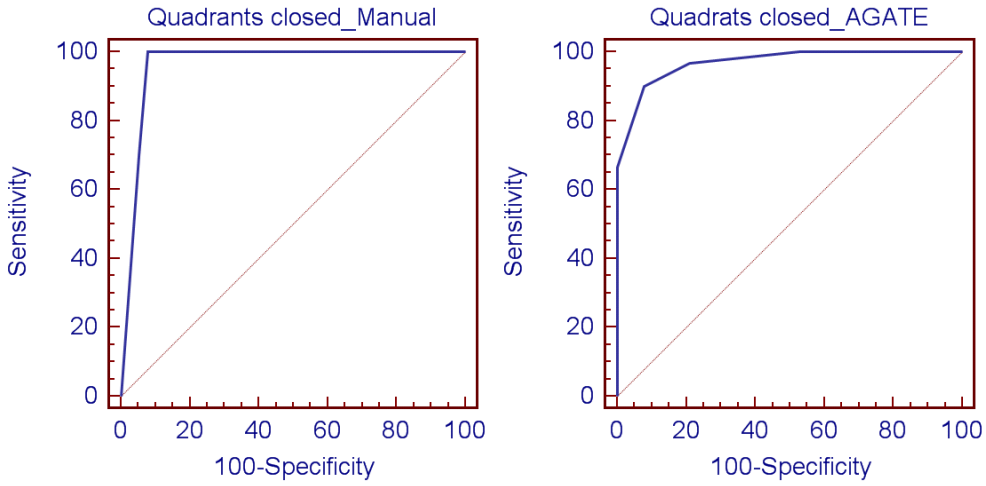

Overall misclassification rate with automated grading for angle assessment was 12.1% (17/140 eyes) with 7.9% false positives (i.e. 11 closed angle eyes), while it was 5.7% (8/140 eyes) and 2.1% (3/140 eyes) with manual grading respectively. Most open angles on gonioscopy had very light TM pigmentation (6/11) or dense pigmentation (4/11) leading to erroneous marking by automated grading as closed angles; while closed angles were marked as open if it was partial angle closure (3/6) or if the angle had a pigmented Schwalbe's line (3/6) in that quadrant. Other reasons for error in automated grading was the presence of a convex iris, obscuring angle details and masquerading as closed angle.

Discussion

We report the clinical utility of the first automated software for EyeCam goniophotographic angle assessment. The agreement of this software in comparison to gonioscopy was found to be very good for the 2 and 3 quadrant definitions of angle closure.

Several anterior segment imaging methods have been developed to address reproducibility and contact issues inherent in gonioscopic angle assessment. While such techniques can quantitatively assess the anterior chamber angle, none can claim to completely replace gonioscopy for several reasons. [20] Assessing the distribution and degree of pigmentation in the trabecular meshwork, 360° circumferential angle view and detection of peripheral anterior synechiae are few of the advantages with gonioscopy. Furthermore, the low specificity of these devices may limit their usefulness in screening for angle closure.[21] Reported practice patterns of ophthalmologists reveal only 50% utilize gonioscopy in comprehensive eye examinations, and follow up documentation of the angle is poor even among glaucomatologists.[22] To improve this, one must deconstruct gonioscopy into its constitutive parts. First there is the technical aspect of image capture, followed by the interpretation and grading. Image capture can be done by

EyeCam-fluent technicians while the software algorithm in our study can fulfill the unmet need of interpretation and grading. This tool may probably be utilized for education and documentation of the angle and it can be easily adapted to goniophotography. Its uptake in screening for angle closure is unfortunately subject to other external factors such as the cost and patient acceptability.

Individual quadrant angle closure diagnosis did not show very good agreement with gonioscopy for either manual or automated methods of EyeCam angle grading. This could be due to the nasal bridge obstructing the bulky probe, altering the angle view of the temporal quadrant. Misclassification of open or closed angles with either method was often due to heavy or light pigmentation and partial angle closure. In a study of 291 subjects including Afro-Americans, "far-east" Asians and Caucasians, Oh YG et al[23]suggested that refractive error and racial origin may influence iris insertion leading to variation in gonioscopic angle assessment. These limitations may have less bearing on EyeCam™ grading. Partial angle closure in a quadrant (which was misclassified by the software as open angles) in this study could be due to inclusion of subjects who have undergone LPI.

Our study had a few limitations. Gonioscopy was performed by a single observer. Misclassification error rates due to lightly pigmented angles or heavily pigmented TM may need to be addressed. Feature extraction methods may identify angle structures irrespective of TM pigmentation.Human observation of the images may still be needed to avoid gross misclassification, especially in a few angle closure eyes. Even though, inclusion of subjects who underwent LPI in this study did not affect the overall results, it might be possible for the heavy pigmentation occurring after LPI to skew automated grading.

In summary, we evaluated a novel automated angle assessment software tool and reported very good diagnostic performance in comparison to gonioscopy. We believe that EyeCam™ imaging with automated angle assessment has potential to be a useful adjunct in clinical evaluation and documentation of the irido-corneal angle.

3.6 References: (Chapter 3)

1. Weinreb RN, Friedman DS. “Laser and medical treatment of Primary Angle Closure Glaucoma.” Angle Closure and Angle Closure Glaucoma. Ed. R.N. Weinreb, D.S. Friedman. Netherlands: Krugler, 2006. 37-54.
2. Nonaka A, Iwawaki T, Kikuchi M, Fujihara M, Nishida A, Kurimoto Y. Quantitative evaluation of iris convexity in primary angle closure. Am J Ophthalmol 2007;143:695-7.
3. Nolan WP, Foster PJ, Devereux JG, et al. YAG laser iridotomy treatment for primary angle-closure in east Asian eyes. Br J Ophthalmol 2000;84:1255–9.
4. He M, Friedman DS, Ge J, et. al. Laser peripheral iridotomy in eyes with narrow drainage angles: ultrasound biomicroscopy outcomes. The Liwan Eye Study. Ophthalmology 2007;114:1513-9.
5. Nolan WP, Foster PJ, Devereux JG, et al. YAG laser iridotomy treatment for primary angle closure in east Asian eyes. Br J Ophthalmol 2000;84:1255-9.
6. Foster PJ, Devereux JG, Alsbirk PH, et al. Detection of gonioscopically occludable angles and primary angle closure glaucoma by estimation of limbal chamber depth in Asians: modified grading scheme. Br J Ophthalmol 2000;84:186-92.
7. Friedman DS, He M. Anterior chamber angle assessment techniques. Surv Ophthalmol 2008;53:250-73.
8. Ahmed I, MacKeen L. A New Approach to Imaging the Angle. Glaucoma Today. 2007;4:1-3.

9. Ang MH, Baskaran M, Kumar RS, et al. National survey of ophthalmologists in Singapore for the assessment and management of asymptomatic angle closure. J Glaucoma 2008;17:1-4.
10. See JL, Chew PT, Smith SD, et al. Changes in anterior segment morphology in response to Illumination and after laser iridotomy in Asian eyes: an anterior segment OCT study. Br J Ophthalmol 2007; 91: 1485-9.
11. Gazzard G, Friedman DS, Devereux JG, Chew P, Seah SK. A prospective ultrasound biomicroscopy evaluation of changes in anterior segment morphology after laser iridotomy in Asian eyes. Ophthalmology 2003;110:630-8.
12. Memarzadeh F, Li Y, Chopra V, et al. Anterior segment optical coherence tomography for imaging the anterior chamber after laser peripheral iridotomy. Am J Ophthalmol. 2007;143: 877-9.
13. Nolan WP, See JL, Chew PT et al. Detection of Primary Angle Closure Using Anterior Segment Optical Coherence Tomography in Asian Eyes. Ophthalmology 2007**;**114:33-39
14. Sakata LM., Lavanya R, Friedman DS, et al. Comparison of Gonioscopy and Anterior Segment Ocular Coherence Tomography in Detecting Angle Closure in Different Quadrants of the Anterior Chamber Angle. Ophthalmology 2008;115;5:769-774.
15. Forbes M. Gonioscopy with corneal indentation; a method for distinguishing between appositional closure and synechial closure. Arch. Ophthal. 1966; 76:488-492.
16. Radhakrishnan S, Goldsmith J et al. Comparison of optical coherence tomography and ultrasound biomicroscopy for detection of narrow anterior chamber angles. Arch

Ophthalmol 2001; **123**:1053–9.

17. Radhakrishnan S, Rollins AM et al. Real-time optical coherence tomography of the anterior segment at 1310 nm. Arch Ophthalmol 2001; **119**:1179–85.
18. Kim DY, Sung KR, Kang SY et al. Characteristics and reproducibility of anterior chamber angle assessment by anterior-segment optical coherence tomography. Acta Ophthalmol 2011; **89**: 435-41.
19. Micallef L, Rodgers P. euler*APE*: Drawing Area-proportional 3-Venn Diagrams Using Ellipses. PLoS ONE 2014;9(7): e101717. doi:10.1371/journal.pone.0101717. http://www.eulerdiagrams.org/eulerAPE
20. Smith SD, Singh K, Lin SC,. Evaluation of the anterior chamber angle in glaucoma: a report by the american academy of ophthalmology. Ophthalmology. 2013 Oct;120(10):1985-97. doi:10.1016/j.ophtha.2013.05.034. Epub 2013 Aug 23. Review.
21. Lavanya R, Foster PJ, Sakata LM et al. Screening for narrow angles in the singapore population: evaluation of new noncontact screening methods. Ophthalmology. 2008 Oct;115(10):1720-7.
22. Quigley HA, Friedman DS, Hahn SR. Evaluation of practice pattern for the care of open angle glaucoma compared with claims data: the Glaucoma Adherence and Persistence Study. Ophthalmology 2007 11(9):1599-606.
23. Oh YG, Minelli S, Spaeth GL, Steinman WC. The anterior chamber angle is different in different racial groups: a gonioscopic study. Eye (Lond). 1994;8 (Pt 1):104-8.

Chapter 4: Circumferential imaging of angle closure by swept source optical coherence tomography (Aim 2)

4.1 Inter and Intra observer reproducibility of Iris-trabecular index: a novel parameter for angle closure detection

Abstract

Purpose. To evaluate the inter- and intra-observer agreement of measurement of the iris-trabecular contact (ITC) index, a measure of the degree of angle closure, using swept source optical coherence tomography (SSOCT, CASIA SS-1000, Tomey Corporation, Nagoya, Japan).

Methods. One randomly selected eye of 60 subjects was imaged under dark room conditions. The SSOCT 3-dimensional angle scan simultaneously obtains 128 radial scans of the anterior chamber for the entire circumference of the angle. Post-imaging analysis estimated the ITC index using in-built software. For intra-observer agreement for image grading, one examiner performed the grading twice in a masked fashion and random order after a one-week interval. A second examiner graded images to assess inter-observer agreement for image grading. For intra-observer agreement for image acquisition, a single operator imaged patients twice. For inter-observer agreement for image acquisition, a single observer graded two sets of images acquired by two different operators on the same patient. Bland-Altman plots and 95% limits of agreement (LOA) were reported.

Results. Study subjects were predominantly Chinese (54/60, 90%) and female (42/60, 70%) with a mean age of 65.5 years. The median ITC index for eyes with open angles (31/60) and closed angles was 20% (95% Confidence Interval [CI] - 13.6, 27.8) and 49% (95%CI – 35.5, 69.2) respectively. The mean difference (95% LOA) for intra-observer agreement for image grading

and image acquisition were -0.8% (-8.2, 6.5) and 0.6% (-10.9, 9.7); corresponding inter-observer agreement were 0.1% (-10, 10.1) and -0.3% (-11.1, 10.5) respectively.

Conclusions. The inter- and intra-observer agreement of the ITC index, as a measure of extent of angle closure using SSOCT, was good.

Introduction

Objective imaging modalities like anterior segment optical coherence tomography (ASOCT) have addressed some of the shortcomings of in gonioscopy such as artifacts, poor reproducibility and patient discomfort.[1-6] Spectral or Fourier domain optical coherence tomography (OCT) technology has recently been introduced to increase the imaging resolution.[7,8] All of these obtain cross-sectional images of the angle which provide less information than the traditional examination of all 360 degrees of the angle when assessed by gonioscopy**.**

The swept source optical coherence tomography (SSOCT, CASIA SS-1000, Tomey Corporation, Nagoya, Japan) is a novel anterior segment imaging device based on the Fourier domain system. Uniquely, the SSOCT's low density 3-dimensional (3D) angle analysis scan, simultaneously obtains multiple radial scans of the entire circumference of the anterior chamber angle. In-built semi-automated analysis software, analyzes the extent of iris-trabecular contact (ITC) across 360° of the angle and calculates the extent of angle closure as the ITC index. This delivers, an estimation of angle closure analogous to that derived from gonioscopy.

The aim of this study was to evaluate the inter- and intra-observer agreement of measurement of the ITC index using the SS-OCT.

Methods (specific to this study)

SS-OCT imaging

All subjects underwent SSOCT imaging of one randomly selected eye before any contact procedure, under dark room conditions. The operator elevated the upper eyelid and gently pulled the lower eyelid down so that the anterior chamber angles could be seen in the scan window, taking care to avoid inadvertent pressure on the globe. Subjects were asked to focus on an internal fixation target and once the subject had been optimally positioned, each eye was scanned with the 3D angle analysis scan (which takes 2.4 seconds) using the auto alignment function. This algorithm takes 128 consecutive meridional scans, each consisting of 512 A-scans covering a distance of 16 mm across the anterior chamber. Each eye was scanned 3 times by two experienced operators. The first and third image was scanned by operator A and the second image was scanned by operator B in order to assess for inter- and intra-examiner agreement of image acquisition.

Analysis of images

The CASIA built-in software (Type and Version 6J.3, 2012.6.8.3) was used to measure the ITC index, which is a semi-quantitative measure of the extent of angle closure. ITC analysis uses full length meridional images of the anterior segment (which are not corrected for index of refraction) to analyze the extent of contact between the iris and angle wall. For our analysis, we restricted the number to 16 out of 128 frames. Other options for frame selection built into the machine were 8, 32, 64 and 128 frames). These 16 frames were automatically selected by the software and were placed at intervals of 11.25 degrees apart. This selection of 16 frames was

made for an accurate and acceptable representation of the angle, and was more stringent than the minimum prescribed 8 frames by the manufacturer.

In each anterior segment image frame, the scleral spur (SS) and the ITC end point (EP) were marked manually by a single examiner with colored "x" mark and "+" mark respectively for both quadrants in the image (**Figure 1a**). SS was identified as the point at which a change in curvature of corneoscleral interface occurs. The EP was identified as the most anterior point of iris contact to the angle wall. The program allowed omitting some frames without marking these points when they could not be identified. When all the 16 frames were marked, the "ITC" button on the screen was clicked to enable the ITC index to be calculated. The software then uses the information from the plotted SS and EP points in these 16 frames to calculate this index.

The results are reflected in an ITC chart as shown in **Figure 1b**. The ITC chart is analogous to a goniogram used in clinical practice. The red circular line represents the SS. The dotted circles represent 0.25, 0.50 and 0.75 mm landmarks anterior to the SS, along the angle wall. The blue area represents the extent of angle closure and if positive, represents angle closure (i.e. ITC) and if negative or neutral, represents open angle areas.

The ITC analysis output also includes 2 parameters:

- the "**ITC index**" which represents the **ratio** of positive ITC (angle closure) in degrees (blue area in the ITC chart) to the total angle with visible scleral spur and end points in degrees; this represents **the extent of angle closure** as a **percentage** (Unit - %).
- the 'invisible range' represents the circumferential extent (in degrees) throughout which either the SS or EP could not be determined in the meridional frames. Minimum of 7 points were needed to be identified for each eye for the calculation of ITC index (as per the manufacturer) and this criterion was used for quality control.

Figure 1: (a) Single frame of the cross-section of the anterior chamber. The colored "x" are the scleral spur (SS) markings and the "+" are the iris-trabecular contact end point (EP)-both points are marked by the observer grading the image. (b) Iris-trabecular contact (ITC) chart with the blue area representing the amount and distribution of iris-trabecular contact. (c) Iris-trabecular contact (ITC) graph with Y axis representing ITC (in arbitrary units) and the X axis representing the degree of the angle. The green graph above the red line (representing SS) denotes the amount of angle closure (measured as the ITC index).

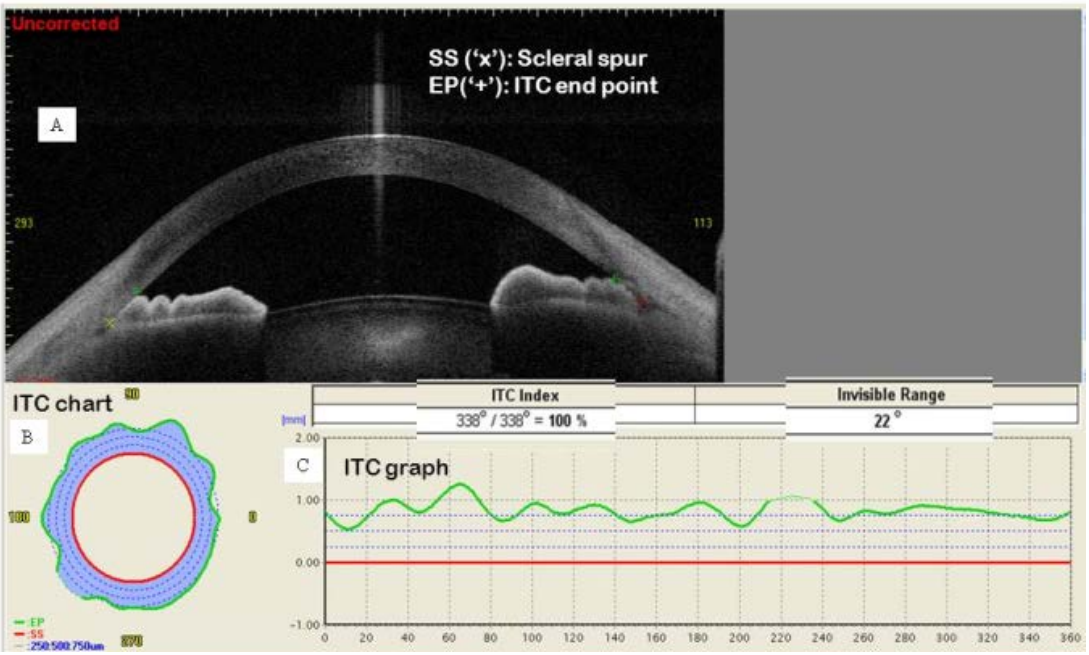

Figure 2: Kernel density estimate of iris-trabecular index with Gaussian approximation with a bandwidth of 13.02, with normal curve overlaid shows slight positively skewed distribution.

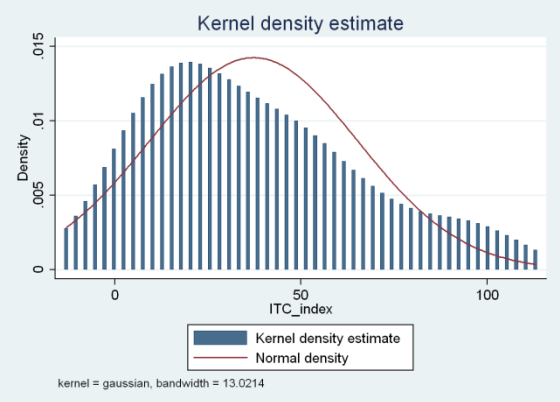

The extent of angle closure circumferentially is also displayed as a graph (**Figure 1c**). A positive ITC (angle closure) is shown as above the red line (which represents the scleral spur) and a negative ITC (open angle) is shown below the line.

Statistical analysis

Inter- and intra-observer agreement was analysed separately for image grading and image acquisition. In order to assess intra-observer agreement for image grading, one examiner performed the grading twice, allowing for a one-week interval before grading the same set of images (n=60). The grader was masked to gonioscopic findings and the second sets of images were scrambled according to a computer generated random number sequence, produced using statistical software (Medcalc v12.0, Meriakerke, Belgium). Twenty images were randomly selected by the same computer generated number sequence from the above set of 60 images and were graded by a second examiner to assess inter-observer agreement for image grading.

In order to assess inter-observer agreement for image acquisition, one examiner graded two sets of images after a one week interval, each set consisting of 60 eyes acquired by two different operators A and B. For intra-examiner agreement for image acquisition, images obtained by operator A twice on the same patient were graded by a single examiner. All grading was performed masked to gonioscopic (Modified Shaffer grading system)[9] and clinical findings.

Demographic parameters were summarized by mean, median, 95% confidence intervals (CI) and interquartile ranges for continuous variables. Skewness and normality test results were assessed. Kernel density probability estimate for the ITC index distribution was performed. Coefficient of variation for repeated measurements was presented as an estimate of dispersion of ITC index. Bland-Altman plots were used to evaluate the agreement of the ITC index for image grading and image acquisition. Fixed and proportional bias were evaluated using the mean

difference, 95% CI, significance of the regression slope and 95% limits of agreement (LOA). Receiver operating characteristic curve (ROC) analysis was performed to evaluate the area under the ROC curve (AUC) for ITC index compared to gonioscopic angle closure as the reference standard. All statistical analyses were performed using MedCalc for Windows v12.0 (Mariakerke, Belgium).

Results

A total of 60 eyes of 60 patients were examined; of these 29 eyes had two quadrants or more angle closure on gonioscopy. The mean age of subjects was 65.5 (Standard deviation [SD] 7.1) years and the majority of subjects were Chinese (54/60, 90%, **Table 1**). The overall mean ITC index was 37.3 (28.0), median was 30 and the index was positively skewed in distribution **(Table 2)**. **Figure 2** shows the kernel density estimate of ITC index depicting a slight positive skew of the data and suggestive of a bimodal distribution. The mean ITC index for the open angle group was 22.5% and 53.0%, for the closed angle group, while the corresponding medians were 20% and 49% respectively.

Agreement of ITC index: Image grading

The inter-observer agreement of ITC index for grading of the images showed that the mean difference (95% LOA) was 0.1% (-10, 10.1, **Table 3, Figure 3a)** and the coefficient of variation (COV) was 11.71%. The intra-observer agreement of ITC index (image grading) showed that the mean difference (95% LOA) was -0.8% (-8.2, 6.5, **Figure 3b**) and the COV was 7.16%. There was no fixed bias noted from the mean difference values. The regression slope for the intra-observer agreement measurements showed proportional bias ($p = 0.0099$) suggesting that there was less agreement in the measurements for extremes of ITC indices for the same

Table 1: Demographic and clinical features of study participants (n=60)

	Patients with open angles (n=31)	**Patients with closed angles (n=29)**	**P value**
Age (mean/SD)	64.6 (6.52)	65.5 (7.09)	0.571
Gender (Male:Female)	11:20	7:22	0.405
Ethnicity (Chinese: Malays:Indian:Others)	27:1:3:0	27:1:0:1	0.672
Eye (Right:Left)	12:19	15:14	0.436
Axial Length (mm) (mean/SD)	23.68 (1.09)	22.84 (0.84)	0.005
ACD (mm) (mean/SD)	3.02 (0.41)	2.74 (0.40)	0.01
Lens Thickness (mm) (mean/SD)	4.31 (0.69)	4.50 (0.80)	0.330
Gonioscopic grade (mean/SD)	3.65 (0.57)	1.16 (0.69)	0.0001

SD – Standard deviation; ACD – Anterior Chamber Depth; ITC – Iris Trabecular Contact Index

Table 2: Distribution of Iris-trabecular contact index (n=60)

	Overall	**Eyes with Open angles**	**Eyes with Closed angles**
Mean (Percentage, 95% CI) †	37.3 (30.07, 44.52)	22.65 (16.36, 28.93)	52.97 (41.92, 64.01)
Median (Percentage, 95% CI)†	30 (21, 45)	20 (13.59, 27.83)	49 (35.53, 69.23)
Interquartile Range (Percentage)	65.5	12.75	44
Coefficient of Skewness	0.74* (positive skew)	0.48	0.19
D'Agostino-Pearson Test for normality (p value)	0.0649	0.26	0.14

†p=<0.0001, SD, *p=0.0204, CI – Confidence Interval

Table 3: Inter- and Intra-Observer agreement for Iris-Trabecular Contact Index Measurement (n=60)

	Bland-Altman plots mean difference (95% CI)	Fixed bias	Proportional bias	95% Limits of Agreement	
				Lower bound	Upper bound
Inter-observer agreement for image grading (n=20)	0.1* (-2.4,2.5)	No	No	-10	10.1
Intra-observer agreement for image grading (n=60)	-0.8 (-1.8, 0.14)	No	Yes[†]	-8.2	6.5
Inter-observer agreement for images acquired by two technicians (n=60)	-0.3 (-1.72, 1.15)	No	No	-11.1	10.5
Intra-observer agreement for images by the same operator(n=60)	0.6 (-1.92, 0.79)	No	No	-10.9	9.7

*All measurements are in percentages, CI –Confidence Interval, [†]Regression equation (y=0.81-0.04x, p=0.0099)

Related publication: Ho SW, **Baskaran M,** Zheng C, Tun TA, Perera SA, Narayanaswamy AK, Friedman DS, Aung T. Swept source optical coherence tomography measurement of the iris-trabecular contact (ITC) index: a new parameter for angle closure. Graefes Arch Clin Exp Ophthalmol. 2013 Apr;251(4):1205-11.

Figure 3: Bland-Altman plots show the mean difference and 95% limits of agreement for intra-observer agreement (a) and inter-observer agreement (b) for Iris Trabecular Contact index (ITC index) if same images are graded. Arrow indicates a single outlier.

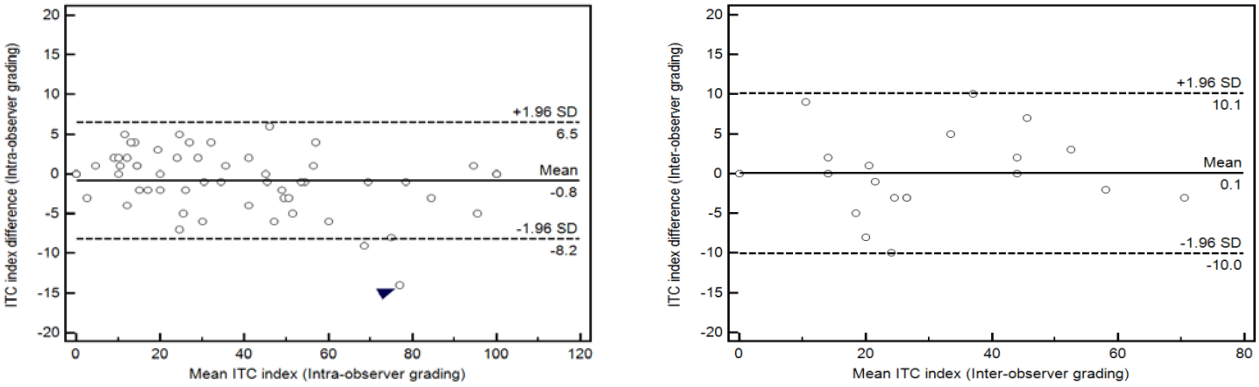

Figure 4: Bland-Altman plots show the mean difference and 95% limits of agreement for intra-observer agreement (a) and inter-observer agreement (b) for Iris Trabecular Contact index (ITC index) using images acquired at different examinations. Arrows indicate single outliers.

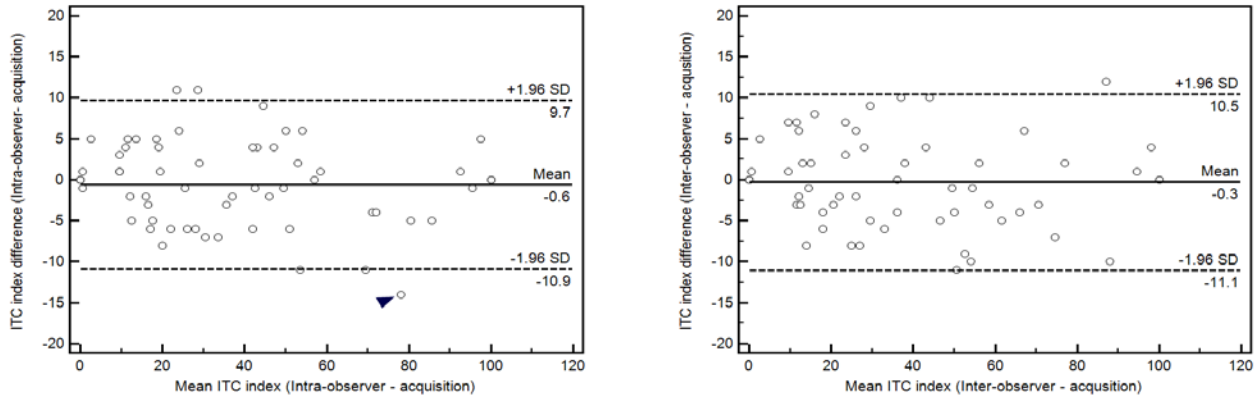

examiner grading the images. However, this could be an initial learning curve for the grader as we did not find a significant proportional bias in the other agreement analyses. Further, the regression plots for the absolute residuals did not show any significant bias in the measurements. The results suggest that the agreement for grading of images was within clinically acceptable limits.

Agreement of ITC index: Image acquisition

The inter-observer agreement of ITC index for image acquisition showed that the mean difference (95% LOA) was -0.3% (-11.1, 10.5) and COV was 13.12%. The intra-observer agreement of ITC index (image acquisition) showed that the mean difference (95% LOA) was 0.6% (-10.9, 9.7) and COV was 9.41% (**Table 3, Figure 4a&b).** There was no fixed bias or proportional bias noted in the repeated measurements. The regression plots for the absolute residuals did not show any significant bias in the measurements. The results suggest that image acquisition by different examiners may lead to more variations in the ITC index compared to a single examiner. However, the differences appear to be within clinically acceptable limits.

ROC analysis

The AUC for ITC index diagnostic performance to detect gonioscopic angle closure was 0.804 (95% Confidence Interval [CI], 0.681, 0.895). The optimal threshold with the best performance was for ITC index >29% with a sensitivity of 75.86 (56.5, 89.7), specificity of 70.97 (52, 85.8), positive likelihood ratio of 2.61 (1.5, 4.7) and negative likelihood ratio of 0.34 (0.2, 0.7).

Discussion

We obtained repeatable measurements of the extent of angle closure, using SSOCT to image the entire circumference of the angle. Both inter- and intra-observer agreement of ITC

measurements were good and clinically acceptable, using images graded or acquired twice on the same person by the same examiner and also by two different examiners. Typical values were found to be 30% (or 108°) apart between open and closed angles, with measurement errors more than 10% (or 36°) being very rare, indicating that the ITC index may be useful for discrimination of even borderline closed angle eyes. The image quality for both sets of images obtained in the first and second examinations were similar, suggesting that there is minimal learning curve for performing this imaging. As far as we are aware, this is the first study examining the agreement of the ITC index measured by SSOCT.

Liu et al[10] evaluated angle parameters measured by SSOCT and found that there was good inter- and intra-observer agreement for angle measurements such as the angle opening distance (AOD), the trabecular iris space area (TISA) and the trabecular-iris angle (TIA). However, they noted that variability in the location of measurement, the axial length, iris thickness and angle width are factors which may affect the agreement of angle measurements.

Various researchers have attempted three-dimensional quantitative analysis of the angle as an alternative method to qualitative gonioscopic assessment. Scheimpflug photography, introduced in the 1970s underwent several modifications and in recent years, the rotating Scheimpflug camera is available as a device for rapid 3-dimensional analysis of the anterior chamber.[11] However, the analysis has limitations as the angle cannot be fully visualized with visible light-based imaging. All the OCT based anterior segment imaging modalities currently utilize a few cross sectional images and assess the angle qualitatively or by certain surrogate quantitative parameters. This may result in inaccurate quantification of angle closure. The novelty of the ITC index lies in the fact that it utilizes 360° angle data as a measure of the percentage of angle closure and represents this information in the form of a chart, similar to a

goniogram. This method of analysis can be easily interpreted for clinical diagnosis and follow-up in angle closure disease, provided it is found to be reliable and accurate. However, manually marking the SS and EP in all images is a tedious and time-consuming process, making clinical use of the ITC index limited. Further refinement and automation of the ITC index will be necessary before the index can be used as a summary measure for angle closure evaluation, especially in clinical decision making and follow-up of patients.

There are several limitations to our study. Firstly, the SS could not be determined in some frames. When we were unable to locate the SS, the software extrapolated the location of SS based on the adjacent SS points. None of the eyes were excluded or rejected for the analysis since we were able to mark at least 7 plots (as per the manufacturer's requirement) with the semi-automated software, hence, the image analysis criterion was fulfilled for all subjects' images. Secondly, we chose 16 instead of 128 frames for the analysis. Sixteen frames offer a reasonable surrogate because if we chose 128 frames, it would be too time-consuming for the examiner to plot all the points in each frame. Even though each frame represented 11.25 degrees of the angle, and was adequate for the analysis of the ITC index, analyzing 128 frames may have yielded a more accurate analysis, not just by including more meridians for analysis, but also by decreasing the invisible range. Thirdly, poor quality images were, likely due to movement of the subject or eyelids during image capture. Capturing images proved ergonomically cumbersome at times. The difficulty lay in capturing the image over the large image console whilst simultaneously stretching to open the subjects' eyelids. Liu et al[10] instructed participants to pull down their own lower eyelids while the technician elevated the upper eyelids to circumvent these issues. However, any method of manual stretching of eyelids might introduce artifacts in the angle configuration by exerting some pressure on the globe. Fourthly, inherent to all OCT scans

is the inability to distinguish between appositional and synechial closure. Lastly, the agreement demonstrated in this study may not be replicated in a clinic-based scenario because of the rigid inclusion criteria used in this study where in eyes with pathologies such as corneal opacity were excluded. Eyes with dense arcus and pterygium can result in degradation of images and identification of landmarks such as SS and EP may not be determined with precision.[6] In relation to the feasibility of the ITC as a measure of the proportion of angle closure, we found that up to 8.3% of eyes had ≥50% of invisible range. We may overcome this limitation if more frames are included for angle assessment in ITC analysis; however, the SS and EP markings need to be automated to enable such a task. It may also be necessary for the manufacturers to provide better image processing algorithms to overcome this problem.

In conclusion, we found good and clinically acceptable intra- and inter-observer agreement of the measurement of the ITC index using SSOCT. The ITC index has the potential to provide objective information about the extent of circumferential angle closure and we consider the assessment of agreement as a first step towards further clinical applications in the future. However, current requirements for manual grading of the images and lack of automation of ITC index limit the clinical utility of this application.

4.2 Comparison of Iris-trabecular index with Gonioscopy

Abstract

Purpose. To evaluate the diagnostic performance of the iris trabecular contact (ITC) index, a measure of the degree of angle closure, using swept source optical coherence tomography (SSOCT, CASIA SS-1000, Tomey Corporation, Nagoya, Japan) in comparison to gonioscopy.

Methods. SSOCT 3-dimensional angle scans, that obtain radial scans for the entire circumference of the angle, were performed under dark conditions and analyzed using customized software by a single examiner masked to the subjects' clinical details (N=140). The ITC index was calculated as a percentage of the angle that was closed on SSOCT images. First-order agreement coefficient statistics (AC1) and area under the receiver operating characteristic (AUC) curve analyses were performed for angle closure based on ITC index in comparison to gonioscopy.

Results. Study subjects were predominantly Chinese (95.7%) and female (70.7%) with a mean age of 59.2 (standard deviation, SD = 8.9) years. The median ITC index for gonioscopically open angle eyes (n=108) was 15.24% and for closed angle eyes (n=32) was 48.5% (p=0.0001). The agreement for angle closure based on ITC index cut-offs (>35% and ≥50%) and gonioscopic angle closure was 0.699 and 0.718 respectively. The AUC for angle closure detection using ITC index was 0.83 (95% confidence interval, CI = 0.76, 0.89) with ITC index >35% having sensitivity of 71.9% and specificity of 84.3%.

Conclusions. The ITC index is a summary measure of the circumferential extent of angle closure as imaged with SSOCT. The index had moderate agreement and good diagnostic performance for angle closure with gonioscopy as the reference standard.

The aim of this study was to examine the agreement and diagnostic accuracy of the ITC index measured using SS-OCT, compared to the clinical reference standard, gonioscopy.

Methods and Statistical analysis were as described earlier (n =152). In addition, the sensitivity, specificity, positive predictive value (PPV), negative predictive value (NPV), positive and negative likelihood ratios (+LR and –LR) for the best ITC cut-off values (>35%, ≥50% and >70%) were reported for various quadrant closure definitions. We have chosen optimal ITC index cut-off based the best sensitivity and specificity values given by the statistical software (>35%), mean value (≥50%) and providing an arbitrary stricter criterion for angle closure (>70%). Further, sensitivity values and associated criteria for fixed specificities were calculated for ITC index against two quadrant closure definition on gonioscopy.

Results

Out of the 152 subjects recruited for the study, the image from one subject was not analyzable due to poor scan quality, and 11 others had more than 180° "invisible range" (unable to identify scleral spur) and so we excluded these eyes from analysis leaving 140 (92.1%) eyes eligible for final analysis. There was no significant difference in the proportion of open vs closed angles on gonioscopy among the excluded eyes (6 each). The mean age of the 140 included subjects was 59.2 (standard deviation, SD = 8.9) years and the majority of subjects were Chinese (134/140, 95.7%) and female (99/140, 70.7%). There were 32 (22.9%) subjects who had gonioscopic angle closure, of whom 29 were primary angle closure suspects and 3 had primary angle closure glaucoma.

Closed angle subjects were older than open angle subjects (63.7 versus 57.8 years, $p < 0.05$), had higher ITC index (50.0 versus 17.2, $p=0.0001$) and had higher "invisible range" ($p<$

Table 4: Comparison of clinical and imaging characteristics of gonioscopically open and closed angle subjects (two quadrant definition of angle closure)

	Open Angle (n=108)	**Closed Angle (n=32)**
Age (years)**	57.8 (8.8)	63.7 (8.0)
Eye (Right:Left)	68:40	19:13
Gender (Male:Female)	33:75	8:24
Ethnicity* (Chinese:Malay: Indian:Others)	106:0:2:0	28:2:1:1
ITC index (percentage)**		
Mean (SD)	17.2 (19.3)	50.0 (28.9)
Median (min-max)	15.2 (0-74)	48.5 (0-100)
Invisible Range* (degrees)		
Mean (SD)	34.6 (48.0)	54.7 (47.4)
Median (min-max)	0 (0–170)	44 (0-170)
Median number of quadrants closed on gonioscopy	0 (0-1)	3 (2-4)

* = $p < 0.05$, ** = $p < 0001$; ITC index – Irido trabecular contact index; min – minimum; max – maximum.

Table 5: Distribution of angle closure and open angles between gonioscopic quadrants of angle closure vs iris-trabecular contact index (ITC) cut-offs

Gonioscopic quadrants of angle closure	**ITC>35%***		**ITC≥50%***		**ITC>70%***		**Total**
	Open	**Closed**	**Open**	**Closed**	**Open**	**Closed**	
0	87	11	93	5	97	1	98 (70.0%)
1	4	6	6	4	9	1	10 (7.1%)
2	1	1	2	0	2	0	2 (1.4%)
3	7	10	13	4	15	2	17 (12.1%)
4	1	12	3	10	7	6	13 (9.3%)
Total	100 (71.4%)	40 (28.6%)	117 (83.6%)	23 (16.4%)	130 (92.9%)	10 (7.1%)	140 (100%)

*p<0.0001 (Chi-square for trend) for all cut-off values

0.05, **Table 4**). The number of quadrants closed on gonioscopy was positively correlated with the ITC index (Spearman's $\rho = 0.578$, p=0.0001).

Table 5 shows the comparative distribution of open and closed angles between gonioscopy (quadrant-wise) and various ITC cut-offs. Even when using ITC cut-off of ≥50%, 6.4% (9/140) of eyes showed closed angles with SSOCT, while the gonioscopist noted none or one quadrant closure. The trend for increasing number of closed angles on SSOCT was noted for all cut-off values as the number of closed quadrants increased on gonioscopy (Chi-square for trend; p<0.0001).

Table 6, shows the agreement for two ITC index cut-off values (>35% and ≥50%) with different quadrant-wise definitions of angle closure. The agreement for ITC index (>35% and ≥ 50%) and 4 quadrants of closed angles on gonioscopy was moderate to good for the 2 cut-off values (0.689 for ITC >35% and 0.842 for ITC≥50%). We considered AC1 statistic to Kappa statistic as the prevalence rates for positive classification, in this instance, closed angles, was low. The AC1 statistic for a two quadrant definition of angle closure for >35% and ≥50%, were found to be moderate at 0.699 and 0.718 respectively. Good agreement (AC1 = 0.842) was seen for a higher cut-off value of ≥50%, as the severity of gonioscopic angle closure increased to four quadrant closure. There was slight over estimation of closed angles (32/140 vs 40/140, p=0.17, McNemar test) for ITC >35% and under estimation (32/140 vs 23/140, p=0.12) for ITC ≥50%, for two quadrant closure on gonioscopy.

The classification of open vs closed angles between gonioscopy and ITC index cut-offs was found to be statistically similar across various definitions except for one quadrant closure definition with ≥50% cut-off value, (42/140 vs 18/140, p=0.0008, McNemar test) and for four

Table 6: Agreement between the various definitions of iris-trabecular contact (ITC) index by swept source optical coherence tomography vs gonioscopy for angle status

Gonioscopic angle closure	Agreement (AC1) between gonioscopy vs ITC index	
	ITC >35%	ITC ≥50%
1 or more quadrants closed*	0.71	0.68
2 or more quadrants closed	0.70	0.72
3 or more quadrants closed	0.69	0.73
4 quadrants closed**	0.69	0.84

AC1 – First order agreement coefficient statistics; *p value = 0.0008 for comparison with ITC index ≥50% (McNemar test); ** p value < 0.0001 for comparison with ITC index >35% (McNemar test)

Table 7: Diagnostic performance indicators for different cut-off values of irido trabecular (ITC) index with gonioscopic angle closure definitions

Gonioscopic angle closure	AUC	ITC index cut-off criteria	Sensitivity (95% CI)	Specificity (95% CI)	PPV (95% CI)	NPV (95% CI)	+LR (95% CI)	-LR (95% CI)
1 or more quadrants closed	0.855 (0.786-0.909)	**>35%**	**69.05 (52.9-82.4)**	**88.78 (80.8-94.3)**	**72.5 (55.9-85.5)**	**87 (78.8-92.9)**	**6.15 (3.4-11.1)**	**0.35 (0.2-0.6)**
		≥50%	42.86 (27.7-59)	94.9 (88.5-98.3)	78.3 (55.7-92.8)	79.5 (71-86.4)	8.40 (3.3-21.1)	0.6 (0.5-0.8)
		>70%	21.43 (10.3-36.8)	98.98 (94.4-100)	90 (55.5-99.7)	74.6 (66.2-81.8)	21 (2.7-160.6)	0.79 (0.7-0.9)
2 or more quadrants closed	0.829 (0.756-0.887)	**>35%**	**71.87 (53.3–86.3)**	**84.26 (76-90.6)**	**57.5 (40.9-73%)**	**91 (83.6-95.8)**	**4.57 (2.8 - 7.4)**	**0.33 (0.2 - 0.6)**
		≥50%	43.75 (26.4-62.3)	91.67 (84.8-96.1)	60.9 (38.5-80.3)	84.6 (76.7-90.6)	5.25 (2.5-11)	0.61 (0.4-0.8)
		>70%	25 (11.5-43.4)	98.15 (93.5-99.8)	80 (42.2-97.9)	81.5 (73.8-87.8)	13.5 (3-60.4)	0.76 (0.6-0.9)
3 or more quadrants closed	0.828 (0.755-0.886)	**>35%**	**70.97 (52-85.8)**	**83.49 (75.2-89.9)**	**55 (38.5-70.7)**	**91 (83.6-95.8)**	**4.48 (2.8-7.2)**	**0.32 (0.2 - 0.6)**
		≥50%	45.16 (27.3-64)	91.74 (84.9-96.2)	60.9 (38-80.7)	85.5 (77.8-91.3)	5.7 (2.7-11.9)	0.58 (0.4-0.8)
		>70%	25.81 (11.9-44.6)	98.17 (93.5-99.8)	80 (44.4-97.5)	82.3 (74.6-88.4)	14.67 (3.3-65.5)	0.75 (0.6-0.9)
4 quadrants closed	0.907 (0.846-0.949)	**>35%**	**92.31 (64-99.8)**	**77.95 (69.7-84.8)**	**30 (16.6-46.5)**	**99 (94.5-100)**	**4.19 (2.9-6)**	**0.099 (0.01-0.7)**
		≥50%	76.92 (46.2-95)	89.76 (83.1-94.4)	43.5 (23.2-65.5)	97.4 (92.7-99.5)	7.51 (4.1-13.6)	0.26 (0.1-0.7)
		>70%	46.15 (19.2-74.9)	96.85 (92.1-99.1)	60 (26.2-87.8)	94.6 (89.2-97.8)	14.65 (4.7-45.3)	0.56 (0.3-0.9)

Area under the receiver operating characteristic curve (AUC) was based on Delong et al, 1988; CI-Confidence Interval; PPV-Positive Predictive Value; NPV-Negative Predictive Value; +LR-Positive Likelihood Ratio; -LR-Negative Likelihood ratio

Figure 5: The receiver operating characteristic curve (ROC) for Iris trabecular contact index against the gonioscopic reference standard.

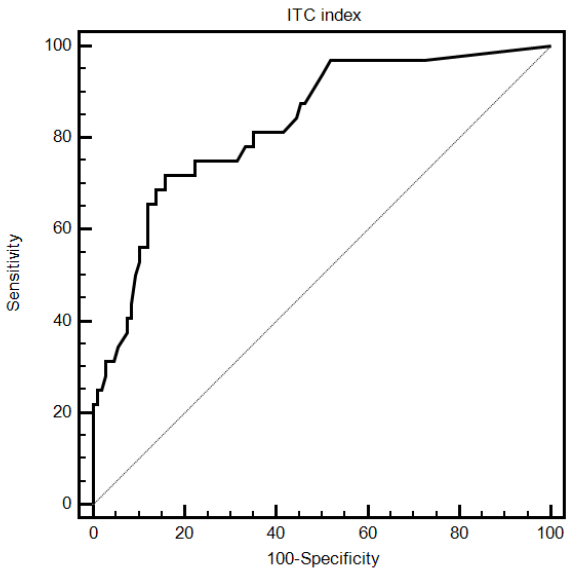

Table 8: Estimated sensitivity at fixed specificities and the associated iris-trabecular contact (ITC) index cut-off values for angle closure (for 2 quadrant closure on gonioscopy)

Specificity	Sensitivity (95% CI)	ITC index cut-off criterion
80	71.87 (50-81.25)	>31.4
90	52.5 (24.65-75.27)	>47.2
95	32.5 (15.63-54.37)	>58.2
97.5	27.19 (9.38-41.65)	>69.3

CI – Confidence interval

Related publication: Baskaran M, Ho SW, Tun TA, How AC, Perera SA, Friedman DS, Aung T. Assessment of circumferential angle-closure by the iris-trabecular contact index with swept-source optical coherence tomography. Ophthalmology. 2013 Nov;120(11):2226-31.

quadrant closure definition with >35% cut-off value (13/140 vs 40/140, p<0.0001, McNemar test, **Table 6**.

Table 7 shows the diagnostic performance of the various ITC index values in the form of AUC, sensitivity, specificity and predictive values. The diagnostic accuracy was good between 0.83 and 0.91 for various definitions of angle closure suggesting uniform performance. The AUC using the two quadrants closed on gonioscopy definition of angle closure was 0.83 (95% CI, 0.76-0.89, **Figure 5**). ITC index of >35% was found to be optimal for the best classification for angle closure across various gonioscopic angle closure definitions with a sensitivity of 71.9% (95% CI, 53.3-86.3%) and a specificity of 84.3% (95% CI,76-90.6%) for two quadrant angle closure. The predictive values and likelihood ratios were provided in **Table 7** for the various definitions. For a two quadrant closure definition on gonioscopy, if the ITC index cut-off of >35% was chosen, the NPV was 91% with a moderate +LR of 4.57. If specificity is fixed at 90%, then the sensitivity dropped to 52.5% (95% CI, 37.4-68.5%, **Table 8**.

Discussion

This study uniquely compares two types of circumferential angle assessment. The ITC index produced by the SSOCT device had moderate to good agreement with gonioscopic angle closure findings, and has good overall diagnostic performance for detecting angle closure.

We found that the ITC index can grossly simulate gonioscopic interpretation in some ways such as circumferential interpretation of angle status, easier interpretation of the extent of angle closure and a pictorial depiction of angle closure, similar to a goniogram. However, as the ITC index is a compilation of multiple non-contact cross-sectional images, it cannot identify synechial angle closure as compared to indentation gonioscopy. Gonioscopy and the SSOCT

device use slightly different landmarks to define angle closure. The ITC index is based on "any" ITC anterior to the SS, while gonioscopic angle closure requires that the pigmented posterior trabecular meshwork not be visible. The mean ITC index for two quadrant closure on gonioscopy in our study was 50% and the best cut-off value for diagnostic performance was found to be >35% with only 4 subjects (2.8%) having an ITC index of 100%. Furthermore, 12% of eyes (17/140) were found to be closed for >35% on SSOCT compared to one quadrant or less on gonioscopy. This higher rate of angle closure with the ITC index suggests that gonioscopy may miss angle closure in some patients and this could be due to inadvertent opening of the angles by compression from the gonioscopy lens, or pupil constriction from slit lamp illumination during gonioscopy. The cut-off values mentioned in this study might likely vary if more frames (>16) were added to the analysis. However, we felt that more frames may be difficult to analyze or not feasible in a clinical setting. In this context, it may be useful to have automated solutions for the entire analysis, where there would be no dependency on landmarks.

There are several limitations to our study. SS could not be identified in some frames, resulting in the "invisible range" to ≥50% in 8.3% eyes. However, the proportion of gonioscopically open and closed angles was similar in the excluded eyes and so this would not have unduly affected the overall diagnostic performance of the ITC index. We carefully removed such images with excess invisible range, and included the manufacturers' recommended minimum of 7 frames in the analysis. Capturing images proved ergonomically cumbersome at times, due to movement of the globe or eyelids during image capture. Another discrepancy lies in the way that the gonioscopy and SSOCT assess the amount of angle closure respectively. Whereas the gonioscopist grades the extent of angle closure by quadrant, the ITC index measures in degrees of closure over the entire circumference of the angle. Overall, while the diagnostic

performance for the ITC index was found to be good across various definitions of angle closure, the predictive values, positive and negative likelihood ratios appear to be moderate and variable.

In conclusion, we describe for the first time, moderate agreement and good diagnostic performance of a novel parameter, the ITC index, assessed using SSOCT, for the interpretation of the extent of angle closure, in comparison to gonioscopy as the reference standard. We believe that with further improvement and automation of the ITC index measurement, SSOCT may be a novel and improved way to clinically document the extent of angle closure over 360 degrees.

4.3 Automated grading of angle closure for 3-D SSOCT images

Abstract

Purpose. To identify angle closure with SSOCT images using image processing and machine learning based framework.

Methods. In digital SSOCT scans, the method automatically localizes the anterior chamber angle (ACA) region, which is the primary structural image cue for clinically identifying angle closure. Next, visual features are extracted from this region to classify the angle as open angle (OA) or angle-closure (AC).

Results and Conclusion. This proposed method has three major contributions that differ from existing methods. First, the ACA localization from OCT images is fully automated and efficient for different ACA configurations. Second, it can directly classify ACA as OA/AC based on visual features and other algorithms, which is different from previous work for ACA measurement that relies on clinical features. Third, it demonstrates that higher dimensional visual features outperform low dimensional clinical features in terms of angle closure classification accuracy.

From tests on a clinical dataset comprising of 3840 images, the proposed method only requires 0.26s per image. The framework achieves a 0:91±0.051 AUC (area under curve) value and 80.3%±7.4% balanced accuracy at 85% specificity, which outperforms existing methods based on clinical features.

Introduction

Several methods are utilized to automate the ACA assessment in literature. Examples are edge detection with line fitting,[1] Schwalbe's line bounded area (SLBA),[12] image feature based classification, such as Histograms of Oriented Gradients (HOG)[13] or Histogram Equalization Pixels (HEP)[13] feeding into machine learning tools. However, they are not fully automated and lack accuracy.[13]

We worked in collaboration with Institute of Infocomm Research (I2R, A-STAR) team to develop automated SSOCT software based on feature extraction and reconstruction based approach based on Similarly-Weighted Linear Reconstruction (SWLR) in addition to several other algorithms.

Methods

A total of 3840 images were obtained from circular SSOCT scan videos, each with 128 frames, of 30 patient eyes, 16 of which are from eyes with closed angles (based on two quadrant angle closure by gonioscopy) and the other 14 with open angles. The tests were based on classification of each individual ACA, with the ground truth label provided by an ophthalmologist. Approximately, 50% images were considered as training data and the rest as test data for validation.

The main steps involved in this work are: **(Figure 6)**

a) Preprocessing to eliminate corneal artifacts
b) Alignment of the frame by (a) Rotation adjustment, (b) horizontal shift adjustment, (c) vertical shift adjustment
c) ACA vertex localization
d) ACA classification using reconstruction based methods mentioned above

Figure 6: Steps involved in automation of 3 dimensional SSOCT image analysis (a) Corneal reflex removal, (b) Rotation registration, (c) Anterior chamber angle localization and (d) Average binarized image ready for classification

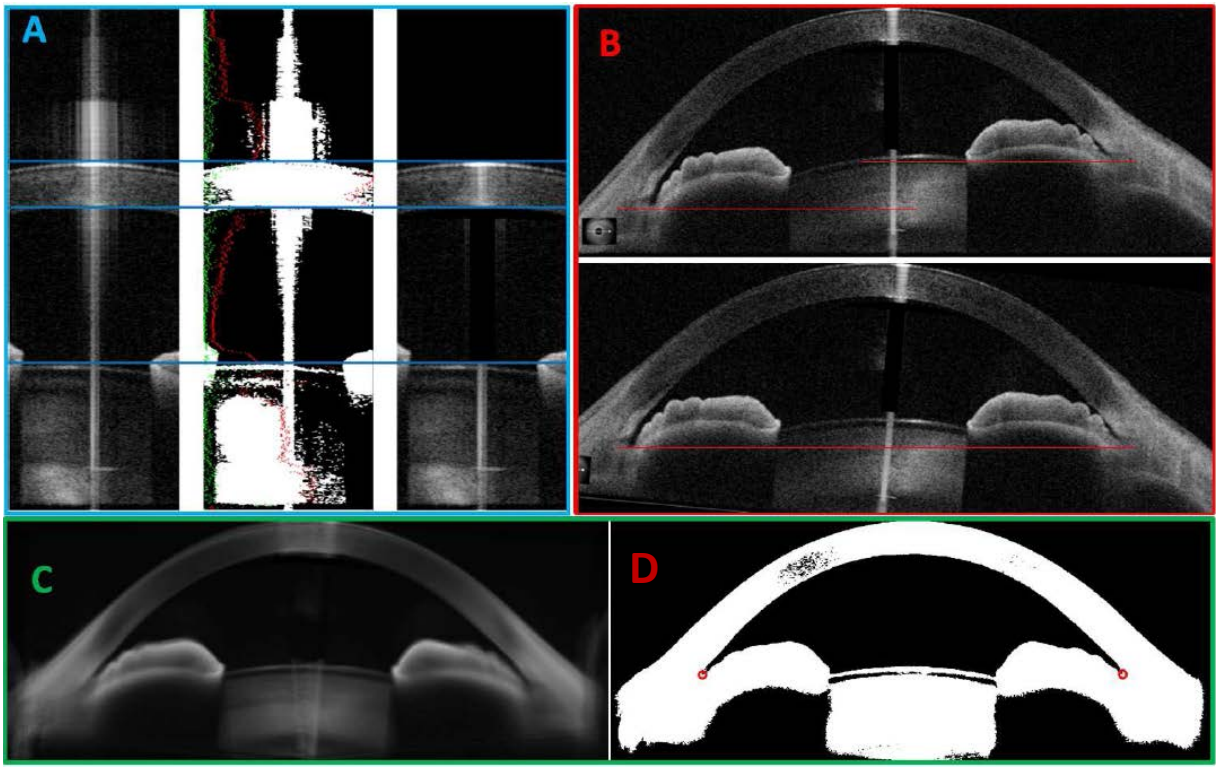

Related publication: Xu Y, Liu J, Cheng J, Lee BH, Wong DW, **Baskaran M,** Perera S, Aung T. Automated anterior chamber angle localization and glaucoma type classification in OCT images. Conf Proc IEEE Eng Med Biol Soc. 2013;2013:7380-3.

Our proposed method (SWLR) was compared with other Machine Learning Algorithms (MLA, which are algorithms that can learn from input data and build models for decision making), such as locally linear embedding (LLE) method, k-nearest neighbours (k-NN), HEP and HOG methods. In brief, LLE is a pattern recognition algorithm which identifies nearest neighbours of a region of interest and computes a set of weights for each point that best describe the point as a linear combination of its neighbouring points. Finally it uses optimization technique to find low-dimensional embedding of points to describe the area as linear combination of neighbouring points. k-NN is the simplest of pattern recognition MLAs and uses non-parametric method for classification and regression of the nearest points. HEP and HOG are methods which uses histogram based visual feature classification.

Statistical analysis was performed using the classification outputs from the MLAs (open or closed angles) in comparison to the clinical ground truth binary classification by glaucoma fellowship trained examiner (Author). AUC, Balanced accuracy (Sens+Spec/2) at 85% specificity was reported.

Results

The AUC for SWLR method was 0.905±0.051, with balanced accuracy of 80.3±7.4 at 85% specificity for detection of angle closure in comparison to clinical grading of images. SWLR outperformed LLE, k-NN, HEP and HOG methods (AUC ranging from 0.838 to 0.888).

The speed of ACA localization was 1.2 seconds per image, which was slower than other methods but robust in accuracy.

Discussion

We have successfully developed a fully automated software tool (named AGAR) for

analysis of 360° circumferential SSOCT scans which can be incorporated in the OCT device to be used clinically. The accuracy of the algorithm outperformed other MLAs..

The proposed automated ACA analysis system has the following novelties:

1) The proposed angle closure detection system is fully automated and having high accuracy and robustness.

2) The cross-sectional ASOCT frame alignment is effective and efficient, which can be integrated into the OCT instrument. This module is good for image stabilization, speckle reduction, ACA localization and alignment, thus can improve overall performance from system level.

3) The proposed SWLR (similarity-weighted linear reconstruction) shows higher ACA classification accuracy and it is also very efficient.

4) The proposed dictionary expansion strategy leads to better translational alignment between reference and test images, thus further improving the ACA classification accuracy through reconstruction approaches.

Limitations of this automated software are that the speed of processing is slower in classifying 128 scans (even though it is less than a minute at present). Further, it can classify as “open” or “closed” angles, but cannot provide intermediate options. The speed can be refined by optimizing number of scans that need to be processed so that similar accuracy of diagnosis is achieved.

In conclusion, the demonstration of an accurate software tool for automated analysis of circumferential SSOCT scans can provide a viable option for screening strategies for angle closure detection. Further validation of this software is required to compare with reference standard gonioscopy.

4.4 References (Chapter 4)

1. Leung CK, Yung WH, Yiu CK, Lam SW, Leung DY, Tse RK, Tham CC, Chan WM, Lam DS. Novel approach for anterior chamber angle analysis: anterior chamber angle detection with edge measurement and identification algorithm (ACADEMIA).Arch Ophthalmol 2006;124:1395–1401.
2. Foster PJ, Johnson GJ. Glaucoma in China: how big is the problem? Br J Ophthalmol 2001;85:1277–1282.
3. Wu RY, Nongpiur ME, He MG, Sakata LM, Friedman DS, Chan YH, Lavanya R, Wong TY, Aung T. Association of narrow angles with anterior chamber area and volume measured with anterior-segment optical coherence tomography. Arch Ophthalmol 2011;129:569-574.
4. Congdon N, Wang F, Tielsch JM. Issues in the epidemiology and population based screening of primary angle-closure glaucoma. SurvOphthalmol 1992;36:411-423.
5. Yi JH, Hong S, Seong GJ, Kang SY, Ma KT, Kim CY. Anterior chamber measurements by pentacam and AS-OCT in eyes with normal open angles. Korean J Ophthalmol 2008;22:242-245.
6. Narayanaswamy A, Sakata LM, He MG, Friedman DS, Chan YH, Lavanya R, Baskaran M, Foster PJ, Aung T. Diagnostic performance of anterior chamber angle measurements for detecting eyes with narrow angles: an anterior segment OCT study. Arch Ophthalmol 2010;128:1321-1327.
7. Wong HT, Lim MC, Sakata LM, Aung HT, Amerasinghe N, Friedman DS, Aung T. High-Definition Optical Coherence Tomography Imaging of the Iridocorneal Angle of the Eye. Arch Ophthalmol 2009;127:256-260.

8. Wylegała E, Teper S, Nowinska AK, Milka M, Dobrowolski D. Anterior segment imaging: Fourier-domain optical coherence tomography versus time-domain optical coherence tomography. J Cataract Refract Surg 2009;35:1410-14.
9. Sasidharan R. South East Asia Glaucoma Interest Group. Appendix 6A. Gonioscopy. Asia Pacific Glaucoma Guidelines. Scientific Communications International, HongKong 2008.
10. Liu S, Yu M, Ye C, Lam DS, Leung CK. Anterior chamber angle imaging with swept-source optical coherence tomography: an investigation on variability of angle measurement. Invest Ophthalmol Vis Sci 2011;52:8598-8603.
11. Rabsilber TM, Khoramnia R, Auffarth GU. Anterior chamber measurements using Pentacam rotating Scheimpflug camera. J Cataract Refract Surg 2006;32:456-9.
12. Tian J, Marziliano P, Wong HT. automatic detection of Schwalbe's line in the anterior chamber angle of the eye using HD-OCT images. In Proc. 32nd Annual International Conference of the IEEE Engineering in Medicine and Biology Society, 2010:3013-16.
13. Xu Y, Liu J, Tan NM, Lee BH, Wong D, Baskaran M, Perera S, Aung T. Anterior Chamber Angle Classification Using Multiscale Histograms of Oriented Gradients for Glaucoma Subtype Identification. In Proc. 34th Annual International Conference of the IEEE Engineering in Medicine and Biology Society, 2012:3167–70.

Chapter 5. Dual mode irido-corneal angle imaging probe (Aim 3)

5.1 Development of a dual mode (optical + infrared) angle imaging probe

Abstract

Purpose. To design and develop an imaging probe integrating a miniaturized CCD camera, LED light source and an infrared laser source, which enables evaluation of the irido-corneal region of the eye in dual mode such as in visible spectrum and infrared light.

Methods. The efficiency of the prototype probe instrument was illustrated in cadaveric porcine eyes, live rabbit eyes and primates.

Results. Clear delineation of the irido-corneal angle was achieved uniformly across different species' eyes using a coupling gel interface in contact mode at the limbus.

Conclusion. The proposed methodology and developed scheme is expected to find potential application in irido-corneal angle documentation, angle closure glaucoma diagnosis and management.

Introduction

Photographic based documentation allows eye care clinicians to document and refer to the earlier images for abnormalities in the anterior segment of the eye and angle. The RetCam™ was primarily designed for wide-field retinal imaging in children, specifically to document premature retinal growth in a condition called "retinopathy of prematurity". Later it was modified to document the anterior chamber angle in the form of EyeCam™ . However, imaging of the anterior chamber angle using EyeCam™ takes longer than gonioscopy (about 5-10 min per eye) and the device is more expensive than gonioscopy.

While visible light is used to document the angle structures, it can interfere with the pupil and angle configuration is then altered. Infrared light source can be a useful combination with visible light to document angle closure status accurately. A gel-assisted imaging technology for angle imaging using this dual mode probe was designed, in order to have an exclusive wide angle imaging probe, which is non-bulky, inexpensive and that can be attached to a slit lamp or as stand-alone, providing the flexibility to be used by a non-technical person.

Methods

Imaging system

The distal end to support the optics was designed in SolidWorks CAD software and built as a separate module. The centre channel has an internal diameter 3 mm and is meant for the 3mm X 3mm Micro CCD video camera (An IntroSpicio^{TM} 115, Medigus Ltd, Israel), which is employed as the image capturing device. The distal end has four channel slots of internal diameter 5 mm for light emitting diode (LED) illumination purpose that are drilled at an angle of 71^0 surrounding the camera slot so as to provide adequate illumination across the field of view of the micro CCD. The LEDs have viewing angle of 20^0. The slot angle and viewing angle of LEDs are such that the focus area of the camera has adequate illumination at the irido-corneal angle area for imaging capture.

The probe distal end which houses four illumination channels and one micro CCD conduit has a diameter of 26 mm for compactness and easy handling, with sufficient working distance from the eye. These slots house two white LEDs (visible), one Near Infrared (NIR) LED (945 nm) and one NIR laser source with wavelength of 808 nm. The fiber-coupled IR-diode laser (wavelength 808 nm) with a maximum power 2 mW was used in this study. The micro camera head is connected to the video controller that controls the video signal from and to the camera

head by a cable. The video controller controls the video signal from and to the camera head. The main input to the device is 100-240 AC (auto switching). This video camera system is used together with a white light source for eye imaging. The camera resolution was 500H x 582V with 140° FOV. **Figure 1** illustrates the photograph of the assembled probe and the distal end is shown in the inset.

The imaging device comprises an eye imaging probe having a central axis and a corneal contact surface. An imaging sensor is located at the central axis of the probe and has variable resolution at different depth which is configured for capturing the interior of the eye when contact surface is placed at the cornea or at limbus of the eye through a coupling gel. The four LEDs viewing angle and slot angle are designed such that the illumination region covers the targeted iridocorneal angle region optimally and provide required luminescence throughout the region. The positioning of LEDs is based on lambertian approach aimed to illuminate the targeted area in a controlled manner. To be precise, the uniform distribution of the light emitted by the source (combination of LEDs) has the same brightness or luminescence when viewed from any angle. Further, the brightness of LEDs can be controlled by using a potentiometer. The probe and sensors are connected to a processor which process captured images for display through a display panel or storage in a media storage device.

Preparation of sample and experimental animals

One randomly selected eye of four pigs (Sus scrofa domestica) was enucleated from the local abattoir and used within 6 hours of death. The ex-vivo samples were transported on ice to the laboratory to maintain its “freshness”. Each sample was fixed onto a custom eye holder, which was mounted on a translation stage with micrometer accuracy. Extra-ocular tissues such as the conjunctiva and lacrimal gland were removed from the samples.

Figure 1: Illustration of the developed dual-modality probe prototype

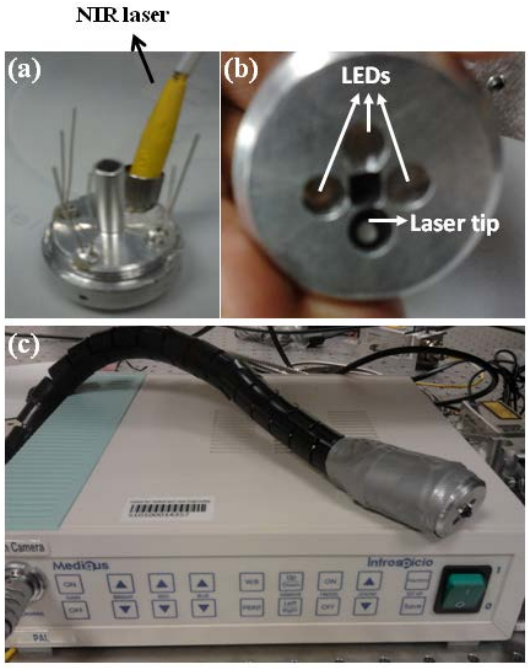

Figure 2: (a) Cadaveric porcine angle imaging using the probe, (b) and (c) Dual mode imaging in a live rabbit, (d) Rabbit angle imaging and (e) Primate angle imaging using the probe

a b c

d e

With due IACUC approval, live rabbits and primates were utilized in this study. The animals were given short acting anesthesia before imaging.

Results

The imaging probe is placed near the iridocorneal angle to image the opposite angle. With the use of a coupling gel (e.g. vidisic gel, Bausch & Lomb, NY, USA), the micro CCD camera can visualize structures in the anterior segment in a manner similar to direct gonioscopy. Users have the option to capture still images or record video stream from which images can be extracted at a later stage.

In our experiment, the porcine eye was chosen since it was much more available than those of nonhuman primates. Also, the porcine eye is similar in size to the human eye, approximately 22 mm in length compared to 24 mm in humans. The porcine eyes were obtained from a local abattoir immediately after the animal's death. The eye was fixed on a support device and imaging of anterior chamber was carried out. The camera used in this study has a field of view of 140^0. Hence imaging was performed on four different sides of eye to have a complete view of angle region inside eye. The obtained result on cadaveric porcine eye is shown in **Figure 2a**. The results from the dual mode imaging are illustrated in rabbit eyes in **Figures 2b and 2c. Figures 2d** illustrate a live rabbit eye angle while **Figure 2e** shows its comparison to a primate angle imaged using the probe. The resolution of the NIR angle images can be improved using a CCD camera sensitive to NIR range.

Such a device is safe for routine clinical use. According to International Commission on Non-ionizing Radiation Protection (ICNIRP), no evaluation for retinal hazard is required if the visible light has a luminance of less than 10,000 candela/m^2.[1] The LED sources such as the one used in our study (Maximum luminous Intensity 7000 mcd) has smaller degree of spatial

coherence than laser light sources leads to distribution of light over a relatively larger area are well within the maximum permissible limit. The cleaning and maintenance of the device includes customary chemicals such as 4% sodium hypochlorite solution for rinsing or 75% iso-propyl alcohol wipes for cleaning the tip of the camera lens. Thus, it does not require specialised cleaning solutions or protocol.

Discussion

With our proposed device, angle imaging can be carried out in a sitting position. The angle measurement for all four quadrants can be carried out in less than 2 minutes. No technical expertise is required for the assessment. This device is easily portable, non-bulky, can be attached to a slit lamp and can be connected to any desktop/laptop PC that is installed with the interfacing software. In the NIR laser mode imaging, the micro CCD we used was mainly meant for visible light. The reduced sensitivity in the NIR region affects the quality of image in the laser mode. It can be overcome by using a CCD which has sensitivity in the NIR region.

The clinical application of such a device is not just for the documentation of irido-corneal angle findings in angle closure disease, but also in pre-operatively assessing and documenting the ‘openness’ of the irido-corneal angle during micro invasive glaucoma surgeries (MIGS) such as various stent procedures and in goniosynechiolysis. There is a growing trend of using such devices to reside or in contact with the anterior chamber and angle; and there are possibilities of long-term migration or erosion of these devices. It is only prudent to have a good documentation of the position of these devices and the changes in the surrounding irido-corneal angle. The above described device can be an objective alternative for clinician documented

evidence in clinical practice, especially with an increasingly medico-legal environment. Further, such a device can be used in small to large animals for irido-corneal angle and anterior segment documentation as it does not depend on a fixed type of goniolens which restricts its use vis-à-vis variable corneal diameter in such animals.

Inclusion of infra-red mode of imaging with a wide-field choice along with the visible spectrum of light source as a dual mode will be an ideal combination. The infra-red mode will remove the effects of light on pupil dynamics (as present in gonioscopy, goniophotography and Eyecam) and allows imaging of the angle in its physiological state which is important for accurate diagnosis and documentation of angle closure. Wide-field imaging with visible light can image the entire angle and provide more qualitative details.

Conclusion

The imaging of anterior chamber angle region was performed using this novel imaging probe on cadaveric porcine eye, live rabbit eye and primates. The developed hand-held imaging system can be used to continuously display, capture and record images of structures within a patient's eye, such as the iridocorneal angle and anterior segment. The system can also be used for the management of glaucoma such that landmark identification monitors during device implantation procedures. This instrument can be a cheaper alternative to gonioscopic based angle detection which can permanently document the angle findings through a photographic imaging technique with good quality images and will be an important adjunct requirement in clinical ophthalmology.

Related publication: Shinoj VK, Murukeshan VM, **Baskaran M,** Aung T. Integrated flexible handheld probe for imaging and evaluation of iridocorneal angle. J Biomed Opt. 2015 Jan 1;20(1):16014.

5.2 References (Chapter 5)

1. I. C. O. N.-I. R. Protection, "Guidelines on limits of exposure to broad-band incoherent optical radiation (0.38 to 3 μm)," *Health Phys* 1997;**73**(3), 539-554.

Chapter 6: Summary and recommendations for future research

6.1 Summary

This thesis evaluated two main modes of circumferential angle imaging viz. EyeCam™ and Casia SSOCT for reproducibility of angle grading and agreement with gonioscopic evaluation of angle closure. Furthermore, the devices were compared with other existing imaging methods such as goniophotography and ASOCT for diagnostic performance in detecting gonioscopic angle closure. We also developed software tools to completely automate the angle grading using these two devices. Finally, we designed and developed a novel biomedical imaging device which is capable of angle evaluation in visible and infrared mode, which is an ideal combination for clinical use.

The salient findings from our various studies are discussed below:

Chapter 3: EyeCam and angle closure evaluation

1. EyeCam™ (manual grading) showed good agreement with gonioscopy for detecting quadrant wise angle closure. However, there was a higher rate of angle closure diagnosed by EyeCam™ compared to gonioscopy. EyeCam™ can demonstrate angle widening after LPI in serial documentation.

These findings provide us reliable indication that this device can be used for clinical application for evaluating the angle, (similar to gonioscopy) barring certain limitations such as PAS detection and misclassification rates. Serial documentation of angle for evaluating the effect of interventions such as LPI and surgical procedures can be useful in clinical practice. We have not evaluated the video mode of this device which can be useful for certain dynamic observations e.g. Valsalva manoeuvre, dark-light changes etc.

2. Eyecam^{TM} and goniophotography have similarly high sensitivity and specificity for the detection of gonioscopic angle closure.

The above finding is important evidence for the high diagnostic performance of EyeCam in detection of angle closure under clinical settings. This was achievable due to the nature of the documentation which is similar to gonioscopic evaluation. Further, EyeCam is more comfortable in comparison to goniophotography. However, the diagnostic performance for angle closure detection may not be the same, if an inexperienced technician operates the EyeCam. Validation studies are needed to gather further evidence in this regard.

3. The diagnostic performance of EyeCam^{TM} was better than ASOCT in detecting angle closure when gonioscopic grading was used as the reference standard. The agreement between the two imaging modalities was moderate.

ASOCT is a cross-sectional imaging modality, and used only at four angle points. This limited information, combined with artifacts and limitations in definition of angle closure between methods, could have led to this conclusion. The non-contact mode in ASOCT is an advantage over EyeCam use. Further, information from circumferential angle imaging such as SSOCT with robust definitions for angle closure, (closer to gonioscopic definition) may prove beneficial in bridging this gap.

4. Customized software for automated grading (Agate version 1.0, developed in collaboration with Institute of Infocomm research, Singapore) of EyeCam^{TM} angle images was found to have good agreement with gonioscopy. Human observation of the images may still be needed to avoid gross misclassification, especially in a few angle closure eyes.

The high performance of automated method of angle evaluation seen in this study can be very useful in clinic based angle closure detection. In high volume eye care centres, this may prove to be useful if integrated to a suitable goniophotographic device. However, as described, gonioscopic confirmation in very high risk individuals may still be needed due to artifacts reported in this study. Further, the cost of EyeCam and the need for training can be disadvantages in widespread use of this device.

Chapter 4: SSOCT and angle closure evaluation

5. The Iris trabecular contact (ITC) index is a summary measure of the circumferential extent of angle closure as imaged with SSOCT. The inter- and intra-observer agreement of the ITC index, as a measure of extent of angle closure using Casia SSOCT, was good.
6. The ITC index had moderate agreement and good diagnostic performance for angle closure with gonioscopy as the reference standard.

ITC index is a novel marker incorporated in Casia SSOCT by the manufacturer and it proves to be a useful method for angle closure evaluation in this study. However, the need for marking SS in multiple scans, the invisible range and the unstandardized method of identifying extent of ITC contact could have underestimated the true agreement, in comparison to gonioscopy. These issues need to be addressed before which this parameter can be clinically applicable.

7. The automated angle grading software for Casia SSOCT (AGAR version 1.0, developed in collaboration with Institute of Infocomm research) image scans achieved good

diagnostic performance in comparison to manual grading of images, and outperformed existing methods based on clinical features.

The automation of SSOCT angle image scans for detection of angle closure can change the clinical practice and may prove to be a major application in diagnosis and screening strategies in the management of PACG blindness. Optimisation of this tool is needed with further validation in comparison to reference standard gonioscopy.

Chapter 5: Development of a novel dual mode angle imaging device

8. A dual mode (visible + infrared laser), portable probe has been successfully designed and developed for angle imaging. The angle imaging capability was demonstrated in animal experiments.

We have completed the prototype which is capable of dual mode angle imaging, however, we need validation in human subjects. Once performed, the above combination is ideal to document angle in physiological state and there is scope for wider clinical application for this device if miniaturization and refinement are achieved with low cost.

Summary of comparison of current and novel imaging methods with gonioscopy:

The diagnostic performance for various methods in the detection of 2 quadrants gonioscopic angle closure in this study is summarized in **Table 1**, which includes the accuracy and precision components of diagnostic performance. It is to be noted that the gold standard for reference was gonioscopy in all these studies. From various literature reviews, we know that it is a flawed standard due to inaccuracies and subjectivity. However, in the lack of a viable and accepted alternative, we are committed to utilize it as the “gold standard” in our studies. The reader should keep this caveat in mind while coming to conclusions.

From the studies we conducted, we found that the **EyeCam** angle photography method can be **utilized in a clinical set up for angle closure detection** in high risk clinical patients, especially in combination with the automated tool. **Cross-sectional ASOCT imaging** has disagreement to gonioscopic grading of angle images, however, this could be due to differences in definition and effect of light on pupil dynamics. While the former problem needs to be refined for clinical application using ASOCT, the latter is an advantage for ASOCT as discussed earlier. However, the **lack of circumferential imaging is a major disadvantage** in the current ASOCT set up. **Casia SSOCT** with its automated analysis tool shows greater promise in terms of angle closure detection as well as a **screening tool in clinical set up and community for high risk population** (i.e. subjects above 50 years of age, Asians and subjects with family history of glaucoma). Further refinement of the automated tool in comparison to gonioscopy needs to be studied. However, the **cost of these instruments is a major disadvantage in implementation and cheaper devices need to be innovated**. One such attempt is the hardware device that we proposed in aim 3 (similar to EyeCam). There are attempts to make cheaper alternatives to the Casia SSOCT and if that succeeds, the gap in the unmet need for angle closure screening can be bridged to some extent.

The high accuracy and precision seen for the automated software tools is encouraging. This may indicate clinical relevance and adaptability as screening tools. The high NPV indicates exclusion of angle closure if the test is negative and this can be used to advantage in screening patients before dilatation.

Figure 1: Summary of AUC, Accuracy, Precision (PPV) and NPV for various diagnostic modalities

Comparison of modalities	**Method**	**AUC**	**Accuracy (%)**	**Precision (PPV%)**	**NPV (%)**
EyeCam Vs Gonioscopy* (n=140)	Manual	0.974	94.29	94.91	93.83
Agate Vs Gonioscopy (n=140)	**Automated**	**0.923**	**87.14**	**82.09**	**91.78**
ASOCT Vs Gonioscopy (n=93)	Manual	0.847	77.42	66.07	94.59
ITC index Vs Gonioscopy (n=140)	Manual	0.829	81.43	71.88	84.26
AGAR (SSOCT) Vs Clinical grading of images (n=3840)	**Automated**	**0.91**	**80.3**	**84.69**	**83.33**

*Gonioscopic angle closure defined as 2 quadrants of angle closure; AUC - Area under the receiver operating characteristic curve; PPV – Positive predictive value; NPV – Negative predictive value

6.2 Main strengths and limitations of the studies

Strengths: Standard definitions and grading systems were adopted for investigations performed in this study. Data from subjects used in testing phase of the software tools were not utilized in the validation phase. A systematic approach was adopted in evaluating the diagnostic methods in comparison to gonioscopy. Careful quality control was adopted in excluding images with artifacts. However, we found that we were able to include acceptable number of subjects in analysis. Masking the gonioscopist from imaging technician helped in avoiding misclassification bias. Clear clinical practice guidelines could be offered from the studies regarding the clinical application of the diagnostic tests. Automation of image grading using robust tools was a novel approach which could alter future diagnostic approach in angle closure.

Limitations: A single gonioscopist performed the examination in most of the subjects. This might increase the probability of systematic bias. However, this is offset by the masking to imaging tests. Moderate to poor reproducibility seen for individual quadrants in EyeCam grading might be a problem due to artifacts, which need to be examined. Position of patient was different between gonioscopy and EyeCam; the effect of which was not evaluated in the studies. These studies were clinic based and may not represent community based populations. Replication of imaging and scans by other less experienced technicians may yield variable results. The cost of both EyeCam and Casia SSOCT may be a limitation to adapt the outcomes of this study widely. Torque effects and uncorrected images in SSOCT scans may yield variable results. Further, the 'invisible range" in ITC index evaluation was a potential confounder. Automated software for SSOCT scans need to be validated using further studies.

Apart from the above technical issues, the main limitation of the techniques used in this study (and not the limitations of the study per se) is the cost-effectiveness of the instruments in comparison to conventional technique, i.e. gonioscopy. Both EyeCam and Casia SSOCT are costlier than conventional gonioscopy in direct costs presently. Development of instruments to replace EyeCam (such as in Aim 3) and SSOCT, and automated solutions for interpretation of the angle closure may further provide a paradigm shift in use of objective instruments in comparison to the subjective gonioscopic technique, at the screening level.

6.3 Future directions

Angle closure detection and screening in high risk population is considered a viable option to combat glaucoma blindness, in a scenario of ageing population across Asia. Management of high risk individuals in the primary care setting will inevitably shift under the care of non-expert paramedical personnel in future. In this regard, clinicians need better clinical tools which can be adapted by non-clinicians using simple guidelines. Automation with robust safety features in diagnostics is the need of the hour.

Outcomes from this dissertation provide some interesting opportunities to explore important future directions in the diagnosis, screening and management of glaucoma, especially PACG. Some of these studies have commenced while other ideas can be explored in future.

1. Integration of the automated software tools (such as automated angle image grading in EyeCam or SSOCT scans) described in this study to commercial devices.
2. Validation clinical studies (using the integrated automated software tool) across commercial instruments such as Cirrus ASOCT (Carl Zeiss Meditec, Dublin, CA) and

Spectralis ASOCT (Heidelberg Engg., Dosenheim, Germany) in comparison to gonioscopy.

3. Community based screening studies for angle closure using the automated software in high risk populations.
4. Cost effectiveness studies of screening using the automated tools compared to manual screening strategies for angle closure.
5. Refinement of the automated software for SSOCT using quantitative algorithms and optimizing the number of scans (and quadrants) needed for faster and accurate diagnostic performance
6. Refinement, miniaturization and validation of the dual mode angle imaging probe.
7. Clinical application of the dual mode probe can be explored in clinical and surgical conditions related to glaucoma.
8. High resolution imaging of the trabecular meshwork is an unmet need.

ELSEVIER LICENSE
TERMS AND CONDITIONS

Jan 21, 2015

This is a License Agreement between Baskaran Mani ("You") and Elsevier ("Elsevier") provided by Copyright Clearance Center ("CCC"). The license consists of your order details, the terms and conditions provided by Elsevier, and the payment terms and conditions.

All payments must be made in full to CCC. For payment instructions, please see information listed at the bottom of this form.

Supplier	Elsevier Limited The Boulevard,Langford Lane Kidlington,Oxford,OX5 1GB,UK
Registered Company Number	1982084
Customer name	Baskaran Mani
Customer address	05-01, SNEC building Singapore, 168751
License number	3553610264924
License date	Jan 21, 2015
Licensed content publisher	Elsevier
Licensed content publication	American Journal of Ophthalmology
Licensed content title	Demonstration of Angle Widening Using EyeCam After Laser Peripheral Iridotomy in Eyes With Angle Closure
Licensed content author	None
Licensed content date	June 2010
Licensed content volume number	149
Licensed content issue number	6
Number of pages	5
Start Page	903
End Page	907
Type of Use	reuse in a thesis/dissertation
Portion	full article
Format	both print and electronic
Are you the author of this Elsevier article?	Yes
Will you be translating?	No
Order reference number	2
Title of your	Novel methods of meridional and circumferential anterior chamber

Title: Angle Assessment by EyeCam, Goniophotography, and Gonioscopy.

Author: Baskaran, Mani; DO, DNB; Perera, Shamira; Nongpiur, Monisha; Tun, Tin; Park, Judy; Kumar, Rajesh; Friedman, David; MD, PhD; Aung, Tin

Publication: Journal of Glaucoma

Publisher: Wolters Kluwer Health

Date: Jan 1, 2012

This reuse is free of charge. No permission letter is needed from Wolters Kluwer Health, Lippincott Williams & Wilkins. We require that all authors always include a full acknowledgement. Example: AIDS: 13 November 2013 - Volume 27 - Issue 17 - p 2679-2689. Wolters Kluwer Health Lippincott Williams & Wilkins© No modifications will be permitted.

BACK CLOSE WINDOW

JOHN WILEY AND SONS LICENSE TERMS AND CONDITIONS

Jan 21, 2015

This Agreement between Baskaran Mani ("You") and John Wiley and Sons ("John Wiley and Sons") consists of your license details and the terms and conditions provided by John Wiley and Sons and Copyright Clearance Center.

License Number	3553611378145
License date	Jan 21, 2015
Licensed Content Publisher	John Wiley and Sons
Licensed Content Publication	Acta Ophthalmologica
Licensed Content Title	Comparison of EyeCam and anterior segment optical coherence tomography in detecting angle closure
Licensed Content Author	Mani Baskaran,Tin Aung,David S. Friedman,Tin A. Tun,Shamira A. Perera
Licensed Content Date	Aug 31, 2012
Pages	1
Type of use	Dissertation/Thesis
Requestor type	Author of this Wiley article
Format	Print and electronic
Portion	Full article
Will you be translating?	No
Order reference number	3
Title of your thesis / dissertation	Novel methods of meridional and circumferential anterior chamber angle imaging
Expected completion date	Jan 2015
Expected size (number of pages)	300
Requestor Location	Baskaran Mani 05-01, SNEC building 11 Third hospital avenue Singapore, Singapore 168751 Attn: Baskaran Mani
Billing Type	Invoice
Billing Address	Baskaran Mani 05-01, SNEC building 11 Third hospital avenue Singapore, Singapore 168751 Attn: Baskaran Mani
Total	0.00 USD

Title:	Focal edge association to glaucoma diagnosis
Conference Proceedings:	Engineering in Medicine and Biology Society, EMBC, 2011 Annual International Conference of the IEEE
Author:	Jun Cheng; Jiang Liu; Wong, D.W.K.; Ngan Meng Tan; Beng Hai Lee; Cheung, C.; Baskaran, M.; Tien Yin Wong; Tin Aung
Publisher:	IEEE
Date:	Aug. 30 2011-Sept. 3 2011

Thesis / Dissertation Reuse

The IEEE does not require individuals working on a thesis to obtain a formal reuse license, however, you may print out this statement to be used as a permission grant:

Requirements to be followed when using any portion (e.g., figure, graph, table, or textual material) of an IEEE copyrighted paper in a thesis:

1) In the case of textual material (e.g., using short quotes or referring to the work within these papers) users must give full credit to the original source (author, paper, publication) followed by the IEEE copyright line © 2011 IEEE.
2) In the case of illustrations or tabular material, we require that the copyright line © [Year of original publication] IEEE appear prominently with each reprinted figure and/or table.
3) If a substantial portion of the original paper is to be used, and if you are not the senior author, also obtain the senior author's approval.

Requirements to be followed when using an entire IEEE copyrighted paper in a thesis:

1) The following IEEE copyright/ credit notice should be placed prominently in the references: © [year of original publication] IEEE. Reprinted, with permission, from [author names, paper title, IEEE publication title, and month/year of publication]
2) Only the accepted version of an IEEE copyrighted paper can be used when posting the paper or your thesis on-line.
3) In placing the thesis on the author's university website, please display the following message in a prominent place on the website: In reference to IEEE copyrighted material which is used with permission in this thesis, the IEEE does not endorse any of [university/educational entity's name goes here]'s products or services. Internal or personal use of this material is permitted. If interested in reprinting/republishing IEEE copyrighted material for advertising or promotional purposes or for creating new collective works for resale or redistribution, please go to http://www.ieee.org/publications_standards/publications/rights/rights_link.html to learn how to obtain a License from RightsLink.

If applicable, University Microfilms and/or ProQuest Library, or the Archives of Canada may supply single copies of the dissertation.

SPRINGER LICENSE
TERMS AND CONDITIONS

Jan 21, 2015

This is a License Agreement between Baskaran Mani ("You") and Springer ("Springer") provided by Copyright Clearance Center ("CCC"). The license consists of your order details, the terms and conditions provided by Springer, and the payment terms and conditions.

All payments must be made in full to CCC. For payment instructions, please see information listed at the bottom of this form.

License Number	3553620077949
License date	Jan 21, 2015
Licensed content publisher	Springer
Licensed content publication	Graefe's Archive for Clinical and Experimental Ophthalmology
Licensed content title	Swept source optical coherence tomography measurement of the iris–trabecular contact (ITC) index: a new parameter for angle closure
Licensed content author	Sue-Wei Ho
Licensed content date	Jan 1, 2012
Volume number	251
Issue number	4
Type of Use	Thesis/Dissertation
Portion	Full text
Number of copies	1
Author of this Springer article	Yes and you are the sole author of the new work
Order reference number	4
Title of your thesis / dissertation	Novel methods of meridional and circumferential anterior chamber angle imaging
Expected completion date	Jan 2015
Estimated size(pages)	300
Total	0.00 USD
Terms and Conditions	

Introduction

The publisher for this copyrighted material is Springer Science + Business Media. By clicking "accept" in connection with completing this licensing transaction, you agree that the following terms and conditions apply to this transaction (along with the Billing and Payment terms and conditions established by Copyright Clearance Center, Inc. ("CCC"), at the time that you opened your Rightslink account and that are available at any time at http://myaccount.copyright.com).

Limited License

With reference to your request to reprint in your thesis material on which Springer Science

ELSEVIER LICENSE
TERMS AND CONDITIONS

Dec 25, 2014

This is a License Agreement between Baskaran Mani ("You") and Elsevier ("Elsevier") provided by Copyright Clearance Center ("CCC"). The license consists of your order details, the terms and conditions provided by Elsevier, and the payment terms and conditions.

All payments must be made in full to CCC. For payment instructions, please see information listed at the bottom of this form.

Supplier	Elsevier Limited The Boulevard,Langford Lane Kidlington,Oxford,OX5 1GB,UK
Registered Company Number	1982084
Customer name	Baskaran Mani
Customer address	05-01, SNEC building Singapore, 168751
License number	3535210493916
License date	Dec 24, 2014
Licensed content publisher	Elsevier
Licensed content publication	Ophthalmology
Licensed content title	Assessment of Circumferential Angle-Closure by the Iris–Trabecular Contact Index with Swept-Source Optical Coherence Tomography
Licensed content author	None
Licensed content date	November 2013
Licensed content volume number	120
Licensed content issue number	11
Number of pages	6
Start Page	2226
End Page	2231
Type of Use	reuse in a thesis/dissertation
Portion	full article
Format	both print and electronic
Are you the author of this Elsevier article?	Yes
Will you be translating?	No
Title of your thesis/dissertation	Novel methods of meridional and circumferential anterior chamber angle imaging
Expected completion date	Jan 2015
Estimated size (number of pages)	

Title:	Anterior chamber angle classification using multiscale histograms of oriented gradients for glaucoma subtype identification
Conference Proceedings:	Engineering in Medicine and Biology Society (EMBC), 2012 Annual International Conference of the IEEE
Author:	Yanwu Xu; Jiang Liu; Ngan Meng Tan; Beng Hai Lee; Wong, D.W.K.; Baskaran, M.; Perera, S.A.; Tin Aung
Publisher:	IEEE
Date:	Aug. 28 2012-Sept. 1 2012

Thesis / Dissertation Reuse

The IEEE does not require individuals working on a thesis to obtain a formal reuse license, however, you may print out this statement to be used as a permission grant:

Requirements to be followed when using any portion (e.g., figure, graph, table, or textual material) of an IEEE copyrighted paper in a thesis:

1) In the case of textual material (e.g., using short quotes or referring to the work within these papers) users must give full credit to the original source (author, paper, publication) followed by the IEEE copyright line © 2011 IEEE.
2) In the case of illustrations or tabular material, we require that the copyright line © [Year of original publication] IEEE appear prominently with each reprinted figure and/or table.
3) If a substantial portion of the original paper is to be used, and if you are not the senior author, also obtain the senior author's approval.

Requirements to be followed when using an entire IEEE copyrighted paper in a thesis:

1) The following IEEE copyright/ credit notice should be placed prominently in the references: © [year of original publication] IEEE. Reprinted, with permission, from [author names, paper title, IEEE publication title, and month/year of publication]
2) Only the accepted version of an IEEE copyrighted paper can be used when posting the paper or your thesis on-line.
3) In placing the thesis on the author's university website, please display the following message in a prominent place on the website: In reference to IEEE copyrighted material which is used with permission in this thesis, the IEEE does not endorse any of [university/educational entity's name goes here]'s products or services. Internal or personal use of this material is permitted. If interested in reprinting/republishing IEEE copyrighted material for advertising or promotional purposes or for creating new collective works for resale or redistribution, please go to http://www.ieee.org/publications_standards/publications/rights/rights_link.html to learn how to obtain a License from RightsLink.

If applicable, University Microfilms and/or ProQuest Library, or the Archives of Canada may supply single copies of the dissertation.

Title:	Automated anterior chamber angle localization and glaucoma type classification in OCT images
Conference Proceedings:	Engineering in Medicine and Biology Society (EMBC), 2013 35th Annual International Conference of the IEEE
Author:	Yanwu Xu; Jiang Liu; Jun Cheng; Beng Hai Lee; Wong, D.W.K.; Baskaran, M.; Perera, S.; Aung, T.
Publisher:	IEEE
Date:	3-7 July 2013

Thesis / Dissertation Reuse

The IEEE does not require individuals working on a thesis to obtain a formal reuse license, however, you may print out this statement to be used as a permission grant:

Requirements to be followed when using any portion (e.g., figure, graph, table, or textual material) of an IEEE copyrighted paper in a thesis:

1) In the case of textual material (e.g., using short quotes or referring to the work within these papers) users must give full credit to the original source (author, paper, publication) followed by the IEEE copyright line © 2011 IEEE.
2) In the case of illustrations or tabular material, we require that the copyright line © [Year of original publication] IEEE appear prominently with each reprinted figure and/or table.
3) If a substantial portion of the original paper is to be used, and if you are not the senior author, also obtain the senior author's approval.

Requirements to be followed when using an entire IEEE copyrighted paper in a thesis:

1) The following IEEE copyright/ credit notice should be placed prominently in the references: © [year of original publication] IEEE. Reprinted, with permission, from [author names, paper title, IEEE publication title, and month/year of publication]
2) Only the accepted version of an IEEE copyrighted paper can be used when posting the paper or your thesis on-line.
3) In placing the thesis on the author's university website, please display the following message in a prominent place on the website: In reference to IEEE copyrighted material which is used with permission in this thesis, the IEEE does not endorse any of [university/educational entity's name goes here]'s products or services. Internal or personal use of this material is permitted. If interested in reprinting/republishing IEEE copyrighted material for advertising or promotional purposes or for creating new collective works for resale or redistribution, please go to http://www.ieee.org/publications_standards/publications/rights/rights_link.html to learn how to obtain a License from RightsLink.

If applicable, University Microfilms and/or ProQuest Library, or the Archives of Canada may supply single copies of the dissertation.

AIP PUBLISHING LLC LICENSE TERMS AND CONDITIONS

Jan 21, 2015

All payments must be made in full to CCC. For payment instructions, please see information listed at the bottom of this form.

License Number	3553630693066
Order Date	Jan 21, 2015
Publisher	AIP Publishing LLC
Publication	Review of Scientific Instruments
Article Title	Note: A gel based imaging technique of the iridocorneal angle for evaluation of angle-closure glaucoma
Author	V. K. Shinoj,V. M. Murukeshan,M. Baskaran, et al.
Online Publication Date	Jun 10, 2014
Volume number	85
Issue number	6
Type of Use	Thesis/Dissertation
Requestor type	Author (original article)
Format	Print and electronic
Portion	Excerpt (> 800 words)
Will you be translating?	No
Order reference number	5
Title of your thesis / dissertation	Novel methods of meridional and circumferential anterior chamber angle imaging
Expected completion date	Jan 2015
Estimated size (number of pages)	300
Total	0.00 USD

Terms and Conditions

AIP Publishing LLC -- Terms and Conditions: Permissions Uses

AIP Publishing LLC ("AIPP"") hereby grants to you the non-exclusive right and license to use and/or distribute the Material according to the use specified in your order, on a one-time basis, for the specified term, with a maximum distribution equal to the number that you have ordered. Any links or other content accompanying the Material are not the subject of this license.

1. You agree to include the following copyright and permission notice with the reproduction of the Material:"Reprinted with permission from [FULL CITATION]. Copyright [PUBLICATION YEAR], AIP Publishing LLC." For an article, the copyright and permission notice must be printed on the first page of the article or book chapter. For photographs, covers, or tables, the copyright and permission notice may appear with the Material, in a footnote, or in the reference list.
2. If you have licensed reuse of a figure, photograph, cover, or table, it is your responsibility to ensure that the material is original to AIPP and does not contain the copyright of another entity, and that the copyright notice of the figure, photograph, cover, or table does not indicate that it was reprinted by AIPP, with permission, from another source. Under no circumstances does AIPP, purport or intend to grant permission to reuse material to which it does not hold copyright.

32nd Annual International Conference of the IEEE EMBS
Buenos Aires, Argentina, August 31 - September 4, 2010

Closed Angle Glaucoma Detection in RetCam Images

Jun Cheng, Jiang Liu, Beng Hai Lee, Damon Wing Kee Wong, Fengshou Yin
Tin Aung, Mani Baskaran, Perera Shamira, Tien Yin Wong

Abstract—**Closed/Open angle glaucoma classification is important for glaucoma diagnosis. RetCam is a new imaging modality that captures the image of iridocorneal angle for the classification. However, manual grading and analysis of the RetCam image is subjective and time consuming. In this paper, we propose a system for intelligent analysis of iridocorneal angle images, which can differentiate closed angle glaucoma from open angle glaucoma automatically. Two approaches are proposed for the classification and their performances are compared. The experimental results show promising results.**

I. INTRODUCTION

GLAUCOMA is an optic nerve disease resulting in loss of vision. It is often associated with increased pressure of fluid inside the eye. Glaucoma can be roughly divided into two main types: open angle glaucoma (OAG) and closed angle glaucoma (CAG). The iridocorneal angle between the iris and the cornea is the key to differentiate OAG and CAG. When the iridocorneal angle is open, it is OAG. When the iridocorneal angle is narrow or even closed, it is CAG. A more detailed explanation with description of the angle structures can be found in [1]. Here we briefly explain the reason that the iridocorneal angle is the key for the glaucoma diagnosis. As you know, the iris located between the cornea and the lens controls the amount of light entering the eye. The iris, cornea, and lens are bathed in a liquid called aqueous humor, which is continually produced by nearby tissues. It moves out of the eye via a drainage canal called the trabecular meshwork. Blocking of the canal would lead to the increased fluid pressure and a CAG. Thus, the iridocorneal angle is the key.

OAG accounts for more than 90% of glaucoma patients. It is usually chronic and progresses gradually. OAG is a leading cause of blindness. It is particularly dangerous as it can progress gradually and go unnoticeable for years. CAG affects less than 10 percent of patients with glaucoma. It is often inherited and occurs more commonly in farsighted elderly people. A CAG attack is usually acute, occurring when the drainage area is blocked. CAG must be treated quickly; otherwise, it may result in blindness within hours to days of the attack. As a result, it is critical to detect CAG in time to have proper treatment. Because of different causes and specific treatments for different types of glaucoma as well as the necessity of urgent treatment of CAG, it is important to determine the type of the glaucoma [2], which implies that it is essential to visualize the iridocorneal angle to make a correct diagnosis of the disease.

Gonioscopy is an eye examination looking at the front part of the eye between the cornea and the iris. It is to visualize the structure of the angle including the trabecular meshwork. The trabecular meshwork is a key in assessing the angle. The angle is said to be open if the trabecular meshwork can be seen, otherwise, closed. Gonioscopy is considered as one of the most practical methods to assess the angle, however, it is subjective and difficult to quantify [1]. Moreover, it is not easy to operate as patients often blink their eyes, squeeze their eyelids together, and etc. The success of gonioscopy therefore requires considerable photographic skill and effort as well as a full knowledge of the angle structures [3].

RetCam (Clarity Medical Systems, Inc., Pleasanton, CA) is a fundus camera traditionally been used to capture the image of retina. With some technical modifications, the camera can be used to capture the image of iridocorneal angle, iris, and cornea [3]. RetCam has some advantages compared with standard gonioscopy. In RetCam imaging, subjects are in a supine position on a bed or reclining chair. An advantage of this is that the patients cannot pull away from the camera lens' tip, which is a common problem when using gonio lenses. The tip of the RetCam's lens is smaller than the standard gonio lens and does not sit on the patient's lower eyelid. Thus, patients are less likely to squeeze their eyelids shut and to struggle against the stimulus of a foreign object in their eyes. Because the illumination from the camera sweeps across their pupils, patients are also less likely to experience discomfort from the light's intensity, so angle-related artifact is minimal. According to doctors' experience, patients undergoing imaging with the RetCam find the technique to be comfortable and noninvasive. As a summary, the RetCam makes goniography fast, easy, and effective.

The new RetCam imaging modality enhances the use of the camera as a clinical, educational, and research tool. The accompany issue is how to grade these RetCam images. Manual grading is currently adopted clinically. As we can

Manuscript received March 30, 2010.
This work was supported in part by the Agency for Science, Technology and Research, Singapore, under SERC grand 092-148-0073.
J. Cheng, J. Liu, B. H. Lee, D. W. K. Wong and F. Yin are with the Institute for Infocomm Research, A*STAR, 1 Fusionopolis Way, #21-01 Connexis, Singapore 138632 (email: jcheng@i2r.a-star.edu.sg).
T. Aung, M. Baskaran and P. Shamira are with Singapore Eye Research Institute.
T. Yin Wong is with the Singapore Eye Research Institute and National University of Singapore.

see that manual grading of medical images is usually tedious and time consuming. This holds true for RetCam images as well. Moreover, the angle usually lies in a small portion in the RetCam image which makes the manual grading more difficult. Manual grading is often subjective by the grader and thus the reproducibility is a concern. To facilitate large-scale clinical use, it is essential to have a precise, efficient system to grade the angle images automatically.

In this paper, we present a closed angle glaucoma detection system, which extracts features from RetCam images and detects closed angles automatically. In Section I, we have given an introduction of the background and motivation for the system. In Section II, we introduce the system and methods in details. Section III shows the experimental results, followed by the conclusions in the last section.

II. METHOD

Before introducing the proposed system, we first introduce the RetCam images. In RetCam imaging, the doctors examine four different sides of the eye including: inferior, superior, nasal and temporal side. Fig. 1 shows four typical RetCam images from the four sides of the eye. In these images, the inner black area is the pupil. The yellowish area surrounding the pupil is the iris. The whitish area is the cornea. The angle which is of our interest is located at the boundary between the iris and the cornea. Similar to gonioscopy, an iridocorneal angle is considered as open if the trabecular meshwork can be seen in the RetCam image, otherwise, closed.

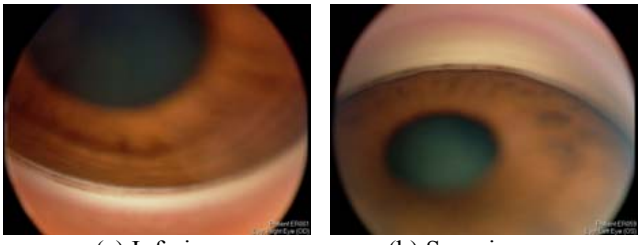

(a) Inferior (b) Superior

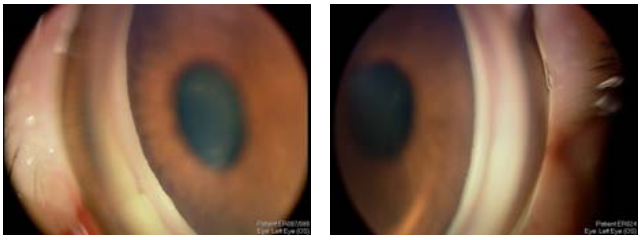

(c) Nasal (d) Temporal

Fig. 1 Sample RetCam Images

We propose a system for automatic analysis of the angle images for glaucoma diagnosis. The system will be verified using a RetCam image database collected in Singapore. Fig. 2 shows the architecture of the RetCam image analysis system. It contains the following main steps: edge detection, arc detection and closed angle glaucoma detection. The edge detection is a preprocessing for the arc detection. The arc detection is to locate the boundary between different angle structures. The last step would tell whether an angle is open or closed for a basic grading.

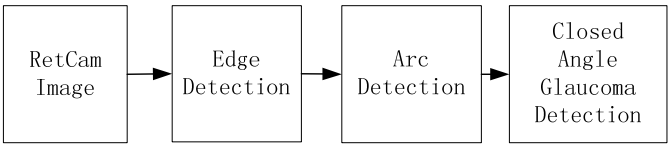

Fig. 2 Architecture of the RetCam Image Analysis System

A. Edge Detection

The edge detection is to find the candidate region of interest. The Canny edge [4] is applied. The edges close to black pixels are excluded as they are not of our interest. Fig. 3 shows the output of edge detection for the sample images in Fig. 2. From these output, we observe noise, false edges, broken edges, and etc. Thus, further processing is necessary.

(a) (b)

(c) (d)

Fig. 3 Edges of Sample Images

B. Arc Detection

From our observation, the edges in the angle area are approximately in an arc shape, i.e., part of a circle. Thus, we apply arc detection algorithms to detect true arcs, remove false arcs, and connect broken edges.

The task here is to detect a known shape arc with unknown parameters including location and radius of the arc. Hough transform is suitable for solving such a problem [5]. Since the edges are approximately part of a circle, a circular Hough transform is applied. Different from Hough transform for line detection, circular Hough transform has three unknowns instead of two: the locations of centre in the 2D coordinates and the radius. The output of the Hough transform is an accumulator, where the local maxima

correspond to centres of the arcs. The algorithm for circular Hough transform can be summarized as follows [6]:

1) Find the edge points.
2) For each edge point, draw a circle with center in the edge point with radius *r* and increment all coordinates that the perimeter of the circle passes through in the accumulator.
3) Find one or several local maxima in the accumulator.

In the application here, we put some constraints on the three unknowns to reduce the computational load. E.g., restrict the range of the radius *r* based on prior knowledge. We also need to exclude false arcs as the RetCam image may contain other structures. Fig. 3(d) is an example with a false arc (the right side arc) which is from other structures instead of the angle. In such a scenario, we can exclude it as it locates far away from the inner true arc. Detect the local maxima that corresponds to arc centre in the accumulator map is not easy. In our detection, we only accept local maxima greater than an empirically determined threshold. Moreover, the relative locations of the detected local maxima should satisfy the following conditions: For images of the inferior and superior side of the eye, the coordinates of the local maxima should differ more in the vertical direction than horizontal, for images of the nasal and temporal side of the eye, the coordinates should differ more in the horizontal than vertical. Otherwise, the one with lower value in the accumulator is excluded. Fig. 4 shows part of accumulator map of Hough transform output. In the accumulator map, we use '*' to denote the local maxima we detected.

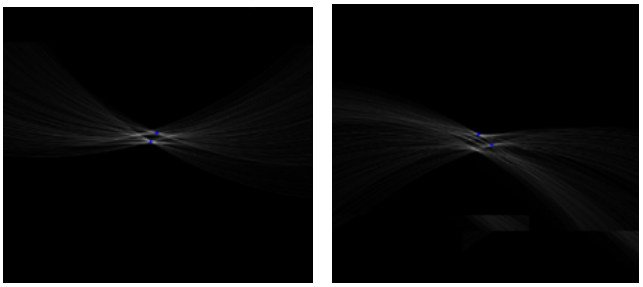

(a) Two peaks (b) Two peaks

(c) Single peak (d) Single peak

Fig. 4 Accumulator of Hough transform and the corresponding local maxima with (a) (b) from RetCam images clinically graded as open angle and (c) (d) from RetCam images clinically graded as closed angle.

C. Closed Angle Glaucoma Detection

After locating the angle area in the arc detection, we can now tell whether the angle is closed or open. Here, we propose two approaches to differentiate closed angle from open angle.

Arc Amount Based Approach

When an angle is closed or nearly closed, the two rays of the angle would be overlapping in the RetCam image. In term of the arcs, we would be able to detect one arc only. Our idea is verified by the output from the sample images. The results from Fig. 3 and Fig. 4 suggest that Fig. 2 (a) and (b) are from open angle while the rest two are from closed angle. It is consistent with clinical grading of the images. We classify it as OAG if we can detect two or more arcs from the RetCam image, otherwise, CAG.

Angle Width Based Approach

The second approach is inspired by the fact that angle width is a key factor to evaluate the angle by the doctors. Based on this, we compute the width of the angle. In the RetCam image, the angle width is the distance between the most inner and outer arcs. For example, the angle width for the case in Fig. 3 (b) is the distance between the two major arcs; the angle width for the cases in Fig. 3 (c) is only one pixel as there is only one arc. In order to compute the angle width, the strongest arc is obtained from the arc detection. Then, the surrounding area of the arc is considered as the region of interest. A closing process is applied to so that the angle width can be measured. As the angle width varies often along the arc; the mean angle width is used. Then, it is compared with a threshold to determine the angle type. If the mean width is greater than the threshold, it is considered as OAG, otherwise, CAG.

III. EXPERIMENTAL RESULTS

The RetCam image analysis system is tested in the eye studies at the Singapore Eye Research Institute (SERI). SERI is the national research institute for ophthalmic and vision research in Singapore, serving as the research institute of the Singapore National Eye Centre. SERI housed the state-of-the-art equipments and facilities with dedicated team of clinical staff and research scientists drawn from leading institutions around the world.

A collection of 1866 images from 99 patients is collected at SERI, which includes 1083 images from 54 patient eyes with OAG and 783 images from 45 patient eyes with CAG. For each patient eye, the examination is done on all the four sides of the eye, i.e., inferior, superior, nasal and temporal. For each side, multiple images are taken. For each image, we can make a classification of closed or open angle by the above mentioned two approaches. However, as four sides of each patient eye are examined with multiple images, the decision of open/closed angle glaucoma for each patient eye can be made by combining the results from all four sides of images. In our experiments, we first look at the performance

if the diagnosis is based on a single image for each eye. Then we look at the performance if the diagnosis is based on all the images captured on each eye. In the second case, a patient eye is said to have OAG if more than half of the images of that eye suggest OAG, otherwise, CAG.

The output of the system is compared with decisions based on manual grading to compute the accuracies. The results are summarized as follows. Table I shows the specificity (the percentage of OAG classified as OAG) and the sensitivity (the percentage of CAG classified as CAG) for 1866 images if the diagnosis is made from individual image by the two approaches. Table II shows the specificity and the sensitivity for 99 patient eyes if the diagnosis is made from a combination of all images from each patient eye.

Table I specificity and sensitivity based on individual image

	Specificity	Sensitivity
Arc Amount	69.6%	75.5%
Angle Width	78.6%	81.9%

Table II specificity and sensitivity based on all images of each patient eye

	Specificity	Sensitivity
Arc Amount	83.3%	86.7%
Angle Width	92.6%	97.8%

As we can see from the results, the width based approach performs better. A possible reason is that variation from one image to another would require variant sensitivity in the edge detection. However, it is difficult to achieve that perfectly. Thus, the intermittent edges appear and affect the detection of arcs sometimes. The computing of mean angle width in the width based approach is less affected by the intermittent edges and thus the width based approach performs better. For the width based approach, an empirically selected threshold is used to make the decision. It is necessary to know how the threshold selection affects the performance.

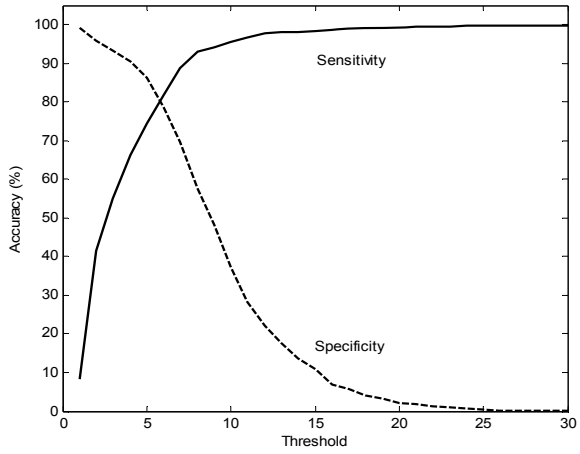

Fig. 5 Sensitivity and specificity versus threshold for diagnosis based on individual image

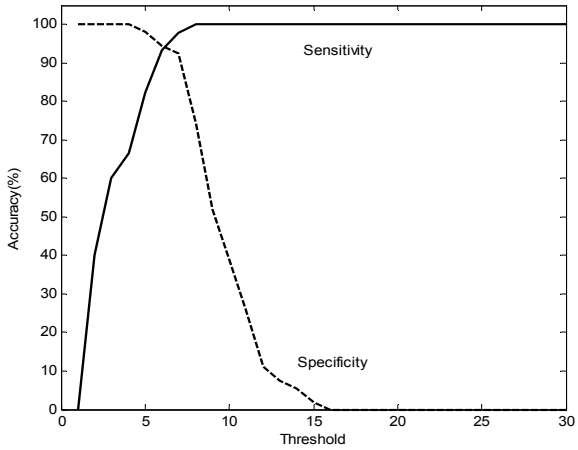

Fig. 6 Sensitivity and specificity versus threshold for diagnosis based on all images from each patient eye

Fig. 5 and Fig. 6 show how the sensitivity (solid line) and specificity (dash line) change when the threshold is changed for the diagnosis based on individual image and multiple images, respectively. This gives the overall picture of the performance of the width based approach. From the figures, we observe that a threshold around 7 is good for minimizing the overall error. However, a lower or higher threshold may be used, depending on the clinically requirements on the sensitivity and specificity. Another observation is that by combining multiple images from four sides of the eye, the performance of the system is improved. Thus, the doctors can make a more confident diagnosis by combining the results from multiple images.

IV. Conclusions

We propose an intelligent system for the analysis of RetCam images for automatic closed/open angle classification. The algorithms show promising & encouraging results. More images would be included to evaluate the performance of the system. Further analysis of the angle would be done to improve the performance as well as to identify eye structures for more advanced grading to tell the degree of closure and potential to become closed.

References

[1] D Minckler, P Foster and PT Hung, Angle Closure Glaucoma Classification and Racial Variation, *Asian Journal of Ophthalmology*, vol. 3, no. 3, 4, 2001.

[2] John F. Salmon, The diagnostic importance of gonioscopy, http://www.glaucomaworld.net/english/019/e019a01t.html

[3] I. I. K. Ahmed AND L. D. Mackeen, A new approach for imaging the angle, *Glaucoma Today*, pp. 27-30, JULY/AUGUST 2007.

[4] J. Canny, A Computational Approach To Edge Detection, *IEEE Trans. Pattern Analysis and Machine Intelligence*, vol. 8, pp. 679–698, 1986.

[5] D. H. Ballard, Generalizing the Hough Transform to Detect Arbitrary Shapes, *Pattern Recognition,* vol. 13, no. 2, pp. 111-122, April 1981.

[6] Bryan S. Morse. Lecture 15: Segmentation (edge based, Hough transform). Brigham Young University: Lecture Notes, 2000.

Demonstration of Angle Widening Using EyeCam After Laser Peripheral Iridotomy in Eyes With Angle Closure

SHAMIRA A. PERERA, DESMOND T. QUEK, MANI BASKARAN, TIN A. TUN, RAJESH S. KUMAR, DAVID S. FRIEDMAN, AND TIN AUNG

• PURPOSE: To evaluate EyeCam in detecting changes in angle configuration after laser peripheral iridotomy (LPI) in comparison to gonioscopy, the reference standard.
• DESIGN: Prospective comparative study.
• METHODS: Twenty-four subjects (24 eyes) with primary angle-closure glaucoma (PACG) were recruited. Gonioscopy and EyeCam (Clarity Medical Systems) imaging of all 4 angle quadrants were performed, before and 2 weeks after LPI. Images were graded according to angle structures visible by an observer masked to clinical data or the status of LPI, and were performed in a random order. Angle closure in a quadrant was defined as the inability to visualize the posterior trabecular meshwork. We determined the number of quadrants with closed angles and the mean number of clock hours of angle closure before and after LPI in comparison to gonioscopy.
• RESULTS: Using EyeCam, all 24 eyes showed at least 1 quadrant of angle widening after LPI. The mean number of clock hours of angle closure decreased significantly, from 8.15 ± 3.47 clock hours before LPI to 1.75 ± 2.27 clock hours after LPI ($P < .0001$, Wilcoxon signed rank test). Overall, gonioscopy showed 1.0 ± 1.41 (95% CI, 0.43-1.57) quadrants opening from closed to open after LPI compared to 2.0 ± 1.28 (95% CI, 1.49-2.51, $P = .009$) quadrants with EyeCam. Intra-observer reproducibility of grading the extent of angle closure in clock hours in EyeCam images was moderate to good (intra-class correlation coefficient 0.831).
• CONCLUSIONS: EyeCam may be used to document changes in angle configuration after LPI in eyes with PACG. (Am J Ophthalmol 2010;149:903–907. © 2010 by Elsevier Inc. All rights reserved.)

LASER PERIPHERAL IRIDOTOMY (LPI) IS THE RECOMmended first-line intervention in both acute and chronic forms of primary angle-closure glaucoma (PACG).[1] LPI eliminates pupil block, the primary underlying mechanism for the condition;[2] causes flattening of iris convexity; and may cause widening of the anterior chamber angle.[3,4]

Gonioscopy, the current reference standard for assessing angle structures, is limited by its dependency on single-observer interpretation and is difficult to perform in a reproducible fashion.[5,6] Gonioscopy requires the placement of a contact lens on the eye of the patient, and gonioscopic findings may vary with the type of lens used as well as ambient lighting conditions.[7] Although 1 study found that one may document angle opening after LPI with gonioscopy, this is difficult to do in an objective manner. Imaging devices such as ultrasound biomicroscopy (UBM)[4] and anterior segment optical coherence tomography (ASOCT)[8] have been used to measure quantitative changes in angle parameters after LPI, but these were based on angle measurements.

The EyeCam (Clarity Medical Systems, Pleasanton, California, USA) is a new technology that was originally designed to obtain wide-field photographs of the fundus. With recent modifications of the lens angulation, the device can be used to visualize structures in the angle in a manner similar to direct gonioscopy. The EyeCam is able to record images that can be saved on a computer, thus allowing comparisons to be made over time. This may be useful to track angle changes with disease progression as well as after treatment. In this study, we evaluated the use of EyeCam in detecting changes in angle configuration after LPI in PACG eyes in comparison to gonioscopy, the reference standard.

METHODS

WE RECRUITED 24 CONSECUTIVE PACG PATIENTS FROM glaucoma clinics of the Singapore National Eye Centre who were undergoing LPI. All eyes had angle closure (defined as the presence of at least 180 degrees of angle in which the posterior pigmented trabecular meshwork was not visible on non-indentation gonioscopy in the primary position) with glaucomatous optic neuropathy (GON) (defined as the presence of vertical cup-to-disc ratio ≥0.7 or cup-to-disc asymmetry ≥0.2 or focal neuroretinal rim notching, with corresponding visual field changes). A glaucomatous visual field defect was defined if the following were found: 1) glaucoma hemifield test (GHT) outside normal limits, and 2) a cluster of 3 or more, non-edge,

Accepted for publication Jan 5, 2010.
From the Singapore National Eye Centre & Singapore Eye Research Institute, Singapore (S.A.P., D.T.Q., M.B., T.A.T., R.S.K., T.A.); Wilmer Eye Institute, Johns Hopkins University, Baltimore, Maryland (D.S.F.); and Yong Loo Lin School of Medicine, National University of Singapore, Singapore (T.A.).
Inquiries to A/Prof Tin Aung, Singapore National Eye Centre, 11 Third Hospital Ave, Singapore 168751; e-mail: tin11@pacific.net.sg

0002-9394/$36.00
doi:10.1016/j.ajo.2010.01.013

contiguous points, not crossing the horizontal meridian with a probability of <5% of the age-matched normal on the pattern deviation plot on 2 separate occasions. Exclusion criteria were a history of previous cataract surgery or any corneal opacities or abnormalities that precluded EyeCam imaging, as well as eyes with secondary angle closure. Sequential argon-yttrium-aluminum-garnet (YAG) LPI was performed in all cases with standardized settings (argon laser 0.7-1.0 W, spot size 50 μm, duration 0.1 seconds, 10-30 shots followed by neodymium (Nd)-YAG laser 2-5 mJ, 3-5 shots).[9]

• **EYECAM IMAGING:** EyeCam imaging was performed before and approximately 2 weeks after LPI. Patients lay flat on a couch, and after application of topical anesthetic drops, coupling gel was applied to the lens probe and images of the superior, inferior, nasal, and temporal quadrants of the angle were obtained (4 images per eye). The lens probe was placed on a coupling gel without compression of the cornea, minimizing alteration of angle configuration. The probe was positioned at the limbus opposite to the angle being photographed, and light from the fiberoptic probe was directed into the angle of interest and then tilted downward to bring the angle structures into view. The patient looked away from the probe to improve visualization of angle structures and all imaging was performed in the dark.

Gonioscopy was performed in the dark in all cases by a single glaucoma-fellowship trained examiner (S.A.P.) who was masked to EyeCam findings. A 1-mm light beam was reduced to a narrow slit and the vertical beam was offset horizontally for assessing superior and inferior angles and was offset vertically for nasal and temporal angles. Static gonioscopy was performed using a Goldmann 2-mirror lens at high magnification (×16), with the eye in the primary position of gaze. If there was any doubt as to the state of the angle or any suspicion of peripheral anterior synechiae (PAS), this was confirmed on indentation gonioscopy with a Sussman lens. Care was taken to avoid light falling on the pupil and to avoid accidental indentation during examination. Slight tilting of the gonioscopy lens was permitted to gain a view over the convexity of the iris.

Both gonioscopy and EyeCam were performed on the same days both before and after LPI (which was confirmed to be patent by transillumination in all cases). The light intensity at various instances of examination was examined using a lux meter (Sekonic, Studio Deluxe III, L-398A; Sekonic Corporation, Tokyo, Japan). The following luminance levels were found in this study: dark room, 0 lux; slit-beam illumination during gonioscopic examination, 32.28 lux; EyeCam illumination at the time of image capture, 129.12 lux; and standard room illumination, 430.4 lux.

• **GRADING OF IMAGES:** EyeCam images were graded at the end of the study by an independent observer (M.B.) masked to gonioscopic data and the status of LPI, and were performed in a random order. However, status of LPI could not be completely masked since a patent LPI was seen in some of the images. Images were graded for their quality as follows: grade 1 if the angle details were clear and well focused in all quadrants; grade 2 if angle images were blurred in any quadrant but some details discerned; grade 3 if the angle structures were blurred in at least 1 quadrant such that no details could be discerned; and grade 4 if the structures were blurred in all 4 quadrants and no angle details were discerned. Images were excluded if they were assessed to be grade 3 or 4.

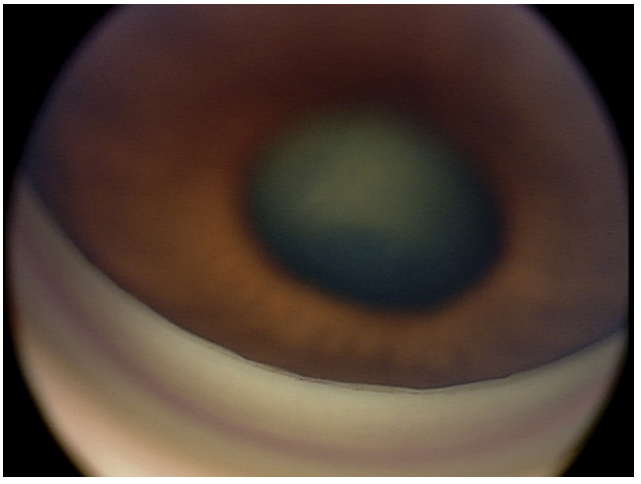

FIGURE 1. An EyeCam image of the closed angle where the trabecular meshwork is not visible before laser peripheral iridotomy.

The angle-grading scheme for each quadrant was the same for both gonioscopy and EyeCam images and was based on anatomic structures observed in the angle. Angle closure in a quadrant was defined as the inability to visualize the posterior trabecular meshwork (Figure 1) in that quadrant. For EyeCam images, we further quantified the extent of angle closure in a quadrant by number of clock hours.

In order to assess for intra-observer reproducibility, 30 pre- and post-LPI EyeCam images were randomly selected and graded by the same examiner twice over 2 sessions. These images were graded for angle closure status, angle structures visible, and the extent of angle closure in clock hours. Inter-observer reproducibility was assessed after grading of these 30 images by another glaucoma fellowship–trained examiner (R.S.K.).

• **STATISTICAL ANALYSIS:** Statistical analysis was performed using Medcalc version 10. 0 (Medcalc, Mariakerke, Belgium). The extent of angle closure before and after LPI was compared using Wilcoxon signed rank nonparameteric test for paired samples. Extent of angle widening between quadrants was compared using Kruskal-Wallis test. Post-LPI angle status for number of quadrants

TABLE 1. Angle Status Before and After Laser Peripheral Iridotomy as Assessed by Both Gonioscopy and EyeCam

	Closed Before LPI			Closed After LPI			Widened From Closed to Open After LPI		
	Gonioscopy	EyeCam	*P* Value[a]	Gonioscopy	EyeCam	*P* Value[a]	Gonioscopy	EyeCam	*P* Value[a]
Median (range)	4 (2 to 4)	3 (0 to 4)	.0035	4 (0 to 4)	1 (0 to 4)	.0002	0 (0 to 4)	2 (0 to 4)	.005
Number of Quadrants				Number of Eyes (n=24)					
0	0	1	—	4	10	—	13	2	—
1	0	0	—	1	8	—	5	8	—
2	1	6	—	1	2	—	2	4	—
3	0	6	—	5	3	—	1	7	—
4	23	11	—	13	1	—	3	3	—

LPI = laser peripheral iridotomy.
[a]Mann-Whitney test.

TABLE 2. Intra-observer and Inter-observer Reproducibility of Grading Angle Structures Visible (by Quadrant) and Extent of Angle Closure (in Clock Hours) in EyeCam Images

	Intra-observer Reproducibility			Inter-observer Reproducibility		
	Angle Closure[a] (Closed or Open Status)	Angle Structures Visible	Extent of Angle Closure (Clock Hours)	Angle Closure[a] (Closed or Open Status)	Angle Structures Visible	Extent of Angle Closure (Clock Hours)
Quadrants	Weighted kappa	ICC (95% CI)	ICC (95% CI)	Weighted kappa	ICC (95% CI)	ICC (95% CI)
Inferior	—	0.37	0.55 (0.27-0.74)	—	0.44	0.71 (0.27-0.74)
Nasal	—	0.53	0.62 (0.34-0.8)	—	0.42	0.44 (0.08-0.70)
Temporal	—	0.49	0.82 (0.65-0.91)	—	0.40	0.40 (0.05-0.66)
Superior	—	0.52	0.76 (0.56-0.88)	—	0.25	0.40 (0.05-0.66)
Overall	0.73	—	0.83 (0.68-0.92)	0.48	—	0.55 (0.11-0.78)

CI = confidence interval; ICC = intra-class correlation coefficient.
[a]Closed status defined as posterior trabecular meshwork not visible for at least 2 quadrants.

open with gonioscopy and EyeCam was compared using Mann-Whitney test. Intra- and inter-observer reproducibility was analyzed using weighted kappa statistic (for angle structure grading) and intraclass correlation coefficient (for extent of angle closure). Statistical significance was reported if $P < .05$.

RESULTS

TWENTY-FOUR SUBJECTS (24 EYES) WITH PACG WERE RECRUITED. There were 23 Chinese and 1 Indian subjects, with a mean age of 61.8 ± 7.9 years, and 62.5% (15/24) were women.

A total of 192 EyeCam images (96 quadrants each, before and after LPI) were recorded. Images were either grade 1 (66.7% [128/192]) or grade 2 (33.3% [64/192]) in quality, and all angle images could be analyzed.

Using EyeCam, all 24 eyes showed at least 1 quadrant of angle widening after LPI (Figure 2). Of these, 12 of 24 eyes had 4 quadrants of angle widening after LPI, 6 of 24 eyes had 3 quadrants, 4 of 24 eyes had 2 quadrants, and 2 of 24 eyes had 1 quadrant of angle widening after LPI. No quadrants became narrower after LPI. The mean (± SD) number of clock hours of angle closure decreased significantly, from 8.15 ± 3.47 before LPI to 1.75 ± 2.27 after LPI ($P < .0001$, Wilcoxon signed rank test). There was no significant difference in the change in clock hours of angle closure between the superior, inferior, nasal, and temporal quadrants after LPI ($P > .5$; Kruskal-Wallis test). While the pre-LPI apposition in clock hours between quadrants was found to be similar ($P = .5$; Kruskal-Wallis test), post-LPI apposition between the inferior compared to the rest of the quadrants showed a significant difference ($P = .0006$; Kruskal-Wallis test). This suggested maximum apposition in the inferior quadrant both before and after LPI.

• **COMPARISON OF ANGLE STATUS AFTER LASER PERIPHERAL IRIDOTOMY BY GONIOSCOPY VERSUS EYECAM:** Table 1 shows the number of eyes and quadrants that were open using EyeCam and gonioscopy. The angle status of 22 eyes was more open in at least 1 quadrant after LPI, and remained unchanged (and closed) in 2 eyes with gonioscopy, whereas with EyeCam, all angles opened up at least 1 quadrant. Overall, gonioscopy showed 1.0 ± 1.41 (95% CI, 0.43-1.57) quadrants opening from closed to

open after LPI compared to 2.0 ± 1.28 (95% CI, 1.49-2.51, $P = .009$) quadrants with EyeCam. Gonioscopy consistently revealed more closed quadrants than EyeCam, before and after LPI (Table 1).

• **REPRODUCIBILITY ANALYSIS FOR EYECAM IMAGES:** The weighted kappa statistic for intra-observer agreement for angle structures seen on EyeCam images was fair to moderate (Table 2), and for identifying angle closure status as closed or open it was moderate. The inferior quadrant had the largest discrepancy between the 2 modalities assessing visible angle structures with a weighted kappa of 0.37. The intraclass correlation coefficient (ICC) for grading extent of angle closure (in clock hours) in Eyecam images was found to be moderate to good (Table 2). The inter-observer agreement was moderate for angle closure status (kappa = 0.48, 95% CI, 0.14-0.82) and extent of angle closure (ICC = 0.55, 95% CI, 0.11-0.78).

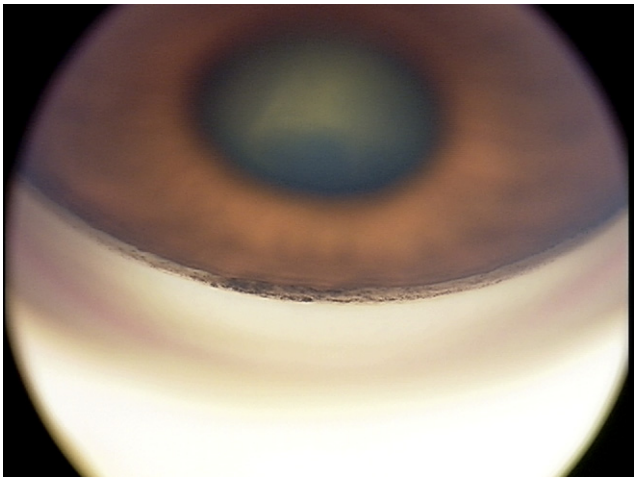

FIGURE 2. An EyeCam image of the same quadrant where the angle has opened up after laser peripheral iridotomy. The trabecular meshwork is now visible.

DISCUSSION

IN THIS STUDY, WE FOUND THAT CHANGES IN ANGLE width after LPI could be documented with the EyeCam in eyes with angle closure. All eyes had at least 1 quadrant of angle widening, and there was a significant reduction in the mean number of clock hours of angle closure from 8.15 ± 3.47 before LPI to 1.75 ± 2.27 after LPI. The EyeCam is thus a new method of documenting changes in the angle, using a photographic method that is similar to angle photography. The images produced would be easy for clinicians to interpret, as the angle appears similar to what is seen during gonioscopy. "Goniographic" documentation by EyeCam allows for monitoring of angle changes if serial examinations are done over time. Demonstration of angle widening pre and post LPI with EyeCam images may serve as a tool for patient education. The EyeCam may also have potential for telemedicine in which the angle can be assessed by a remote observer to make recommendations for treatment.

Overall, good-quality images of the angle were obtained with EyeCam, with all images of grade 1 (66.7% [128/192]) or grade 2 (33.3% [64/192]) quality. We found the images to have high resolution with easy identification of angle structures.

We found that the inferior angle had the most apposition both before and after LPI. While we are unable to explain this unusual finding, this result should be interpreted with caution as the inferior angle had the most discrepancy between EyeCam and gonioscopy for visible angle structures (kappa = 0.37) and the least intra-observer reproducibility for angle closure assessment (ICC = 0.55).

The EyeCam has several advantages over gonioscopy. As compared to gonioscopy, which requires coupling a contact lens to the cornea, EyeCam imaging requires minimal contact, reducing the possibility of mechanically altering the angle configuration. The EyeCam images can be recorded and stored for comparison at another time. Disadvantages of EyeCam are that the procedure takes longer than gonioscopy (about 5 minutes per eye) and the device is expensive. The light source from the EyeCam, delivered via a fiberoptic cable, is 4 times brighter than slit illumination for gonioscopy and may cause pupil constriction, which opens the angle somewhat. When EyeCam findings were compared to that of gonioscopy, we found that gonioscopy consistently revealed more closed quadrants than EyeCam and this may be attributable to this light effect or secondary to the supine positioning. Because of the above-mentioned reasons, it is possible that EyeCam may overestimate angle width in clinical practice and delay the diagnosis of angle closure in some subjects in comparison to gonioscopy. Failing to detect gonioscopically closed angles may also lead to under-diagnosis of angle closure glaucoma. When we tried to assess for the presence of peripheral anterior synechiae, we found that this was difficult to discern with EyeCam, as one is unable to indent the angle, unlike with dynamic gonioscopy. Iris processes in particular may be confused with PAS in EyeCam images. Additionally, we were unable to determine iris configuration with the 2-dimensional images obtained with EyeCam. Another disadvantage of EyeCam imaging of the angle is that for repeat imaging, images may not be obtained over the exact same location. Unless certain landmarks on the iris are used as anchors, each repeat photograph may be slightly rotated. Finally, it is not known if the angulation of the EyeCam probe alters the view of angle structures, causing some discrepancy with the gonioscopic findings. This is because the EyeCam probe is held over the limbus in the quadrant opposite to the one being imaged, and the angulation of the probe when held against the eye may affect the view of the angle structures.

Some variability may be introduced according to how the operator holds the probe. The results obtained from EyeCam may thus not be interchangeable with those from gonioscopy.

Other imaging techniques have been used to document changes in the angle after LPI. Using ASOCT, See and associates quantified the change in angle configuration after LPI by measuring the angle opening distance (AOD) at 500 μm anterior to the scleral spur (AOD500) and trabecular-iris space area (TISA) up to 750 μm from the scleral spur (TISA750). Both mean AOD500 and TISA750 were shown to significantly increase following LPI, with angles twice as wide on average in the dark after LPI than before LPI.[10] Ultrasound biomicroscopy (UBM) has also previously been used to demonstrate anterior chamber angle (ACA) widening following LPI. By prospectively comparing 55 fellow eyes of patients presenting with acute primary angle closure, Gazzard and associates showed that the AOD at 250 and 500 μm from the scleral spur (AOD250 and AOD500, respectively) and angle recess area (ARA), all measures of ACA depth, significantly increased after sequential laser iridotomy.[11,12] Although the EyeCam is unable to provide quantitative measurements of anterior chamber depth like the ASOCT or UBM, it provides 90 degrees of angle visualization per image, compared to the ASOCT and UBM, which can only provide a cross-sectional view of 1 point through the angle. In addition, the EyeCam provides real-time color images similar to gonioscopic appearance, with which clinicians are familiar.

Our study has several limitations. The use of a single operator for EyeCam imaging and a single observer for image analysis could result in a systematic bias. Despite masking of the observer to the status of LPI during analysis of angle images, a patent LPI could be seen in some images of the superior quadrants post-LPI. The grading systems used for gonioscopy and EyeCam were different: while the Modified Shaffer system used for gonioscopy estimated angle width, EyeCam grading was based on angle structures visible in the EyeCam images. The intra- and inter-observer variability in our study suggests that reproducibility was only moderate for consistent interpretation of angle structures using EyeCam. Further research comparing angle findings by EyeCam with gonioscopy is warranted in order to evaluate the use of this device in actual clinical practice.

In conclusion, the EyeCam can be used to document angle changes after LPI in eyes with angle closure. However, the EyeCam's current disadvantages, such as variable angle of view, intense illumination, inability to distinguish appositional from synechial closure, and subjectivity of image grading, may limit its clinical application. Figure 2.

THE STUDY WAS SUPPORTED BY GRANTS FROM SINGAPORE NATIONAL EYE CENTRE, SINGHEALTH FOUNDATION, AND National Medical Research Council. Dr T Aung has received travel support and honoraria from Clarity Medical Systems. Drs Perera and Quek contributed equally to this study. Involved in design of the study (T.A., S.A.P.); conduct of the study (S.A.P., T.A., T.A.T., R.S.K., M.B.); collection (S.A.P., T.A.T., R.S.K., M.B., T.A.), management (T.A., S.A.P.), analysis (M.B., S.A.P., T.A., R.S.K.), and interpretation of the data (T.A., R.S.K., M.B., S.A.P., D.S.F.); and preparation, review, and approval of manuscript (S.A.P., M.B., D.T.Q., R.S.K., T.A., D.S.F.). Informed consent for this research was obtained from all participants, and the study had the approval of the Institutional Review Board of the Singapore Eye Research Institute and adhered to the tenets of the Declaration of Helsinki.

REFERENCES

1. Weinreb RN, Friedman DS. Laser and medical treatment of primary angle closure glaucoma. In: Weinreb RN, Friedman DS, eds. Angle Closure and Angle Closure Glaucoma. Netherlands: Krugler; 2006:37–54.
2. Nonaka A, Iwawaki T, Kikuchi M, Fujihara M, Nishida A, Kurimoto Y. Quantitative evaluation of iris convexity in primary angle closure. Am J Ophthalmol 2007;143:695–697.
3. Nolan WP, Foster PJ, Devereux JG, et al. YAG laser iridotomy treatment for primary angle-closure in east Asian eyes. Br J Ophthalmol 2000;84:1255–1259.
4. He M, Friedman DS, Ge J, et al. Laser peripheral iridotomy in eyes with narrow drainage angles: ultrasound biomicroscopy outcomes. The Liwan Eye Study. Ophthalmology 2007; 114:1513–1519.
5. Nolan WP, Foster PJ, Devereux JG, et al. YAG laser iridotomy treatment for primary angle closure in east Asian eyes. Br J Ophthalmol 2000;84:1255–1259.
6. Foster PJ, Devereux JG, Alsbirk PH, et al. Detection of gonioscopically occludable angles and primary angle closure glaucoma by estimation of limbal chamber depth in Asians: modified grading scheme. Br J Ophthalmol 2000;84:186–192.
7. Friedman DS, He M. Anterior chamber angle assessment techniques. Surv Ophthalmol 2008;53:250–273.
8. Ahmed I, MacKeen L. A new approach to imaging the angle. Glaucoma Today 2007;4:1–3.
9. Ang MH, Baskaran M, Kumar RS, et al. National survey of ophthalmologists in Singapore for the assessment and management of asymptomatic angle closure. J Glaucoma 2008; 17:1–4.
10. See JL, Chew PT, Smith SD, et al. Changes in anterior segment morphology in response to illumination and after laser iridotomy in Asian eyes: an anterior segment OCT study. Br J Ophthalmol 2007;91:1485–1489.
11. Gazzard G, Friedman DS, Devereux JG, Chew P, Seah SK. A prospective ultrasound biomicroscopy evaluation of changes in anterior segment morphology after laser iridotomy in Asian eyes. Ophthalmology 2003;110:630–638.
12. Memarzadeh F, Li Y, Chopra V, et al. Anterior segment optical coherence tomography for imaging the anterior chamber after laser peripheral iridotomy. Am J Ophthalmol 2007;143:877–879.

Use of EyeCam for Imaging the Anterior Chamber Angle

Shamira A. Perera,[1,2] *Mani Baskaran,*[1] *David S. Friedman,*[3,4] *Tin A. Tun,*[2] *Hla M. Htoon,*[2] *Rajesh S. Kumar,*[2] *and Tin Aung*[2,5]

Purpose. To compare EyeCam (Clarity Medical Systems, Pleasanton, CA) imaging with gonioscopy for detecting angle closure.

Methods. In this prospective, hospital-based study, subjects underwent gonioscopy by a single observer and EyeCam imaging by a different operator. EyeCam images were graded by two masked observers. The anterior chamber angle in a quadrant was classified as closed if the trabecular meshwork could not be seen. The eye was classified as having angle closure if two or more quadrants were closed.

Results. One hundred fifty-two subjects were studied. The mean age was 57.4 years (SD 12.9) and there were 82 (54%) men. Of the 152 eyes, 21 (13.8%) had angle closure. The EyeCam provided clear images of the angles in 98.8% of subjects. The agreement between the EyeCam and gonioscopy for detecting angle closure in the superior, inferior, nasal, and temporal quadrants based on agreement coefficient (AC1) statistics was 0.73, 0.75, 0.76, and 0.72, respectively. EyeCam detected more closed angles than did gonioscopy in all quadrants ($P < 0.05$). With gonioscopy, 21/152 (13.8%) eyes were diagnosed as angle closure compared to 41 (27.0%) of 152 with EyeCam ($P < 0.001$, McNemar Test), giving an overall sensitivity of 76.2% (95% confidence interval [CI], 54.9%–90.7%), specificity of 80.9% (95%CI, 73.5%–87.3%), and an area under the receiver operating characteristic curve (AUC) of 0.79.

Conclusions. The EyeCam showed good agreement with gonioscopy for detecting angle closure. However, it detected more closed angles than did gonioscopy in all quadrants. (*Invest Ophthalmol Vis Sci.* 2010;51:2993–2997) DOI:10.1167/iovs.09-4418

Gonioscopy is the current reference standard for assessing the anterior chamber angle (ACA). The advantages of gonioscopy include the ability to visualize a whole quadrant of the ACA at one time, the use of the corneal wedge to help identify landmarks in the angle such as Schwalbe's line, and the ability to dynamically indent the angle and distinguish peripheral anterior synechiae (PAS) from appositional closure. Various grading schemes have been developed to categorize eyes on the basis of gonioscopic assessment of the ACA,[1–3] but such schemes are based on subjective and at best semiquantitative assessments. However, factors such as the type of lens used, the technique used, and the skill of the observer affect the variability of gonioscopy findings.[4] Documentation of gonioscopic findings is often poor, with most clinicians recording them in charts without images or photographic records.

The EyeCam (Clarity Medical Systems, Pleasanton, CA) is an imaging modality that was originally designed to obtain wide-field photographs of the fundus. It has recently been used in glaucoma management to image the optic disc[5] and the anterior chamber angle.[6] With the use of 120° and 130° wide-field lenses, high-resolution anterior segment images of the iris and ACA can be obtained (Fig. 1). The hardware consists of a hand-held digital video camera connected fiberoptically to a light-emitting control unit and computer assembly. The operator controls focus, illumination, and the acquisition of images with a foot switch. Images are automatically saved to a computer hard drive. Alternatively, a short video stream can be captured, with still frames selected from the video and saved at the end of the imaging session.

The purpose of this study was to evaluate the use of the EyeCam for angle imaging and to assess its diagnostic performance in detecting angle closure using gonioscopy as the reference standard.

Methods

Consecutive subjects were recruited from a glaucoma clinic at a Singapore hospital from July to October 2008. Written informed consent was obtained from all participants. The study had the approval of the hospital's Institutional Review Board and adhered to the tenets of the Declaration of Helsinki.

After an interview about medical and ophthalmic history, each subject underwent the following examinations on the same day: visual acuity, gonioscopy, and imaging with the EyeCam. Subjects were excluded if they were taking any topical medications that had an effect on the pupil size, had a history of cataract surgery or any corneal opacity or abnormalities that precluded EyeCam imaging. A history laser iridotomy was not an exclusion criterion.

Gonioscopy

Gonioscopy was performed in the dark in all cases by a single examiner with glaucoma fellowship training (SAP), who was masked to EyeCam findings. A 1-mm light beam was reduced to a narrow slit and the vertical beam was offset horizontally for assessing superior and inferior angles and offset vertically for nasal and temporal angles. Static gonioscopy was performed with a Goldmann two-mirror lens at high magnification (×16), with the eye in the primary position of gaze. Care was taken to avoid light falling on the pupil and to avoid accidental indentation during examination. In some cases, the gonioscopy lens was tilted minimally to permit a view of the angle over the convexity of the iris, avoiding distortion of angle. The angle in each quadrant was graded using the Scheie grading system according to the anatomic structures observed during gonioscopy.[1] The ACA was considered

From the [1]Singapore National Eye Center, Singapore; the [2]Singapore Eye Research Institute, Singapore; the [3]Wilmer Eye Institute and [4]The Johns Hopkins Bloomberg School of Public Health, The Johns Hopkins Hospital, Baltimore, Maryland; and the [5]Department of Ophthalmology, Yong Loo Lin School of Medicine, National University of Singapore, Singapore.

Supported by grants from the National Medical Research Council, Singapore and Singhealth Foundation.

Submitted for publication August 1, 2009; revised November 5 and December 7, 2009; accepted December 28, 2009.

Disclosure: **S.A. Perera**, None; **M. Baskaran**, None; **D.S. Friedman**, None; **T.A. Tun**, None; **H.M. Htoon**, None; **R.S. Kumar**, None; **T. Aung**, Clarity Medical Systems (R)

Corresponding author: Tin Aung, Singapore National Eye Center, 11 Third Hospital Avenue, Singapore, 168751; tin11@pacific.net.sg.

closed in that quadrant if the posterior pigmented trabecular meshwork (TM) could not be seen in the primary position without indentation. The eye was classified as having angle closure if there were two or more quadrants of closure. Any doubt as to the state of the angle or any suspicion of PAS was confirmed on indentation gonioscopy with a Sussman lens. PAS were defined as abnormal adhesions of the iris to the angle that were present to the level of the anterior trabecular meshwork or higher, and were deemed to be present if apposition between the peripheral iris and angle structures could not be broken despite indentation gonioscopy.

EyeCam Imaging

After gonioscopy, EyeCam imaging was performed on subjects who lay supine on a couch in a darkened room. Images were captured by a single trained technician (TAT) in all four quadrants of the left eye of all subjects, unless any exclusion criteria were present, in which case the right eye was imaged. The technician was trained on the technical details of EyeCam imaging and had basic knowledge of angle anatomy and structures. After instillation of topical anesthetic eye drops (proparacaine hydrochloride 0.5% ophthalmic solution; Alcon Laboratories, Inc., Fort Worth, TX), coupling gel was applied to the anesthetized eye, before imaging proceeded with a 130° lens held next to the limbus. The illumination light was pointed at the angle rather than the pupil, to minimize any pupillary dilatation. If the angle was not visible due to pronounced convexity of the iris, the probe was moved anteriorly within 10° of the limbus to gain a view over the convexity of the iris. The illumination was adjusted using the foot pedal to avoid overexposure. Clear still images were captured to the hard disc of the attached computer for subsequent grading. Imaging of all four quadrants of the eye was performed in less than 5 minutes.

Grading of the Images

EyeCam images were graded in each quadrant by two fellowship-trained glaucoma specialists (TA and MB) working together, who were masked to the gonioscopic data. Images were first graded for their quality as follows: grade 1 if the angle details were clear and well focused in all quadrants; grade 2 if angle images were blurred in any quadrant but some details discerned; grade 3 if the angle structures were blurred in at least one quadrant such that no details can be discerned; and grade 4 if the structures were blurred in all four quadrants and no angle details were discerned. Images were excluded if they were assessed to be grade 3 or 4.

The angle-grading scheme for each quadrant was similar to that used for gonioscopy and was based on anatomic structures observed in the ACA (Fig. 2A). The final grading of a quadrant was determined by the most prevalent grade seen in that quadrant. For EyeCam images, angle closure in any quadrant was defined as the inability to visualize the TM in that quadrant (Fig. 2B), and the eye was considered to have angle closure if the TM was not visible in at least two quadrants.

To examine for intraobserver reproducibility of image grading, the images from 40 (26.31%) of 152 randomly selected eyes were graded again at a different session by one of the examiners (MB), masked to previous grading, for angle structures in each quadrant and for angle

FIGURE 1. EyeCam imaging in a supine subject.

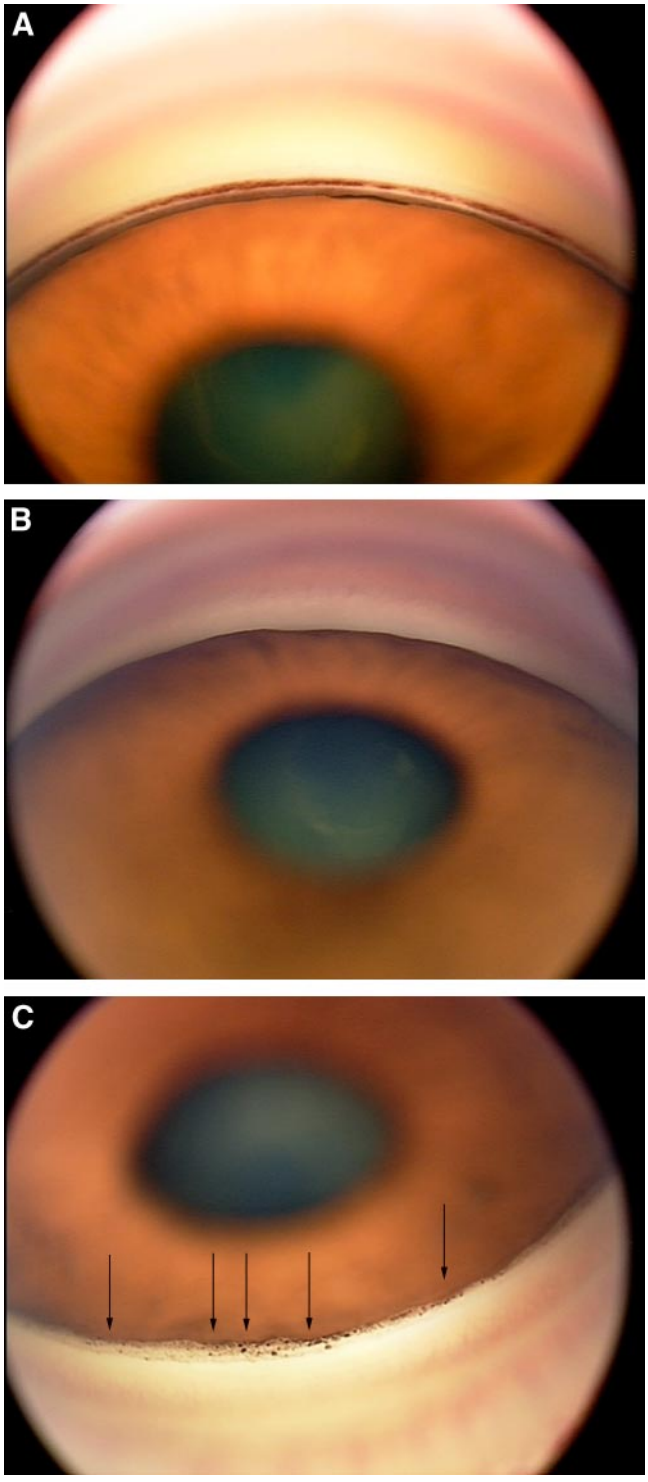

FIGURE 2. (**A**) A wide-open quadrant shown on EyeCam, where the ciliary body can be seen. (**B**) A closed angle where only the Schwalbe's line can be identified. (**C**) An annotated EyeCam image showing possible peripheral anterior synechiae (PAS, *arrows*) and angle pigmentation. The presence of PAS was confirmed by indentation gonioscopy.

TABLE 1. Analysis of the Eyes with Closed Quadrants Detected by EyeCam and Gonioscopy (n = 152)

	Gonioscopy *n* (%, 95% CI)	EyeCam *n* (%, 95% CI)	*P**	AC1†
Eyes with the following number of closed quadrants				
1	15 (9.9, 5.9–15.4)	7 (4.6, 2–8.89)	0.1	0.86
2	8 (5.3, 2.5–10.2)	11 (7.2, 4–12.6)	0.63	0.73
3	7 (4.6, 2.1–9.4)	10 (6.6, 3.5–11.8)	0.61	0.89
4	6 (4, 1.6–8.5)	20 (13.2, 8.6–19.5)	<0.01	0.86
Eyes with closed quadrants by location				
Superior	23 (15.1, 10–21.5)	34 (22.5, 16.4–29.7)	0.04	0.73
Inferior	23 (15.1, 10–21.5)	35 (23, 16.9–30.2)	0.03	0.75
Nasal	21 (13.8, 8.9–20)	36 (23.8, 17.6–31.1)	0.004	0.76
Temporal	10 (6.6, 3.4–11.4)	34 (22.4, 16.3–29.5)	<0.001	0.72
Eyes with angle closure using different definitions				
≥Two quadrants	21 (13.8, 8.9–20)	41 (27, 20.4–34.5)	<0.001	0.71
≥Three quadrants	13 (8.6, 5–14.2)	30 (19.7, 14.2–26.8)	<0.001	0.78

* McNemar test

† Interinstrument agreement based on AC1 statistics.

closure in the eye. For interobserver agreement, the images were also graded by a separate glaucoma fellowship–trained examiner (RSK) who was masked to previous grading results. To assess reproducibility of image acquisition, EyeCam angle imaging was repeated in the same eye by the same technician after 30 minutes in a subgroup of 20 subjects.

Statistical Analysis

Only eyes that had complete data for all four quadrants by both modalities were included for statistical analysis. Parametric and nonparametric tests were used to compare continuous variables, according to data distribution. The χ^2 test was used to compare categorical data. The McNemar test was used to compare differences in distribution of a categorical variable between two related samples. The κ statistic was used to assess the agreement between categorical variables. However, as the κ statistic may be affected by trait prevalence (distribution) and base rates,[7,8] Agreement coefficient (AC1) statistics were used to assess the agreement between graders in situations where the prevalence of positive classifications may lead to inconsistent results. $P < 0.05$ was considered statistically significant (JMP 5; SAS Institute, Inc., Cary, NC, and MedCalc ver. 8.1.0.0; MedCalc, Mariakerke, Belgium).

RESULTS

Of the 169 subjects recruited, 15 were excluded for incomplete or missing data. Two subjects (1.2%) were excluded due to poor quality (grade 3 or 4) of EyeCam images. A total of 152 eyes of 152 subjects were finally analyzed, comprising 23 (3.8%) of 608 images that were grade 2 and 585 (96.2%) of 603 images that were grade 1. The mean age was 57.4 years (SD 12.9 years) and there were 82 (54%) men. The majority of subjects were Chinese (80.3%), and the remainder were Malay (4.6%), Indian (7.9%), and other races (7.2%). Of the 152 eyes, 21 eyes (13.8%) had angle closure (6 had suspected primary angle closure [PACS], 4 primary angle closure [PAC], and 11 were primary angle closure glaucoma [PACG]). Among these, 15 eyes had previous laser peripheral iridotomy performed.

The agreement between EyeCam and gonioscopy in detecting a closed angle in the superior, inferior, nasal, and temporal quadrants based on AC1 statistics was 0.73, 0.75, 0.76, and 0.72, respectively (Table 1). EyeCam detected more closed angles than gonioscopy in all quadrants ($P < 0.05$).

With gonioscopy, 21 (13.8%) of 152 eyes were diagnosed as angle closure compared with 41 (27.0%) with EyeCam ($P < 0.001$, McNemar Test), giving an overall sensitivity of 76.2% (95% confidence interval [CI], 54.9%–90.7%), specificity of 80.9% (95% CI, 73.5%–87.3%), and an area under the receiver operating characteristic curve (AUC) of 0.79. The agreement between the two modalities, according to AC1 stats, varied depending on the definition of angle closure used (summarized in Table 1).

Reproducibility Analysis

The intraobserver reproducibility (image grading) for detecting angle closure in two quadrants or more using EyeCam images was 0.57 (AC1) and 0.43 (κ; 95% CI, 0.13–0.74); and that of interobserver agreement was 0.64 (AC1) and 0.49 (κ; 95% CI, 0.20–0.79; Table 2) respectively. In terms of reproducibility of image acquisition, there was good intraobserver reproducibility for angle closure detection (0.84 [AC1] and 0.73 [κ; 95% CI, 0.38–1.08]).

TABLE 2. The Inter- and Intraobserver Agreement in Detecting Closed Quadrants and Detecting Overall Angle Closure Status Using EyeCam and Gonioscopy

	Interobserver Agreement		Intraobserver Agreement	
Quadrants	**κ (95% CI)**	**AC1**	**κ (95% CI)**	**AC1**
Superior	0.63 (0.38–0.88)	0.67	0.52 (0.23–0.82)	0.67
Inferior	0.59 (0.31–0.87)	0.70	0.65 (0.4–0.91)	0.74
Nasal	0.39 (0.06–0.72)	0.58	0.57 (0.27–0.86)	0.71
Temporal	0.40 (0.06–0.75)	0.65	0.48 (0.16–0.80)	0.68
Angle closure*	0.49 (0.20–0.79)	0.64	0.43 (0.13–0.74)	0.57

* Defined as closure in two quadrants or more.

Discussion

In this study, we found good agreement between EyeCam angle imaging and clinical gonioscopy for detecting quadrants with closed angles. However, for detecting eyes with angle closure, there was a higher rate of angle closure diagnosed by EyeCam compared with gonioscopy, with a sensitivity and specificity of 76.2% and 80.9% respectively (AUC 0.79), using the two quadrant definition of angle closure. The EyeCam was able to obtain clear images of the angles in 98.8% of studied individuals, with imaging performed by a technician.

This difference in findings between the EyeCam and gonioscopy could be due to numerous factors including patient positioning (the patient is supine for the EyeCam and seated for gonioscopy), different degrees of illumination (although light is needed for both assessments), and the optics used in the EyeCam to image the angle. Of note, the light used for EyeCam is quite bright and although no flash was used, the light would have an effect on pupillary constriction. The probe is placed 180° across from the angle being imaged and requires a direct line of sight to see angle structures. However, a convex iris profile can block the camera from angle structures. EyeCam imaging revealed a very uniform distribution of closed quadrants across all four quadrant locations of the eye, in contrast to gonioscopy which showed a trend toward more closure in the inferior and superior quadrants, supporting previous gonioscopic and anterior segment optical coherence tomography (AS-OCT) data.[9,10]

The EyeCam offers advantages over other angle imaging methods. It provides a direct, color view of the angle with excellent optical quality, similar to that provided by gonioscopy. The number of poor-quality images is low (~1% in our study), and a technician can perform EyeCam easily after a short period of training. In contrast, in a previously published large community-based study of AS-OCT for the detection of angle closure, 16% (a significant proportion) of eyes could not be assessed for angle closure, mainly due to poor quality images or poor visibility of the scleral spur.[11] Goniophotography using a slit lamp–mounted camera is another method of angle imaging that is similar to EyeCam. However, slit lamp goniophotography is technically challenging, and it is not easy to obtain good-quality images. We are currently performing a study comparing EyeCam with slit lamp goniophotography.

In some EyeCam images, we identified structures that resemble PAS (Fig. 2C). However as indentation could not be performed, the EyeCam could not be used to conclusively differentiate PAS from iris processes. This is a limitation of the device. Indentation gonioscopy is the reference standard approach to distinguish between appositional and synechial angle closure.[12] Furthermore, being unable to dynamically indent the eye made it difficult at times to distinguish TM pigment from pigment on Schwalbe's line. The interpretation of EyeCam images in eyes with lightly pigmented TM may be difficult, whereas gonioscopy has the advantage of using the corneal wedge as a landmark to identify the anterior edge of the TM. These reasons may have contributed to the moderate intra- and interobserver agreement found in the interpretation of EyeCam images. This level of agreement is lower than that seen when interpreting AS-OCT images.[13]

Current documentation of the angle in patient records is often subject to a variety of different classification systems and can be difficult to interpret. The EyeCam may have potention for documenting a 360° view of the angle, which could then be interpreted by any observer. This would be useful for documentation in clinical charts. The EyeCam also delivers images that show more than simply the angle width, it can show pigment and new vessels (although not evaluated in this study), that cannot be imaged by the cross-sectional imaging modalities. However, quantitative analysis is not yet possible with the EyeCam. As trained technicians can efficiently capture the images, the EyeCam could be used alongside the ophthalmologist's clinical examination for referral consultations or for education.

Our study has some limitations. The use of a single observer for gonioscopy could have led to a systematic bias. EyeCam was performed on supine patients, whereas gonioscopy was performed on patients sitting at the slit lamp. As mentioned, the lighting conditions for EyeCam and gonioscopy were different. The images seen with the EyeCam gave a good 90° view or more of the angle, but there is some degradation of the images at the periphery that are related to optical aberrations and depth of field. The reproducibility of EyeCam image grading was only moderate. This is a concern because clinical decisions based on the EyeCam images may vary depending on the grader. The proportion of subjects with angle closure was quite low (13.8%) in this sample and may partly explain the wide confidence intervals seen in reproducibility analyses for angle closure detection. Should the EyeCam be used more widely, it may be necessary to devise more elaborate training and create standard photos in an attempt to improve the reproducibility. Overall, we believe that the EyeCam's limitations include the high cost, variable angle of view, effect of illumination and gravity, learning curve for the operator, moderate to poor reproducibility, inability to distinguish appositional from synechial closure as PAS cannot be identified, and difficulty in identifying angle structures in eyes with light pigmentation. The strengths of the study stem from the fact that standard definitions and grading system were used for angle closure and a large number of eyes have been imaged. Also, the assessment of EyeCam images was performed by graders masked to the gonioscopic data.

In summary, this initial study showed a good degree of agreement between EyeCam angle imaging and clinical gonioscopy, with moderate sensitivity and specificity for detecting angle closure. The EyeCam has potential for use in anterior segment imaging, particularly in the clinical setting for documentation of angle findings. However, due to several inherent limitations, it cannot be recommended as a screening tool for detection of angle closure and cannot be used to distinguish PACS from PAC or PACG, as it cannot identify PAS.

References

1. Scheie HG. Width and pigmentation of the angle of the anterior chamber. A system of grading by gonioscopy. *Arch Ophthalmol.* 1957;58:510–512.
2. Schirmer KE. Gonioscopy and artefacts. *Br J Ophthalmol.* 1967; 51:50–53.
3. Spaeth GL. The normal development of the human anterior chamber angle: a new system of descriptive grading. *Trans Ophthalmol Soc UK.* 1971;91:709–739.
4. Gazzard G, Foster PJ, Friedman DS, Khaw PT, Seah S. Light to dark physiological variation in irido-trabecular angle width (video report). *Br J Ophthalmol.* Available at http://bjo.bmjjournals.com/cgi/content/full /88/11/DC1/1.
5. Erraguntla V, MacKeen LD, Atenafu E, et al. Assessment of change of optic nerve head cupping in pediatric glaucoma using the RetCam 120. *J AAPOS.* 2006;10:528–533.
6. Narayanaswamy A, Singh M. RetCam: a useful adjunctive tool to evaluate and manage paediatric glaucomas. *Asian J Ophthalmol.* 2008;109:30–31.
7. Chan YH. Biostatistics 104: correlational analysis. *Singapore Med J.* 2003;44:614–619.
8. Inter-Rater Reliability. Available at: http://www.education.ox.ac.uk/uploaded/3.3%20&%203.4%20Inter-rater%20&%20teach%20expect/3.3.interrater.ppt#. Accessed September 5, 2009.

9. Nolan WP, See JL, Chew PT et al. Detection of primary angle closure using anterior segment optical coherence tomography in Asian eyes. *Ophthalmology.* 2007;114:33–39.
10. See JL, Chew PT, Smith SD, et al. Changes in anterior segment morphology in response to illumination and after laser iridotomy in Asian eyes: an anterior segment OCT study. *Br J Ophthalmol.* 2007;9:1485–1489.
11. Sakata LM., Lavanya R, Friedman DS, et al. Comparison of gonioscopy and anterior segment ocular coherence tomography in detecting angle closure in different quadrants of the anterior chamber angle. *Ophthalmology* 115;5:769–774.
12. Forbes M. Gonioscopy with corneal indentation; a method for distinguishing between appositional closure and synechial closure. *Arch Ophthalmol.* 1966;76:488–492.
13. Radhakrishnan S, See JL, Smith SD, et al. Reproducibility of anterior chamber angle measurements obtained with anterior segment optical coherence tomography. *Invest Ophthalmol Vis Sci.* 2007; 48:3683–3688.

Angle Assessment by EyeCam, Goniophotography, and Gonioscopy

Mani Baskaran, DO, DNB, Shamira A. Perera, BSc(hons), FRCOphth,* Monisha E. Nongpiur, MS,* Tin A. Tun, MD,* Judy Park, MSc,* Rajesh S. Kumar, MS,* David S. Friedman, MD, PhD,† and Tin Aung, FRCS(Ed), PhD*‡*

Purpose: To compare EyeCam (Clarity Medical Systems, Pleasanton, CA) and goniophotography in detecting angle closure, using gonioscopy as the reference standard.

Methods: In this hospital-based, prospective, cross-sectional study, participants underwent gonioscopy by a single observer, and EyeCam imaging and goniophotography by different operators. The anterior chamber angle in a quadrant was classified as closed if the posterior trabecular meshwork could not be seen. A masked observer categorized the eyes as per the number of closed quadrants, and an eye was classified as having angle closure if there were 2 or more quadrants of closure. Agreement between the methods was analyzed by κ statistic and comparison of area under receiver operating characteristic curves (AUC).

Results: Eighty-five participants (85 eyes) were included, the majority of whom were Chinese. Angle closure was detected in 38 eyes (45%) with gonioscopy, 40 eyes (47%) using EyeCam, and 40 eyes (47%) with goniophotography ($P = 0.69$ in both comparisons, McNemar test). The agreement for angle closure diagnosis (by eye) between gonioscopy and the 2 imaging modalities was high ($\kappa = 0.86$; 95% Confidence Interval (CI), 0.75-0.97), whereas the agreement between EyeCam and goniophotography was not as good ($\kappa = 0.72$; 95% CI, 0.57-0.87); largely due to lack of agreement in the nasal and temporal quadrants ($\kappa = 0.55$ to 0.67). The AUC for detecting eyes with gonioscopic angle closure was similar for goniophotography and EyeCam (AUC 0.93, sensitivity = 94.7%, specificity = 91.5%; $P > 0.95$).

Conclusions: EyeCam and goniophotography have similarly high sensitivity and specificity for the detection of gonioscopic angle closure.

Key Words: anterior chamber angle, gonioscopy, goniophotography, imaging, angle closure

(*J Glaucoma* 2012;21:493–497)

Improved methods are needed to assess the anterior chamber angle (ACA). Although gonioscopy offers several advantages such as low cost, the ability to simultaneously visualize an entire quadrant of the ACA, the use of the corneal wedge as a landmark to help identify angle structures and the ability to dynamically indent the angle to confirm the presence of peripheral anterior synechiae (PAS), it remains a subjective examination. Documentation of gonioscopic findings is often poor, as images or photographic records are not routinely taken in clinical practice.[1] A recent chart review of insured patients diagnosed with glaucoma in the United States found that routine gonioscopic examination was not standardized and infrequently performed.[2] In this context, the availability of simple photographic techniques to document angle findings would be an appealing option in clinical practice, especially if imaging provided clinically useful information about the risk of angle closure and can be used for documentation of longitudinal changes.

The EyeCam (Clarity Medical Systems, Pleasanton, CA) is a camera capable of taking wide-field photographs of the fundus,[3] and has recently been assessed for its ability image, the optic disc[3] and the ACA.[4,5] We recently reported good agreement compared with gonioscopy,[6] and demonstrated that the EyeCam detects changes in angle configuration after laser peripheral iridotomy.[7] Goniophotography is a clinical method of documenting gonioscopic findings using a slit-lamp mounted camera and indirect gonioscopic lens. This technique requires some expertize to discern the ocular structures with the gonioscopy lens and for obtaining clear images of the angle.

The aim of this study was to compare EyeCam images with those obtained with goniophotography for angle assessment and to assess their diagnostic performance in detecting angle closure, as identified with gonioscopy.

MATERIALS AND METHODS

This prospective hospital-based study was conducted with the approval of the Ethics Review Board of the Singapore Eye Research Institute and was performed in accordance with the tenets of the Declaration of Helsinki. Written informed consent was obtained from every participant.

Consecutive participants who were above the age of 40 years were recruited from a single glaucoma clinic at a Singapore hospital. The study population was novel and not the same as those in our previous studies on EyeCam.[6,7] Participants with earlier intraocular surgery or penetrating eye injury, or corneal disorders such as corneal endothelial dystrophy, pterygium, or corneal scars that may preclude satisfactory imaging, were excluded from the study. Poor

Received for publication September 14, 2010; accepted February 28, 2011.

From the *Singapore Eye Research Institute and Singapore National Eye Center; ‡Yong Loo Lin School of Medicine, National University of Singapore, Singapore; and †Wilmer Eye Institute and Johns Hopkins Bloomberg School of Public Health, Baltimore, MD.

Financial Disclosure: Dr Aung has received honoraria for travel to conferences from Clarity Medical Systems, Inc. Pleasanton, CA and an instrument loan.

Supported by Grants from the National Medical Research Council, Singapore and Singapore National Eye Centre.

Reprints: Tin Aung, FRCS(Ed), PhD, Glaucoma Service, Singapore National Eye Center, 11 Third Hospital Avenue, Singapore, 168751 (e-mail: tin11@pacific.net.sg).

DOI:10.1097/IJG.0b013e3182183362

quality images from EyeCam and goniophotography, with blurred angle details, were excluded from the study. Patients who had previously undergone laser peripheral iridotomy were also included. After obtaining a detailed ophthalmic history, each patient underwent a standardized examination that included visual acuity assessment, slit-lamp biomicroscopy, Goldmann applanation tonometry, gonioscopy, goniophotography, and imaging with the EyeCam.

Gonioscopy was performed in the dark in all cases by a single examiner with previous glaucoma fellowship training (S.A.P.), who was masked to imaging findings. A 1-mm light beam was reduced to a narrow slit and the vertical beam was used for assessing superior and inferior angles and offset horizontally for nasal and temporal angles. Static gonioscopy was performed using a Goldmann 2-mirror lens (Ocular Instruments Inc, Bellevue, WA) at high magnification ($\times$ 16), with the eye in the primary position of gaze. In some cases, the gonioscopy lens was tilted minimally to permit a view of the angle over the convexity of the iris, avoiding distortion of angle. Care was taken to avoid light falling on the pupil and to avoid inadvertent indentation during examination. The angle in each quadrant was graded as per the Scheie grading system according to the anatomic structures observed during gonioscopy.[8] The ACA was considered "closed" in that quadrant if the posterior pigmented trabecular meshwork (TM) could not be seen in the primary position without indentation (Scheie grade 3 or 4). The eye was classified as having angle closure if there were 2 or more quadrants of closure. Indentation gonioscopy was performed to assess the presence of PAS, however, this information was not used in this study.

Image capture by EyeCam has been described in detail elsewhere.[6,7] This instrument is identical to the Retcam (Clarity Medical Systems, Pleasanton, CA) device used for retinal imaging. In brief, EyeCam imaging was performed on participants in the supine position on a couch, in a darkened room. Images were captured by a single trained technician (T.A.T.) in all 4 quadrants of the eye. After applying topical anesthetic eye drops (Proparacaine hydrochloride 0.5% ophthalmic solution, Alcon Laboratories Inc., FortWorth, TX), coupling gel was applied to the anesthetized eye, before imaging proceeded with a 130 degrees lens held next to the limbus. The illumination light was pointed at the angle rather than the pupil to minimize any pupillary dilatation. If the angle was not visible due to pronounced convexity of iris, the probe was moved anteriorly within 10 degrees of the limbus to gain a view over the convexity of the iris. The illumination was adjusted using the foot pedal to avoid overexposure until the TM and/or the peripheral iris roll was clearly visible. Clear, still images were captured to the hard disk of the attached computer for subsequent grading. Imaging of all 4 quadrants of the eye was performed in < 5 minutes.

Goniophotography was performed using the slit lamp with the MagnaView Goniolens (Ocular Instruments Inc, Bellevue, WA) by an ophthalmologist (M.E.N.), masked to other findings. This is a single mirror goniolens with high magnification ($\times$ 1.3). We used a thin film of goniogel when using this lens to capture images with better clarity. A slit beam of 1 mm width and lowest possible height was used to capture the angle structures in primary gaze. Images of all 4 quadrants of the study eye were documented, taking precautions to avoid pupil constriction during photography. In all images, the slit beam was rotated so as to be radial in each quadrant view.

The resulting EyeCam and goniophotograph images were randomly ordered and graded on separate occasions, by a fellowship trained glaucoma specialist (M.B.) who was masked to gonioscopic data. The methodology for grading the quality of EyeCam images and the method of grading the images have been described elsewhere.[6] The quality of images were graded from 1 to 4 based on the visibility of angle details. Only grade 1 and 2 images were included. Eachquadrant was graded for anatomic structures observed in the ACA. As with gonioscopy, angle closure in a quadrant was defined as the inability to visualize the pigmented TM in that quadrant. This definition was used for both EyeCam and goniophotography images. An eye was considered to have angle closure if the pigmented TM was not visible in at least 2 quadrants. We have not reported on the presence of PAS or iris processes as indentation was not possible using the EyeCam. Further classifications such as 1 quadrant closure or more and 3 quadrants closure or more were considered in the analysis. Intraobserver and interobserver reproducibility for EyeCam and goniophotography grading was analyzed in 30 randomly selected eyes. Images for all 4 quadrants were included and presented to each of the observers (M.B and R.S.K.) in random order. The observers graded the images for angle closure in each quadrant for both modalities on separate occasions, masked to gonioscopic data.

Statistical Analysis

One eye from each patient was randomly selected for analysis if both the eyes were eligible for the study. The McNemar test was used to compare differences in the distribution of categorical variables between 2 related samples. Kappa statistic was used to assess the agreement between categorical variables and for reproducibility analysis. Receiver operating characteristic curves, with calculations of area under the curve (AUC) and 95% confidence intervals (CIs) were used as an index of each instrument's performance for identifying eyes with angle closure, using gonioscopy as the reference standard. A P value < 0.05 was considered statistically significant. The sample size calculation was based on comparison of sensitivities for matched groups in a diagnostic study, as reported by Beam.[9] With an estimated sensitivity of 82%, the numbers of participants required was 78 in this study. Statistical analysis was performed using STATA version 10 (Statacorp, College Station, TX), and Med Calc version 8.1.0.0 (Mariakerke, Belgium).

RESULTS

Of the 90 participants recruited, 5 were excluded due to incomplete, poor quality, or missing goniophotography/EyeCam images in some quadrants. The mean age of the remaining 85 study participants was 61.6 years (SD 12.1 y) and there were 44 female participants (52.9%). The majority of participants were Chinese (74.1%), the rest comprised of Malay (8.2%) and Indian (17.6%) ethnic groups. All images were of gradable quality. Of the 85 eyes analyzed, 38 eyes (44.7%) had angle closure (in 2 quadrants or more) by gonioscopy; whereas EyeCam and goniophotography each identified 40 eyes (47.1%) as having angle closure ($P = 0.69$ in both comparisons, McNemar test). The agreement for angle closure diagnosis (by eye) between gonioscopy and the 2 imaging modalities was high ($\kappa = 0.86$; 95% CI, 0.75-0.97), whereas the agreement between EyeCam and goniophotography was not as good

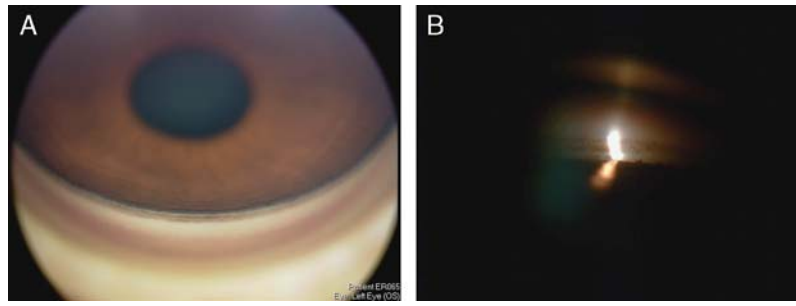

FIGURE 1. EyeCam (A) and goniophotograph (B) images showing open angle in the inferior quadrant of the same patient.

($\kappa = 0.72$; 95% CI, 0.57-0.87). Figures 1A and B show an open angle seen in the inferior quadrant for the same participant using EyeCam and goniophotography. Figure 2 shows the comparison of the above classification of angle closure between the 3 modalities. When defining angle closure as 1, 2, or 3 quadrants or more closed on gonioscopy, EyeCam and gonioscopy had good-to-excellent agreement (Table 1). Agreement was best when defining angle closure as 2 or more quadrants closed on gonioscopy. In a quadrant-wise analysis of angle closure, goniophotography and EyeCam imaging had poorer agreement in the nasal and temporal quadrants ($\kappa = 0.55$ vs. 0.67) compared with the superior and inferior quadrants ($\kappa = 0.69$ vs. 0.76, Table 1).

The AUC was more than 90% for each imaging modality when defining angle closure as having 2 or more quadrants closed on gonioscopy (Table 2). The AUC was lower when defining angle closure using more or fewer quadrants closed on gonioscopy.

The interobserver agreement for EyeCam (using 2 or more quadrants closed to define angle closure) was 0.8 (95% CI $\kappa = 0.57$-1) and for goniophotography was 0.67 (95% CI $\kappa = 0.40$-0.93). The intraobserver agreement for the EyeCam was 0.73 (95% CI $\kappa = 0.38$-1.1) and for goniophotography was 0.87 (95% CI $\kappa = 0.69$-1).

DISCUSSION

To the best of our knowledge, this is the first study comparing EyeCam and goniophotography with gonioscopy in a clinical setting. We found good diagnostic performance for both these modalities for detecting angle closure compared with gonioscopy, especially using the 2-quadrant definition of angle closure. Subjective grading of goniophotographs and EyeCam images was reproducible both within and between observers, and identified angle closure as defined by gonioscopy with high accuracy. This study found better agreement between EyeCam and gonioscopy for detecting angle closure than a previous study by our group where the agreement was found to be 0.71 (AC1 stats) for angle closure.[6] We postulate that greater experience with the EyeCam has resulted in better quality images, allowing for more accurate assessment of the angle structures. Furthermore, we have further emphasized the need to avoid illumination across the pupil during imaging, and this may have led to less angle widening during the imaging process. Our current technique is to lower the illumination once the EyeCam is focused on the pigmented TM. If the quadrant is closed and the posterior TM cannot be visualized, the technician should then focus on the peripheral iris or Schwalbe line and once again decrease illumination before obtaining the image. In a previous study,[6] we found more angle closure in EyeCam images compared with gonioscopy. This difference in angle findings could be due to the imaging method used for the EyeCam to image the angle. A highly convex iris profile can block the camera from angle structures and this may be mistaken for angle closure. The focusing of the EyeCam exactly on the angle structures may have been less standardized in the previous study, which may have led to a misclassification bias toward angle closure diagnosis, compared with this study. Gonioscopy could cause some indentation of the angle resulting in a more wider angle appearance compared with the Eyecam, which is noncontact.

Only 5 eligible participants (6%) were excluded due to incomplete or poor quality goniophotograph/EyeCam images. Almost all goniophotographs and EyeCam images were of good quality and could be evaluated in the study. In contrast, as many as 30% of anterior segment optical coherence tomography (AS-OCT) angle images could not be graded in previous studies, mainly due to poor visibility of the scleral spur.[10,11] The EyeCam and goniophotography may have an advantage over present AS-OCT technologies in that a wide field view and documentation of the angle is possible and these images can be easily interpreted by most ophthalmologists.

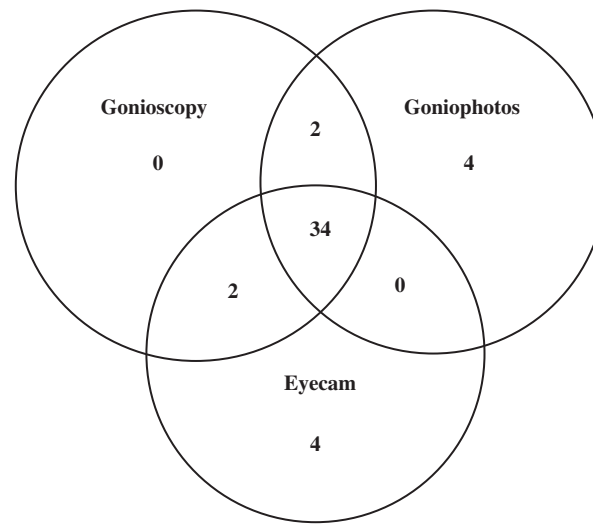

FIGURE 2. Venn diagram showing distribution of closed angles (2 quadrants or more) between gonioscopy (n=38), goniophotography (n=40), and EyeCam (n=40).

TABLE 1. Summary Statistics of Agreement of EyeCam and Goniophotography Compared With Gonioscopy for Different Definitions of Angle Closure

	Agreement Between Methods and k Statistic (95% CI)		
Definition of Closure	**EyeCam Versus Gonioscopy**	**Goniophotography Versus Gonioscopy**	**EyeCam Versus Goniophotography**
1 or more quadrants closed	0.84 (0.62, 1.05)	0.77 (0.56, 0.98)	0.74 (0.60, 0.88)
2 or more quadrants closed	0.86 (0.65, 1.07)	0.86 (0.65, 1.07)	0.72 (0.57, 0.87)
3 or more quadrants closed	0.78 (0.57, 0.99)	0.70 (0.49, 0.91)	0.73 (0.59, 0.88)
Superior quadrant closed	0.83 (0.72, 0.95)	0.76 (0.63, 0.90)	0.69 (0.54, 0.85)
Inferior quadrant closed	0.93 (0.85, 1.01)	0.83 (0.71, 0.95)	0.76 (0.62, 0.90)
Nasal quadrant closed	0.64 (0.47, 0.81)	0.59 (0.41, 0.77)	0.55 (0.37, 0.74)
Temporal quadrant closed	0.68 (0.51, 0.84)	0.59 (0.41, 0.76)	0.67 (0.51, 0.83)

CI indicates confidence interval.

Although goniophotography and EyeCam imaging performed equally well in this study, they differ in important ways. Goniophotography is performed with the patient seated (as is gonioscopy), whereas EyeCam imaging is performed with the patient in the supine position. In theory, body positioning could lead to variation in angle findings and a supine position may be inconvenient for some participants. Goniophotography samples a smaller segment of the angle quadrant. To minimize the impact of illumination on angle findings, the photographer must use a narrow slit of light, analogous to the cross-sectional scans attained by the AS-OCT,[12] rather than the full quadrant view afforded by EyeCam. Goniophotography is also more cumbersome to obtain. Although we did not measure the time needed to obtain goniophotographs, we found that the procedure was relatively time consuming and more operator-dependent than image acquisition with the EyeCam. Goniophotography requires a technician familiar with gonioscopy (in this study, an ophthalmologist performed the goniophotography) to place the goniolens on the eye and to focus on the angle structures. In contrast, a less trained individual can perform EyeCam imaging. Goniophotography may have advantages over the EyeCam, including the ability to capture the corneal wedge to help identify Schwalbe line, and the use of less light (32.28 lux compared with 129.12 lux with EyeCam).[7] The agreement in identifying angle closure between EyeCam and goniophotography, while good, was lower than the agreement between each modality with the reference standard, gonioscopy. Agreement was lowest in the nasal quadrant, followed by the temporal quadrant. The latter may be due to difficulties in image capture due to the nasal bridge; however, we are unable to explain the poor agreement in the nasal quadrant. The inability of both modalities to perform indentation and detect PAS, and the use of illumination (which may cause pupil constriction with widening of angle) are significant drawbacks.[12]

Our study had several limitations. This clinic-based population may not be representative of community-based populations, as many had been examined with lenses touching the eye, and therefore may have been more cooperative with the examination. This could have led to better results than would be obtained in nonclinic settings. Second, the operators performing the tests were well trained and experienced. Whether or not others could be trained to obtain such high-quality images is uncertain. Only 1 examiner performed gonioscopy, which is a potential limitation of the study. In addition, the difference in position adopted by the study participants when undergoing gonioscopy (seated) and EyeCam (supine) may have affected the results. The cost of EyeCam, being higher than either gonioscopy or goniophotography, may be a limitation to its routine use in clinical practice. Finally, we did not determine if images taken over time by different technicians would have performed equally well. Although grading of the images was reproducible, more attention to overall reproducibility will be needed as these technologies evolve.

In summary, this study showed that both EyeCam and goniophotography can be used to document angle findings, and analysis of the images was consistent with findings on gonioscopy. Both modalities showed good diagnostic performance for detecting angle closure, with good agreement between each other, and with gonioscopy. EyeCam may have advantages over goniophotography such as easier image capture, a wider field of view of the angle, higher quality images, and greater patient comfort. However, as these techniques are technically demanding and time consuming, they are unlikely to replace gonioscopy but may be a useful adjunct to document gonioscopic findings in clinical practice.

TABLE 2. ROC Analysis to Compare EyeCam and Goniophotography With Gonioscopy for Various Definitions of Angle Closure

	EyeCam Versus Gonioscopy			Goniophotography Versus Gonioscopy			
Definition of Closure	**AUC (95% CI)**	**Sensitivity**	**Specificity**	**AUC (95% CI)**	**Sensitivity**	**Specificity**	***P****
1 or more quadrants closed	0.92 (0.84, 0.97)	0.95	0.89	0.89 (0.79, 0.94)	0.95	0.82	0.38
2 or more quadrants closed	0.93 (0.85, 0.97)	0.95	0.92	0.93 (0.85, 0.97)	0.95	0.92	> 0.95
3 or more quadrants closed	0.89 (0.79, 0.94)	0.94	0.87	0.85 (0.7, 0.92)	0.81	0.89	0.22

*P value to test equality of the 2 ROC curves, based on the method of De Long.
AUC indicates area under ROC curve; CI, confidence interval; ROC, receiver operating characteristic.

REFERENCES

1. Schirmer KE. Gonioscopy and artefacts. *Br J Ophthalmol*. 1967;51:50–53.
2. Quigley HA, Friedman DS, Hahn SR. Evaluation of practice pattern for the care of open angle glaucoma compared with claims data: the Glaucoma Adherence and Persistence Study. *Ophthalmology*. 2007;11:1599–1606.
3. Erraguntla V, MacKeen LD, Atenafu E, et al. Assessment of change of optic nerve head cupping in pediatric glaucoma using the RetCam 120. *J AAPOS*. 2006;10:528–533.
4. Narayanaswamy A, Singh M. RetCam—a useful adjunctive tool to evaluate and manage paediatric glaucomas. *Asian J Ophthalmol*. 2008;109:30–31.
5. Ahmed I, MacKeen L. A new approach to imaging the angle. *Glaucoma Today*. 2007;4:1–3.
6. Perera SA, Baskaran M, Friedman DS, et al. Use of EyeCam for imaging the anterior chamber angle. *Invest Ophthalmol Vis Sci*. 2010;51:2998–3002.
7. Perera SA, Quek DT, Baskaran M, et al. Demonstration of angle widening using EyeCam after laser peripheral iridotomy in eyes with angle closure. *Am J Ophthalmol*. 2010;149: 903–907.
8. Scheie HG. Width and pigmentation of the angle of the anterior chamber? A system of grading by gonioscopy. *Arch Ophthalmol*. 1957;58:510–512.
9. Beam CA. Strategies for improving power in diagnostic radiology research. *AJR*. 1992;159:631–637.
10. Nolan WP, See JL, Chew PT, et al. Detection of primary angle closure using anterior segment optical coherence tomography in asian eyes. *Ophthalmology*. 2007;114:33–39.
11. Sakata LM, Lavanya R, Friedman DS, et al. Comparison of gonioscopy and anterior segment ocular coherence tomography in detecting angle closure in different quadrants of the anterior chamber angle. *Ophthalmology*. 2008;115:769–774.
12. Forbes M. Gonioscopy with corneal indentation; a method for distinguishing between appositional closure and synechial closure. *Arch Ophthal*. 1966;76:488–492.

33rd Annual International Conference of the IEEE EMBS
Boston, Massachusetts USA, August 30 - September 3, 2011

Focal Edge Association to Glaucoma Diagnosis

Jun Cheng, Jiang Liu, Damon Wing Kee Wong, Ngan Meng Tan, Beng Hai Lee,
Carol Cheung, Mani Baskaran, Tien Yin Wong and Tin Aung

***Abstract*—Glaucoma is an optic nerve disease resulting in the loss of vision. There are two common types of glaucoma: open angle glaucoma and angle closure glaucoma. Glaucoma type classification is important in glaucoma diagnosis. Clinically, ophthalmologists examine the iridocorneal angle between iris and cornea to determine the glaucoma type as well as the degree of closure. However, manual grading of the iridocorneal angle images is subjective and often time consuming. In this paper, we propose focal edge for automated iridocorneal angle grading. The iris surface is located to determine focal region and focal edges. The association between focal edges and angle grades is built through machine learning. A modified grading system with three grades is adopted. The experimental results show that the proposed method can correctly classify 87.3% open angle and 88.4% closed angle. Moreover, it can correctly classify 75.0% grade 1 and 77.4% grade 0 for angle closure cases.**

I. Introduction

Glaucoma is an optic nerve disease resulting in loss of vision. It is often associated with increased pressure of fluid inside the eye. Two common types of glaucoma are open angle glaucoma (OAG) and angle closure glaucoma (ACG). Ophthalmologists examine the iridocorneal angle between iris and cornea to determine OAG and ACG. When the angle is open, it is OAG, otherwise, ACG. A detailed description of the angle structures can be found in [1]. Here we briefly explain why the iridocorneal angle is important. The iris, cornea, and lens are bathed in aqueous humor, which is continually produced by nearby tissues. The fluid moves out of the eye via the trabecular meshwork drainage. Blockage in the trabecular meshwork would lead to increased pressure in the eye. The trabecular meshwork is associated with the angle, thus, the iridocorneal angle is important. Because of different causes and specific treatments for different types of glaucoma as well as the necessity of urgent treatment of ACG, it is important to determine the glaucoma type early [2], which implies that it is essential to visualize the iridocorneal angle to make a correct diagnosis of the disease.

Gonioscopy is an eye examination that looks at the front part of the eye between the cornea and the iris. The drawback of this examination is that it requires considerable clinical expertise and effort as well as a full knowledge of the angle structures [3]. A new option with much more convenience is the RetCam (Clarity Medical Systems, Inc., Pleasanton, CA) camera, which is explored to capture the image of iridocorneal angle [3]. Ophthalmologists often examine four quadrants including inferior, superior, nasal and temporal of an eye [4]. Fig. 1(a) shows a typical iridocorneal angle image from inferior quadrant of an eye. The angle which is of our interest is located at the boundary between the iris and the cornea. The arcuate line in Fig. 1(b) indicates the iris surface which is part of angle boundary. When there are other edges on the corneal side of the iris surface, as indicated by the black arrow in Fig. 1(b), it is an open angle, otherwise, closed.

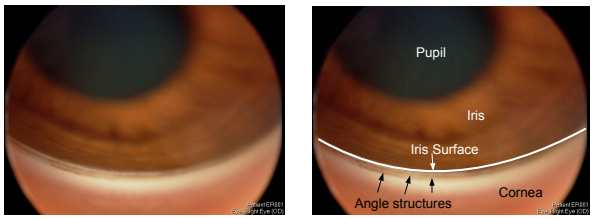

(a) Original Image (b) Iris Surface and angle structures

Fig. 1. Sample Iridocorneal Angle Image

Shaffer grading system [2] is widely used in gonioscopy to evaluate the angle status. Based on the visibility of the angle structures, the system assigns a numerical grade (0-4) to each angle with associated anatomical description and implied clinical interpretations [1]. In this paper, a modified grading system is adopted. Since the anterior trabecular meshwork cannot be identified through the angle images captured by the RetCam, grade 2 cannot be differentiated from grade 1 according to [1]. Thus, grade 2 is merged into grade 1. Moreover, as the clinical interpretation for grade 3 and 4 are the same: 'Closure Impossible', it is not important to differentiate them. In summary, the modified Shaffer grading system contains three grades: 1) Open for 'Closure Impossible', 2) Grade 1 for 'Eventual Closure Probable' and 'Closure Possible', 3) Grade 0 for 'Closure Present or Imminent'. This is a three-class classification problem. Manual grading is currently adopted clinically. However, it is subjective and time consuming due to ambiguous angle structures. Thus, an automated system for angle grading is beneficial to save workload of ophthalmologists.

Limited work has been done for automated angle image grading as the imaging modality appears only recently. In [4], the edges around strongest arc are used to determine ACG or OAG without estimating the degree of closure for ACG. One limitation of the approach is that some edges from inner iris are mistaken as edges from angle structures. In this paper, we propose to first locate the iris surface. The edges on the cornea side of the iris surface are then used. Besides the differentiation between ACG and OAG, we further tell the degree (grade 1 or 0) of closure for ACG. The rest of paper is organized as

This work was supported in part by the Agency for Science, Technology and Research, Singapore, under SERC grant 092-148-0073.

J. Cheng, J. Liu, D. W. K. Wong, N. M. Tan and B. H. Lee are with Institute for Infocomm Research, A*Star, Singapore. C. Cheung and M. Baskaran are with Singapore Eye Research Institute. T. Y. Wong and T. Aung are with Singapore Eye Research Institute and National University of Singapore.

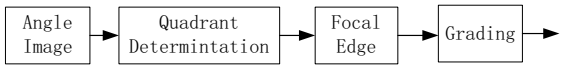

Fig. 2. Architecture of the Angle Image Analysis System

follows. In Section II, we introduce the system and methods in details. Section III shows the experimental results, followed by the conclusions in the last section.

II. Methodology

A system for automatic grading of the angle images is proposed. In the proposed system, focal edge is used for angle evaluation and the association between focal edge and the angle grades is built. Fig. 2 shows the architecture of the system. It contains the following main steps: quadrant determination, focal edge extraction, and grading.

A. Quadrant Determination

As the images can be from the inferior, superior, nasal and temporal quadrants of the eye, one important step for the automated diagnosis is to determine the quadrant. In order to do so, we make use of the strongest arc. The background is removed first by a threshold empirically remove background and selected to segment the effective image area. Then, Canny edge [5] followed by circular Hough transform [6] similar to that in [4] is used to obtain the strongest arc. Assuming (x_i, y_i), $i = 1, 2, \cdots, N$, are the coordinates of all points from the arc, where top-left corner is defined as $(1, 1)$ and bottom-right corner as (m, n), N is the number of points. The function to determine the quadrant Q is given as [1]:

$$Q = \begin{cases} \texttt{Superior}, & \text{if } x_c - \bar{x}_i \geq |y_c - \bar{y}_i| \\ \texttt{Inferior}, & \text{if } \bar{x}_i - x_c \geq |y_c - \bar{y}_i| \\ \texttt{Nasal}, & \text{if } y_c - \bar{y}_i > |x_c - \bar{x}_i| \\ \texttt{Temporal}, & \text{if } \bar{y}_i - y_c > |x_c - \bar{x}_i| \end{cases} \quad (1)$$

where $(\bar{x}_i, \bar{y}_i) = (\frac{1}{N}\sum_{i=1}^{N} x_i, \frac{1}{N}\sum_{i=1}^{N} y_i)$ is the mean of the coordinates, (x_c, y_c) is the center of the detected strongest arc.

B. Focal Edge

Focal edge refers to edges associated with certain objects or structures. In this paper, it refers to edges associated with angle structures. In order to find the focal edges, the strongest arc from the circular Hough transform is first obtained. Then we locate the iris surface, i.e., the arcuate line in Fig. 1(b), as it is visible in both open angle and angle closure. For angle closure, the iris surface is normally the strongest edge in the nearby area of the strongest arc. However, for open angle, edges from other angles structures can be stronger. In this paper, the iris surface is located as follows.

Without losing generality, assuming that the image is from inferior side of an eye as in Fig. 3(a). Given $L_j(x) = I(x, j)$, $x = 1, 2, \cdots, M$, from the j^{th} column of the image I. Assuming L_j crosses with the strongest arc at x_j. Inspired

[1]A left eye is assumed here, swop nasal and temporal for a right eye

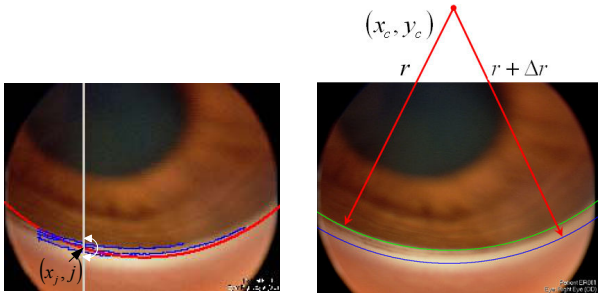

(a) Edge (b) Focal region

Fig. 3. Focal edge: Red: strongest arc, Blue: Canny edge

by the observations on iris surface, we search for the point with strongest ascending edge (from iris to cornea) from pixels around x_j in L_j (the pixels between the two white arrows in Fig. 3(a)) and get its coordinate x_k. Among all ascending Canny edge within $(x_k - w, x_k)$ as well as x_k itself, the point closest to the pupil is used as the candidate iris surface point in this column. Here, w is set to be the estimated maximum angle width. Finally, curve fitting is applied based on all candidate points located in the last step. In this paper, the iris surface is modelled as part of circle and a circular Hough transform is applied again to find the fitted curve with circular center (x_c, y_c) and radius r. After obtaining the estimation of iris surface highlighted in green as shown in Fig. 3(b), another circular arc can be determined based on the same circular center (x_c, y_c) with a larger radius $r + \delta r$. The parameter δr is set to be slightly larger than w. The region in between is the focal region and the edges within the region is the focal edge.

C. Grading

In manual grading, the ophthalmologists examine the structures seen and then convert to grades (0, 1, or Open). In the automated grading, we use the estimated iris surface as the start point of the angle. In the following, we estimate the end point of the angle and the distance between them is computed as the width of the angle.

1) Angle Width Profile Computation: As mentioned in [4], the angle width is a critical measurement. The angle width is the distance between two imaginary tangent lines constructed to the inner surface of the trabecular meshwork and the anterior iris surface, respectively. In last section, we have estimated the iris surface. However, identification of trabecular meshwork requires much efforts especially in the presence of other angle structures. In this paper, we use the Canny edge as well as the iris surface in the focal region as possible angle boundary. For images taken from the superior and inferior quadrants, we take the top and bottom edges from each column as borders of angle area. The distance in between is the computed angle width in this column. The distance values from all columns form the width profile. For columns without Canny edges within the focal region, the angle width is zero. For images from the nasal and temporal quadrants, the computation is similar except that we process on each row and we take the leftmost and rightmost edges in rows. As the width

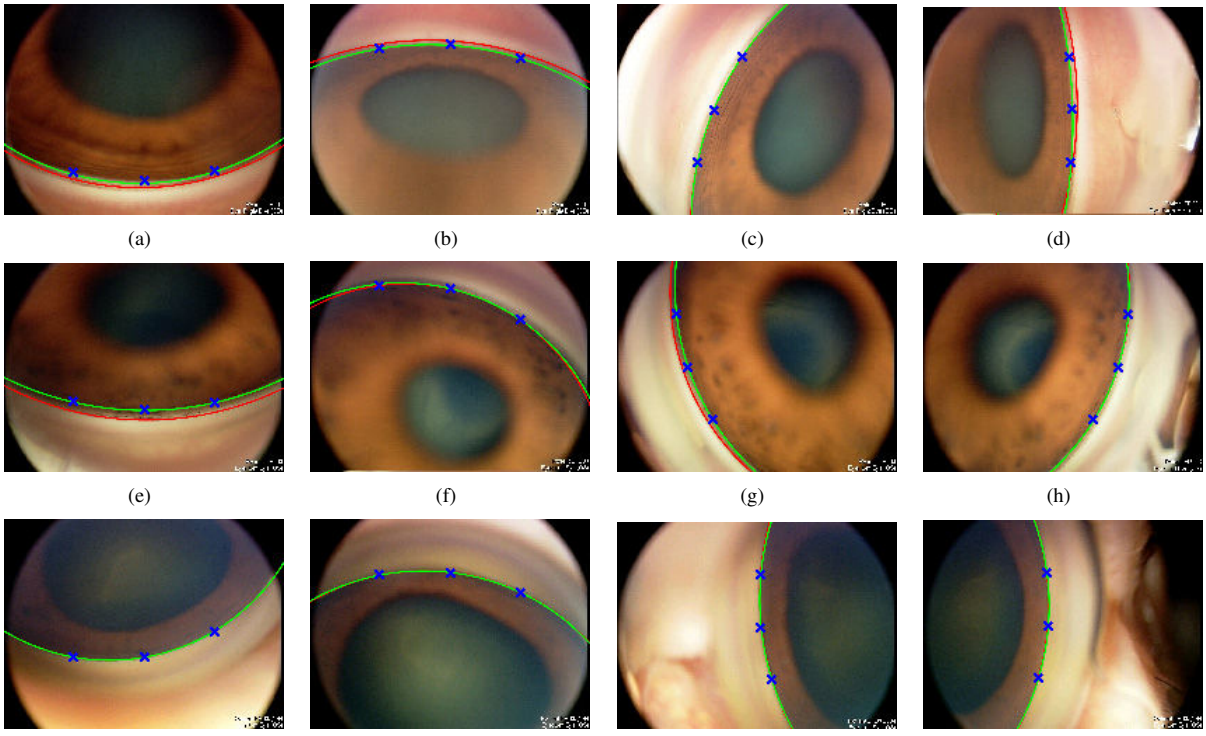

Fig. 4. Strongest arc and estimated iris surface for some iridocorneal angle images: Red: strongest arc, Green: estimated iris surface, Blue: ground truth points. The first and second rows are from eyes with OAG and the last row is from an eye with ACG.

profiles from different quadrant often have different lengths, the profile cannot be compared directly. In order to get unified feature with same dimension, we use same amount of widths sampled from the width profile. Moreover, as the blur happens often in two sides of the image, we use central portion only. By doing so, we extract an unified feature from the image.

One major difference between the approach here and the approach in [4] is that the strongest arc from previous approach can be any part from the angle structures. Thus, edges from both sides of the strongest arc are used previously. When iris surface is located, only the edges on the corneal side need to be considered. Thus, the chance of false detection of the edges from inner iris as angle structures is reduced.

2) Classification: Recall in the threshold approach in [4], the mean angle width is computed and a threshold T_1 is used to differentiate open angle from angle closure. As mentioned earlier in the introduction, we further tell the degree of closure for angle closure glaucoma. For the threshold approach, we can introduce another threshold T_2 to differentiate grade 1 from grade 0. We compute the mean width $\overline{w}$ as in [4]. For an image with mean width $\overline{w}$, its grade $G(\overline{w})$ is computed as:

$$G(\overline{w}) = \begin{cases} Open & \overline{w} \geq T_1 \\ 1 & T_1 > \overline{w} > T_2 \\ 0 & \overline{w} \leq T_2 \end{cases} \quad (2)$$

Although the threshold approach is simple and straightforward, the computing of the mean angle width may overlook some information, e.g., the width distribution, and etc. In practice, some angles can be partially closed. In this paper, we propose to use the width profile as the feature instead of its mean. Machine learning is applied for the classification of images with different grades.

We use support vector machines as the optimization tools for solving machine learning problems. The LIBSVM [7] is used in our experiments as a powerful classifier. In our method, we implement a three-class classifier using a two-tier system with two sub-classifiers. Classifier one is trained to get the classification between angle closure and open angle. Classifier two is trained to differentiate grade 0 from grade 1. In the testing, classifier one is applied first to differentiate angle closure from open angle. For angle closure, it would be further classified to grade 1 or grade 0 using classifier two.

III. Experimental Results

A total of 1866 images as in [4] are used. The images are graded by ophthalmologists manually. The breakdown of the images are as follows: 1149 images are graded as open, 421 images are graded as 1, and 296 images are graded as 0. The above grading is used as the ground truth. The results by the proposed method as well as prior method are compared using this ground truth.

Locating the iris surface is a critical step. Fig. 4 shows results from some sample images. The lines in red are the strongest arcs obtained by method as in [4]. The lines in green are the estimated iris surface by the proposed method. Although ground truth is difficult to obtain for all points in all images, we manually mark three points evenly along the iris surface as ground truth points, as shown by the crosses in blue.

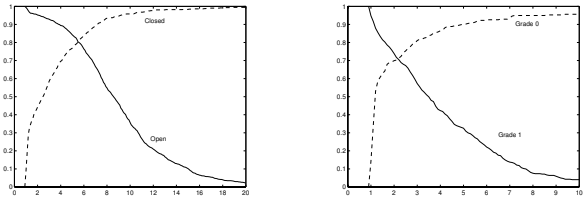

(a) Open vs. Closed (b) 1 vs. 0

Fig. 5. Accuracies of gradings by two classifiers at different thresholds

Method		Prior [4]	Proposed
Classifier One	Open	80.3%	87.3%
	Close	80.3%	88.4%
Classifier Two	1	70.6%	75.0%
	0	71.3%	77.4%

TABLE I
PERFORMANCE OF THE TWO-CLASS CLASSIFIERS

The distances between these points and the two lines in green and red (not visible if it overlaps with the green line) are the localization errors. The first two rows are from patients with OAG. The third row is from patients with ACG. Comparing the lines in green with the stars in blue, the proposed method estimates the iris surface well while the strongest arc does not work well for most OAG examples. However, it is too tedious to manually mark the ground truth for all images. Instead, the grading accuracy is used as the measurement.

In the threshold based approach, the selection of the two thresholds are critical. In order to select them properly to have best performance, we look into how the threshold selection affects the classifications, as shown in Fig. 5. Two thresholds T_1 and T_2 are determined to maximize the total accuracies in the classification between grade open vs. closed and grade 1 vs. grade 0, respectively.

In the machine learning approach, two classifiers are trained. In the first classifier for classification between open and angle closure, half of the images from all grades are used as set one and the other half are used as set two. The images from same eye quadrants are either in set one or set two, but not both. In the training, same number of images from angle closure and open angle from set one are used. A cross-validation is used in the training to determine parameters for the LIBSVM [7]. The trained model is used to test on set two. After that we swop the two sets and applied the training and testing again to get the performance on set one. Finally, the accuracy is computed as the average of the two testing. In the second classifier for grade 1 and grade 0, a similar procedure is done. It should be noted that we achieve the three-class classification through a two-tier system instead of one against one or one against all as in [8] as the classification between angle closure and open angle is more important than that of grade 1 and grade 0.

Table I shows the results of the two-class classifiers in comparison with prior method [4]. As shown in Table I, the proposed method improves the accuracies by 7.0% and 8.1% compared prior method for classification between open and closed angle. For classification between grade 1 and grade 0, it improves by 4.4% and 6.1%.

	Grading	Predicted		
		Open	1	0
Actual	Open	80.3%	14.5%	5.2%
	1	29.5%	43.2%	27.3%
	0	8.8%	19.9%	71.3%

TABLE II
CONFUSION MATRIX BY PRIOR METHOD

	Grading	Predicted		
		Open	1	0
Actual	Open	87.3%	6.8%	5.9%
	1	13.8%	64.6%	21.6%
	0	8.5%	18.9%	72.6%

TABLE III
CONFUSION MATRIX BY PROPOSED METHOD

We then compute the confusion matrices of the three-class classifiers. Table II shows the results by the mean angle width approach as similar in [4], extended to three-class. Table III shows the results by the proposed method. Comparing them, we can see that the machine learning approach improves the accuracies by 7.0%, 23.4%, and 1.3% for open, 1, and 0, respectively. The improvement for grade 0 is minimal as the width distribution does not provide much more information.

IV. CONCLUSION

In this paper, we propose a new system for automated iridocorneal angle image grading. The proposed method uses focal edge via locating the iris surface. The association between focal edge and angle grades is built through machine learning. Experimental results show good agreement with manual grading in ACG and OAG classification. It provides an automatic classification of angle closure and open angle. Moreover, for angle closure, it tells the degree of closure by grading 1 or 0. Automatic grading of the iridocorneal images is a challenging work due to ambiguous angle structures in some images. Further analysis of the angle would be done to improve the grading accuracy. More images from new patients would be included to evaluate the performance of the system.

REFERENCES

[1] D. Minckler, P. Foster, and P.T. Hung, "Angle closure glaucoma classification and racial variation," *Asia Journal of Ophthalmology*, vol. 3, no. 3,4, pp. 3–9, 2001.

[2] John F. Salmon, "The diagnostic importance of gonioscopy," available at: http: //www.glaucomaworld.net/english/019/e019a01t.html/.

[3] I. I. K. Ahmed and L. D. Mackeen, "A new approach for imaging the angle," *Glaucoma Today,*, pp. 27–30, 2007.

[4] J. Cheng, J. Liu, B. H. Lee, D. Wong, F. Yin, and P. Shamira T. Y. Wong T. Aung, M. Baskaran, "Closed angle glaucoma detection in retcam images," in *Int. Conf. of the IEEE Engineering in Medicine and Biology Society*, 2010, pp. 4096–4099.

[5] J. Canny, "A computational approach to edge detection,," *IEEE Trans. Pattern Analysis and Machine Intelligence*, vol. 8, pp. 679–698.

[6] B. S. Morse, "Segmentation (edge based, hough transform), brigham young university: Lecture notes," 2000.

[7] Chih-Chung Chang and Chih-Jen Lin, *LIBSVM: a library for support vector machines*, 2001, Software available at http://www.csie.ntu.edu.tw/ cjlin/libsvm.

[8] Chih wei Hsu and Chih-Jen Lin, "A comparison of methods for multi-class support vector machines," 2001.

Acta Ophthalmologica

Comparison of EyeCam and anterior segment optical coherence tomography in detecting angle closure

Mani Baskaran,[1] Tin Aung,[1,2] David S. Friedman,[3] Tin A. Tun[1] and Shamira A. Perera[1]

[1]Singapore Eye Research Institute & Singapore National Eye Center, Singapore
[2]Yong Loo Lin School of Medicine, National University of Singapore, Singapore
[3]Wilmer Eye Institute and Johns Hopkins Bloomberg School of Public Health, Baltimore, Maryland, USA

ABSTRACT.

Purpose: **To compare the diagnostic performance of EyeCam (Clarity Medical Systems, Pleasanton, CA, USA) and anterior segment optical coherence tomography (ASOCT, Visante; Carl Zeiss Meditec, Dublin, CA, USA) in detecting angle closure, using gonioscopy as the reference standard.**

Methods: **Ninety-eight phakic patients, recruited from a glaucoma clinic, underwent gonioscopy by a single examiner, and EyeCam and ASOCT imaging by another examiner. Another observer, masked to gonioscopy findings, graded EyeCam and ASOCT images. For both gonioscopy and EyeCam, a closed angle in a particular quadrant was defined if the posterior trabecular meshwork was not visible. For ASOCT, angle closure was defined by any contact between the iris and angle anterior to the scleral spur. An eye was diagnosed as having angle closure if ≥2 quadrants were closed. Agreement and area under the receiver operating characteristic curves (AUC) were evaluated.**

Results: **The majority of subjects were Chinese (69/98, 70.4%) with a mean age of 60.6 years. Angle closure was diagnosed in 39/98 (39.8%) eyes with gonioscopy, 40/98 (40.8%) with EyeCam and 56/97 (57.7%) with ASOCT. The agreement (kappa statistic) for angle closure diagnosis for gonioscopy versus EyeCam was 0.89; gonioscopy versus ASOCT and EyeCam versus ASOCT were both 0.56. The AUC for detecting eyes with gonioscopic angle closure with EyeCam was 0.978 (95% CI: 0.93–1.0) and 0.847 (95% CI: 0.76–0.92, $p < 0.01$) for ASOCT.**

Conclusion: **The diagnostic performance of EyeCam was better than ASOCT in detecting angle closure when gonioscopic grading was used as the reference standard. The agreement between the two imaging modalities was moderate.**

Key words: angle closure – anterior chamber angle – anterior segment optical coherence tomography – EyeCam – gonioscopy – imaging

Acta Ophthalmol. 2012: 90: e621–e625

doi: 10.1111/j.1755-3768.2012.02510.x

Introduction

Assessment of the anterior chamber angle (ACA) is important for the identification of patients with angle closure and the correct classification of glaucoma. Clinically, this is performed using static and dynamic indentation gonioscopy, which is the current reference standard. Gonioscopy confers several advantages such as low cost, the ability to simultaneously visualize a large circumferential area of the ACA, the use of the corneal wedge to accurately delineate Schwalbe's line and the ability to dynamically indent the angle. However, gonioscopy has significant shortcomings including the subjectivity of the assessment, the need for rigorous training, the fact that the lens must contact the eye and the inability to revisit the findings in the absence of documentation (photographing the angle is difficult). The use of various types of gonioscopic lenses and noncomparable grading systems for describing the angle reduces reproducibility across graders. Photographic techniques on the other hand may offer high resolution, wide-field views of the angle which can overcome many of these limitations by documenting angle structures in an objective and standardized manner.

The EyeCam™ (Clarity Medical Systems, Pleasanton, CA, USA) is an imaging system that was designed to obtain wide-field photographs of the fundus (Retcam™, Clarity Medical Systems, Pleasanton, CA, USA), primarily for the diagnosis and management of paediatric posterior segment disease. The instrument has recently been used to image the optic disc (Erraguntla et al. 2006) and the ACA (Narayanaswamy et al. 2008). We recently reported good agreement compared to gonioscopy (Perera & Baskaran 2010) and demonstrated that the EyeCam was sensitive enough to detect changes in angle configuration after laser peripheral iridotomy (Perera & Quek 2010). Anterior segment optical coherence tomography (ASOCT) on the other hand offers a rapid, noncontact method of angle assessment, which can be qualitative as well as quantitative. Its diagnostic capabilities have been described in detail, and angle assessment using ASOCT has been documented to correlate moderately well with gonioscopy (Nolan et al. 2007).

The aim of this study was to compare the use of EyeCam and ASOCT for angle imaging and to assess their diagnostic performance in detecting angle closure using gonioscopy as the reference standard.

Materials and Methods

This prospective hospital-based study was conducted with the approval of the Ethics Review Board of the Singapore Eye Research Institute and was performed in accordance with the tenets of the Declaration of Helsinki. Written informed consent was obtained from every participant.

Consecutive eligible subjects who were above the age of 40 years were recruited from a single glaucoma clinic at a Singapore hospital. The study population was novel and not the same as those in our previous studies on EyeCam (Perera & Baskaran 2010; Perera & Quek 2010). Exclusion criteria included subjects with prior intraocular surgery or penetrating eye injury, the presence of corneal disorders such as corneal endothelial dystrophy, pterygium or corneal scars that may preclude satisfactory imaging or those on medications that act on the pupil. Patients who had previously undergone laser peripheral iridotomy were not excluded. After obtaining a detailed ophthalmic history, each subject underwent a standardized examination that included visual acuity assessment, slit-lamp biomicroscopy, Goldmann applanation tonometry, gonioscopy, ASOCT and imaging with the EyeCam.

Gonioscopy was performed in the dark in all cases by a single examiner with glaucoma fellowship training (SAP), who was masked to imaging findings. A 1-mm light beam was reduced to a narrow slit and the vertical beam was used for assessing superior and inferior angles and offset horizontally for nasal and temporal angles. Static gonioscopy was performed using a Goldmann 2-mirror lens (Ocular Instruments Inc, Bellevue, WA, USA) at high magnification (×16), with the eye in the primary position of gaze. Care was taken to avoid light falling on the pupil and to avoid inadvertent indentation during examination. The angle in each quadrant was graded as per the Scheie grading system according to the anatomical structures observed during gonioscopy (Scheie 1957). The ACA was considered 'closed' in that quadrant if the posterior pigmented trabecular meshwork (TM) could not be seen in the primary position without indentation (Scheie grade 3 or 4). The eye was classified as having angle closure if there were two or more quadrants of angle closure.

Image capture by EyeCam has been described in detail elsewhere (Perera & Baskaran 2010; Perera & Quek 2010). In summary, EyeCam imaging was performed on participants in the supine position, in a darkened room. Images were captured by a single trained technician (TAT) for all four quadrants of the eye. After applying topical anaesthetic eye drops (Proparacaine hydrochloride 0.5% ophthalmic solution; Alcon Laboratories Inc., FortWorth, TX, USA), coupling gel was applied to the anesthetized eye, before imaging proceeded with a 130° lens held next to the limbus. The illumination light was pointed at the angle rather than the pupil to minimize any pupillary constriction. If pronounced convexity of iris precluded visibility of the angle, the probe was moved anteriorly within 1 mm of the limbus to gain a view over the convexity of the iris. The illumination was adjusted using the foot pedal to avoid over-exposure until the trabecular meshwork and/or the peripheral iris roll was clearly visible. Clear, focused images were captured onto the hard disk of the attached computer for subsequent grading. Imaging of all four quadrants of the eye was performed in < 5 min.

The resulting set of four EyeCam images per patient were randomly ordered and graded (on separate occasions to the ASOCT images) by a fellowship trained glaucoma specialist (MB), who was masked to gonioscopic data. The methodology for grading the quality of EyeCam images and the method of grading the images have been described elsewhere (Perera & Baskaran 2010). In brief, each quadrant was graded for anatomical structures observed in the ACA using the same grading system used for gonioscopy to ensure comparability. As with gonioscopy, angle closure in a quadrant was defined as the inability to visualize the pigmented TM in that quadrant. An eye was considered to have angle closure if the pigmented TM was not visible in at least two quadrants.

Anterior segment imaging was obtained using a commercially available ASOCT device (Visante; Carl Zeiss Meditec, Dublin, CA, USA). The details of ASOCT imaging technology have been described previously (Radhakrishnan & Rollins 2001; Radhakrishnan & Goldsmith 2005). Briefly, this technology permits image acquisition at a rate of eight frames per second (2000 A scans per second) with a transverse and an axial resolutions of 60 and 10–20 μm, respectively. The combination of wide-field scanning optics (16 mm) and a deep axial scan range (8 mm) allows ASOCT to image a cross section of the anterior chamber in one image frame. The scanned images are then processed by customized dewarping software, which compensates for index of refraction transitions to correct the physical dimensions of the images (Goldsmith et al. 2005). Seated subjects were examined by a single examiner who was masked to gonioscopic findings. Three ASOCT images of each eye were obtained in dark conditions: one image scanning the angle at

the 3 and 9-o'clock hour positions, one scanning the superior angle at 12 o'clock and one scanning the inferior angle at 6 o'clock. Because of interference from the eyelids with image acquisition of the ACA at 6 and 12 o'clock, the lower lid was pulled down gently by the operator to image the inferior angle, and the upper lid was elevated gently to image the superior angle, taking care to avoid inadvertent pressure on the globe. Imaging was repeated once if the scleral spur visibility was poor, to select the best set of images. The ASOCT image files were exported to a personal computer and were evaluated for the presence of a closed or open ACA by two examiners with glaucoma subspecialty training (MB and TA working together) who were masked to other test results. A closed angle in a particular quadrant was defined as any contact between the iris and angle wall anterior to the scleral spur on the ASOCT images.

Statistical analysis

One eye from each patient was randomly selected for imaging if both eyes were eligible for the study. The McNemar test was used to compare differences in the distribution of categorical variables between two related samples. Kappa statistic was used to assess the agreement between categorical variables and for reproducibility analysis. Receiver operating characteristic (ROC) curves with calculations of area under the curve (AUC) and 95% confidence intervals (CI) were used as an index of each instrument's performance for identifying eyes with angle closure, using gonioscopy as the reference standard. A p-value < 0.05 was considered statistically significant. The sample size calculation was based on comparison of sensitivities for matched groups in a diagnostic study (Beam 1992). With an estimated sensitivity of 82%, the numbers of subjects required was 78 in this study. Statistical analysis was performed using STATA version 10 (Statacorp, College Station, TX, USA), and MED CALC version 8.1.0.0 (Mariakerke, Belgium).

Results

Of the 140 subjects (140 eyes) recruited, all EyeCam images were gradable. The initial 98 subjects (98 eyes) underwent ASOCT also and were eligible for comparison with EyeCam data. Five eyes had poor scleral spur identification in atleast one quadrant in ASOCT images. All the remaining images were gradable in all four quadrants. The majority of study subjects were Chinese (69/98, 70%) with a mean age of 60.7 (SD – 12.6) years and there were an equal number of men and women. Of the 98 eyes analysed, 39 (39.8%) had angle closure (in ≥2 quadrants) by gonioscopy.

Angle closure was present in 40/98 (40.8%) with EyeCam and 56/97 (57.7%) with ASOCT. Although five eyes had some incomplete/nongradable quadrants, if an eye satisfied the criteria for a diagnosis of angle closure in the available two quadrants, they were graded as having angle closure instead of being totally excluded. Overall, 97 eyes were included for ROC analysis in the ASOCT group.

The kappa agreement between the two imaging modalities was moderate at 0.56. The kappa statistic for agreement varied between 0.62 and 0.89 for EyeCam against gonioscopy and between 0.45 and 0.56 for ASOCT and gonioscopy, depending on the definition of angle closure by number of quadrants closed (Table 1). The highest agreement was seen with a definition of two or more quadrants closed for both devices. The inferior quadrant showed the highest agreement with gonioscopy using both devices. Using our definition of angle closure as two or more quadrants closed on gonioscopy, both sensitivity and specificity using the EyeCam was 95% while they were 92% and 65% respectively for ASOCT. The AUC for EyeCam was 0.978 (95% CI 0.926–0.997) and that for ASOCT was 0.847 (95% CI 0.758–0.914) (Table 2 & Fig. 1).

Table 1. Kappa values using EyeCam and anterior segment optical coherence tomography (ASOCT) compared to gonioscopy.

	Agreement between methods – Kappa statistic (95% CI)		
Definition of closure	EyeCam versus gonioscopy (n = 98)	ASOCT versus gonioscopy (n = 93)	EyeCam versus ASOCT (n = 93)
1 or more quadrants closed	0.86 (0.75, 0.96)	0.54 (0.38, 0.70)	0.54 (0.38, 0.70)
2 or more quadrants closed	0.89 (0.80, 0.99)	0.56 (0.41, 0.72)	0.56 (0.41, 0.72)
3 or more quadrants closed	0.80 (0.68, 0.92)	0.56 (0.39, 0.72)	0.65 (0.49, 0.80)
4 quadrants closed	0.62 (0.43, 0.80)	0.45 (0.26, 0.64)	0.46 (0.28, 0.65)
Superior quadrant closed	0.85 (0.74, 0.96)	0.46 (0.30, 0.62)*	0.42 (0.27, 0.58)*
Inferior quadrant closed	0.94 (0.87, 0.99)	0.57 (0.41, 0.73)*	0.55 (0.39, 0.71)*
Nasal quadrant closed	0.67 (0.51, 0.83)	0.53 (0.37, 0.70)*	0.63 (0.47, 0.79)*
Temporal quadrant closed	0.67 (0.52, 0.83)	0.52 (0.35, 0.68)*	0.57 (0.41, 0.74)*

* n = 95 (superior quadrant); 96 (inferior quadrant); 98 (for nasal and temporal quadrants).

Table 2. Receiver operating characteristic curve (ROC) analysis to compare EyeCam and anterior segment optical coherence tomography (ASOCT) with Gonioscopy for various definitions of angle closure.

	EyeCam versus gonioscopy			ASOCT versus gonioscopy			
Definition of closure	AUC (95% CI)	Sensitivity	Specificity	AUC (95% CI)	Sensitivity	Specificity	p-value*
1 or more quadrants closed	0.957 (0.896, 0.988)	0.93	0.93	0.884 (0.801, 0.941)	0.95	0.61	0.076
2 or more quadrants closed	0.978 (0.926, 0.997)	0.95	0.95	0.847 (0.758, 0.914)	0.92	0.65	0.002
3 or more quadrants closed	0.945 (0.879, 0.981)	0.94	0.89	0.877 (0.792, 0.936)	0.84	0.75	0.137
4 quadrants closed	0.891 (0.812, 0.945)	0.77	0.88	0.795 (0.699, 0.872)	0.77	0.76	0.102

AUC, area under the ROC curve.
* Comparison of independent ROC curves between EyeCam and ASOCT.

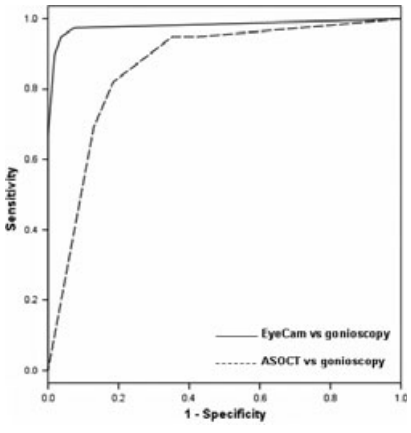

Fig. 1. Receiver operating characteristic curve (ROC) analysis comparing EyeCam vs gonioscopy and ASOCT vs gonioscopy for angle closure.

Discussion

The EyeCam accurately identified angle closure in this clinic-based mostly Chinese population and performed better than ASOCT when both were compared to gonioscopy. Not only was the AUC substantially and significantly higher using the EyeCam, but also, almost all EyeCam images were gradable, while close to 5% of ASOCT images were not, mainly due to poor identification of the scleral spur inspite of repeated imaging. Our previous study using a different population showed more modest results: EyeCam imaging had an AUC of 0.79 for detecting eyes with gonioscopic angle closure (Perera & Baskaran 2010). Although the definitions remained the same, perhaps this case mix had more obvious examples of closed angles with 4/4 quadrants closed, yielding a very high AUC of 0.978. Alternatively, there could be a learning curve in the accurate utilization of this device.

That said the current reference standard, gonioscopy, may not in fact be ideal as it is subjective, and long-term studies documenting outcomes based on gonioscopic assessment are lacking. Therefore, even though the EyeCam gave results highly similar to gonioscopy, it will await future long-term studies to determine whether the EyeCam or ASOCT are more able to predict disease onset or progression.

The disagreement between EyeCam and ASOCT may be due to several technical and operational reasons. Firstly, ASOCT is performed in the dark and does not require contact with the eye; inadvertent indentation and excessive light during gonioscopy (or EyeCam) would open the ACA artificially (Nolan et al. 2007). On gonioscopy, nonvisibility of the pigmented trabecular meshwork is used to define a closed angle. On ASOCT, the trabecular meshwork itself is rarely seen, and hence, any contact anterior to the scleral spur (used as a surrogate marker) defines angle closure. As the scleral spur lies posterior to the pigmented trabecular meshwork, the ASOCT definition uses a more lenient definition of angle closure. Cumulatively, all these discrepancies would lead to a relative overestimation of angle closure by ASOCT.

Operationally, each modality has specific nuances in imaging particular quadrants. With gonioscopy, viewing the temporal and nasal angles can be difficult because of the horizontal positioning of the light beam. With EyeCam imaging, the temporal angle may be more challenging in deep-set eyes, because of obtaining the correct angulation of the probe via a nasal approach. Imaging the superior and inferior quadrants with ASOCT can be difficult as manipulations to move the lids out of the way prior to ASOCT may alter the appearance of the angle (Sakata et al. 2008) or because of variable identification of scleral spur during image analysis (Kim et al. 2011).

This study has some limitations. The analysis of the ACA in each quadrant by ASOCT was based on only a cross-sectional image of the angle, and there may be variations throughout the quadrant that may be missed by this single meridional image. In contrast, both gonioscopy and EyeCam give wide-field views of the whole quadrant from which an overall decision can be made. The number of images in which the ACA status cannot be determined may be higher in clinical practice, where technicians and observers may have less expertise in angle assessment. On the other hand, the use of a single gonioscopist in our study could result in a systematic bias for the gonioscopy findings and is a potential weakness, although it does reflect common medical practice. Another limitation relates to the fact that the reproducibility of detecting a closed ACA in ASOCT images was not assessed in this study. A previous study has reported the interobserver variability as moderate with a kappa of 0.48 with respect to angle closure status (Nolan et al. 2007). Studies comparing ASOCT with a more comprehensive gonioscopic grading system such as the Spaeth system, or with other imaging methods of assessing the ACA such as ultrasound biomicroscopy, may provide further insights to the discrepancies between gonioscopy and ASOCT.

In conclusion, the EyeCam discriminated angle closure status better than ASOCT when gonioscopic grading was used as a reference standard. The agreement between the two imaging modalities was moderate.

Acknowledgements

Dr Aung has received travel support and honoraria from Clarity Medical Systems, Inc. Pleasanton, CA, USA, as well as an instrument loan. Dr Aung has received research support, travel support and honoraria from Carl Zeiss Meditec, Dublin, CA, USA, as well as an instrument loan. The Study was supported by grants from the National Medical Research Council, Singapore, and Singhealth Foundation.

References

Beam CA (1992): Strategies for improving power in diagnostic radiology research. AJR Am J Roentgenol **159**: 631–637.

Erraguntla V, Mackeen LD & Atenafu E et al. (2006): Assessment of change of optic nerve head cupping in pediatric glaucoma using the RetCam 120. J AAPOS **10**: 528–533.

Goldsmith JA, Li Y & Chalita MR et al. (2005): Anterior chamber width measurement by high-speed optical coherence tomography. Ophthalmology **112**: 238–244.

Kim DY, Sung KR & Kang SY et al. (2011): Characteristics and reproducibility of anterior chamber angle assessment by anterior-segment optical coherence tomography. Acta Ophthalmol **89**: 435–441.

Narayanaswamy A & Singh M (2008): RetCam — a useful adjunctive tool to evaluate and manage paediatric glaucomas. Asian J Ophthalmol **109**: 30–31.

Nolan WP, See JL & Chew PTK et al. (2007): Detection of primary angle closure using anterior segment optical coherence tomography in Asian eyes. Ophthalmology **114**: 33–39.

Perera SA & Baskaran M (2010): Use of EyeCam for imaging the anterior chamber angle. Invest Ophthalmol Vis Sci **51**: 2998–3002.

Perera SA & Quek DT (2010): Demonstration of angle widening using EyeCam after laser peripheral iridotomy in eyes with angle closure. Am J Ophthalmol **149**: 903–907.

Radhakrishnan S & Goldsmith J (2005): Comparison of optical coherence tomography and ultrasound biomicroscopy for detection of narrow anterior chamber angles. Arch Ophthalmol **123**: 1053–1059.

Radhakrishnan S & Rollins AM (2001): Real-time optical coherence tomography of the anterior segment at 1310 nm. Arch Ophthalmol **119**: 1179–1185.

Sakata LM, Lavanya R & Friedman DS et al. (2008): Comparison of gonioscopy and anterior segment ocular coherence tomography in detecting angle closure in different quadrants of the anterior chamber angle. Ophthalmology **115**: 769–774.

Scheie HG (1957): Width and pigmentation of the angle of the anterior chamber. A system of grading by gonioscopy. Arch Ophthalmol **58**: 510–512.

Received on December 19th 2011.
Accepted on June 18th, 2012.

Correspondence:
Tin Aung, FRCS(Ed), PhD
Singapore National Eye Centre
11, Third Hospital Avenue
168751 Singapore
Tel: + 65 62277255
Fax: + 65 62263395
Email: tin11@pacific.net.sg

Automated Analysis of Angle Closure From Anterior Chamber Angle Images

Mani Baskaran,[1–3] Jun Cheng,[4] Shamira A. Perera,[1] Tin A. Tun,[1] Jiang Liu,[4] and Tin Aung[1–3]

[1]Singapore Eye Research Institute and Singapore National Eye Centre, Singapore
[2]Yong Loo Lin School of Medicine, National University of Singapore, Singapore
[3]Duke-NUS Graduate Medical School, Singapore
[4]Institute of Infocomm Research, Singapore

Correspondence: Tin Aung, Glaucoma Service, Singapore National Eye Centre, 11 Third Hospital Avenue, Singapore 168751; tin11@pacific.net.sg.

Submitted: May 21, 2014
Accepted: October 9, 2014

Citation: Baskaran M, Cheng J, Perera SA, Tun TA, Liu J, Aung T. Automated analysis of angle closure from anterior chamber angle images. *Invest Ophthalmol Vis Sci*. 2014;55:7669–7673. DOI:10.1167/iovs.14-14852

Purpose. To evaluate a novel software capable of automatically grading angle closure on EyeCam angle images in comparison with manual grading of images, with gonioscopy as the reference standard.

Methods. In this hospital-based, prospective study, subjects underwent gonioscopy by a single observer, and EyeCam imaging by a different operator. The anterior chamber angle in a quadrant was classified as closed if the posterior trabecular meshwork could not be seen. An eye was classified as having angle closure if there were two or more quadrants of closure. Automated grading of the angle images was performed using customized software. Agreement between the methods was ascertained by κ statistic and comparison of area under receiver operating characteristic curves (AUC).

Results. One hundred forty subjects (140 eyes) were included, most of whom were Chinese (102/140, 72.9%) and women (72/140, 51.5%). Angle closure was detected in 61 eyes (43.6%) with gonioscopy in comparison with 59 eyes (42.1%, $P = 0.73$) using manual grading, and 67 eyes (47.9%, $P = 0.24$) with automated grading of EyeCam images. The agreement for angle closure diagnosis between gonioscopy and both manual ($\kappa = 0.88$; 95% confidence interval [CI], 0.81–0.96) and automated grading of EyeCam images was good ($\kappa = 0.74$; 95% CI, 0.63–0.85). The AUC for detecting eyes with gonioscopic angle closure was comparable for manual and automated grading (AUC 0.974 vs. 0.954, $P = 0.31$) of EyeCam images.

Conclusions. Customized software for automated grading of EyeCam angle images was found to have good agreement with gonioscopy. Human observation of the EyeCam images may still be needed to avoid gross misclassification, especially in eyes with extensive angle closure.

Keywords: anterior chamber angle, gonioscopy, EyeCam, angle closure, automated grading

Gonioscopy is the established reference standard clinical method for angle evaluation.[1] Objective capture of gonioscopic views can be obtained with standard goniophotography or EyeCam (Clarity Medical Systems, Pleasanton, CA, USA) goniography.[2] Currently, grading of the documented images can be done only manually, but automated solutions are needed to enable clinician independent grading of the angle images.[2–4] In the absence of routine gonioscopy in clinical practice,[1] such automated angle image analysis potentially may serve as a surrogate for gonioscopy by a clinician.

EyeCam is the anterior segment module of Retcam (Clarity Medical Systems), a pediatric wide-angle fundus photography system.[5,6] We have previously evaluated the EyeCam in grading angle status[2] and in detecting the extent of angle opening after laser peripheral iridotomy (LPI).[3] Building on this, we have developed an automated software algorithm to classify open and closed angles in Eye Cam angle images.[7] Further, the algorithm can identify the specific quadrant from its orientation and provide a summary of the number of quadrants that are closed. This article aimed to test this software by comparing automated grading of EyeCam angle images with manual grading of images, with gonioscopy as the reference standard.

Methods

This prospective hospital-based study was approved by the ethics committee of Singapore Eye Research Institute. Written informed consent was obtained from every participant and the study was performed in accordance with the tenets of the Declaration of Helsinki.

Consecutive eligible subjects older than 40 years were recruited from a single glaucoma clinic at a Singapore hospital. After obtaining a detailed ophthalmic history, each subject underwent a standardized examination that included visual acuity assessment, slit-lamp biomicroscopy, Goldmann applanation tonometry, gonioscopy, and imaging with the EyeCam. Subjects with prior intraocular surgery or penetrating eye injury, or corneal disorders, such as corneal endothelial dystrophy, pterygium, or corneal scars that may preclude satisfactory imaging, were excluded from the study. Poor-quality images from EyeCam, with blurred angle details (even in

one quadrant) were excluded from the study. Patients who had previously undergone LPI were not excluded.

Gonioscopy

Gonioscopy was performed in the dark in all cases by a single examiner with previous glaucoma fellowship training (SAP), who was masked to imaging findings. A 1-mm light beam was reduced to a narrow slit and the vertical beam was used for assessing superior and inferior angles and offset horizontally for nasal and temporal angles. Static gonioscopy was performed using a Goldmann 2-mirror lens (Ocular Instruments Inc., Bellevue, WA, USA) at high magnification (×16), with the eye in the primary position of gaze. The gonioscopy lens was tilted minimally to permit a view of the angle over the convexity of the iris, avoiding distortion of angle. Care was taken to avoid light falling on the pupil and to avoid inadvertent indentation during examination. The angle in each quadrant was graded as per the Scheie grading system according to the anatomical structures observed during gonioscopy.[8] The anterior chamber angle (ACA) was considered "closed" in that quadrant if the posterior pigmented trabecular meshwork (TM) could not be seen in the primary position without indentation (Scheie grade 3 or 4). The eye was classified as having angle closure if there were two or more quadrants of closure. Indentation gonioscopy was performed to ascertain angle structures in the presence of a pigmented Schwalbe's line.

EyeCam Angle Imaging

Image capture by EyeCam has been described in detail elsewhere.[3,4] This instrument is identical to the Retcam device used for retinal imaging.[5,6] In brief, EyeCam imaging was performed on participants in the supine position on a couch, in a darkened room. Images were captured by a single trained technician (TAT) in all four quadrants of the eye at least 20 minutes after the gonioscopy was performed, to avoid any distortion of angle status. After applying topical anesthetic eye drops (proparacaine hydrochloride 0.5% ophthalmic solution; Alcon Laboratories, Inc., Fort Worth, TX, USA), coupling gel was applied to the anesthetized eye before imaging proceeded with a 130° lens held next to the limbus. The illumination light was pointed at the angle rather than the pupil to minimize any pupillary dilatation. If the angle was not visible due to pronounced convexity of iris, the probe was moved anteriorly within 10° of the limbus to gain a view over the convexity of the iris. The illumination was adjusted using the foot pedal to avoid overexposure until the TM and/or the peripheral iris roll was clearly visible. Clear, still images were saved to the hard disk of the attached computer for subsequent grading.

Manual and Automated Grading of EyeCam Images

The resulting EyeCam images were randomly ordered and graded on a separate occasion, by a fellowship-trained glaucoma specialist (MB) who was masked to gonioscopic data. The methodology for grading the quality of EyeCam images and the method of grading the images have been described elsewhere.[3] The quality of images was graded from 1 to 4 based on the visibility of angle details. Only grade 1 and 2 images were included. Each quadrant was graded for anatomical structures observed in the ACA. As with gonioscopy, angle closure in a quadrant was defined as the inability to visualize the pigmented TM in that quadrant. An eye was considered to have angle closure if the pigmented TM was not visible in at least two quadrants. We have not reported on the presence of peripheral anterior synechiae (PAS) or iris processes because indentation was not possible using the EyeCam. Further classifications such as one-quadrant closure or more and three-quadrant closure or more were considered in the analysis.

Automated analysis was performed by AGATE (Version 1.0; Institute of Infocomm Research and Singapore Eye Research Institute, Singapore), a software program to analyze the angle images by quadrants and assign the classification as "open" or "closed" based on a training data set. The methodology for the program evaluation and the basis for the program were published earlier.[7,8] The method first determines the quadrant information from the image. Then it detects focal edges associated with angle structures. A circular Hough transform is applied to locate the iris surface. From the iris surface and the quadrant information, a focal region is calculated. Edges within the focal region are extracted and used to estimate the angle width profile. Finally, a classification between "open" and "closed" is given based on the angle width profile.

Reproducibility of Grading Methods

Intra- and interobserver reproducibility for EyeCam manual grading were analyzed in 40 randomly selected eyes by two observers masked to gonioscopic data and were found to be acceptable for two quadrants angle closure (first-order agreement coefficient statistics [AC1] between 0.57 and 0.63).[3]

Automated software (AGATE) reproducibility was excellent ($\kappa = 0.99$) for a sample of 30 eyes (120 images).

Statistical Analysis

One eye from each patient was randomly selected for analysis if both eyes were eligible for the study. The McNemar test was used to compare differences in the distribution of categorical variables between two related samples. Kappa statistic was used to assess the agreement between categorical variables and for reproducibility analysis. First-order agreement coefficient statistics were used to assess the agreement between graders in situations in which the prevalence of positive classifications may lead to inconsistent results. First-order agreement coefficient statistic results are interpreted in a similar manner to κ statistics.[9] Cochran's Q test was performed to test differences in proportions of two or three quadrants of angle closure among the three methods. Receiver operating characteristic (ROC) curves, with calculations of area under the curve (AUC) and 95% confidence intervals (CIs) were used as an index of each instrument's diagnostic performance for identifying eyes with angle closure, using gonioscopy as the reference standard. A P value less than 0.05 was considered statistically significant. The sample size calculation was based on comparison of sensitivities for matched groups in a diagnostic study, as reported by Beam et al.[10] With an estimated sensitivity of 82%, the number of subjects required was 78 in this study. Statistical analysis was performed using MedCalc version 12.3.0.0 (Mariakerke, Belgium). Venn diagrams to scale were generated for either two or three quadrants of angle closure to show overlap among the three methods.[11]

Results

Out of the 145 consecutive eligible subjects, five were excluded due to missing/poor-quality images. One hundred forty eyes were included for analysis using the automated software. The mean age of included subjects was 60.5 (SD 12.9) years with most being Chinese (102/140, 72.9%) and women (72/140, 51.5%). Five subjects had previously undergone LPI. Gonioscopic angle closure was noted in two

Investigative Ophthalmology & Visual Science

Table 1. Kappa Agreement of Manual and Automated Grading of EyeCam Angle Images Compared With Gonioscopy

	Agreement Between Methods					
	Manual vs. Gonioscopy, $n = 140$		Automated vs. Gonioscopy, $n = 140$		Manual vs. Automated, $n = 140$	
Definition of Closure	κ (95% CI)	AC1	κ (95% CI)	AC1	κ (95% CI)	AC1
One or more quadrants closed	0.87 (0.79–0.95)	0.87	0.50 (0.36–0.64)	0.50	0.57 (0.44–0.70)	0.57
Two or more quadrants closed*	0.88 (0.81–0.96)	0.89	0.74 (0.63–0.85)	0.74	0.68 (0.56–0.81)	0.69
Three or more quadrants closed†	0.76 (0.64–0.87)	0.79	0.78 (0.67–0.89)	0.82	0.79 (0.68–0.89)	0.81
Four quadrants closed	0.60 (0.44–0.76)	0.76	0.46 (0.28–0.65)	0.72	0.47 (0.29–0.65)	0.70
Superior quadrant closed	0.81 (0.71–0.91)	0.82	0.69 (0.57–0.81)	0.69	0.73 (0.62–0.84)	0.73
Inferior quadrant closed	0.88 (0.81–0.96)	0.89	0.65 (0.52–0.78)	0.67	0.58 (0.45–0.72)	0.62
Nasal quadrant closed	0.65 (0.51–0.79)	0.74	0.64 (0.50–0.78)	0.72	0.61 (0.47–0.75)	0.67
Temporal quadrant closed	0.67 (0.54–0.80)	0.73	0.37 (0.21–0.53)	0.41	0.48 (0.33–0.62)	0.50

κ, kappa statistic; AC1, first-order agreement coefficient statistic; Cochran's Q test: *$P = 0.12$, †$P = 0.28$.

quadrants or more among 61 eyes (43.6%) in comparison to 59 (42.1%, $P = 0.73$) using manual grading of angle images. Automated grading of angle images graded more angle closure eyes but was statistically insignificant in comparison to gonioscopy (67/140, 47.9%, $P = 0.24$).

Table 1 shows the agreement for various definitions of angle closure among the three methods. Generally, two- or three-quadrant closure definitions showed good agreement among methods. The temporal quadrant showed the least agreement with automated grading in comparison with gonioscopy. Manual versus automated grading comparison showed moderate to good agreement. Figure 1a shows a Venn diagram depicting eyes identified by each method for two-quadrant angle closure definition, with automated grading overestimating angle closure. Figure 1b shows a similar diagram for three-quadrant angle closure definition, suggesting slight overestimation by manual grading. However, this difference in agreement was not statistically significant for two (Cochran's Q test, manual versus automated, 0.88 vs. 0.74, $P = 0.12$) or three quadrants (0.76 vs. 0.78, $P = 0.28$) of angle closure among the methods. The agreement statistics did not change when subjects with previous LPI were removed from the analysis (data not shown). Table 2 shows that the AUC ROC is indistinguishable and very high for both methods in particular for the predominant two-quadrant definition of angle closure by gonioscopy. The AUC for two-quadrant closure (manual versus automated = 0.974 versus 0.954, $P = 0.31$) was slightly better than three-quadrant closure definition (manual versus automated = 0.927 vs. 0.94, $P = 0.67$), but this was not statistically significant.

Figures 2 and 3 depict EyeCam images showing discrepancy with gonioscopic diagnosis of open and closed angles respectively. The Figure 2A image was graded as closed on both manual and automated grading possibly due to a convex

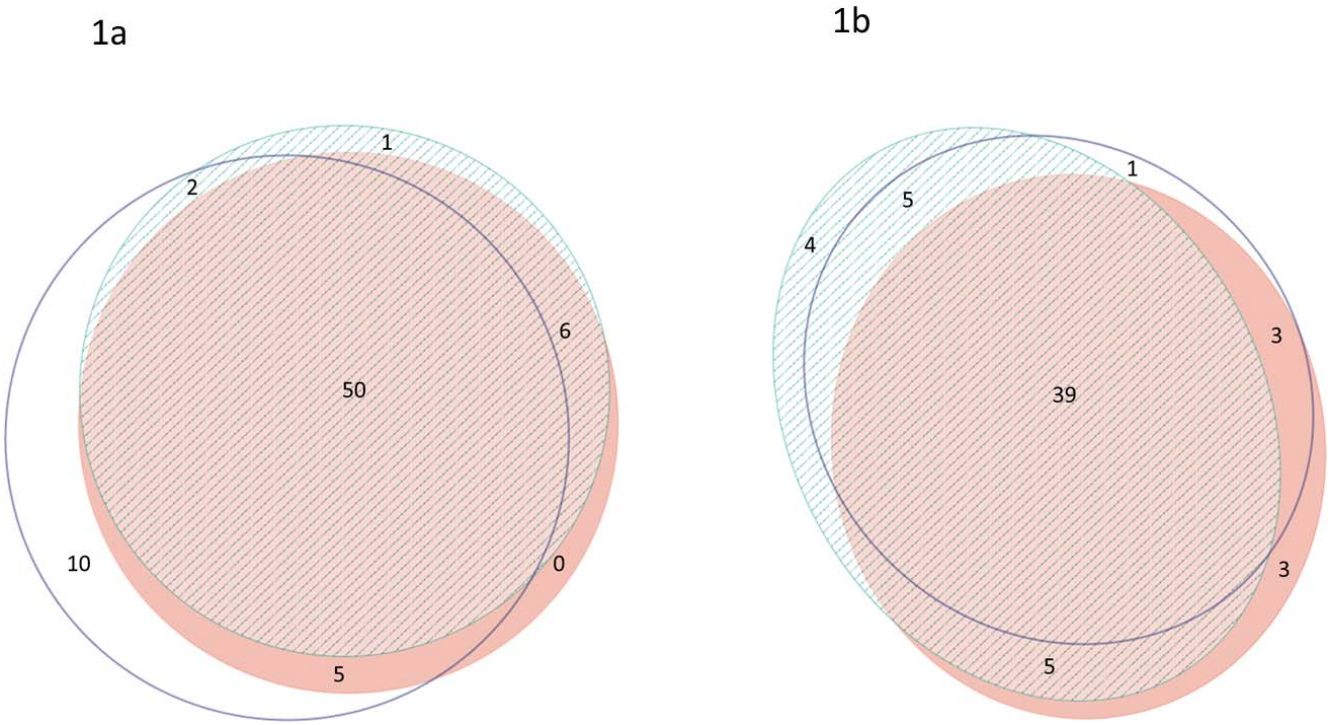

Figure 1. Venn diagrams showing the number of (**a**) two and (**b**) three quadrants closed angle detection by gonioscopy (*solid fill*), EyeCam manual (*stripes*) and automated (*empty*) grading methods, suggesting overestimation by the latter two methods.

Investigative Ophthalmology & Visual Science

Table 2. Receiver Operating Characteristic Curve Analysis to Compare Manual and With Gonioscopy for Various Definitions of Angle Closure

	Manual vs. Gonioscopy, $n = 140$			Automated vs. Gonioscopy, $n = 140$			
Definition of Closure	**AUC (95% CI)**	**Sensitivity**	**Specificity**	**AUC (95% CI)**	**Sensitivity**	**Specificity**	***P* Value***
One or more quadrants closed	0.955 (0.906–0.983)	0.92	0.95	0.923 (0.865–0.961)	0.95	0.55	0.266
Two or more quadrants closed	0.974 (0.933–0.994)	0.92	0.96	0.954 (0.905–0.982)	0.90	0.85	0.306
Three or more quadrants closed	0.927 (0.87–0.964)	0.88	0.89	0.94 (0.886–0.973)	0.84	0.93	0.665
Four quadrants closed	0.891 (0.828–0.938)	0.75	0.88	0.877 (0.811–0.926)	0.56	0.89	0.728

* Comparison of independent ROC curves between manual and automated grading of EyeCam angle images.

iris configuration. The Figures 2B and 2C images were graded as open on manual grading and gonioscopy but closed on automated grading, possibly due to the presence of a lightly pigmented TM or heavy TM pigmentation respectively, thus blurring the demarcation between TM and iris root. The Figure 3A image was graded as open on both gradings due to partial angle closure, whereas Figure 3B was graded as open with automated grading owing to the presence of pigmented Schwalbe's line. Overall misclassification rate with automated grading for angle assessment was 12.1% (17/140 eyes) with 7.9% false positives (i.e., 11 closed-angle eyes), whereas it was 5.7% (8/140 eyes) and 2.1% (3/140 eyes) with manual grading, respectively. Most open angles on gonioscopy had very light TM pigmentation (6/11) or dense pigmentation (4/11), leading to erroneous marking by automated grading as closed angles, whereas closed angles were marked as open if it was partial angle closure (3/6) or if the angle had a pigmented Schwalbe's line (3/6) in that quadrant. Another reason for error in automated grading was the presence of a convex iris, obscuring angle details and masquerading as closed angle.

Discussion

We report the clinical utility of the first automated software for goniophotographic angle assessment. The agreement of this software in comparison with gonioscopy was found to be very good for the two- and three-quadrant definitions of angle closure.

Several anterior segment imaging methods have been developed to address reproducibility and contact issues inherent in gonioscopic angle assessment. Although such techniques can quantitatively assess the anterior chamber angle, none can claim to completely replace gonioscopy for several reasons.[1] Assessing the distribution and degree of pigmentation in the TM, 360° circumferential angle view and detection of peripheral anterior synechiae are a few of the advantages with gonioscopy. Furthermore, the low specificity of these devices may limit their usefulness in screening for angle closure.[12] Reported practice patterns of ophthalmologists reveal only 50% use of gonioscopy in comprehensive eye examinations, and follow-up documentation of the angle is poor even among glaucomatologists.[13] To improve this, one must deconstruct gonioscopy into its constitutive parts. First, there is the technical aspect of image capture, followed by the interpretation and grading. Image capture can be done by EyeCam-fluent technicians, whereas the software algorithm in our study can fulfill the unmet need of interpretation and grading. This tool probably may be used for education and documentation of the angle and it can be easily adapted to goniophotography. Its uptake in screening for angle closure is unfortunately subject to other external factors, such as the cost and patient acceptability.

We have earlier examined the agreement between gonioscopy and manual assessment of angle images[3] using EyeCam, as well as in comparison with goniophotography and anterior segment optical coherence tomography (ASOCT).[14] Although ASOCT showed poor to fair agreement with manual EyeCam images, goniophotography shared better agreement and AUC for two- or three-quadrant angle closure.[2] This is unsurprising, in that they share similarities in acquisition and views. The misclassifications may stem from the fact that gonioscopy is far more versatile and one can use the corneal wedge to exactly identify the Schwalbe's line and evaluate the most open angle to correctly identify the angle anatomy for grading. Dynamic indentation adds another dimension in that it can differentiate between synechial and appositional closure and can help with discerning plateau iris and a prominent peripheral iris roll.

Individual quadrant angle closure diagnosis did not show very good agreement with gonioscopy for either manual or automated methods of EyeCam angle grading. This could be due to the nasal bridge obstructing the bulky probe, altering the angle view of the temporal quadrant. Misclassification of open or closed angles with either method was often due to heavy or light pigmentation and partial angle closure. In a

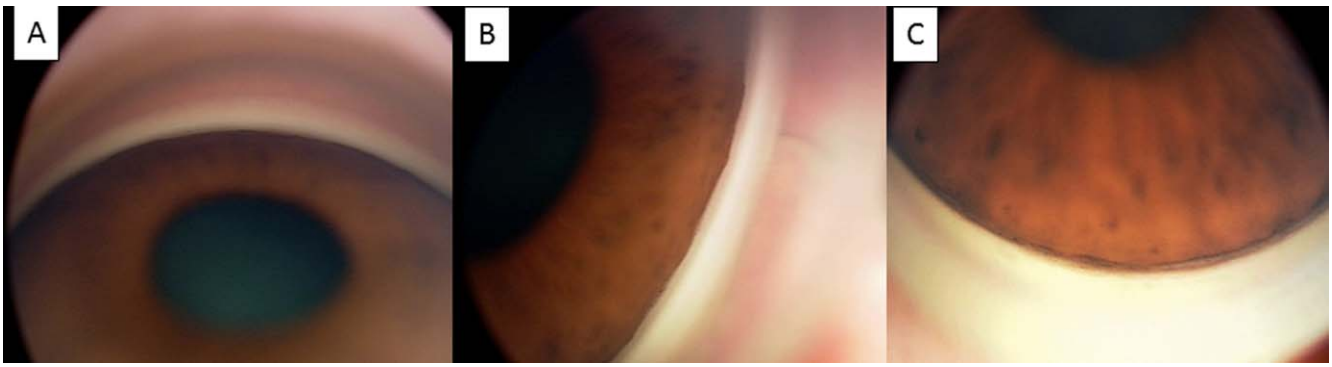

Figure 2. EyeCam images: misclassification into closed angles by automated grading method due to (**A**) convex iris, (**B**) lightly pigmented TM, and (**C**) heavy TM pigmentation.

Investigative Ophthalmology & Visual Science

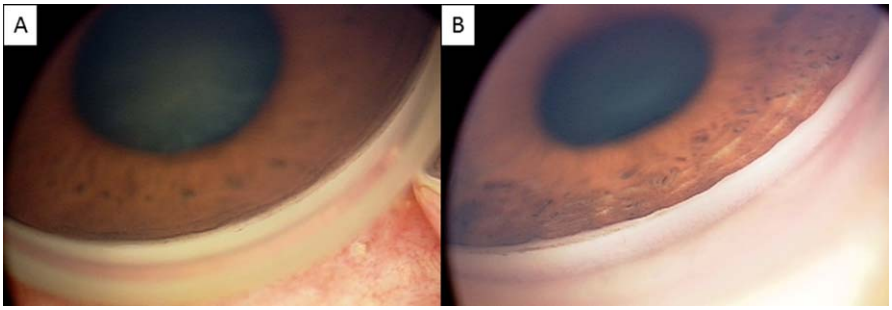

FIGURE 3. EyeCam images: misclassification into open angles by automated grading method due to (**A**) partial angle closure in that quadrant and (**B**) pigmented Schwalbe's line.

study of 291 subjects, including African American, "Far East" Asian, and Caucasian individuals, Oh et al[15] suggested that refractive error and racial origin may influence iris insertion, leading to variation in gonioscopic angle assessment. These limitations may have less bearing on EyeCam grading. Partial angle closure in a quadrant (which was misclassified by the software as open angles) in this study could be due to inclusion of subjects who have undergone LPI. Thus, the actual performance of the software may be better than reported, for as yet untreated angle closure subjects.

Our study had a few limitations. Gonioscopy was performed by a single observer and used the Scheie grading system. Misclassification error rates due to lightly pigmented angles or heavily pigmented TM may need to be addressed using better engineering methods, such as feature extraction techniques. These methods may identify angle structures irrespective of TM pigmentation and may improve the software algorithm in detecting angle closure. Until then, human observation of the images still may be needed to avoid gross misclassification, especially in eyes with extensive angle closure. Although inclusion of subjects who had previously undergone LPI in this study did not affect the overall results, it may be possible that the pigmentation released after LPI may have influenced the automated grading.

In summary, we evaluated a novel automated angle assessment software tool and reported very good diagnostic performance in comparison with gonioscopy. We believe that EyeCam imaging with automated angle assessment has potential to be a useful adjunct in clinical evaluation and documentation of the irido-corneal angle.

Acknowledgments

Supported by grants from the National Medical Research Council, Singapore; SingHealth; and Singapore National Eye Centre, Singapore.

Disclosure: **M. Baskaran**, None; **J. Cheng**, None; **S.A. Perera**, None; **T.A. Tun**, None; **J. Liu**, None; **T. Aung**, None

References

1. Smith SD, Singh K, Lin SC. Evaluation of the anterior chamber angle in glaucoma: a report by the American Academy of Ophthalmology. *Ophthalmology*. 2013;120:1985–1997.
2. Baskaran M, Perera SA, Nongpiur ME, et al. Angle assessment by EyeCam, goniophotography, and gonioscopy. *J Glaucoma*. 2012;21:493–497.
3. Perera SA, Baskaran M, Friedman DS, et al. Use of EyeCam for imaging the anterior chamber angle. *Invest Ophthalmol Vis Sci*. 2010;51:2998–3002.
4. Perera SA, Quek DT, Baskaran M, et al. Demonstration of angle widening using EyeCam after laser peripheral iridotomy in eyes with angle closure. *Am J Ophthalmol*. 2010;149:903–907.
5. Narayanaswamy A, Singh M. RetCam—a useful adjunctive tool to evaluate and manage paediatric glaucomas. *Asian J Ophthalmol*. 2008;109:30–31.
6. Erraguntla V, MacKeen LD, Atenafu E, et al. Assessment of change of optic nerve head cupping in pediatric glaucoma using the RetCam 120. *J AAPOS*. 2006;10:528–533.
7. Cheng J, Liu J, Lee BH, et al. Closed angle glaucoma detection in RetCam images. *Conf Proc IEEE Eng Med Biol Soc*. 2010;1:4096–4099.
8. Scheie HG. Width and pigmentation of the angle of the anterior chamber. A system of grading by gonioscopy. *Arch Ophthalmol*. 1957;58:510–512.
9. Chan YH. Biostatistics 104: correlational analysis. *Singapore Med J*. 2003;44:614–619.
10. Beam CA. Strategies for improving power in diagnostic radiology research. *AJR Am J Roentgenol*. 1992;159:631–637.
11. Micallef L, Rodgers P. eulerAPE: drawing area-proportional 3-Venn diagrams using ellipses. *PLoS One*. 2014;9:e101717.
12. Lavanya R, Foster PJ, Sakata LM, et al. Screening for narrow angles in the Singapore population: evaluation of new noncontact screening methods. *Ophthalmology*. 2008;115:1720–1727.
13. Quigley HA, Friedman DS, Hahn SR. Evaluation of practice pattern for the care of open angle glaucoma compared with claims data: the Glaucoma Adherence and Persistence Study. *Ophthalmology*. 2007;11:1599–1606.
14. Baskaran M, Aung T, Friedman DS, et al. Comparison of EyeCam and anterior segment optical coherence tomography in detecting angle closure. *Acta Ophthalmol*. 2012;90:e621–3625.
15. Oh YG, Minelli S, Spaeth GL, Steinman WC. The anterior chamber angle is different in different racial groups: a gonioscopic study. *Eye (Lond)*. 1994;8:104–108.

Graefes Arch Clin Exp Ophthalmol
DOI 10.1007/s00417-012-2158-6

GLAUCOMA

Swept source optical coherence tomography measurement of the iris–trabecular contact (ITC) index: a new parameter for angle closure

Sue-Wei Ho · Mani Baskaran · Ce Zheng · Tin A. Tun · Shamira A. Perera · Arun K. Narayanaswamy · David S. Friedman · Tin Aung

Received: 7 March 2012 / Revised: 2 September 2012 / Accepted: 4 September 2012

Abstract
Purpose To evaluate the inter- and intra-observer agreement of measurement of the iris–trabecular contact (ITC) index, a measure of the degree of angle closure, using swept source optical coherence tomography (SSOCT, CASIA SS-1000, Tomey Corporation, Nagoya, Japan).
Methods One randomly selected eye of 60 subjects was imaged under dark room conditions. The SSOCT 3-dimensional angle scan simultaneously obtains 128 radial scans of the anterior chamber for the entire circumference of the angle. Post-imaging analysis estimated the ITC index using in-built software. For intra-observer agreement for image grading, one examiner performed the grading twice in a masked fashion and random order after a 1-week interval. A second examiner graded images to assess inter-observer agreement for image grading. For intra-observer agreement for image acquisition, a single operator imaged patients twice. For inter-observer agreement for image acquisition, a single observer graded two sets of images acquired by two different operators on the same patient. Bland–Altman plots and 95 % limits of agreement (LOA) were reported.
Results Study subjects were predominantly Chinese (54/60, 90 %) and female (42/60, 70 %), with a mean age of 65.5 years. The median ITC index for eyes with open angles (31/60) and closed angles was 20 % (95 % confidence interval [CI] — 13.6, 27.8) and 49 % (95%CI — 35.5, 69.2) respectively. The mean difference (95 % LOA) for intra-observer agreement for image grading and image acquisition were −0.8 % (−8.2, 6.5) and 0.6 % (−10.9, 9.7); corresponding inter- observer agreement were 0.1 % (−10, 10.1) and −0.3 % (−11.1, 10.5) respectively.
Conclusions The inter- and intra-observer agreement of the ITC index, as a measure of extent of angle closure using SSOCT, was good.

Keywords Angle closure glaucoma · Swept source optical coherence tomography · Gonioscopy · Iris · Agreement

Financial Support The study was supported by a Translational Clinical Research Program grant, Biomedical Research Council (BMRC), Singapore

S.-W. Ho · M. Baskaran · C. Zheng · T. A. Tun · S. A. Perera · A. K. Narayanaswamy · T. Aung
Singapore Eye Research Institute
and Singapore National Eye Centre,
Singapore, Singapore

M. Baskaran · C. Zheng · T. Aung
Yong LooLin School of Medicine,
National University of Singapore,
Singapore, Singapore

D. S. Friedman
Dana Center for Preventive Ophthalmology and Johns Hopkins Bloomberg School of Public Health, Wilmer Eye Institute,
Baltimore, MD, USA

T. Aung (✉)
Singapore National Eye Centre,
11 Third Hospital Avenue,
Singapore 168751, Singapore
e-mail: tin11@pacific.net.sg

Introduction

Primary angle closure glaucoma (PACG) is a leading cause of blindness, especially in Asian populations [1–3]. Proper examination of the anterior chamber angle is essential for the correct categorization of individuals suspected of having

Published online: 23 September 2012

angle closure [4]. Currently, gonioscopy is the reference standard for this clinical examination. However, gonioscopic examination is subjective, requires the expertise of a trained examiner, and has poor intra- and inter-observer agreement [5]. Objective imaging modalities like anterior segment optical coherence tomography (ASOCT) have addressed some of these shortcomings [6]. Spectral- or Fourier-domain optical coherence tomography (OCT) technology has recently been introduced to increase the imaging resolution [7, 8]. All of these obtain cross-sectional images of the angle which provide less information than the traditional examination of all 360° of the angle when assessed by gonioscopy.

The swept source optical coherence tomography (SSOCT, CASIA SS-1000, Tomey Corporation, Nagoya, Japan) is a novel anterior segment imaging device based on the Fourier-domain system. It employs a swept laser source at a wavelength of 1,310 nm and a scan speed of 30,000 A-scans per second. The device has a wide scanning range of 16 mm, which allows an entire cross section of the anterior chamber to be captured simultaneously. Uniquely, the SSOCT's low density 3-dimensional (3D) angle analysis scan simultaneously obtains multiple radial scans of the entire circumference of the anterior chamber angle. In-built semi-automated analysis software, which requires observer input, analyzes the extent of iris–trabecular contact (ITC) across 360° of the angle, and calculates the extent of angle closure as the ITC index. This delivers, for the first time, an estimation of angle closure which is more analogous to that derived from gonioscopy.

The aim of this study was to evaluate the inter- and intra-observer agreement of measurement of the ITC index using the SS-OCT.

Methods

This was a prospective observational study that was conducted in accordance with the tenets of the Declaration of Helsinki and was approved by the hospital's Institutional Review Board. Written informed consent was obtained from all participants.

Phakic subjects aged 40 years and above were recruited from glaucoma clinics at a Singapore hospital. Subjects with corneal disease that precluded imaging of the anterior segment, or those with previous uveitis, intraocular surgery or lid abnormalities were excluded. Subjects who had had laser peripheral iridotomy were not excluded. After demographic data were recorded; each subject underwent a standardized ophthalmic examination which included static and dynamic indentation gonioscopy. A glaucoma fellowship-trained ophthalmologist (MB) performed indentation gonioscopy in a dark room using a Sussman four-mirror goniolens (Ocular Instruments Inc, Bellevue, WA, USA). The angle in each quadrant was graded as per the modified Shaffer grading system, according to the anatomical structures observed during gonioscopy [9]. The anterior chamber angle (ACA) was considered 'closed' in that quadrant if the posterior pigmented trabecular meshwork (TM) could not be seen in the primary position without indentation (Modified Shaffer grade 0 to 2). The eye was classified as having angle closure if there were two or more closed quadrants.

SS-OCT imaging

All subjects underwent SSOCT imaging of one randomly selected eye before any contact procedure, under dark-room conditions. The operator elevated the upper eyelid and gently pulled the lower eyelid down so that the anterior chamber angles could be seen in the scan window, taking care to avoid inadvertent pressure on the globe. Subjects were asked to focus on an internal fixation target and once the subject had been optimally positioned, each eye was scanned with the 3D angle analysis scan (which takes 2.4 s) using the auto alignment function. This algorithm takes 128 consecutive meridional scans, each consisting of 512 A-scans covering a distance of 16 mm across the anterior chamber. Each eye was scanned 3 times by two experienced operators. The first and third image were scanned by operator A (TAT) and the second image was scanned by operator B (CZ), in order to assess for inter- and intra-examiner agreement of image acquisition.

Analysis of images

The CASIA built-in software (Type and Version 6 J.3, 2012.6.8.3) was used to measure the ITC index, which is a semi-quantitative measure of the extent of angle closure. ITC analysis uses full-length meridional images of the anterior segment (which are not corrected for index of refraction) to analyze the extent of contact between the iris and angle wall. For our analysis, we restricted the number to 16 out of 128 frames. Other options for frame selection built into the machine were eight, 32, 64, and 128 frames. These 16 frames were automatically selected by the software, and were placed at intervals of 11.25° apart. This selection of 16 frames was made for an accurate and acceptable representation of the angle, and was more stringent than the minimum prescribed eight frames by the manufacturer.

In each anterior segment image frame, the scleral spur (SS) and the ITC end point (EP) were marked manually by a single examiner (SWH) with colored "x" mark and "+" mark respectively for both quadrants in the image (Fig. 1a). SS was identified as the point at which a change in curvature of corneoscleral interface occurs. The EP was identified as the most anterior point of iris contact to the angle wall. The program made it possible to omit some frames without

Fig. 1 **a** Single frame of the cross-section of the anterior chamber. The colored "*x*"s are the scleral spur (*SS*) markings and the "+" are the iris–trabecular contact end point (*EP*)—both points are marked by the observer grading the image. **b** Iris–trabecular contact (ITC) chart with the *blue area* representing the amount and distribution of iris–trabecular contact. **c** Iris–trabecular contact (*ITC*) graph with *Y*-axis representing ITC (in arbitrary units) and the *X*-axis representing the degree of the angle. The *green graph above the red line* (representing SS) denotes the amount of angle closure (measured as the ITC index)

marking these points when they could not be identified. When all the 16 frames were marked, the "ITC" button on the screen was clicked to enable the ITC index to be calculated. The software then used the information from the plotted SS and EP points in these 16 frames to calculate this index.

The results are reflected in an ITC chart, as shown in Fig. 1b. The ITC chart is analogous to a goniogram used in clinical practice. The red circular line represents the SS. The dotted circles represent 0.25, 0.50 and 0.75 mm landmarks anterior to the SS, along the angle wall. The blue area represents the extent of angle closure and if positive, represents angle closure (i.e., ITC) and if negative or neutral, represents open angle areas.

The ITC analysis output also includes two parameters:

- the "ITC index" which represents the ratio of positive ITC (angle closure) in degrees (blue area in the ITC chart) to the total angle with visible scleral spur and end points in degrees; this essentially represents the extent of angle closure as a percentage.
- the 'invisible range' represents the circumferential extent (in degrees) throughout which either the SS or EP could not be determined in the meridional frames. A minimum of seven points needed to be identified for each eye for the calculation of ITC index (as per the manufacturer), and this criterion was used for quality control.

Table 1 Demographic and clinical features of study participants

	Patients with open angles (n=31)	Patients with closed angles (n=29)	P value
Age (mean/SD)	64.6 (6.52)	65.5 (7.09)	0.571
Gender (male:female)	11:20	7:22	0.405
Ethnicity (Chinese: Malays:Indian: others)	27:1:3:0	27:1:0:1	0.672
Eye (right:left)	12:19	15:14	0.436
Axial length (mm) (mean/SD)	23.68 (1.09)	22.84 (0.84)	0.005
ACD (mm) (mean/SD)	3.02 (0.41)	2.74 (0.40)	0.01
Lens thickness (mm) (mean/SD)	4.31 (0.69)	4.50 (0.80)	0.330
Gonioscopic grade (mean/SD)	3.65 (0.57)	1.16 (0.69)	0.0001

SD standard deviation; *ACD* anterior chamber depth; *ITC* iris trabecular contact index

Table 2 Distribution of Iris-trabecular contact index

	Overall	Eyes with open angles	Eyes with closed angles
Mean (percentage, 95 % CI) †	37.3 (30.07, 44.52)	22.65 (16.36, 28.93)	52.97 (41.92, 64.01)
Median (percentage, 95 % CI)†	30 (21, 45)	20 (13.59, 27.83)	49 (35.53, 69.23)
Interquartile range (percentage)	65.5	12.75	44
Coefficient of skewness	0.74* (positive skew)	0.48	0.19
D'Agostino–Pearson test for normality (p value)	0.0649	0.26	0.14

† p=<0.0001, SD, *p=0.0204, *CI* confidence interval

The extent of angle closure circumferentially is also displayed as a graph (Fig. 1c). A positive ITC (angle closure) is shown as above the red line (which represents the scleral spur) and a negative ITC (open angle) is shown below the line.

Agreement analysis

Inter- and intra-observer agreement was analysed separately for image grading and image acquisition. In order to assess intra-observer agreement for image grading, one examiner (SWH) performed the grading twice, allowing for a 1-week interval before grading the same set of images (n=60). The grader was masked to gonioscopic findings and the second sets of images were scrambled according to a computer generated random number sequence, produced using statistical software (Medcalc v12.0, Meriakerke, Belgium). Twenty images were randomly selected by the same computer-generated number sequence from the above set of 60 images, and were graded by a second examiner (TAT) to assess inter-observer agreement for image grading.

In order to assess inter-observer agreement for image acquisition, one examiner (SWH) graded two sets of images after a 1-week interval, each set consisting of 60 eyes acquired by two different operators A and B. For intra-examiner agreement for image acquisition, images obtained by operator A twice on the same patient were graded by a single examiner (SWH). All grading was performed masked to gonioscopic and clinical findings.

Demographic parameters were summarized by mean, median, 95 % confidence intervals (CI) and interquartile ranges for continuous variables. Skewness and normality test results were assessed. Kernel density probability estimate for the ITC index distribution was performed. Coefficient of variation for repeated measurements was presented as an estimate of dispersion of ITC index. Bland–Altman plots were used to evaluate the agreement of the ITC index for image grading and image acquisition. Fixed and proportional bias were evaluated using the mean difference, 95 % CI, significance of the regression slope, and 95 % limits of agreement (LOA). Receiver operating characteristic curve (ROC) analysis was performed to

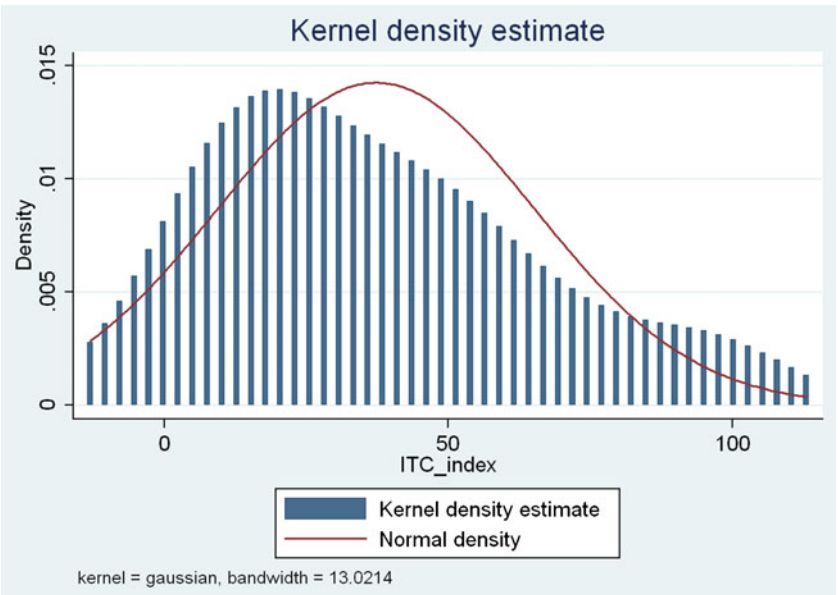

Fig. 2 Kernel density estimate of iris–trabecular index with Gaussian approximation with a bandwidth of 13.02, with normal curve overlaid shows slight positively skewed distribution

Table 3 Inter- and intra-observer agreement for iris–trabecular contact index measurement

	Bland–Altman plots mean difference (95 % CI)	Fixed bias	Proportional bias	95 % Limits of agreement	
				Lower bound	Upper bound
Inter-observer agreement for image grading (n=20)	0.1* (−2.4,2.5)	No	No	−10	10.1
Intra-observer agreement for image grading (n=60)	−0.8 (−1.8, 0.14)	No	Yes†	−8.2	6.5
Inter-observer agreement for images acquired by two technicians (n=60)	−0.3 (−1.72, 1.15)	No	No	−11.1	10.5
Intra-observer agreement for images by the same operator(n=60)	0.6 (−1.92, 0.79)	No	No	−10.9	9.7

*All measurements are in percentages, *CI* confidence interval, † Regression equation (y=0.81-0.04x, p=0.0099)

evaluate the area under the ROC curve (AUC) for ITC index compared to gonioscopic angle closure as the reference standard. All statistical analyses were performed using MedCalc for Windows v12.0 (Mariakerke, Belgium).

Results

A total of 60 eyes of 60 patients were examined; of these, 29 eyes had two quadrants or more angle closure on gonioscopy. The mean age of subjects was 65.5 (standard deviation [SD] 7.1) years, and the majority of subjects were Chinese (54/60, 90 %, Table 1). The overall mean ITC index was 37.3 (28.0), median was 30, and the index was positively skewed in distribution (Table 2). Figure 2 shows the kernel density estimate of ITC index, depicting a slight positive skew of the data and suggestive of a bimodal distribution. The mean ITC index for the open angle group was 22.5 % and 53.0 % for the closed angle group, while the corresponding medians were 20 % and 49 % respectively.

Agreement of ITC index: image grading

The inter-observer agreement of ITC index for grading of the images showed that the mean difference (95 % LOA) was 0.1 % (−10, 10.1, Table 3, Fig. 3a), and the coefficient of variation (COV) was 11.71 %. The intra-observer agreement of ITC index (image grading) showed that the mean difference (95 % LOA) was −0.8 % (−8.2, 6.5, Fig. 3b) and the COV was 7.16 %. There was no fixed bias noted from the mean difference values. The regression slope for the intra-observer agreement measurements showed proportional bias (p=0.0099), suggesting that there was less agreement in the measurements for extremes of ITC indices for the same examiner grading the images. However, this could be an initial learning curve for the grader, as we did not find a significant proportional bias in the other agreement analyses. Further, the regression plots for the absolute residuals did not show any significant bias in the measurements.

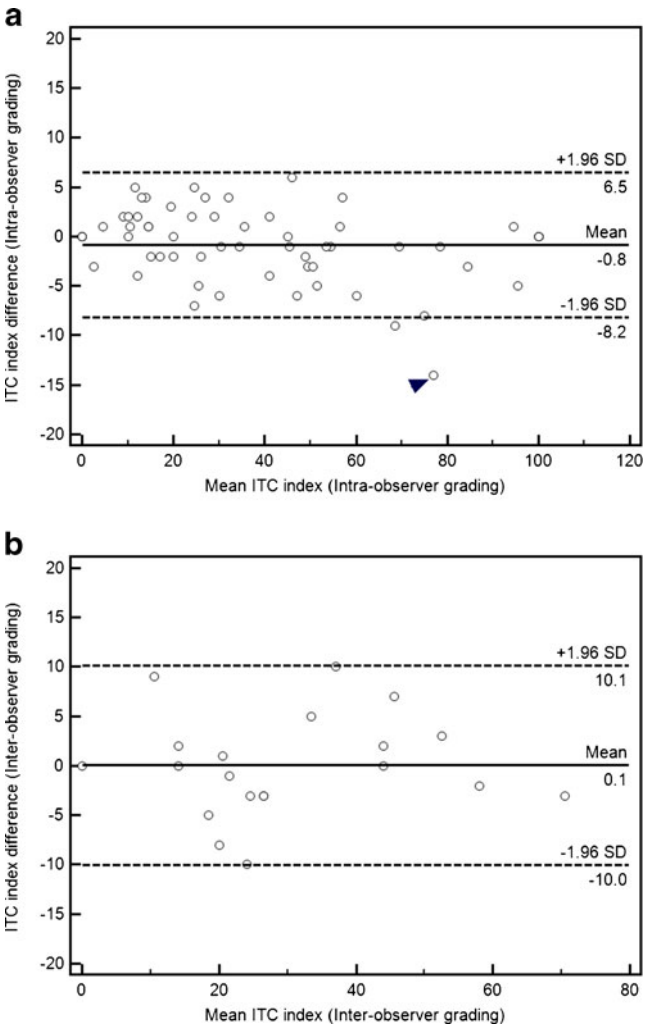

Fig. 3 Bland–Altman plots show the mean difference and 95 % limits of agreement for intra-observer agreement (**a**) and inter-observer agreement (**b**) for iris–trabecular contact index (ITC index) if same images are graded. *Arrow* indicates a single outlier

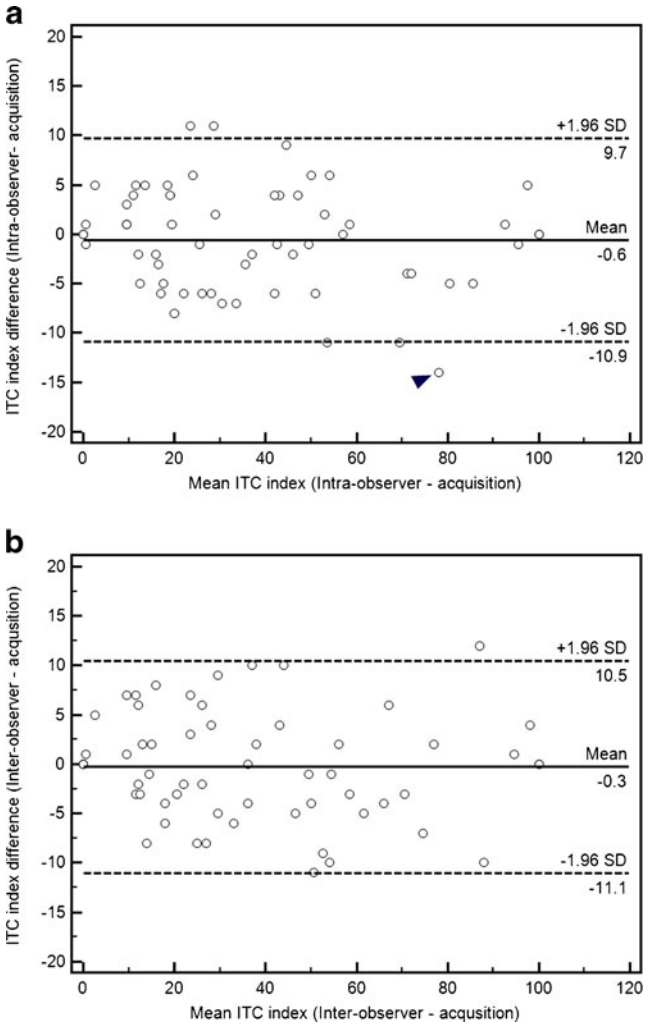

Fig. 4 Bland–Altman plots show the mean difference and 95 % limits of agreement for intra-observer agreement (**a**) and inter-observer agreement (**b**) for iris–trabecular contact index (ITC index) using images acquired at different examinations. *Arrows* indicate single outliers

The results suggest that the agreement for grading of images was within clinically acceptable limits.

Agreement of ITC index: image acquisition

The inter-observer agreement of ITC index for image acquisition showed that the mean difference (95 % LOA) was −0.3 % (−11.1, 10.5) and COV was 13.12 %. The intra-observer agreement of ITC index (image acquisition) showed that the mean difference (95 % LOA) was 0.6 % (−10.9, 9.7) and COV was 9.41 % (Table 3, Fig. 4a&b). There was no fixed bias or proportional bias noted in the repeated measurements. The regression plots for the absolute residuals did not show any significant bias in the measurements. The results suggest that image acquisition by different examiners may lead to more variations in the ITC index compared to a single examiner. However, the differences appear to be within clinically acceptable limits.

ROC analysis

The AUC for ITC index diagnostic performance to detect gonioscopic angle closure was 0.804 (95 % confidence interval [CI], 0.681, 0.895). The optimal threshold with the best performance was for ITC index >29 %, with a sensitivity of 75.86 (56.5, 89.7), specificity of 70.97 (52, 85.8), positive likelihood ratio of 2.61 (1.5, 4.7), and negative likelihood ratio of 0.34 (0.2, 0.7).

Discussion

We obtained repeatable measurements of the extent of angle closure, using SSOCT to image the entire circumference of the angle. Both inter- and intra-observer agreement of ITC measurements were good and clinically acceptable, using images graded or acquired twice on the same person by the same examiner and also by two different examiners. Typical values were found to be 30 % (or 108°) apart between open and closed angles, with measurement errors more than 10 % (or 36°) being very rare, indicating that the ITC index may be useful for discrimination of even borderline closed angle eyes. The image quality for both sets of images obtained in the first and second examinations were similar, suggesting that there is minimal learning curve for performing this imaging. As far as we are aware, this is the first paper examining the agreement of the ITC index measured by SSOCT.

Liu et al. [10] recently evaluated angle parameters measured by SSOCT, and found that there was good inter- and intra-observer agreement for angle measurements such as the angle opening distance (AOD), the trabecular iris space area (TISA), and the trabecular-iris angle (TIA). However, they noted that variability in the location of measurement, the axial length, iris thickness, and angle width are factors which may affect the agreement of angle measurements.

Various researchers have attempted three-dimensional quantitative analysis of the angle as an alternative method to qualitative gonioscopic assessment. Scheimpflug photography, introduced in the 1970s, has undergone several modifications and in recent years, the rotating Scheimpflug camera is available as a device for rapid 3-dimensional analysis of the anterior chamber [11]. However, the analysis has limitations, as the angle cannot be fully visualized with visible-light-based imaging. All the OCT-based anterior segment imaging modalities currently utilize a few cross-sectional images, and assess the angle qualitatively or by certain surrogate quantitative parameters. This may result in inaccurate quantification of angle closure. The novelty of

the ITC index lies in the fact that it utilizes 360° angle data as a measure of the percentage of angle closure, and represents this information in the form of a chart, similar to a goniogram. This method of analysis can be easily interpreted for clinical diagnosis and follow-up in angle-closure disease, provided it is found to be reliable and accurate. However, manually marking the SS and EP in all images is a tedious and time-consuming process, making clinical use of the ITC index limited. Further refinement and automation of the ITC index will be necessary before the index can be used as a summary measure for angle-closure evaluation, especially in clinical decision making and follow-up of patients.

There are several limitations to our study. Firstly, the SS could not be determined in some frames. When we were unable to locate the SS, the software extrapolated the location of SS based on the adjacent SS points. None of the eyes were excluded or rejected for the analysis, since we were able to mark at least seven plots (as per the manufacturer's requirement) with the semi-automated software; hence, the image analysis criterion was fulfilled for all subjects' images. Secondly, we chose 16 instead of 128 frames for the analysis. Sixteen frames offer a reasonable surrogate because if we chose 128 frames, it would be too time-consuming for the examiner to plot all the points in each frame. Even though each frame represented 11.25° of the angle, and was adequate for the analysis of the ITC index, analyzing 128 frames might have yielded a more accurate analysis, not just by including more meridians for analysis, but also by decreasing the invisible range. Thirdly, poor-quality images were probably due to movement of the subject or eyelids during image capture. Capturing images proved ergonomically cumbersome at times. The difficulty lay in capturing the image over the large image console while simultaneously stretching to open the subjects' eyelids. Liu et al. [10] instructed participants to pull down their own lower eyelids while the technician elevated the upper eyelids to circumvent these issues. However, any method of manual stretching of eyelids might introduce artifacts in the angle configuration by exerting some pressure on the globe. Fourthly, inherent to all OCT scans is the inability to distinguish between appositional and synechial closure. Lastly, the agreement demonstrated in this study may not be replicated in a clinic-based scenario because of the rigid inclusion criteria used in this study, in which eyes with pathologies such as corneal opacity were excluded. Eyes with dense arcus and pterygium can result in degradation of images, and identification of landmarks such as SS and EP may not be determined with precision [6]. In relation to the feasibility of the ITC as a measure of the proportion of angle closure, we found that up to 8.3 % of eyes had ≥50 % of invisible range. We may overcome this limitation if more frames are included for angle assessment in ITC analysis; however, the SS and EP markings need to be automated to enable such a task. It may also be necessary for the manufacturers to provide better image processing algorithms to overcome this problem.

In conclusion, we found good and clinically acceptable intra- and inter-observer agreement of the measurement of the ITC index using SSOCT. The ITC index has the potential to provide objective information about the extent of circumferential angle closure, and we consider the assessment of agreement as a first step towards further clinical applications in the future. However, current requirements for manual grading of the images limit the clinical utility of this application.

Conflict of Interest None of the authors have any financial/conflicting interests.

References

1. Leung CK, Yung WH, Yiu CK, Lam SW, Leung DY, Tse RK, Tham CC, Chan WM, Lam DS (2006) Novel approach for anterior chamber angle analysis: anterior chamber angle detection with edge measurement and identification algorithm (ACADEMIA). Arch Ophthalmol 124:1395–1401
2. Foster PJ, Johnson GJ (2001) Glaucoma in China: how big is the problem? Br J Ophthalmol 85:1277–1282
3. Wu RY, Nongpiur ME, He MG, Sakata LM, Friedman DS, Chan YH, Lavanya R, Wong TY, Aung T (2011) Association of narrow angles with anterior chamber area and volume measured with anterior-segment optical coherence tomography. Arch Ophthalmol 129:569–574
4. Congdon N, Wang F, Tielsch JM (1992) Issues in the epidemiology and population based screening of primary angle-closure glaucoma. SurvOphthalmol 36:411–423
5. Yi JH, Hong S, Seong GJ, Kang SY, Ma KT, Kim CY (2008) Anterior chamber measurements by pentacam and AS-OCT in eyes with normal open angles. Korean J Ophthalmol 22:242–245
6. Narayanaswamy A, Sakata LM, He MG, Friedman DS, Chan YH, Lavanya R, Baskaran M, Foster PJ, Aung T (2010) Diagnostic performance of anterior chamber angle measurements for detecting eyes with narrow angles: an anterior segment OCT study. Arch Ophthalmol 128:1321–1327
7. Wong HT, Lim MC, Sakata LM, Aung HT, Amerasinghe N, Friedman DS, Aung T (2009) High-definition optical coherence tomography imaging of the iridocorneal angle of the eye. Arch Ophthalmol 127:256–260
8. Wylegała E, Teper S, Nowinska AK, Milka M, Dobrowolski D (2009) Anterior segment imaging: Fourier-domain optical coherence tomography versus time-domain optical coherence tomography. J Cataract Refract Surg 35:1410–1414
9. Sasidharan R (2008) South East Asia Glaucoma Interest Group. Appendix 6A. Gonioscopy. Asia Pacific glaucoma guidelines. Scientific Communications International, HongKong
10. Liu S, Yu M, Ye C, Lam DS, Leung CK (2011) Anterior chamber angle imaging with swept-source optical coherence tomography: an investigation on variability of angle measurement. Invest Ophthalmol Vis Sci 52:8598–8603
11. Rabsilber TM, Khoramnia R, Auffarth GU (2006) Anterior chamber measurements using Pentacam rotating Scheimpflug camera. J Cataract Refract Surg 32:456–459

34th Annual International Conference of the IEEE EMBS
San Diego, California USA, 28 August - 1 September, 2012

Anterior Chamber Angle Classification Using Multiscale Histograms of Oriented Gradients for Glaucoma Subtype Identification*

Yanwu Xu[1], Jiang Liu[1], Ngan Meng Tan[1], Beng Hai Lee[1], Damon Wing Kee Wong[1], Mani Baskaran[2], Shamira A. Perera[2] and Tin Aung[2,3]

Abstract— **Glaucoma subtype can be identified according to the configuration of the anterior chamber angle(ACA). In this paper, we present an ACA classification approach based on histograms of oriented gradients at multiple scales. In digital optical coherence tomography (OCT) photographs, our method automatically localizes the ACA, and extracts histograms of oriented gradients (HOG) features from this region to classify the angle as an open angle (OA) or an angle-closure(AC). This proposed method has three major features that differs from existing methods. First, the ACA localization from OCT images is fully automated and efficient for different ACA configurations. Second, the ACA is directly classified as OA/AC by using multiscale HOG visual features only, which is different from previous ACA assessment approaches that on clinical features. Third, it demonstrates that visual features with higher dimensions outperform low dimensional clinical features in terms of angle closure classification accuracy. Testing was performed on a large clinical dataset, comprising of 2048 images. The proposed method achieves a 0.835 ± 0.068 AUC value and $75.8\% \pm 6.4\%$ balanced accuracy at a 85% specificity, which outperforms existing ACA classification approaches based on clinical features.**

I. Introduction

Glaucoma is the second leading cause of blindness worldwide (behind cataracts) as well as the foremost cause of irreversible blindness [1], with a mean prevalence of 2.4% for all age groups and 4.7% for ages 75 years and above. It currently affects about 60 million people [2], and is responsible for approximately 5.2 million cases of blindness (15% of world total) according to the data from the World Health Organization [1]. As illustrated in Fig. 1, *glaucoma is classified according to the configuration of the angle* (formed by the intersection of the cornea and iris) into open angle (OA) and angle-closure (AC) glaucoma. Primary angle closure glaucoma (PACG) is a major form of glaucoma in Asia [3], compared to primary open angle glaucoma (POAG), which is more common in Caucasians and Africans [4]. The high visual morbidity from PACG is related to the destructive nature of the asymptomatic form of the disease.

*This work was supported in part by the Agency for Science, Technology and Research, Singapore, under BMRC grant 10/1/35/19/674.

[1]Y.-W. Xu, J. Liu, N.-M. Tan, B.-H. Lee and D.W.K. Wong are with the Institute for Infocomm Research, Agency for Science, Technology and Research, 138632, Singapore {yaxu, jliu, nmtan, benghai, wkwong} at i2r.a-star.edu.sg

[2]M. Baskaran, S.A. Perera and T. Aung are with the Singapore Eye Research Institute, 168751, Singapore baskaran.mani at seri.com.sg, shamira.perera at snec.com.sg, aung.tin at snec.com.sg

[3]T. Aung is also with the Department of Ophthalmology, National University of Singapore, 119074, Singapore

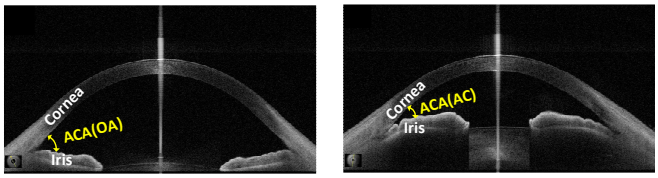

Fig. 1. Open angle (OA, left) and angle-closure (AC, right).

Early detection of anatomically narrow angles is important and the subsequent prevention of visual loss from PACG depends on an accurate classification of the ACA [5].

Angle closure is a result of obstruction of the trabecular meshwork by the iris, impeding the drainage of aqueous humour in the angle of the eye, causing an increase in intraocular pressure (IOP). As reported in [6], a shallow central anterior chamber depth (ACD), a thick and anterior lens position and short axial length (AL) are anatomical risk factors for angle closure. Amongst these, a shallow ACD is regarded as a cardinal risk factor for PACG. However, only a small proportion of subjects with shallow ACD ultimately develop PACG according to a population study [7]. Thus other ocular factors related to PACG development need to be discovered.

In the literature, automated glaucoma subtype classification has been studied on color RetCam images [8], in which the biologically inspired features (BIF) are extracted from the ACA regions for classification. For other image modalities, several automatic ACA assessment methods have been proposed. For example, an edge detection and line fitting approach is proposed for ACA measurement [9] in ultrasound biomicroscopy (UBM) images. Similarly, a segmentation, edge detection and linear regression based approach is proposed for ACA assessment in OCT images [10].

In this work, we study ACA classification based on histograms of oriented gradients (HOG) features to identify glaucoma subtype in OCT images, which has the advantages of being non-invasive and non-contact [11] compared to UBM. An OCT image captures a cross-section of the eye as a grayscale image, and several features can be extracted for ACA measurement, such as anterior chamber open depth (AOD) [9][10], trabeculariris angle (TIA) [12], trabecular-iris space area (TISA) [12] and Schwalbe's line bounded area (SLBA) [13]. *In clinical practice, these features are used for ACA classification.*

978-1-4577-1787-1/12/$26.00 ©2012 IEEE

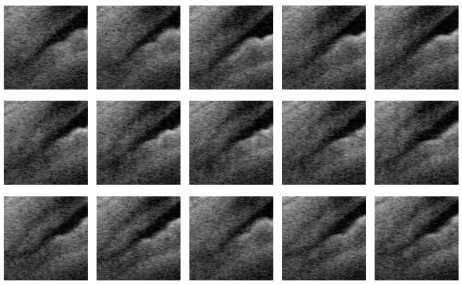

Fig. 2. Illustration of the varying of ACA closed and open. The ACAs in the top and bottom rows are clinically labeled as closed, the ACAs in middle row are labeled as open; however, these ACAs are intermediate cases and very hard to classify.

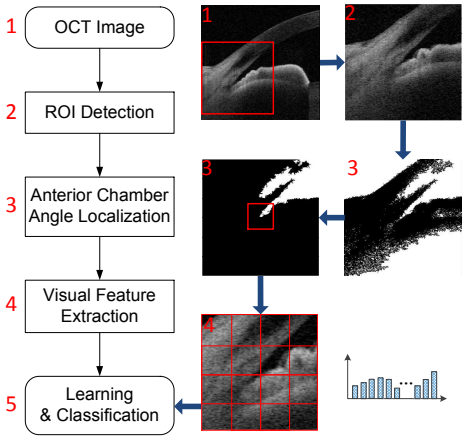

Fig. 3. Flowchart of the proposed ACA localization and classification.

ACA detection in OCT images can be relatively straightforward since the images are generally clean and are approximately aligned during image acquisition process. However, ACA classification is a challenging task since there are intermediate cases (see in Fig. 2) that are difficult to classify as AC or OA using the same clinical features, even for human experts. Based on image classification experience, using only one or two dimensional clinical features is insufficient to achieve good performance, since the eigen dimension of this problem might be much higher, *as observed clinically* [7].

In this paper, we propose an image processing and learning based framework for efficient ACA localization and classification, which has the following main features: 1) the image processing based ACA localization in OCT images is fully automated and efficient for different ACA configurations; 2) it can directly classify ACA as OA/AC based on only visual features, which is different from previous work for ACA measurement that relies on clinical features; 3) it demonstrates that visual features with higher dimensions outperform low dimensional clinical features in terms of angle closure classification accuracy. With the proposed framework, other existing visual features and learning algorithms can be introduced to elevate performance.

II. ACA Localization and Classification Framework

To classify an ACA as open or closed angles, our solution is to follow the method of a human expert. As shown in Fig. 3, for a given OCT image, we first localize the ACA region by using image processing approaches, and then extract certain visual features (*e.g., HOG*) in the region and apply the SVM classifier to identify whether it is closed. In previous work, the ACA regions are marked manually [12] or are automatic determined by using edge detection [9]. Based on our observations, we extended the edge detection approach by combining edge detection with weighting and connected component labeling segmentation (CCLS) [10], which is robust to different ACA configurations and can localize the ACAs with their vertices roughly aligned. To classify an ACA as AC or OA, the simple thresholding method is clinically used with several clinical features (*e.g.*, depth, angle and area) for ACA measurement. However, we believe that the context around the ACA region can provide additional information to increase classification accuracy, since the eigen dimension of this problem might be much higher. Thus we introduce HOG features at multiple scales with higher dimension and SVM classifier for ACA classification.

A. ACA localization

A coarse-to-fine scheme is used to efficiently localize the ACA from input OCT image. As shown in Fig. 3, first, a 400×400 region of interest (ROI) covering the exact ACA is cropped out at a fixed position from the 834×900 input image; second, the ROI is quantized to a binary image (0 for black and 1 for white) using a small valued threshold in order to preserve more details of the angle (a large/adaptive threshold will lose more details at the extreme end of the ACA, which is very important for classification); third, a morphological operation is performed to remove isolated noise points; fourth, weighting and CCLS algorithm are used to segment the ACA candidate in the ROI; fifth, a post processing step is applied to remove other components connected to the exact ACA in the candidate region; lastly, the ACA is localized with an $n \times n$ bounding box centered at its detected vertex.

1) ROI detection: For ROI detection, many existing computer vision methods can be used, such as the well-known sliding window method [14][15]. However, for the relatively clean OCT images, line fitting based cornea detection is accurate and much more efficient to obtain the ROI, since the ACA is between the cornea and iris (see in Fig. 1). As shown in Fig. 4, Sobel edge detection is first applied on the OCT image, and then the top-most white point of each column is obtained, thus the fitted smooth line of these points is treated as the upper boundary of the cornea. The lowest point of the boundary is selected as the reference point (*i.e.*, the center point of the left boundary of the ROI), and then a 400×400 rectangle referred to this point is cropped as the ROI.

2) ACA segmentation: The ROI is first converted to binary image (0 for black and 1 for white) using a small valued

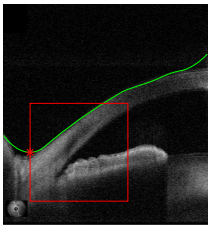

Fig. 4. Illustration of ROI detection. The green line is the detected cornea upper boundary and the red bounding box is the ROI.

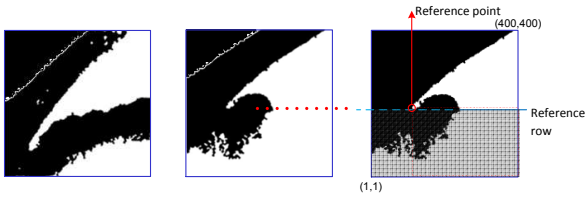

Fig. 5. Clear ACA (left), bottom connected ACA (middle) and an illustration of post processing (right) for the bottom connected case.

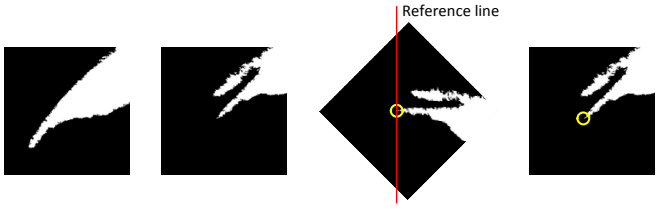

Fig. 6. Two ACA profiles: single clear angle (first) and multiple angles (second), and illustration of ACA vertex localization (third and fourth) for an ACA region.

threshold, and the pixels above the cornea upper boundary is set to black to avoid further processing. Thus each 4-connected white region can be separated and labeled by using CCLS algorithm [10], and the candidate ACA region is selected by choosing the one with maximum pixel number. With the candidate ACA region obtained, a post processing step illustrated in Fig. 5 is applied to deal with the case that the bottom part of the ACA is connected with other white regions. This occurs when *the iris is not fully captured during the imaging process*, resulting in that at least one row is completely white in the bottom half of the right-most rows. First, the top-most white point of each column is located; second, the difference between each pair of neighboring columns is computed; third, the first column from the left that has a difference greater than 30 (pixels) is found and then the reference point of the ACA segmentation can be obtained; lastly, for the region from the reference point to the right-bottom, a zero value (black) is given to all the pixels below the reference row which has the minimum number of white pixels.

3) ACA vertex localization: As shown in Fig. 6, by this step, the obtained ACA regions can be categorized into two profiles according to our observations, *i.e.*, the clear case (when the ACA vertex is the left-bottom-most white point) and the multiple angles case. To localize the true vertex of the ACA in both cases, the image is first rotated 45 degree clockwise with respect to the bottom-left point, and then the left-most white point is located (if there are multiple such points, choose the bottom-most one) and its original position on the non-rotated image can be calculated. After the vertex is localized, a $n \times n$ (n is set to 150 in the experiments) region centered at the vertex is cropped *from the original image*, as the ACA localization result to extract visual features for classification.

B. ACA feature representation and classification

1) HOG feature extraction: In this work, HOG features [14] is used for ACA representation, because HOG features have demonstrated great success in various object detection and recognition problems. Moreover, HOG features are related to the edge information, which is important for ACA assessment; and we did not use BIF features [8] which are related to textures, computational expensive and are more suitable for color images. At this stage, each ACA region is represented by a $n \times n$ grayscale image. To extract HOG features, the gradient of each pixel in the region is computed, and then the gradient magnitude is inserted into one of nine histogram bins that span a 180 degree range. The ACA region is divided into $d \times d$ cells, and 2×2 cells form a block. Each block half overlaps each of its neighbors, and is normalized using the L2-norm. With a specific d, the HOG vector is composed of all normalized block histograms. Multiscale strategy is introduced to boost up the performance, *i.e.*, different values of d are used to extract HOG features at different scales, and the final feature is composed of all HOG vectors extracted at every scale. For more details of the HOG features, the readers are referred to [14].

2) Linear SVM classification: For efficiency, a simple linear SVM classifier is employed, with a weight vector ω trained to estimate the class label y (+1 for AC and -1 for OA) of a given feature vector $\mathbf{f}$, according to $y = \omega^T \mathbf{f}$. In the experiments, we use the LIBLINEAR toolbox [16] to train the SVM models.

III. Experiments

In this section, we describe the evaluation criteria and experimental setting, then analyze the classification accuracy in our framework, through comparisons of using visual features and clinical features.

A. Experimental setup

Our approach is implemented with Matlab and tested on a four-core 3.4GHz PC with 12GB RAM. A dataset comprised of 2048 images is used for the experiments, which is much larger than the datasets used in the literature [9][13]. The images are from 8 circular scan videos of 8 patient eyes with glaucoma, 4 of them with PACG and other 4 with POAG. Each video contains 128 frames, and each frame is split into 2 images since it contains two angles and the right angle image is flipped horizontally. The evaluation is based on each single image, which is labeled as AC or OA by three

TABLE I

PERFORMANCE COMPARISONS OF ACA CLASSIFICATION WITH DIFFERENT FEATURES AND PARAMETERS

Feature	HOG				AOD	SLBA
d	3	6	10	{3,6,10}	–	–
AUC	0.807 ±0.073	0.818 ±0.088	0.796 ±0.094	**0.835 ±0.068**	0.745 ±0.166	0.697 ±0.108
$\bar{P}(\%)$	66.8 ±10.0	72.3 ±10.0	67.8 ±7.8	**75.8 ±6.4**	63.9 ±11.7	62.1 ±7.5

ophthalmologists from Singapore Eye Research Institute. All ACA localization results are manually checked and all ACA regions are correctly cropped out. For the ACA classification evaluation, we follow the widely used leave-one-out (LOO) approach, *i.e.*, for each testing round, 512 images from one PACG and one POAG patients are used for testing while others are used for training, thus 16 rounds are performed to test all cases. We assess the performance using a balanced accuracy with a fixed 85% specificity and area under ROC curve (AUC) *which evaluates the overall performance*. The balanced accuracy ($\bar{P}$), sensitivity (P_+) and specificity (P_-) are defined as

$$\bar{P} = \frac{P_+ + P_-}{2}, \quad P_+ = \frac{TP}{TP + FN}, \quad P_- = \frac{TN}{TN + FP}, \tag{1}$$

where TP and TN denote the number of true positives and negatives, respectively, and FP and FN denote the number of false positives and negatives, respectively.

B. Comparison of ACA classification

In this section, we compare classification methods using HOG features [14] with different cell numbers ($d = 3, 6, 10$) and two clinical features (*i.e.*, AOD [10] and SLBA [13]). From the results shown in Table I, we have the following observations:

1) The HOG feature based methods outperform the clinical feature based ones, which demonstrate high dimensional visual features provide more information for classification and thus lead to higher performance. In addition, the performance drops significantly in some videos because the video contains a lot of intermediate cases which are difficult to classify even for human experts.
2) Among methods based on the HOG features with different parameter d, the highest accuracy (*i.e.*, largest AUC and $\bar{P}$) is obtained when setting $d = 6$, for which the cell size is not too small to lose useful information nor too big to introduce more noises.
3) Comparing HOG feature based methods with and without a multiscale scheme, it shows that the multiscale scheme leads to a higher accuracy, as expected.

In terms of processing speed, each ACA costs about 0.09s for feature extraction and classification with a Matlab implementation, which can be further accelerated with a C++ implementation.

IV. CONCLUSION

To identify glaucoma subtype, an image processing and learning based framework was proposed to localize and classify ACA, based on multiscale HOG features. Our method was tested on a clinical dataset comprised of 2048 images with two evaluation criteria. The results indicate that it outperforms clinical feature based methods. In future work, we plan to extend the classification framework to multiple level angle closure grading, in order to elevate precision and better deal with intermediate cases.

REFERENCES

[1] B. Thylefors, A.D. Negrel, R. Pararajasegaram, and K.Y. Dadzie. Global data on blindness, *Bull WHO*, vol. 73, no. 1, pp. 115–21, 1995.

[2] T.Y. Wong, S. Loon, and S.M. Saw. The epidemiology of age related eye diseases in asia, *British Journal of Ophthalmology*, vol. 90, no. 4, pp. 506–11, 2006.

[3] P.J. Foster and G.J. Johnson. Glaucoma in China: how big is the problem? *British Journal of Ophthalmology*, vol. 85, pp. 1277–82, 2001.

[4] B.E. Klein, R. Klein, W.E. Sponsel, T. Franke, L.B. Cantor, J. Martone, and M.J. Menage. Prevalence of glaucoma. The Beaver Dam Eye Study. *Ophthalmology*, vol. 99, pp. 1499–504, 992.

[5] D.T.L. Quek, M.E. Nongpiur, S.A. Perera, and T. Aung. Angle imaging: Advances and challenges, *Indian Journal of Ophthalmology*, vol. 59, no. 7, pp. 69–75, 2011.

[6] N.G. Congdon, Q. Youlin, H. Quigley, P.T. Hung, T.H. Wang, T.C. Ho, and J.M. Tielsch. Biometry and primary angle-closure glaucoma among Chinese, white, and black populations. *Ophthalmology*, vol. 104, pp. 1489–95, 1997.

[7] N.L. Wang, H.P. Wu, and Z.G. Fan. Primary angle closure glaucoma in Chinese and Western populations, *Chinese Medical Journal*, vol. 115, pp. 1706–15, 2002.

[8] J. Cheng, D. Tao., J. Liu, D.W.K. Wong, B.H. Lee, M. Baskaran, T.Y. Wong, and T. Aung. Focal biologically inspired feature for glaucoma type classification, In *Int. Conf. Medical Image Computing and Computer Assisted Intervention*, 2011, vol. 6893, pp. 91–8.

[9] C.K. Leung, W.H. Yung, C.K. Yiu, S.W. Lam, D.Y. Leung, R.K. Tse, C.C. Tham, W.M. Chan, and D.S. Lam. Novel approach for anterior chamber angle analysis: anterior chamber angle detection with edge measurement and identification algorithm (ACADEMIA), *Arch Ophthalmol*, vol. 124, no. 10, pp. 1395–401, 2006.

[10] J. Tian, P. Marziliano, M. Baskaran, H.T. Wong, and T. Aung. Automatic anterior chamber angle assessment for HD-OCT images, *IEEE Trans. on Bio. Eng.*, vol. 58, no. 11, pp. 3242–9, 2011.

[11] C.K. Leung, C.Y. Cheung, H. Li, S. Dorairaj, C.K. Yiu, A.L. Wong, J. Liebmann, R. Ritch, R.N. Weinreb, and D.S. Lam. Dynamic analysis of darkLight changes of the anterior chamber angle with anterior segment OCT, *Invest. Ophthalmol. Vis. Sci.*, vol. 48, no. 9, pp. 4116–22, 2007.

[12] C.K. Leung, H. Li, R.N. Weinreb, J. Liu, C.Y. Cheung, R.Y. Lai, C.P. Pang, and D.S. Lam. Anterior chamber angle measurement with anterior segment optical coherence tomography: a comparison between slit lamp OCT and visante OCT, *Invest. Ophthalmol. Vis. Sci.*, vol. 49, no. 8, pp. 3469–74, 2008.

[13] J. Tian, P. Marziliano, and H.T. Wong. Automatic detection of Schwalbe's line in the anterior chamber angle of the eye using HD-OCT images, In *Int. Conf. IEEE Engin. in Med. and Biol. Soc.*, 2010, pp. 3013–6.

[14] N. Dalal and B. Triggs. Histograms of oriented gradients for human detection, In *IEEE Conf. Computer Vision and Pattern Recognition*, 2005, vol. 1, pp. 1886–93.

[15] Y. Xu., D. Xu, S. Lin, J. Liu, J. Cheng, C.Y. Cheung, T. Aung, and T.Y. Wong. Sliding window and regression based cup detection in digital fundus images for glaucoma diagnosis, In *Int. Conf. Medical Image Computing and Computer Assisted Intervention*, 2011, vol. 6893, pp. 1–8.

[16] R.E. Fan, K.W. Cheng, C.J. Hsieh, X.R. Wang, and C.J. Lin. LIBLINEAR: A library for large linear classification, *Journal of Machine Learning Research*, vol. 9, pp. 1871–4, 2008.

Assessment of Circumferential Angle-Closure by the Iris–Trabecular Contact Index with Swept-Source Optical Coherence Tomography

Mani Baskaran, DNB,[1,2] Sue-Wei Ho, MBBCh, BAO,[1] Tin A. Tun, MBBS,[1] Alicia C. How, FRCS(Ed),[1] Shamira A. Perera, FRCOphth,[1] David S. Friedman, MD,[3] Tin Aung, FRCS(Ed), PhD[1,2]

Purpose: To evaluate the diagnostic performance of the iris–trabecular contact (ITC) index, a measure of the degree of angle-closure, using swept-source optical coherence tomography (SSOCT, CASIA SS-1000, Tomey Corporation, Nagoya, Japan) in comparison with gonioscopy.

Design: Prospective observational study.

Participants: A total of 108 normal subjects and 32 subjects with angle-closure.

Methods: The SSOCT 3-dimensional angle scans, which obtain radial scans for the entire circumference of the angle, were performed under dark conditions and analyzed using customized software by a single examiner masked to the subjects' clinical details. The ITC index was calculated as a percentage of the angle that was closed on SSOCT images. First-order agreement coefficient (AC1) statistics and area under the receiver operating characteristic curve (AUC) analyses were performed for angle-closure on the basis of the ITC index in comparison with gonioscopy.

Main Outcome Measures: Angle-closure on gonioscopy was defined as nonvisibility of posterior trabecular meshwork for at least 2 quadrants. Agreement of the ITC index with gonioscopically defined angle-closure was assessed using the AC1 statistic.

Results: Study subjects were predominantly Chinese (95.7%) and female (70.7%), with a mean age of 59.2 (standard deviation, 8.9) years. The median ITC index was 15.24% for gonioscopically open-angle eyes (n = 108) and 48.5% for closed-angle eyes (n = 32) ($P = 0.0001$). The agreement for angle-closure based on ITC index cutoffs (>35% and ≥50%) and gonioscopic angle-closure was 0.699 and 0.718, respectively. The AUC for angle-closure detection using the ITC index was 0.83 (95% confidence interval, 0.76–0.89), with an ITC index >35% having a sensitivity of 71.9% and specificity of 84.3%.

Conclusions: The ITC index is a summary measure of the circumferential extent of angle-closure as imaged with SSOCT. The index had moderate agreement and good diagnostic performance for angle-closure with gonioscopy as the reference standard.

Financial Disclosure(s): The author(s) have no proprietary or commercial interest in any materials discussed in this article. *Ophthalmology 2013;120:2226-2231 © 2013 by the American Academy of Ophthalmology.*

Current approaches to anterior chamber angle (ACA) imaging mostly depend on obtaining a single cross-sectional slice view across the anterior segment, which means that the rest of the angle is not visualized or considered in determining angle status.[1–3] Furthermore, quantitative analysis using these images needs interpretation by an expert. Newer approaches using swept-source ocular coherence tomography (SSOCT) allow for imaging of the entire ACA over 360 degrees and provide a summary measure of the extent of angle-closure.[1]

Glaucoma is highly prevalent and increasing because of the aging population.[4] An estimated 37.4 million people will have glaucoma in Asia by the year 2020, of whom approximately 18 million will have primary angle-closure glaucoma (PACG). Better diagnostic and therapeutic approaches for PACG are thus needed to prevent PACG blindness.[4] However, gonioscopy, the current clinical method of angle assessment, lacks objectivity, has limited agreement between observers, and is uncomfortable for the patient. Many ophthalmologists do not routinely perform gonioscopy on patients with glaucoma.[2,5–7] Anterior chamber angle imaging devices could aid angle-closure diagnosis.[8–11] However, the paucity of simple algorithms for angle status assessment that can be easily interpreted by general ophthalmologists presently restricts their use to glaucoma subspecialty clinics.[8]

A new imaging modality that uses SSOCT (CASIA SS-1000, Tomey Corporation, Nagoya, Japan) uses a swept laser source at a wavelength of 1310 nm and a scan speed of 30 000 A-scans/s. The device has a wide scanning range of 16 mm, which allows an entire cross-section of the anterior

ISSN 0161-6420/13/$ - see front matter
http://dx.doi.org/10.1016/j.ophtha.2013.04.020

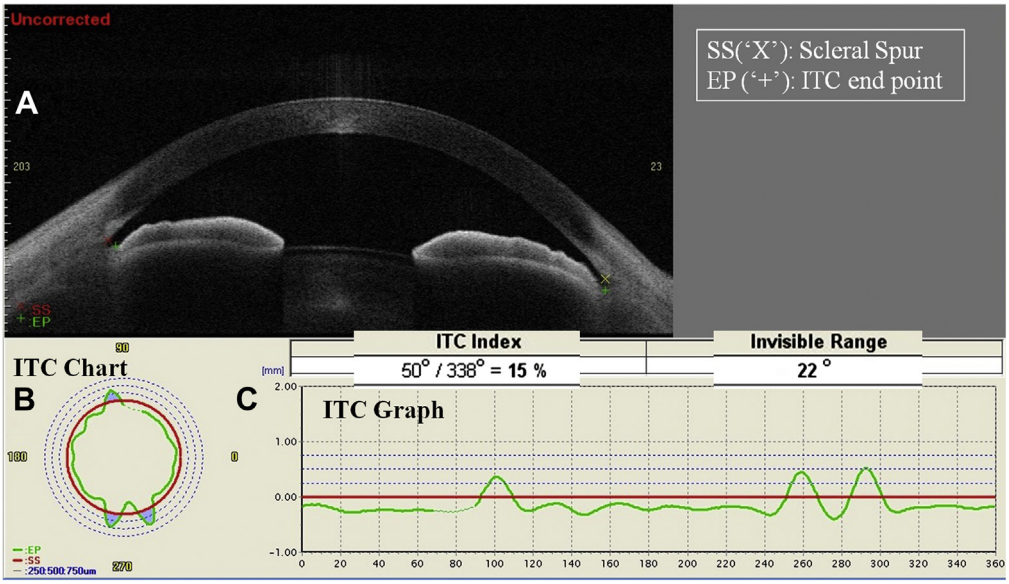

Figure 1. The iris–trabecular contact (ITC) index analysis for an open angle. **A,** Single frame of the cross-section of the anterior chamber. The colored "x" represents the scleral spur (SS) markings, and the "+" represents the ITC end point (EP). Both points are marked by the observer grading the image. **B,** The ITC chart with the blue area represents the amount and distribution of ITC. **C,** The ITC graph with the Y axis represents ITC (in arbitrary units), and the X axis represents the degree of the angle. The green graph above the *red line* (representing SS) denotes the amount of angle-closure (measured as the ITC index).

chamber to be captured simultaneously. The SSOCT's low-density 3-dimensional angle analysis scan simultaneously obtains multiple radial scans of the whole anterior chamber for the entire circumference of the angle.[12] In-built software analysis then analyzes the extent of iris–trabecular contact (ITC) across 360° of the angle and calculates the extent of angle-closure as the ITC index.[13]

The aim of this study was to examine the agreement and diagnostic accuracy of the ITC index measured using SS-OCT compared with the clinical reference standard, gonioscopy.

Methods

This was a prospective observational study conducted in accordance with the tenets of the Declaration of Helsinki and approved by the hospital's institutional review board. Written informed consent was obtained from all participants.

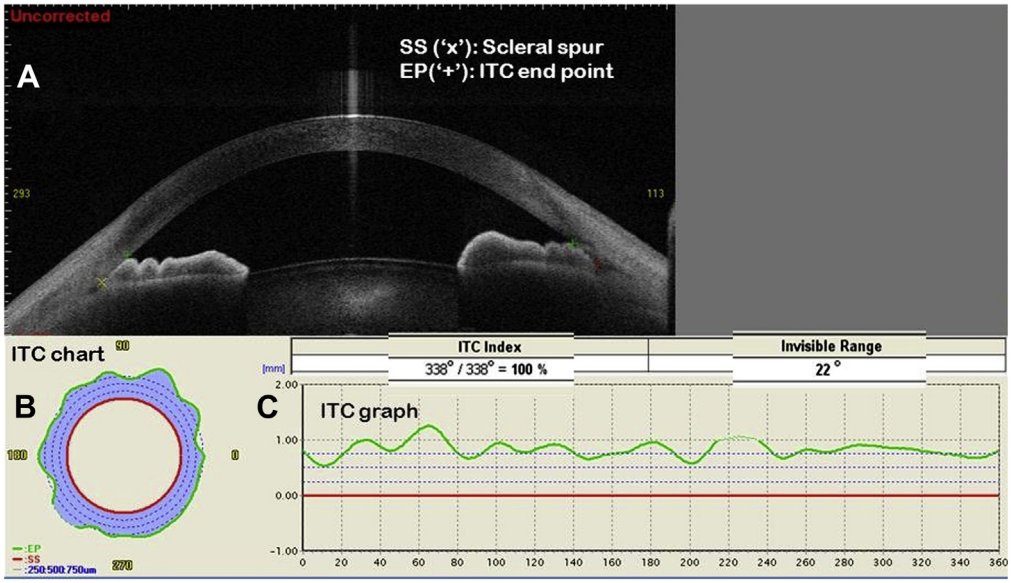

Figure 2. The iris–trabecular contact (ITC) index analysis for a closed-angle. **A,** Single frame of the cross-section of the anterior chamber. The colored "x" represents the scleral spur (SS) markings, and the "+" represents the ITC end point (EP). Both points are marked by the observer grading the image. **B,** The ITC chart with the blue area represents the amount and distribution of ITC. **C,** The ITC graph with the Y axis represents ITC (in arbitrary units), and the X axis represents the degree of the angle. The green graph above the *red line* (representing SS) denotes the amount of angle-closure (measured as the ITC index).

Phakic subjects aged 40 years or older were recruited from glaucoma clinics at an eye hospital between January 2011 and July 2011. Subjects with corneal disease that precluded imaging of the anterior segment and those with previous uveitis, intraocular surgery, or lid abnormalities were excluded. Subjects who had laser peripheral iridotomy were not excluded. Subjects who had laser trabeculoplasty and laser iridoplasty were excluded from the study. Imaging of the anterior segment was performed for 152 consecutive eligible subjects who provided informed consent.

After demographic data were recorded, each subject underwent a standardized examination that included slit-lamp examination, intraocular pressure measurement with Goldman applanation tonometry, indentation gonioscopy, and examination of the optic disc.

Gonioscopy

Indentation gonioscopy was performed in the dark in all cases by a glaucoma fellowship−trained ophthalmologist (M.B.) using a Sussman 4-mirror goniolens (Ocular Instruments Inc, Bellevue, WA). This examiner was masked to imaging results. A 1-mm light beam was reduced to a narrow slit, and the vertical beam was offset horizontally for evaluating nasal and temporal angles and maintained vertically for assessing superior and inferior angles. The examination was performed with the subject's eye in the primary position of gaze. Care was taken to avoid light from falling on the pupil and to avoid inadvertent indentation during examination. In some cases, the gonioscopy lens was tilted slightly to allow a view of the angle over the convexity of the iris, avoiding ocular distortion. The angle in each quadrant was graded per the modified Shaffer grading system, according to the anatomic structures observed during gonioscopy.[14] The ACA was considered "closed" in that quadrant if the posterior pigmented trabecular meshwork could not be seen in the primary position without indentation (Modified Shaffer grade 0 to 2). The eye was classified as having angle-closure if there were 2 or more closed quadrants.

Swept-Source Optical Coherence Tomography Imaging

All subjects underwent SSOCT imaging before any contact procedure, under dark room conditions. The upper eyelid was gently elevated and the lower eyelid was gently pulled down by the operator so that the ACAs could be seen in the scan window, taking care to avoid inadvertent pressure on the globe. Patients were asked to focus on an internal fixation target, and once the patient had been optimally positioned, each eye was scanned with the 3-dimensional angle analysis scan (which takes 2.4 seconds) using the auto alignment function. This algorithm takes 16 consecutive meridional scans, each consisting of 512 A-scans covering a distance of 16 mm across the anterior chamber. The 16 frames are selected by the software, and although manufacturers do not provide the details of the method of selection of frames, we presume that these are selected at equal intervals, that is, at 11.25 degrees apart for the 360 degrees of the angle. (The other options for frame selection were 8, 32, 64, and 128 frames.)

Definitions

Primary angle-closure suspect was defined as an eye with narrow angles (in which the pigmented posterior trabecular meshwork was not visible on gonioscopy for at least 180 degrees in the primary position) and an intraocular pressure of $\leq$21 mmHg in the absence of glaucomatous optic neuropathy or peripheral anterior synechiae. Primary angle-closure glaucoma was defined as eyes with narrow angles associated with glaucomatous optic neuropathy (defined as loss of neuroretinal rim with a vertical cup-to-disc ratio of 0.7 or an inter-eye asymmetry of 0.2, or notching attributable to glaucoma) with corresponding visual field loss.

Analysis of Images

The CASIA built-in software was used to measure the ITC index, which is a semiquantitative measure of the extent of angle-closure expressed as a percentage. The ITC analysis uses cross-sectional meridional images of the anterior segment (which are not corrected for index of refraction) to analyze the extent of contact between the iris and the angle wall.

Figures 1 and 2 represent examples of open and closed angles on SSOCT ITC analysis, respectively. In each anterior segment image frame, the scleral spur (SS) and the ITC end point (EP) were marked manually by a single examiner (S-W.H.) with a red "x" mark and green "+" mark, respectively, for both quadrants in the image (Figs 1A and 2A). The SS was identified as the point at which a change in curvature of corneo-scleral interface occurs. The EP was identified as the most anterior point of iris contact to the angle wall. The program allowed omitting some frames without marking these points when they could not be identified (identified as invisible range). In such cases, attempts were made to replace those images with the nearest scans with visible SS and EP. When all the 16 frames were marked, the "ITC" button on the screen was clicked to enable the ITC index to be calculated. The software uses the information from the plotted SS and EP points in these 16 frames to calculate this index.

The results are reflected in an ITC chart as shown in Figures 1B and 2B. The ITC chart is analogous to a goniogram used in clinical practice. The red circular line represents the SS markings. The dotted circles represent 0.25-, 0.50-, and 0.75-mm landmarks anterior to the SS, along the angle wall. The red line represents the SS, and the green line represents the anterior ITC EP. The blue area represents the extent of angle-closure and if positive, indicates angle-closure (i.e., ITC) and if negative or neutral, represents open-angle areas.

The ITC analysis output also includes 2 parameters: (1) The "ITC index," which represents the ratio of positive ITC (angle-closure) in degrees (blue area in the ITC chart) to the total angle with visible SS and EP in degrees; this essentially represents the extent of angle-closure in percentage. (2) The "invisible range" represents the circumferential extent (in degrees) throughout which the SS or EP could not be determined in the meridional frames. A minimum of 7 points were needed in which SS and EP could be identified to calculate the ITC index (as per the manufacturer), and this criterion was used for quality control and exclusion.

The extent of angle-closure is displayed as a graph in Figures 1C and 2C. A positive ITC (angle-closure) is shown above the red line (the red line represents the SS), and a negative ITC (open angle) is shown below the line.

We previously reported that the intra- and inter-examiner agreement for the ITC index was good (mean difference for Bland−Altman test ranged from −0.8 to 0.6%, and 95% limits of agreement ranged from −11.1 to 10.5%).[15]

Statistical Analysis

One eye from each patient was randomly selected for analysis if both eyes were eligible for the study. Demographic parameters were summarized by mean and standard deviation for continuous variables. Median and range were used where appropriate. McNemar's test was used to compare differences in the distribution of categoric variables between 2 related samples. First-order agreement coefficient (AC1) statistics were used to assess the agreement between categoric variables.[16,17] Receiver operating characteristic curves, with calculations of area under the curve (AUC) and 95% confidence intervals (CIs), were used to assess the

performance of the ITC index for identifying eyes with angle-closure, using gonioscopy as the reference standard. The sensitivity, specificity, positive predictive value, negative predictive value, positive likelihood ratio (+LR), and negative likelihood ratio (−LR) for the best ITC cutoff values (>35%, ≥50%, and >70%) were reported for various quadrant closure definitions. We have chosen the optimal ITC index cutoff on the basis of the best sensitivity and specificity values given by the statistical software (>35%) and mean value (≥50%), and providing an arbitrary stricter criterion for angle-closure (>70%). Further, sensitivity values and associated criteria for fixed specificities were calculated for the ITC index against 2-quadrant closure definition on gonioscopy. A P value <0.05 was considered statistically significant for all comparisons. Statistical analyses were performed using MedCalc version for Windows v12.0 (Mariakerke, Belgium).

Results

Of the 152 subjects recruited for the study, the image from 1 subject was not analyzable because of poor scan quality, and 11 others had more than 180° "invisible range" (unable to identify SS); thus, we excluded these eyes from analysis, leaving 140 eyes (92.1%) eligible for final analysis. There was no significant difference in the proportion of open versus closed angles on gonioscopy among the excluded eyes (6 each). The mean age of the 140 included subjects was 59.2 (standard deviation, 8.9) years, and the majority of subjects were Chinese (134/140, 95.7%) and female (99/140, 70.7%). There were 32 subjects (22.9%) who had gonioscopic angle-closure, of whom 29 were primary angle-closure suspects and 3 had primary angle-closure glaucoma.

Closed-angle subjects were older than open-angle subjects (63.7 vs. 57.8 years, $P < 0.05$), had higher ITC index (50.0 vs. 17.2, $P = 0.0001$), and had higher "invisible range" ($P < 0.05$, Table 1). Figure 3A and B (available at http://aaojournal.org) show the distribution of the ITC index, suggesting a positively skewed distribution for open angles. The number of quadrants closed on gonioscopy was positively correlated with the ITC index (Spearman's $\rho = 0.578$, $P = 0.0001$).

Table 2 (available at http://aaojournal.org) shows the comparative distribution of open and closed angles between gonioscopy (quadrant-wise) and various ITC cutoffs. Even when using an ITC cutoff of ≥50%, 6.4% (9/140) of eyes showed closed angles with SSOCT, whereas the gonioscopist noted zero or 1-quadrant closure. The trend for increasing number of closed angles on SSOCT was noted for all cutoff values as the number of closed quadrants increased on gonioscopy (chi-square for trend; $P < 0.0001$). Table 3 (available at http://aaojournal.org) shows the agreement for 2 ITC index cutoff values (>35% and ≥50%) with different quadrant-wise definitions of angle-closure. The agreement for the ITC index (>35% and ≥50%) and 4 quadrants of closed angles on gonioscopy was moderate to good for the 2 cutoff values (0.689 for ITC >35% and 0.842 for ITC ≥50%). We considered that the AC1 statistic to Kappa statistic as the prevalence rate for positive classification (in this instance, closed angles) was low. The AC1 statistic for a 2-quadrant definition of angle-closure for >35% and ≥50% was found to be moderate at 0.699 and 0.718, respectively. Good agreement (AC1 = 0.842) was seen for a higher cutoff value of ≥50%, because the severity of gonioscopic angle-closure increased to 4-quadrant closure. There was slight overestimation of closed angles (32/140 vs. 40/140, $P = 0.17$, McNemar test) for ITC >35% and underestimation (32/140 vs. 23/140, $P = 0.12$) for ITC ≥50%, for 2-quadrant closure on gonioscopy. The classification of open versus closed angles between gonioscopy and ITC index cutoffs was found to be statistically similar across various definitions except for 1-quadrant closure definition with ≥50% cutoff value, (42/140 vs. 18/140, $P = 0.0008$, McNemar test) and for 4-quadrant closure definition with >35% cutoff value (13/140 vs. 40/140, $P < 0.0001$, McNemar test, Table 2, available at http://aaojournal.org).

Table 1. Comparison of Clinical and Imaging Characteristics of Gonioscopically Open- and Closed-Angle Subjects (2-Quadrant Definition of Angle-Closure)

	Open-Angle (n = 108)	Closed-Angle (n = 32)
Age (yrs)*	57.8 (8.8)	63.7 (8.0)
Eye (right:left)	68:40	19:13
Gender (male:female)	33:75	8:24
Ethnicity† (Chinese:Malay: Indian:others)	106:0:2:0	28:2:1:1
ITC index (percentage)*		
Mean (SD)	17.2 (19.3)	50.0 (28.9)
Median (min−max)	15.2 (0−74)	48.5 (0−100)
Invisible range* (degrees)		
Mean (SD)	34.6 (48.0)	54.7 (47.4)
Median (min−max)	0 (0−170)	44 (0−170)
Median no. of quadrants closed on gonioscopy	0 (0−1)	3 (2−4)

ITC = iris−trabecular contact; max = maximum; min = minimum; SD = standard deviation.
*$P < 0.0001$.
†$P < 0.05$.

Table 4 shows the diagnostic performance of the various ITC index values in the form of AUC, sensitivity, specificity, and predictive values. Figure 4 shows the receiver operating characteristic curve for the performance of ITC index. The diagnostic accuracy was good between 0.83 and 0.91 for various definitions of angle-closure, suggesting uniform performance. The AUC using the 2 quadrants closed on gonioscopy definition of angle-closure was 0.83 (95% CI, 0.76−0.89). The ITC index of >35% was found to be optimal for the best classification for angle-closure across various gonioscopic angle-closure definitions with a sensitivity of 71.9% (95% CI, 53.3−86.3) and a specificity of 84.3% (95% CI, 76−90.6) for 2-quadrant angle-closure. The predictive values and LRs are provided in Table 4 for the various definitions. For a 2-quadrant closure definition on gonioscopy, if the ITC index cutoff of >35% was chosen, the negative predictive value was 91% with a moderate +LR of 4.57. If specificity is fixed at 90%, then the sensitivity decreased to 52.5% (95% CI, 37.4−68.5) (Table 5, available at http://aaojournal.org).

Discussion

This study uniquely compares 2 types of circumferential angle assessment. The ITC index produced by the SSOCT device had moderate to good agreement with gonioscopic angle-closure findings and good overall diagnostic performance for detecting angle-closure.

Liu et al[12] recently evaluated angle parameters measured by SSOCT and found that there was good inter- and intraobserver reproducibility for angle measurements, such as the angle opening distance, trabecular−iris space area, and trabecular−iris angle. The intraclass correlation coefficients were ≥0.83 for all measurements. They noted that variability in the location of measurements, the axial length, the iris thickness, and the angle width are factors that may affect the reproducibility of angle measurements. However, the ITC

Table 4. Diagnostic Performance Indicators for Different Cutoff Values of Iris–Trabecular Contact Index with Gonioscopic Angle-Closure Definitions

Gonioscopic Angle-Closure	AUC	ITC Index Cutoff Criteria	Sensitivity (95% CI)	Specificity (95% CI)	PPV (95% CI)	NPV (95% CI)	+LR (95% CI)	−LR (95% CI)
≥1 quadrants closed	0.855 (0.786–0.909)	**>35%**	**69.05 (52.9–82.4)**	**88.78 (80.8–94.3)**	**72.5 (55.9–85.5)**	**87 (78.8–92.9)**	**6.15 (3.4–11.1)**	**0.35 (0.2–0.6)**
		≥50%	42.86 (27.7–59)	94.9 (88.5–98.3)	78.3 (55.7–92.8)	79.5 (71–86.4)	8.40 (3.3–21.1)	0.6 (0.5–0.8)
		>70%	21.43 (10.3–36.8)	98.98 (94.4–100)	90 (55.5–99.7)	74.6 (66.2–81.8)	21 (2.7–160.6)	0.79 (0.7–0.9)
≥2 quadrants closed	0.829 (0.756–0.887)	**>35%**	**71.87 (53.3–86.3)**	**84.26 (76–90.6)**	**57.5 (40.9–73%)**	**91 (83.6–95.8)**	**4.57 (2.8–7.4)**	**0.33 (0.2–0.6)**
		≥50%	43.75 (26.4–62.3)	91.67 (84.8–96.1)	60.9 (38.5–80.3)	84.6 (76.7–90.6)	5.25 (2.5–11)	0.61 (0.4–0.8)
		>70%	25 (11.5–43.4)	98.15 (93.5–99.8)	80 (42.2–97.9)	81.5 (73.8–87.8)	13.5 (3–60.4)	0.76 (0.6–0.9)
≥3 quadrants closed	0.828 (0.755–0.886)	**>35%**	**70.97 (52–85.8)**	**83.49 (75.2–89.9)**	**55 (38.5–70.7)**	**91 (83.6–95.8)**	**4.48 (2.8–7.2)**	**0.32 (0.2–0.6)**
		≥50%	45.16 (27.3–64)	91.74 (84.9–96.2)	60.9 (38–80.7)	85.5 (77.8–91.3)	5.7 (2.7–11.9)	0.58 (0.4–0.8)
		>70%	25.81 (11.9–44.6)	98.17 (93.5–99.8)	80 (44.4–97.5)	82.3 (74.6–88.4)	14.67 (3.3–65.5)	0.75 (0.6–0.9)
4 quadrants closed	0.907 (0.846–0.949)	**>35%**	**92.31 (64–99.8)**	**77.95 (69.7–84.8)**	**30 (16.6–46.5)**	**99 (94.5–100)**	**4.19 (2.9–6)**	**0.099 (0.01–0.7)**
		≥50%	76.92 (46.2–95)	89.76 (83.1–94.4)	43.5 (23.2–65.5)	97.4 (92.7–99.5)	7.51 (4.1–13.6)	0.26 (0.1–0.7)
		>70%	46.15 (19.2–74.9)	96.85 (92.1–99.1)	60 (26.2–87.8)	94.6 (89.2–97.8)	14.65 (4.7–45.3)	0.56 (0.3–0.9)

CI = confidence interval; +LR = positive likelihood ratio; −LR = negative likelihood ratio; NPV = negative predictive value; PPV = positive predictive value. The AUC was based on Delong et al.[18]
Letters in boldface represent indicators for optimal cut-off value (i.e., >35%).

index may be less affected by the subtle changes in these variables because it gives an overall summary measure of angle-closure. Moreover, this index may be easily interpretable by clinicians compared with the other angle parameters because it is more similar to the method used in gonioscopy.

We previously reported good intra- and interexaminer repeatability of the ITC index analyzed from the same or different image acquisitions.[15] We found that the ITC index can grossly simulate gonioscopic interpretation in some ways, such as circumferential interpretation of angle status, easier interpretation of the extent of angle-closure, and a pictorial depiction of angle-closure, similar to a goniogram. However, because the ITC index is a compilation of multiple noncontact cross-sectional images, it cannot identify synechial angle-closure compared with indentation gonioscopy. Gonioscopy and the SSOCT device use slightly different landmarks to define angle-closure. The ITC index is based on "any" ITC anterior to the SS, whereas gonioscopic angle-closure requires that the pigmented posterior trabecular meshwork not be visible. The mean ITC index for 2-quadrant closure on gonioscopy in our study was 50%, and the best cutoff value for diagnostic performance was >35%, with only 4 subjects (2.8%) having an ITC index of 100%. Furthermore, 12% of eyes (17/140, Table 2, available at http://aaojournal.org) were found to be closed for >35% on SSOCT compared with 1 quadrant or less on gonioscopy. This higher rate of angle-closure with the ITC index suggests that gonioscopy may miss angle-closure in some patients, and this could be due to inadvertent opening of the angles by compression from the gonioscopy lens or pupil constriction from slit-lamp illumination during gonioscopy. The cutoff values mentioned in this study might likely vary if more frames (>16) were added to the analysis. However, we thought that more frames may be difficult to analyze or not feasible in a clinical setting. In this context, it may be useful to have automated solutions for the entire analysis, where there would be no dependency on landmarks.

Study Limitations

The SS could not be identified in some frames, resulting in the "invisible range" to ≥50% in 8.3% eyes. However, the proportion of gonioscopically open and closed angles was similar in the excluded eyes, and so this would not have unduly affected the overall diagnostic performance of the ITC index. We carefully removed such images with excess invisible range and included the manufacturers' recommended minimum of 7 frames in the analysis. Capturing images proved ergonomically cumbersome at times

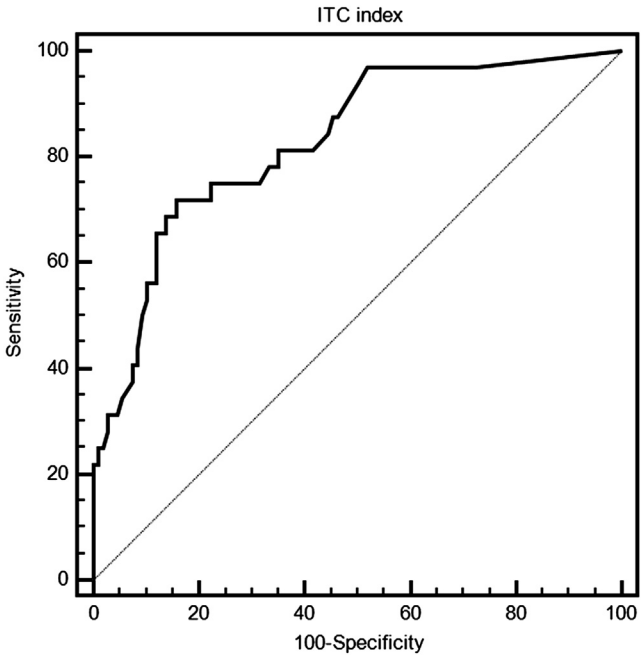

Figure 4. Receiver operating characteristic for the iris–trabecular contact (ITC) index against the gonioscopic reference standard.

because of movement of the globe or eyelids during image capture. Another discrepancy lies in the way that gonioscopy and SSOCT assess the amount of angle-closure. Whereas the gonioscopist grades the extent of angle-closure by quadrant, the ITC index measures in degrees of closure over the entire circumference of the angle. Overall, although the diagnostic performance for the ITC index was found to be good across various definitions of angle-closure, the predictive values and +LR and −LR seem to be moderate and variable.

In conclusion, we describe for the first time moderate agreement and good diagnostic performance of a novel parameter, the ITC index, assessed using SSOCT, for the interpretation of the extent of angle-closure in comparison with gonioscopy as the reference standard. With further improvement and automation of the ITC index measurement, SSOCT may be a novel and improved way to clinically document the extent of angle-closure over the entire 360 degrees.

References

1. Wylegała E, Teper S, Nowińska AK, et al. Anterior segment imaging: Fourier-domain optical coherence tomography versus time-domain optical coherence tomography. J Cataract Refract Surg 2009;35:1410–4.
2. Sakata LM, Lavanya R, Friedman DS, et al. Comparison of gonioscopy and anterior segment ocular coherence tomography in detecting angle closure in different quadrants of the anterior chamber angle. Ophthalmology 2008;115:769–74.
3. Friedman DS, He M. Anterior chamber angle assessment techniques. Surv Ophthalmol 2008;53:250–73.
4. Quigley HA, Broman AT. The number of people with glaucoma worldwide in 2010 and 2020. Br J Ophthalmol 2006;90:262–7.
5. Foster PJ, Baasanhu J, Alsbirk PH, et al. Glaucoma in Mongolia. A population-based survey in Hovsgol province, northern Mongolia. Arch Ophthalmol 1996;114:1235–41.
6. Schirmer KE. Gonioscopy and artefacts. Br J Ophthalmol 1967;51:50–3.
7. Hoskins HD Jr. Interpretive gonioscopy in glaucoma. Invest Ophthalmol 1972;11:97–102.
8. Quek DT, Nongpiur ME, Perera SA, Aung T. Angle imaging: advances and challenges. Indian J Ophthalmol 2011;59(Suppl):S69–75.
9. See JL. Imaging of the anterior segment in glaucoma. Clin Experiment Ophthalmol 2009;37:506–13.
10. Nolan W. Anterior segment imaging: ultrasound biomicroscopy and anterior segment optical coherence tomography. Curr Opin Ophthalmol 2008;19:115–21.
11. Radhakrishnan S, Huang D, Smith SD. Optical coherence tomography imaging of the anterior chamber angle. Ophthalmol Clin North Am 2005;18:375–81. vi.
12. Liu S, Yu M, Ye C, et al. Anterior chamber angle imaging with swept-source optical coherence tomography: an investigation on variability of angle measurement. Invest Ophthalmol Vis Sci 2011;52:8598–603.
13. Fukuda R, Usui T, Tomidokoro A, et al. Noninvasive observations of peripheral angle in eyes after penetrating keratoplasty using anterior segment Fourier-domain optical coherence tomography. Cornea 2012;31:259–63.
14. Gonioscopy. In: South East Asia Glaucoma Interest Group. Asia Pacific Glaucoma Guidelines. 2nd ed. Hong Kong: Scientific Communications International; 2008:79. Available at: http://www.apglaucomasociety.org/toc/APGG2_fullversionNMview.pdf. Accessed April 7, 2013.
15. Ho SW, Baskaran M, Zheng C, et al. Swept source optical coherence tomography measurement of the iris-trabecular contact (ITC) index: a new parameter for angle closure. Graefes Arch Clin Exp Ophthalmol 2013;251:1205–11.
16. Gwet K. The AC1 Coefficients. In: Gwet K, ed. Handbook of Inter-Rater Reliability: The Definitive Guide to Measuring the Extent of Agreement Among Raters. Gaithersburg, MD: Stataxis Publishing Company; 2003:309.
17. Chan YH. Biostatistics 104: correlational analysis. Singapore Med J 2003;44:614–9.
18. DeLong ER, DeLong DM, Clarke-Pearson DL. Comparing the areas under two or more correlated receiver operating characteristic curves: a nonparametric approach. Biometrics 1998;44:837–45.

Footnotes and Financial Disclosures

Originally received: December 14, 2012.
Final revision: April 21, 2013.
Accepted: April 22, 2013.
Available online: June 17, 2013. Manuscript no. 2012-1860.

[1] Singapore National Eye Centre, Singapore and Singapore Eye Research Institute, Singapore.

[2] Yong Loo Lin School of Medicine, National University of Singapore, Singapore.

[3] Wilmer Eye Institute, Dana Center for Preventive Ophthalmology and Johns Hopkins Bloomberg School of Public Health, Baltimore, Maryland.

Financial Disclosure(s):
The author(s) have no proprietary or commercial interest in any materials discussed in this article.

Supported by a Translational Clinical Research Program grant, Biomedical Research Council, Singapore.

Correspondence:
Tin Aung, FRCS(Ed), PhD, Singapore National Eye Centre, 11 Third Hospital Avenue, Singapore 168751. E-mail: aung.tin@snec.com.sg.

35th Annual International Conference of the IEEE EMBS
Osaka, Japan, 3 - 7 July, 2013

Automated Anterior Chamber Angle Localization and Glaucoma Type Classification in OCT Images*

Yanwu Xu, Jiang Liu, Jun Cheng, Beng Hai Lee, Damon Wing Kee Wong,
Baskaran Mani, Shamira Perera and Tin Aung

***Abstract*— To identify glaucoma type with OCT (optical coherence tomography) images, we present an image processing and machine learning based framework to localize and classify anterior chamber angle (ACA) accurately and efficiently. In digital OCT photographs, our method automatically localizes the ACA region, which is the primary structural image cue for clinically identifying glaucoma type. Next, visual features are extracted from this region to classify the angle as open angle (OA) or angle-closure (AC). This proposed method has three major contributions that differ from existing methods. First, the ACA localization from OCT images is fully automated and efficient for different ACA configurations. Second, it can directly classify ACA as OA/AC based on only visual features, which is different from previous work for ACA measurement that relies on clinical features. Third, it demonstrates that higher dimensional visual features outperform low dimensional clinical features in terms of angle closure classification accuracy. From tests on a clinical dataset comprising of 2048 images, the proposed method only requires 0.26s per image. The framework achieves a 0.921 ± 0.036 AUC (area under curve) value and $84.0\% \pm 5.7\%$ balanced accuracy at a 85% specificity, which outperforms existing methods based on clinical features.**

I. Introduction

Glaucoma is a group of heterogeneous optic neuropathies characterized by the progressive loss of axons in the optic nerve. Data from the World Health Organization shows that glaucoma accounts for 5.1 million cases of blindness in the world and is the second leading cause of blindness worldwide (behind cataracts) as well as the foremost cause of irreversible blindness [1]. As illustrated in Fig. 1, *glaucoma is classified according to the configuration of the angle* (the part of the eye between the cornea and iris mainly responsible for drainage of aqueous humor) into open angle (OA) and angle-closure (AC) glaucoma.

Primary angle closure glaucoma (PACG) is a major form of glaucoma in Asia [2] compared to primary open angle glaucoma (POAG), which is more common in Caucasians and Africans [3]. PACG is already responsible for the majority of bilateral glaucoma blindness in Asia, which will affect 20 million people. Previously reported anatomical risk factors for angle closure include a shallow central anterior chamber depth (ACD), a thick and anterior lens position and short axial length (AL) [4]. Amongst these, a shallow ACD is regarded as a sine qua non (cardinal risk factor) for the disease. However, population based data suggest that only a small proportion of subjects with shallow ACD ultimately develop PACG [5]. Therefore, it is likely that other ocular factors relate to PACG development and need to be discovered.

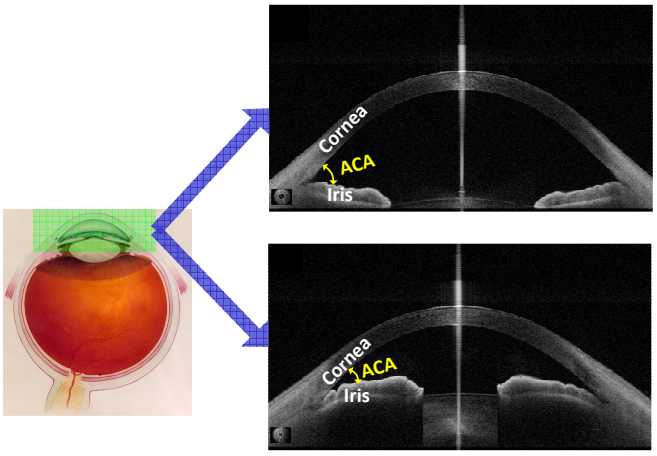

Fig. 1. Open angle (OA, top) and angle-closure (AC, bottom).

In previous work, automated glaucoma type classification has been studied in different image modalities. A BIF feature based learning method was proposed for color RetCam images [6]. An edge detection and line fitting approach was proposed for ACA measurement [7] in ultrasound biomicroscopy (UBM) images. Similarly, a segmentation, edge detection and linear regression based approach was proposed for ACA assessment in OCT images [8].

In this work, we study ACA localization and classification for glaucoma type identification in OCT (optical coherence tomography) images, which has the advantages of being non-invasive and non-contact [9] compared to UBM. An OCT image captures a cross-section of the eye as a grayscale image, and several features (as illustrated in Fig. 2) are extracted based on ACA measurement such as AOD (angle-opening distance) [7], [8], TIA (trabecular-iris angle) [10], TISA (trabecular–iris space area) [8], [10] and SLBA (Schwalbe's line bounded area) [11]. In practice, these clinical features are used for angle closure assessment, *i.e.*, ACA classification.

ACA detection in OCT images can be relatively straight-

*This work was supported in part by the Agency for Science, Technology and Research, Singapore, under BMRC grant 10/1/35/19/674.

Y. Xu, J. Liu, J. Cheng, B. H. Lee and D.W.K. Wong are with the Institute for Infocomm Research, Agency for Science, Technology and Research, 138632, Singapore {yaxu, jliu, jcheng, benghai, wkwong} at i2r.a-star.edu.sg

M. Baskaran, S.A. Perera and T. Aung are with the Singapore Eye Research Institute, 168751, Singapore baskaran.mani at seri.com.sg, shamira.perera at snec.com.sg, aung.tin at snec.com.sg

T. Aung is also with the Department of Ophthalmology, National University of Singapore, 119074, Singapore

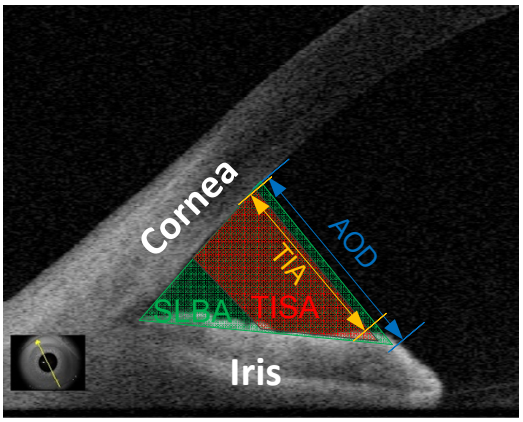

Fig. 2. Features used for ACA measurement clinically. Please refer to the color print for better viewing.

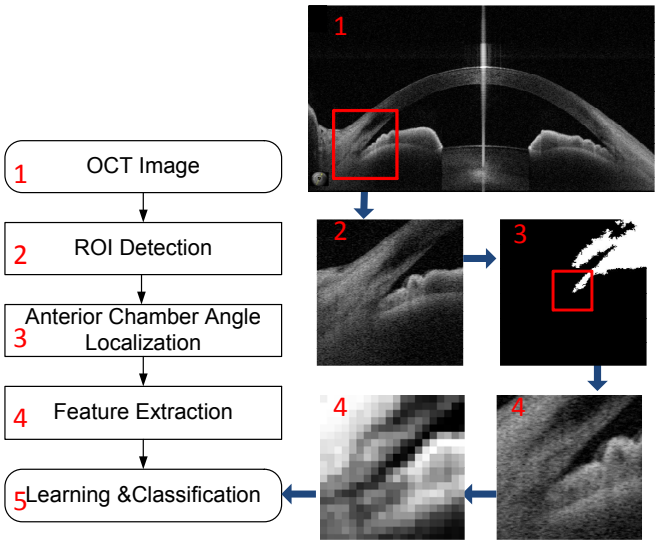

Fig. 3. Flowchart of the proposed ACA localization and classification.

forward since the images are generally clean and are approximately aligned during image acquisition process. However, ACA classification is a challenging task since there are intermediate cases that are difficult to classify as AC or OA using the same clinical features, even for human experts. From our image classification experience, the use of only one or two dimensional clinical features is insufficient to achieve good performance, since the eigen dimension of this problem might be much higher, *as observed clinically* [5].

In this paper, we propose an image processing and learning based framework for efficient ACA localization and classification. With the proposed framework, other existing visual features and learning algorithms can be introduced to improve performance in the future.

II. Angle Closure Classification

To classify an ACA as open or closed, a natural solution is to follow the method of a human expert. Generally, as shown in Fig. 3, for a given OCT image, the ACA region needs to be localized accurately at first, and then certain features and criteria are used to identify whether it is closed.

A. ACA localization

In previous work, the ACA regions are marked manually [10] or are automatic determined by using edge detection [7]. For efficiency, we adopt a coarse-to-fine scheme to localize the ACA from input OCT image, which first segments a candidate ACA region and then localizes its vertex for alignment. The steps are shown in Fig. 3. First, a 400×400 region of interest (ROI) covering the exact ACA is cropped out at a fixed position from the 834×900 input image; second, the ROI is quantized to a binary image (0 for black and 1 for white) using a small valued threshold in order to preserve more details of the angle (a large/adaptive threshold will lose more details at the extreme end of the ACA, which is very important for classification); third, a morphological operation is performed to remove isolated noise points; fourth, weighting and connected component labeling segmentation (CCLS) [8] algorithm are used to segment the ACA candidate in the ROI; fifth, a post processing step is applied to remove other components connected to the exact ACA in the candidate region; lastly, the ACA is localized with an $n \times n$ bounding box centered at its detected vertex. For further details, readers are referred to our recent work [12].

B. ACA feature representation and classification

Each ACA region is represented by a $n \times n$ image, which can be grayscale, binary and/or edges of the ACA. Many existing features from computer vision can be used for classification, such as HOG [13] and BIF [6] which are related to edges and textures, respectively.

In this work, we use the histogram equalized pixel (HEP) values as a feature that is effective and computationally efficient. This is motivated by the intensity of a pixel being a natural feature [14] to classify whether it is on a closed angle. However, using all the pixels in the $n \times n$ region will generate features that are too high dimensional and may also introduce too much noise. Therefore, we downsample the image to reduce the feature dimension. The additional quantization with fewer bins before downsampling enhances the contrast between pixels and provides more distinguishable features.

As illustrated in Fig. 4, the $n \times n$ grayscale image of ACA is first enhanced by quantizing to 8 bins, and then downsampling to $d \times d (d < n)$, so that the vectored image $\mathbf{f}$ is the HEP feature. For efficiency, the simple linear SVM classifier is employed, with a weight vector ω trained to estimate the class label y (+1 for AC and -1 for OA) of a given feature vector $\mathbf{f}$, according to $y = \omega^T \mathbf{f}$. In the experiments, we use the LIBLINEAR toolbox [15] to train the SVM models.

III. Experiments

A. Experimental setup

Our approach is implemented with Matlab and tested on a four-core 3.4GHz PC with 12GB RAM. A total of 2048

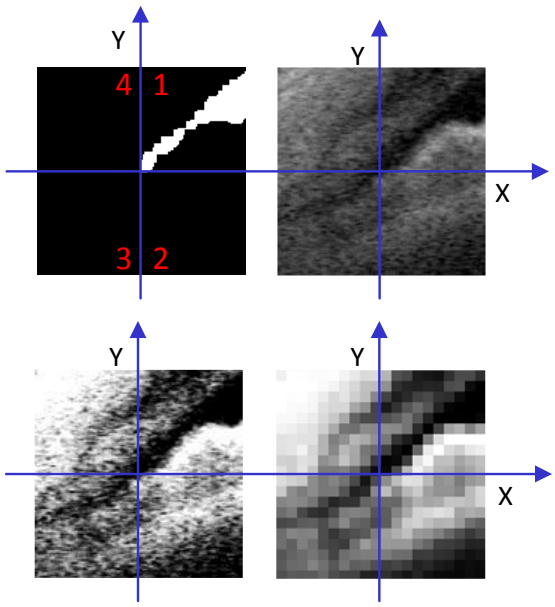

Fig. 4. ACA feature representations (left top to right bottom): binary, grayscale, histogram equalized and HEP.

images are used for the experiments. The images are from 8 circular scan videos of 8 patient eyes with glaucoma, 4 of them with PACG and other 4 with POAG. Each video contains 128 frames, and each frame is split into 2 images since it contains two angles and the right angle image is flipped horizontally.

The experiments are based on each single image, which is labeled as AC or OA by three ophthalmologists from a hospital. For the classification evaluation, we follow the widely used leave-one-out (LOO) method, *i.e.*, for each testing round, 512 images from one PACG and one POAG patients are used for testing while others are used for training, thus 16 rounds are performed to test all cases.

We assess the performance using a balanced accuracy with a fixed 85% specificity and area under ROC curve (AUC) *which evaluates the overall performance*. The balanced accuracy ($\bar{P}$), sensitivity (P_+) and specificity (P_-) are defined as

$$\begin{aligned} \bar{P} &= \frac{P_+ + P_-}{2}, \\ P_+ &= \frac{TP}{TP+FN}, \\ P_- &= \frac{TN}{TN+FP}, \end{aligned} \tag{1}$$

where TP and TN denote the number of true positives and negatives, respectively, and FP and FN denote the number of false positives and negatives, respectively.

B. Comparison of ACA classification

In this section, we compare classification methods with several visual features (*i.e.*, BIF [6], HOG [13] and HEP) with different ACA region sizes ($n = 100, 150, 200$) and two clinical features (*i.e.*, AOD [8] and SLBA [11]). For the HEP feature extraction, d is set to 20 for efficiency reasons.

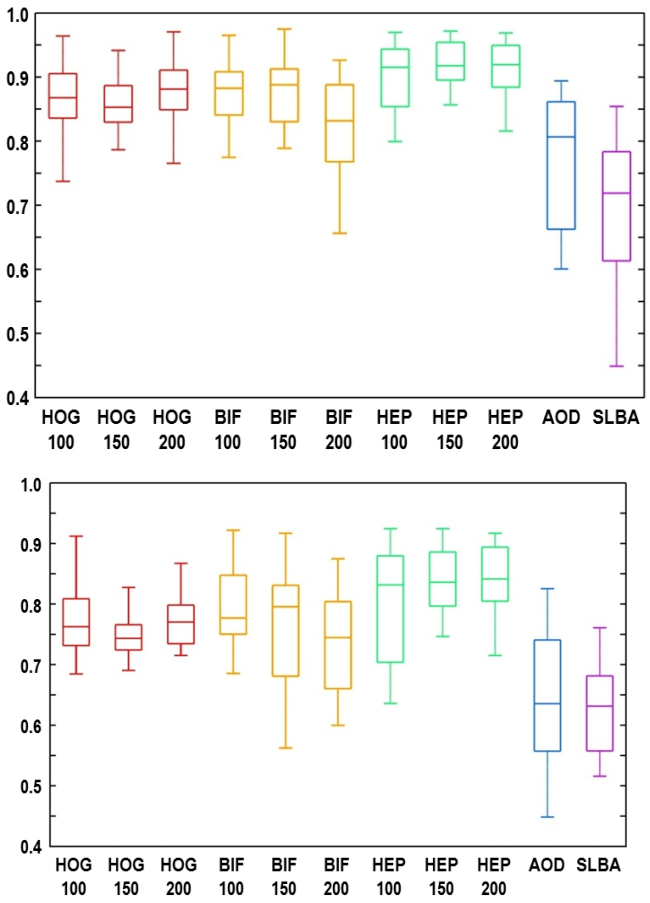

Fig. 5. Performance comparison in terms of AUC (top) and balanced accuracy (bottom).

For HOG and BIF feature extraction, the ACA is divided into 5×5 cells; 2×2 cells form a block for HOG, and 22 feature maps are used for BIF. From the results shown in Fig. 5 and Table I, we have the following observations:

1) The visual feature based methods outperform the clinical feature based ones, demonstrating that high dimensional visual features provide more information for classification and thus leading to higher performance. In addition, the performance drops significantly in some videos that contains a lot of intermediate cases which are difficult to classify even for human experts.
2) Among visual feature based methods, the simplest HEP features outperform HOG and BIF features. A possible explanation is that HOG features introduces noise and BIF is not very suitable for grayscale images.
3) Comparing methods based on the HEP feature with different ACA size n, the results are relatively stable, and the largest AUC is obtained when setting $n = 150$, which was found to be not too small to lose useful information nor too big to introduce too much noises.

We also observed that histogram equalization can lead to about 2–3% relative improvement of AUC compared to downsampling only. In terms of processing speed, each

TABLE I

PERFORMANCE COMPARISONS OF ACA CLASSIFICATION WITH DIFFERENT FEATURES

Feature	HOG			BIF			HEP			AOD	SLBA
n	100	150	200	100	150	200	100	150	200	–	–
AUC	0.865 $\pm$0.058	0.847 $\pm$0.063	0.882 $\pm$0.054	0.877 $\pm$0.054	0.872 $\pm$0.078	0.821 $\pm$0.080	0.899 $\pm$0.059	**0.921 $\pm$0.036**	0.914 $\pm$0.045	0.745 $\pm$0.166	0.697 $\pm$0.108
$\bar{P}(\%)$	76.2 $\pm$7.6	76.0 $\pm$5.6	78.5 $\pm$6.6	79.3 $\pm$7.1	76.8 $\pm$11.0	73.6 $\pm$8.5	80.2 $\pm$9.9	84.0 $\pm$5.7	**84.2 $\pm$6.0**	63.9 $\pm$11.7	62.1 $\pm$7.5

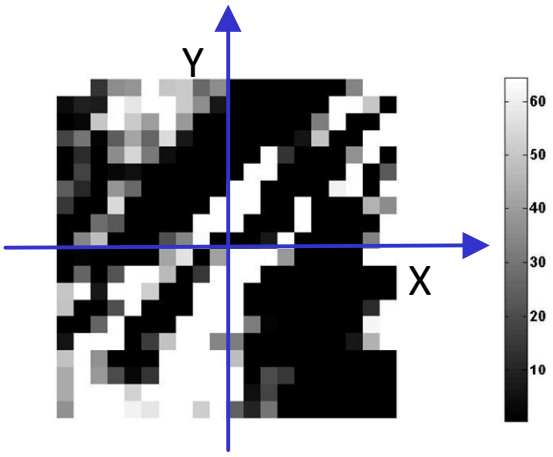

Fig. 6. The learned average weight matrix.

ACA represented by a 400-dimension feature costs about 0.06s for feature extraction and classification with a Matlab implementation, which can be further accelerated with a C++ implementation.

In addition, we found a way to further reduce the feature dimension without significant reduction of accuracy. As shown in Fig. 4, with the proposed ACA localization, each ACA is aligned with its vertex at the center, and then the exact ACA should fall into quadrant 1; however, some ACAs are misaligned since the exact vertex of an ACA is very hard to distinguish when that region is blurred. In this case, the extreme ends of some ACA corners fall into quadrant 3, especially for closed ones. Thus we suppose that quadrant 1 and 3 may provide sufficient information for classification, which is supported by experiments. The average weight vectors $\bar{\omega}$ we obtained in the testing are illustrated in Fig. 6; for each dimension (shown as a block), a higher weight corresponds to a lighter color. One can observe that most of the dimensions with highest weights (in white) are in quadrant 1 and 3, as expected. Thus the performance of using all of the $d \times d$ pixels was compared with only using pixels in quadrants 1 and 3, the AUC reduction is less than 0.3% with a half dimension reduction.

IV. CONCLUSION

For glaucoma type identification, an image processing and machine learning based framework was proposed to localize and classify ACA accurately and efficiently, based on visual features only. We tested our method on a clinical dataset comprised of 2048 images with two evaluation criteria. The results show that it outperforms clinical feature based methods, achieving a 0.921 ± 0.036 AUC value and $84.0\% \pm 5.7\%$ balanced accuracy ($\bar{P}$) at a 85% specificity (P_{-}), while only requiring 0.26s per image. In future work, we plan to extend the classification framework to multiple level angle closure grading, in order to improve precision and better deal with intermediate cases.

REFERENCES

[1] B. Thylefors, A.D. Negrel, R. Pararajasegaram, and K.Y. Dadzie, "Global data on blindness," *Bull WHO*, vol. 73, no. 1, pp. 115–21, 1995.

[2] P.J. Foster and G.J. Johnson, "Glaucoma in china: how big is the problem?," *Br J Ophthalmol*, vol. 85, pp. 1277–82, 2001.

[3] B.E. Klein, R. Klein, W.E. Sponsel, T. Franke, L.B. Cantor, J. Martone, and Menage M.J., "Prevalence of glaucoma. the beaver dam eye study," *Ophthalmology*, vol. 99, pp. 1499–504, 1992.

[4] N.G. Congdon, Q. Youlin, H. Quigley, T.H. Hung, P.T.and Wang, T.C. Ho, and J.M. Tielsch, "Biometry and primary angle-closure glaucoma among chinese, white, and black populations," *Ophthalmology*, vol. 104, pp. 1489–95, 1997.

[5] N.L. Wang, H.P. Wu, and Z.G. Fan, "Primary angle closure glaucoma in chinese and western populations," *Chinese Medical Journal*, vol. 115, pp. 1706–15, 2002.

[6] J. Cheng, D. Tao, J. Liu, D.W.K. Wong, B.H. Lee, M. Baskaran, T.Y. Wong, and T. Aung, "Focal biologically inspired feature for glaucoma type classification," in *MICCAI*, 2011, vol. 6893, pp. 91–8.

[7] W.H. Leung, C.K.and Yung, C.K. Yiu, S.W. Lam, D.Y. Leung, R.K. Tse, C.C. Tham, W.M. Chan, and D.S. Lam, "Novel approach for anterior chamber angle analysis: anterior chamber angle detection with edge measurement and identification algorithm (academia)," *Arch Ophthalmol*, vol. 124, no. 10, pp. 1395–401, 2006.

[8] J. Tian, P. Marziliano, M. Baskaran, H.T. Wong, and T. Aung, "Automatic anterior chamber angle assessment for hd-oct images," *IEEE Transactions on Biomedical Engineering*, vol. 58, no. 11, pp. 3242–9, 2011.

[9] C.K. Leung, C.Y. Cheung, H. Li, S. Dorairaj, C.K. Yiu, A.L. Wong, J. Liebmann, R. Ritch, R.N. Weinreb, and D.S. Lam, "Dynamic analysis of darklight changes of the anterior chamber angle with anterior segment oct," *Invest Ophthalmol Vis Sci*, vol. 48, no. 9, pp. 4116–22, 2007.

[10] C.K. Leung, R.N. Weinreb, j. Liu, C.Y. Cheung, R.Y. Lai, C.P. Pang, and D.S. Lam, "Anterior chamber angle measurement with anterior segment optical coherence tomography: A comparison between slit lamp oct and visante oct," *Invest. Ophthalmol. Vis. Sci.*, vol. 49, no. 8, pp. 3469–74, 2008.

[11] J. Tian, P. Marziliano, and H.T. Wong, "Automatic detection of schwalbe's line in the anterior chamber angle of the eye using hd-oct images," in *EMBC*, 2010, pp. 3013–6.

[12] Y. Xu, J. Liu, N.M. Tan, B.H. Lee, D.W.K. Wong, S. Baskaran, M. amd Perera, and T. Aung, "Anterior chamber angle classification using multiscale histograms of oriented gradients for glaucoma subtype identification," in *EMBC*, 2012.

[13] N. Dalal and B. Triggs, "Histograms of oriented gradients for human detection," in *CVPR*, 2005, vol. 1, pp. 1886–93.

[14] M.J. Gangeh, L. Sørensen, S.B. Shaker, M.S. Kamel, M. de Bruijne, and M. Loog, "A texton-based approach for the classification of lung parenchyma in ct images," in *MICCAI*, 2010, vol. 6363, pp. 595–602.

[15] R.E. Fan, K.W. Chang, C.J. Hsieh, X.R. Wang, and C.J. Lin, "LIBLINEAR: A library for large linear classification," *Journal of Machine Learning Research*, vol. 9, pp. 1871–4, 2008.

AIP | Review of Scientific Instruments

Note: A gel based imaging technique of the iridocorneal angle for evaluation of angle-closure glaucoma

V. K. Shinoj, V. M. Murukeshan, M. Baskaran, and T. Aung

Citation: Review of Scientific Instruments **85**, 066105 (2014); doi: 10.1063/1.4882335
View online: http://dx.doi.org/10.1063/1.4882335
View Table of Contents: http://scitation.aip.org/content/aip/journal/rsi/85/6?ver=pdfcov
Published by the AIP Publishing

Note: A gel based imaging technique of the iridocorneal angle for evaluation of angle-closure glaucoma

V. K. Shinoj,[1,2] V. M. Murukeshan,[1,a)] M. Baskaran,[2] and T. Aung[2]
[1]*Center for Optical and Laser Engineering, School of Mechanical and Aerospace Engineering, Nanyang Technological University, Singapore 639798*
[2]*Singapore Eye Research Institute (SERI) and Singapore National Eye Center (SNEC), 11 Third Hospital Avenue, Singapore 168751*

(Received 24 March 2014; accepted 27 May 2014; published online 10 June 2014)

Noninvasive medical imaging techniques have high potential in the field of ocular imaging research. Angle closure glaucoma is a major disease causing blindness and a possible way of detection is the examination of the anterior chamber angle in eyes. Here, a simple optical method for the evaluation of angle-closure glaucoma is proposed and illustrated. The light propagation from the region associated with the iridocorneal angle to the exterior of eye is considered analytically. The design of the gel assisted probe prototype is carried out and the imaging of iridocorneal angle is performed on an eye model. © *2014 AIP Publishing LLC*. [http://dx.doi.org/10.1063/1.4882335]

Glaucoma is an eye disease normally associated with an increase in intraocular pressure that, if untreated, can ultimately lead to blindness.[1–3] The closed-angle or angle-closure glaucoma is related to closure of iridocorneal angle (ICA) corresponding to the area between the iris and cornea.[4,5] The aqueous humor leaves the anterior chamber through the trabecular meshwork (TM), and passes through Schlemm's canal and collector channels before finally draining into aqueous veins and episcleral vessels.[6] The width of the ICA is associated with the drainage of aqueous humour from eye's anterior chamber. A wide angle permits adequate drainage of aqueous humour through the TM region provided the TM region is not obstructed.[7] A narrow angle may obstruct the drainage system and can lead to acute angle-closure glaucoma. Hence the imaging of the region associated with the ICA has created immense interest among scientific community as it facilitate diagnosing and monitoring of various eye conditions associated with glaucoma.[8,9] The sclera extending into the cornea near ICA however obstructs any direct view of the angle.

In a conventional screening procedure, the opening of the iridocorneal angle is assessed by means of a contact gonioscopic lens.[10] TM imaging in porcine eyes is carried out through multiphoton gonioscopy method.[11] The evaluation using gonioscopic lens involves contact with the cornea and often results in patient discomfort. Furthermore, gonioscopic data can be affected by inadvertent pressure on the gonioscopic lens during the inspection.[12] Since most clinicians record the results in charts without images or photographic records, the documentation of the gonioscopic outcomes are often poor.[13] Though ultrasound biomicroscopy (UBM) imaging technique produces high-resolution, quantitative cross-sectional images of the anterior chamber angle, it is not without disadvantages. Besides time-consuming, this technique is not readily available, is relatively invasive, and requires a highly skilled operator.[14,15]

Different optical probe imaging configurations have been investigated for their miniaturized size and flexibility for various disease diagnostic applications in our group.[16–19] An optical interferometric based method for the measurement of axial eye length has been reported.[20] Also, multispectral optical imaging of the human ocular fundus has been carried out in the recent past using LED illumination.[21] An endoscope based method has been used to obtain retinal images and iridocorneal angle in larger mammals;[22] however, the need for mechanical contact of probe distal end with the cornea by extreme pressure could cause abrasions of the corneal epithelium even with the presence of the gel on the cornea. This paper, in this context, proposes a low-cost clinical probe and related instrumentation that can image the structures of iridocorneal region with good resolution.

Since the direct view of ICA is obstructed due to the sclera overlap, the best approach to observe the TM region is to view from the opposite angle. Consider light transmission from anterior chamber to cornea and then to the outside medium. The angle at which light is refracted is in accordance with Snell's Law as follows:

$$n_1 \sin\theta_1 = n_2 \sin\theta_2, \tag{1}$$

$$n_2 \sin\phi = n_3 \sin\theta_3, \tag{2}$$

where n_1, n_2, and n_3 are the indices of anterior chamber (aqueous humor), cornea, and outside medium, respectively. The angles θ_1, θ_2, and θ_3 depicted in Figure 1 are the respective angles for light incident, and light refracted to corneal and transmitted to outside media at corresponding interfaces, relative to the normal plane of the interface. Since the thickness of cornea (≈0.55 mm) is comparatively small, $\theta_2 = \phi$. Hence,

$$\theta_3 = \sin^{-1}\left(\frac{n_2}{n_3}\sin\left(\sin^{-1}\left(\frac{n_1}{n_2}\sin\theta_1\right)\right)\right)$$
$$\theta_3 = \sin^{-1}\left(\frac{n_1}{n_3}\sin\theta_1\right). \tag{3}$$

a)Electronic mail: mmurukeshan@ntu.edu.sg

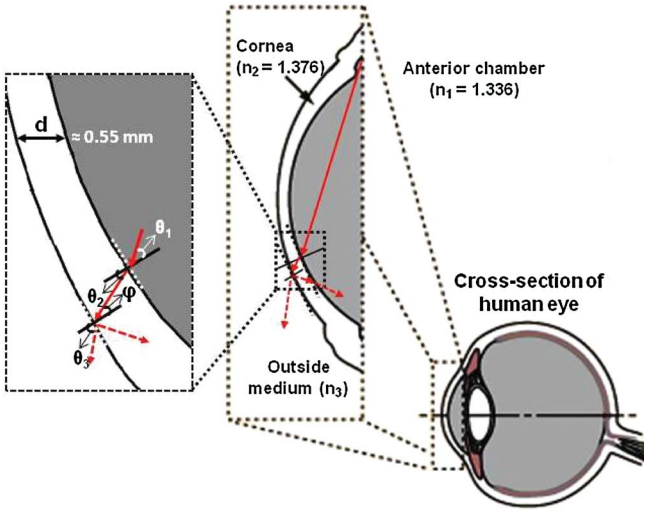

FIG. 1. Schematic diagram showing light transmission from the region of iridocorneal angle to the exterior of eye.

The variations in the real and imaginary part of θ_3 are plotted using Eq. (3) for various incident angles (40°-90°) and outside medium indices (n_3). The obtained result is shown in Figure 2. In order to have a good view of the trabecular meshwork region, the incident angle is estimated to be within 50°-65° using Snell's law. When the outside medium index is air ($n_3 = 1$) or media with indices close to one, the transmitted angle (θ_3) becomes imaginary as depicted in Figure 2. In this case, the complex angle represents the existence of total internal reflection (TIR) at the cornea-air interface. This obstructs the lateral view of iridocorneal angle region. By changing the outside medium index (n_3), the TIR can be avoided. Therefore, to have a clear view of TM region, the immediate media outside the corneal region has to be tailored. Different ocular gel media are available in the market that can be used to track light from the ICA region back to the exterior of the corneal region. In order to avoid further TIR at the gel-air interface, the angle of incidence at this interface has to be minimized. In this viewpoint, we propose an objective lens based probe configuration as shown in Figure 3 where a mirror is employed at the distal end to alter the angle of incidence at the gel-air interface.

A schematic of the proposed configuration is shown in Figure 3(a). The imaging of opposite iridocorneal angle is performed on an ocular eye model (OEM-7; Ocular Instruments Inc., Bellevue, WA) without and with gel. The photograph of eye model is given in Figure 3(b). The eye model includes natural surfaces of human eye including anterior chamber and crystalline lens.[15] A fiber-optic broadband light source is collimated and redirected to illuminate the iridocorneal region. The light reflected from the ICA region is collected through an objective lens and directed to a CCD camera (PL-A741; PixeLINK, Ottawa, Canada). A long working distance (20 mm), infinity-corrected objective lens (Mitutoyo; 20X, 0.4NA) is employed in this study.

The photograph of distal end is given in Figure 3(c). A mirror is used to redirect the beam to the objective lens. The mirror can be rotated to have a clear view of the ICA region.

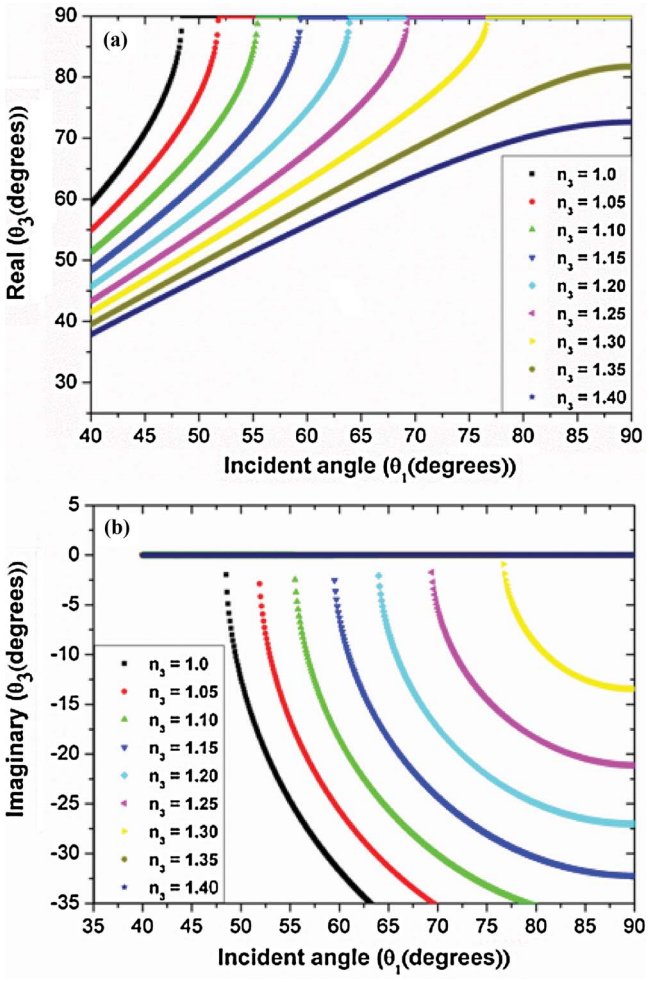

FIG. 2. The variations in the (a) real and (b) imaginary part of θ_3 are plotted using Eq. (3) for various incident angles (θ_1) and at various filling material indices.

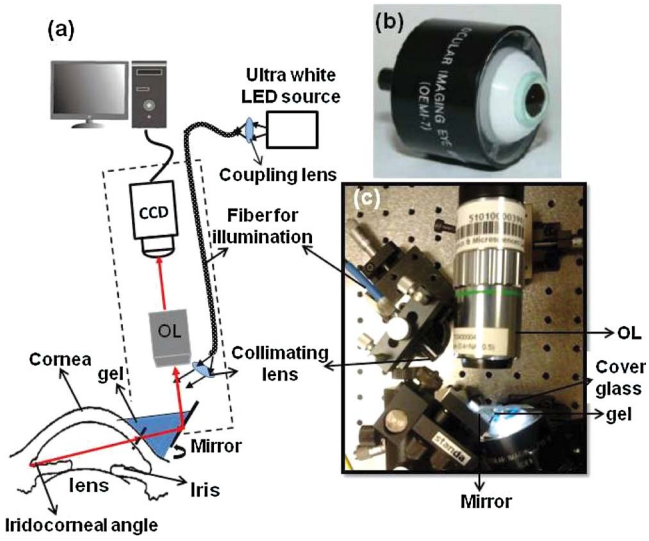

FIG. 3. (a) Schematic of the proposed experimental setup, (b) photograph of Ocular Imaging Eye Model (OEMI-7), and (c) photograph of the distal end of the proposed system.

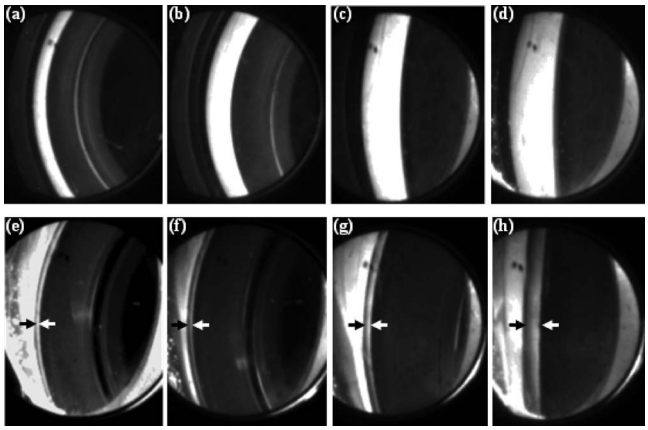

FIG. 4. Imaging of opposite iridocorneal angle region: (a)–(d) Iridocorneal angle is not visible in absence of gel (the images are taken at different objective planes); (e)–(h) Iridocorneal angle is visible with gel (these images are also taken at different objective planes).

The imaging of the region is performed without gel at different objective planes and the obtained result is shown in Figures 4(a)–4(d). It shows that the ICA region view is restricted due to the total internal reflection at the cornea-air interface as expected from the analytical results (Figure 2). A sterile coupling gel (Vidisic gel; Mann, Germany), of refractive index 1.338, was applied to a glass cover slip and pressed to the region between the mirror and the eye model such that a gel-filled coupling medium is formed as shown in Figure 3. This would minimize reflection of light by refractive index matching, thereby optimizing light transmission. In this scheme, the angle of incidence at the gel-air interface is a minimum such that light can be guided to the camera through the objective lens. The results obtained in the presence of gel are shown in Figures 4(e)–4(h). These figures were taken at objective planes corresponding to those in Figures 4(a)–4(d), respectively. The width of the iridocorneal angle region is indicated using arrows, between the margin of cornea and base of iris.

An optical method to examine the iridocorneal angle region that will be promising in the evaluation of angle-closure glaucoma is proposed and illustrated. The light transmission from the anterior chamber to the exterior of eye is analytically considered using Snell's law. Based on this, an experimental probe system is developed for imaging the iridocorneal angle region. The images saved into the computer allow the clinicians to evaluate and compare the changes in angle if serial examinations are to be done over a period of time which would be particularly advantageous in tracking both disease progression as well as treatment effects.

The authors acknowledge the financial support received through NMRC (NIG09nov001) and A*Star-SERC (Grant No. 112 148 0003). The authors also acknowledge the facilities provided through COLE, NTU.

[1]J. E. Oliver, M. G. Hattenhauer, D. Herman, D. O. Hodge, R. Kennedy, M. Fang-Yen, and D. H. Johnson, Am. J. Ophthalmol. **133**(6), 764–772 (2002).
[2]D. A. Lee and E. J. Higginbotham, Am. J. Health-Syst. Pharm. **62**(7), 691–699 (2005).
[3]E. W. Leung, F. A. Medeiros, and R. N. Weinreb, J. Glaucoma **17**(5), 350–355 (2008).
[4]H. A. Quigley, D. S. Friedman, and N. G. Congdon, J. Glaucoma **12**(2), 167–180 (2003).
[5]P. Tarongoy, C. L. Ho, and D. S. Walton, Surv. Ophthalmol. **54**(2), 211–225 (2009).
[6]M. Johnson and R. Kamm, Invest. Ophthalmol. Visual Sci. **24**(3), 320–325 (1983).
[7]P. F. Hoyng and L. M. van Beek, Drugs **59**(3), 411–434 (2000).
[8]A. Konstantopoulos, P. Hossain, and D. F. Anderson, Br. J. Ophthalmol. **91**(4), 551–557 (2007).
[9]W. P. Nolan, J. L. See, P. T. Chew, D. S. Friedman, S. D. Smith, S. Radhakrishnan, C. Zheng, P. J. Foster, and T. Aung, Ophthalmology **114**(1), 33–39 (2007).
[10]L. M. Sakata, R. Lavanya, D. S. Friedman, H. T. Aung, H. Gao, R. S. Kumar, P. J. Foster, and T. Aung, Ophthalmology **115**(5), 769–774 (2008).
[11]O. Masihzadeh, D. A. Ammar, M. Y. Kahook, E. A. Gibson, and T. C. Lei, J. Biomed. Opt. **18**(3), 036009 (2013).
[12]S. Radhakrishnan, D. Huang, and S. D. Smith, Ophthalmol. Clin. North Am. **18**(3), 375–381 (2005).
[13]S. A. Perera, M. Baskaran, D. S. Friedman, T. A. Tun, H. M. Htoon, R. S. Kumar, and T. Aung, Invest. Ophthalmol. Visual Sci. **51**(6), 2993–2997 (2010).
[14]S. F. Riley, J. P. Nairn, F. A. Maestre, and T. J. Smith, Int. Ophthalmol. Clin. **34**(3), 271–282 (1994).
[15]G. L. Spaeth, S. Aruajo, and A. Azuara, Trans. Am. Ophthalmol. Soc. **93**, 337–351 (1995).
[16]V. Murukeshan and N. Sujatha, Rev. Sci. Instrum. **78**(5), 053106 (2007).
[17]S. K. Vengalathunadakal, P. Padmanabhan, V. M. Murukeshan, and S. Padmanabhan, Opt. Eng. **48**(10), 103601 (2009).
[18]M. Valiyambath Krishnan, M. Vadakke Matham, S. Krishnan, P. Parasuraman, J. Joseph, and K. Bhakoo, J. Biomed. Opt. **17**(7), 076010 (2012).
[19]V. K. Shinoj, V. M. Murukeshan, S. B. Tor, N. H. Loh, and S. W. Lye, Appl. Opt. **53**(6), 1083–1088 (2014).
[20]W. J. O. Boyle, G. L. Dick, K. T. V. Grattan, A. W. Palmer, D. N. Wang, and K. Weir, Rev. Sci. Instrum. **64**(11), 3082–3087 (1993).
[21]N. L. Everdell, I. B. Styles, A. Calcagni, J. Gibson, J. Hebden, and E. Claridge, Rev. Sci. Instrum. **81**(9), 093706 (2010).
[22]J.-L. Guyomard, S. G. Rosolen, M. Paques, M.-N. Delyfer, M. Simonutti, Y. Tessier, J. A. Sahel, J.-F. Legargasson, and S. Picaud, Invest. Ophthalmol. Visual Sci. **49**(11), 5168–5174 (2008).

Journal of Biomedical Optics

SPIEDigitalLibrary.org/jbo

Integrated flexible handheld probe for imaging and evaluation of iridocorneal angle

Vengalathunadakal K. Shinoj
Vadakke Matham Murukeshan
Mani Baskaran
Tin Aung

Integrated flexible handheld probe for imaging and evaluation of iridocorneal angle

Vengalathunadakal K. Shinoj,[a,b] Vadakke Matham Murukeshan,[a,*] Mani Baskaran,[b] and Tin Aung[b]
[a]Nanyang Technological University, School of Mechanical and Aerospace Engineering, Center for Optical and Laser Engineering, Singapore 639798, Singapore
[b]Singapore Eye Research Institute (SERI) and Singapore National Eye Center (SNEC), 11 Third Hospital Avenue, Singapore 168751, Singapore

Abstract. An imaging probe is designed and developed by integrating a miniaturized charge-coupled diode camera and light-emitting diode light source, which enables evaluation of the iridocorneal region inside the eye. The efficiency of the prototype probe instrument is illustrated initially by using not only eye models, but also samples such as pig eye. The proposed methodology and developed scheme are expected to find potential application in iridocorneal angle documentation, glaucoma diagnosis, and follow-up management procedures. [DOI: 10.1117/1.JBO.20.1.016014]

Keywords: anterior segment ocular imaging; glaucoma; trabecular meshwork; iridocorneal angle.

Paper 140704R received Oct. 28, 2014; accepted for publication Dec. 17, 2014; published online Jan. 16, 2015.

1 Introduction

The irreversible and progressive nature of the disease makes glaucoma one of the serious ophthalmic diseases.[1,2] Primary angle closure glaucoma (PACG) is one form of glaucoma where the eye's drainage canals become blocked by the iris so that the intraocular pressure rises over time.[3,4] PACG is a major form of glaucoma in Asia and, in contrast to western countries, it responsible for the majority of bilateral blindness in Singapore, China, and India.[5,6] Optical imaging methods have been vital in the area of biomedical imaging for various disease diagnoses.[7–10]

Documentation of the entire angle is needed to identify abnormalities or the status of iridocorneal angle. Most of the current imaging methods based on optical coherence tomography (OCT) are either cross-sectional or expensive and are not extensively used by clinicians.[11,12] Pentacam, based on Scheimpflug's photography principle, can be used to image the anterior chamber through its circumference, where the imaging of an obliquely tilted object can be accomplished with a maximum depth of focus and the least image distortion under given conditions.[13,14] However, the assessment of the iridocorneal angle cannot be done in detail using this method, since direct visualization of the angle recess is not available due to the limitations of visible light penetrating the necessary depth. The main pathology in PACG is a closed anterior chamber angle which is diagnosed clinically using gonioscopy, an instrument that uses a mirror system.[15,16] Gonioscopy is a subjective procedure and the documentation is mainly through various grading procedures.[15–17] The main drawback with this method is patient discomfort and physician compliance.[18] It was reported earlier that 50% of physicians do not perform gonioscopy in clinical examination as it is cumbersome and requires time-consuming methods.[19] Interpretation of gonioscopic findings requires expertise and is subject to substantial disagreement between physicians,[20] in spite of the technique being low cost and simple to use. Multiple reflections from the lens or mirrors used along with the coupling gel cause the quality of the image to be poor. In spite of all this, gonioscopy remains the clinical reference standard as it allows the clinician to observe the angle structures through a cheaper instrument in the clinic and to make note of pathological findings of clinical importance.

Photographic-based documentation allows the eye care clinician to document and refer to the earlier images for abnormalities in the anterior segment of the eye and angle.[21] The RetCam™ was primarily designed for wide-field retinal imaging in children to document premature retinal growth in a condition called "retinopathy of prematurity."[22] Later, it was modified to document the anterior chamber angle in the form of EyeCam™.[23,24] However, imaging of the anterior chamber angle using EyeCam™ takes longer than gonioscopy (about 5 to 10 min per eye) and the device is more expensive compared with gonioscopy. We have recently demonstrated a gel-assisted imaging technology for angle imaging—an exclusive wide angle imaging probe which is nonbulky and inexpensive. The probe can be attached to a slit lamp, providing the flexibility to be used by a nontechnical person.[25]

In this context, we propose a miniaturized integrated charge-coupled diode (CCD) camera and light-emitting diode (LED) light source-based probe system, which enables evaluation of the iridocorneal region inside the eye. Full details of the probe configuration and methodology are given in the following sections.

2 Materials and Method

2.1 *Preparation of Sample*

One randomly selected eye from four pigs (*Sus scrofa domestica*) was enucleated from the local abattoir and used within 6 h of death. The *ex vivo* samples were transported on ice to the laboratory to maintain their "freshness." Each sample was fixed onto a custom eye holder, which was mounted on a

*Address all correspondence to: Vadakke Matham Murukeshan, E-mail: mmurukeshan@ntu.edu.sg

0091-3286/2015/$25.00 © 2015 SPIE

translation stage with micrometer accuracy. Extraocular tissues, such as the conjunctiva and lacrimal gland, were removed from the samples.

2.2 *Imaging System*

The distal end to support the optics is designed in a CAD design software (SolidWorks, USA) and built as a separate module. The probe distal end that houses one micro-CCD conduit and four illumination channels has a diameter of 26 mm, which is suitable for compactness and easy handling, with a sufficient working distance from the eye. The center channel has an internal diameter of 3 mm and is meant for a 3 mm × 3 mm micro-CCD video camera (IntroSpicio™ 115, Medigus Ltd., Israel), which is employed as the image capturing device. The video camera system is used together with a light source. The distal end also has four channel slots of internal diameter 5 mm for LED illumination purposes that are drilled at an angle of 71 deg surrounding the camera slot, so as to provide adequate illumination across the field of view (FOV) of the micro-CCD. The LEDs have a viewing angle of 20 deg. The slot angle and viewing angle of LEDs are such that the focus area of the camera has adequate illumination at the iridocorneal area for image capture. The microcamera head is connected to a camera controller (video processor unit of IntroSpicio™ 115, Medigus Ltd.) that controls the video signal from and to the camera head by a cable. The camera controller can control brightness/contrast, gain, white balance, etc., of the video signal. The main input to the device is 100 to 240 AC (autoswitching). The micro-CCD has 291,000 effective numbers of pixels (500 horizontal × 582 vertical) with an FOV of 140 deg. Figure 1 illustrates the photograph of the assembled probe, and the probe distal end is shown in the inset.

2.3 *Equipment Safety and Maintenance*

The imaging probe fulfils safety directions in routine clinical use as per international standards. According to the International Commission on Non-ionizing Radiation Protection, no evaluation for retinal hazard is required if the visible light has a luminance of less than 10,000 candela/m^2.[26] The LED sources, such as the one used in our study (maximum luminous intensity of 7000 mcd), have a smaller degree of spatial coherence compared with laser light sources and this leads to a distribution of light over a relatively larger area making it well within the maximum permissible limit. The cleaning and maintenance of the probe include customary chemicals such as 4% sodium hypochlorite solution for rinsing or 75% isopropyl alcohol wipes for cleaning the tip of the camera lens. Thus, it does not require specialized cleaning solutions or protocol.

2.4 *Imaging Method*

The imaging scheme is illustrated schematically in Fig. 2. The imaging device comprises an eye imaging probe having a central axis and a corneal contact surface. An imaging sensor is located at the central axis of the probe and has variable resolution at different depths which is configured for capturing the interior of the eye when the contact surface is placed at the cornea or at the limbus of the eye through a coupling gel. The four LEDs' viewing angles and slot angles are designed such that the illumination region optimally covers the targeted iridocorneal angle region and provides the required illumination throughout the region. The LEDs are positioned based on a Lambertian approach to illuminate the targeted area in a controlled manner. To be precise, the uniform distribution of the light emitted by the source (the combination of LEDs) has the same brightness or luminescence when viewed from any angle. Further, the brightness of the LEDs can be controlled using a potentiometer. The probe and sensors are connected via a flexible connection (with flexible wires) to the camera controller. The camera controller in turn is connected to a personal computer using an S-video connector for display and/or for storage in a media storage device.

3 Results and Discussion

The functionality of the imaging probe prototype is tested first on an ocular imaging eye model (OEMI-7, Ocular Instruments Inc., Bellevue, Washington). Figure 3(a) shows the photograph of the eye model. The imaging probe is placed near the limbal region of the cornea to image the opposite iridocorneal angle. With the use of a coupling gel (e.g., Vidisic gel, Bausch & Lomb, New York), the micro-CCD camera can visualize

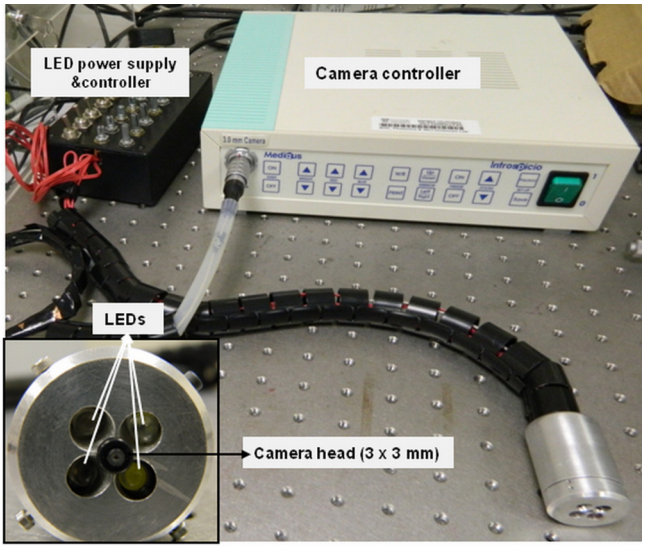

Fig. 1 Photograph of imaging system (inset: probe distal end).

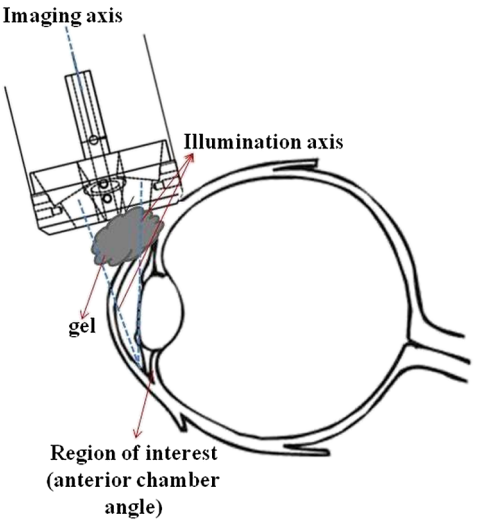

Fig. 2 Illustration of the imaging method.

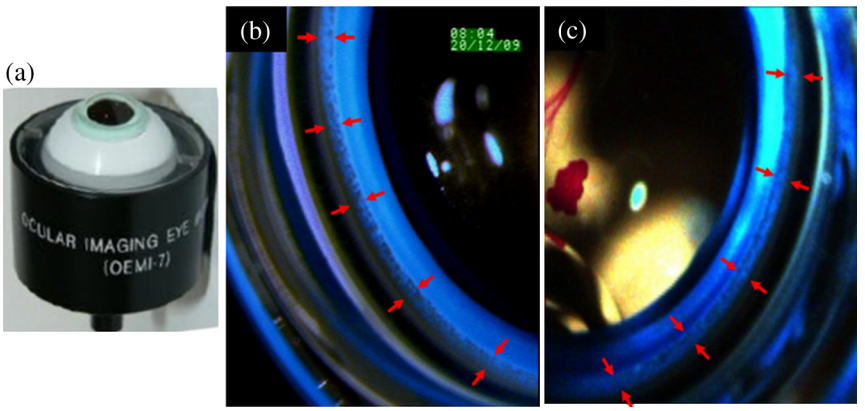

Fig. 3 (a) Ocular eye model; (b) and (c) images of two opposite quadrants of the model eye, and the red arrows highlight the iridocorneal angle region.

structures in the anterior segment in a manner similar to direct gonioscopy. The coupling gel provides an optical interface between the camera's lens and the cornea and eliminates the total internal reflection that naturally occurs at the corneal tear film-air interface, thus allowing rays of light coming from the iridocorneal angle to escape into the microcamera. Users have the options to capture still images or to record video stream from which images can be extracted at a later stage. The obtained results of the two opposite quadrants of the model eye are shown in Figs. 3(b) and 3(c). The opposite iridocorneal angle and the simulated trabecular meshwork of the eye model are visible in the images and are highlighted using red arrows.

In our experiment, the sample used is pig eye due to its resemblance to the features observed in human eyes. It is more easily available compared with those of nonhuman primates. Also, a pig eye is similar in size to the human eye, ≈22 mm in length compared with 24 mm in humans. Pig eye has been used in vision science research involving, but not limited to, glaucoma and corneal transplant studies.[27,28] The pig eyes are obtained from a local abattoir immediately after the animal's death. Imaging of the anterior chamber is carried out after fixing the eye on a support. Imaging is performed on four different sides of the eye to have a complete view of the angle region inside eye since the camera's FOV is 140 deg. The obtained results from four sides of pig eye are shown in Figs. 4(a)–4(d).

Even though Pentacam allows very easy, fast, and noncontact quantification of the anterior chamber parameters, the evaluation of the iridocorneal angle cannot be done in detail since direct visualization of the angle recess is not available. Gonioscopy still remains the clinical reference standard as it allows the clinician to observe the angle structures in the clinic and to make note of the pathological findings of clinical importance. In Eyecam™-based angle assessment, fluid-based optical coupling avoids additional pressure exertion on the cornea as in gonioscopy and hence eliminates the concern for compression artifacts. However, the device is more expensive than gonioscopy and extra space is needed for supine examination that may widen the angle due to the effect of gravity. Devices based on anterior segment optical coherence tomography (AS-OCT) technology can obtain cross-sectional images in the sitting position and provide better resolution of the anterior chamber angle; however, a panoramic view is not available for complete evaluation and documentation of devices placed in the angle.[29] With our proposed device, angle images can be carried out in a sitting position. The angle measurement for all four quadrants can be carried out in less than 2 min. No personnel expertise is required for the assessment. This device is easily portable, nonbulky, can be attached to a slit lamp, and can be connected to any desktop/laptop PC installed with the interfacing software. Table 1 compares the key features of our proposed device with that of other complimentary devices used for anterior chamber angle imaging.

The clinical application of such an imaging probe is gaining more importance in the context not just of the documentation of the iridocorneal angle findings in angle closure disease, but also in preoperatively assessing and documenting the "openness" of the iridocorneal angle during microinvasive glaucoma surgeries (MIGS) such as various stent procedures and in gonio-synechiolysis. There is a growing trend of letting such MIGS devices to reside in contact with the anterior chamber angle, and there are possibilities of long-term migration or erosion of these devices.[30] It is only prudent to have a good documentation of the position of these devices and the changes in the surrounding iridocorneal angle. The above described imaging probe can be

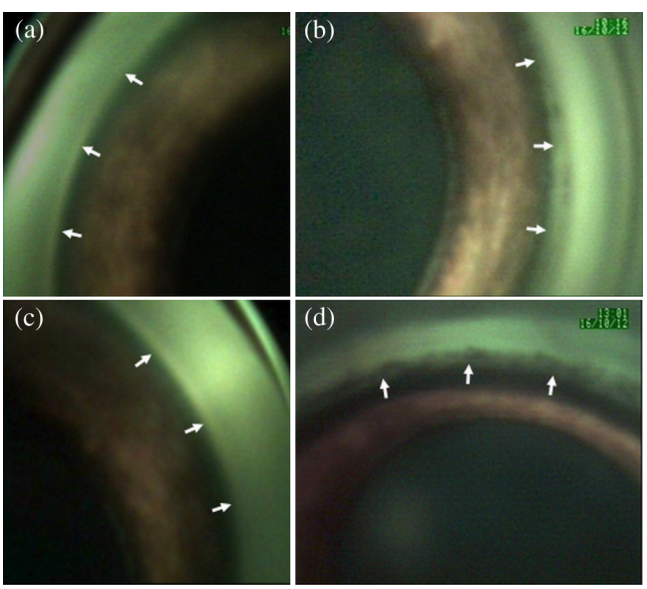

Fig. 4 (a)–(d) Angle images (from four different sides) of the porcine pig eye sample obtained using the developed probe (white arrows highlight the iridocorneal angle region).

Table 1 The comparison of our device parameters with other complementary imaging techniques.

Device/technology	Ease of use	Panoramic view	Clinical interpretation	Cost
Pentacam	Noncontact/ sitting	Yes	Difficult	High
EyeCam	Contact/ supine	Yes	Easy	High
AS-OCT	Noncontact/ sitting	No	Difficult	High
Proposed device in this manuscript	Contact/ sitting	Yes	Easy	Low

an objective alternative for clinician documented evidence in clinical practice, especially in an increasingly medicolegal environment. Further, such a device can be used vis-à-vis variable corneal diameters of animals for the iridocorneal angle and anterior segment documentation, whereas a fixed type of goniolens restricts such use.[31]

4 Conclusion

A handheld ocular imaging probe system is designed, developed, and illustrated to continuously display, capture, and record images of anterior segment and iridocorneal angle regions. The system and methodology are validated using an eye model and pig eyes as test samples. This instrument, which can give good quality digital images, can be a cheaper alternative to gonioscopy-based angle detection schemes. Further, the illustrated handheld probe can also be used in the management of glaucoma for monitoring landmark identification during device implantation procedures.

Acknowledgments

The authors acknowledge the financial support received through NMRC (NIG09nov001) and A*STAR-SERC grant (No. 112 148 0003). The authors have filed a patent (PAT/118/14/14/SG PRV) on the design aspect and imaging methodology of the probe scheme described in this manuscript.

References

1. P. C. Van Veldhuisen et al., "The Advanced Glaucoma Intervention Study (AGIS): 7. The relationship between control of intraocular pressure and visual field deterioration," *Am. J. Ophthalmol.* **130**(4), 429–440 (2000).
2. W. M. Grant and J. F. Burke Jr., "Why do some people go blind from glaucoma?," *Ophthalmology* **89**(9), 991–998 (1982).
3. E. M. Stone et al., "Identification of a gene that causes primary open angle glaucoma," *Science* **275**(5300), 668–670 (1997).
4. W. P. Nolan et al., "Detection of primary angle closure using anterior segment optical coherence tomography in Asian eyes," *Ophthalmology* **114**(1), 33–39 (2007).
5. S. K. Seah et al., "Incidence of acute primary angle-closure glaucoma in Singapore: an island-wide survey," *Arch. Ophthalmol.* **115**(11), 1436–1440 (1997).
6. T. Aung et al., "Anterior chamber depth and the risk of primary angle closure in 2 East Asian populations," *Arch. Ophthalmol.* **123**(4), 527–532 (2005).
7. V. M. Murukeshan, V. K. Shinoj, P. Saraswathi, and P. Padmanabhan, "Diagnostic sensing of specific protein in breast cancer cells using hollow-core photonic crystal fiber," in *Multimodality Breast Imaging: Diagnosis and Treatment*, E. Y. K. Ng, U. Rajendra Acharya, Rangaraj M. Rangayyan, and Jasjit S. Suri, Eds., pp. 475–495, SPIE Press, Bellingham, Washington (2013).
8. V. K. Shinoj and V. M. Murukeshan, "Hollow-core photonic crystal fiber based multifunctional optical system for trapping, position sensing, and detection of fluorescent particles," *Opt. Lett.* **37**(10), 1607–1609 (2012).
9. J. James, V. M. Murukeshan, and L. S. Woh, "Integrated photoacoustic, ultrasound and fluorescence platform for diagnostic medical imaging-proof of concept study with a tissue mimicking phantom," *Biomed. Opt. Express* **5**(7), 2135–2144 (2014).
10. J. G. Fujimoto, "Optical coherence tomography for ultrahigh resolution in vivo imaging," *Nat. Biotechnol.* **21**(11), 1361–1367 (2003).
11. M. E. Nongpiur et al., "Classification algorithms based on anterior segment optical coherence tomography measurements for detection of angle closure," *Ophthalmology* **120**(1), 48–54 (2013).
12. S. Radhakrishnan et al., "Real-time optical coherence tomography of the anterior segment at 1310 nm," *Arch. Ophthalmol.* **119**(8), 1179–1185 (2001).
13. T. Scheimpflug, "Improved method and apparatus for the systematic alteration or distortion of plane pictures and images by means of lenses and mirrors for photography and for other purposes," GB Patent 1196 (1904).
14. R. Jain and S. Grewal, "Pentacam: principle and clinical applications," *J. Curr. Glaucoma Pract.* **3**(2), 20–32 (2009).
15. L. M. Sakata et al., "Comparison of gonioscopy and anterior segment ocular coherence tomography in detecting angle closure in different quadrants of the anterior chamber angle," *Ophthalmology* **115**(5), 769–774 (2008).
16. H. G. Scheie, "Width and pigmentation of the angle of the anterior chamber: a system of grading by gonioscopy," *AMA Arch. Ophthalmol.* **58**(4), 510–512 (1957).
17. N. G. Congdon et al., "A proposed simple method for measurement in the anterior chamber angle: biometric gonioscopy," *Ophthalmology* **106**(11), 2161–2167 (1999).
18. D. T. Quek et al., "Angle imaging: advances and challenges," *Indian J. Ophthalmol.* **59**(7), S69–S75 (2011).
19. A. L. Coleman, F. Yu, and S. J. Evans, "Use of gonioscopy in medicare beneficiaries before glaucoma surgery," *J. Glaucoma* **15**(6), 486–493 (2006).
20. M. Baskaran et al., "Comparison of EyeCam and anterior segment optical coherence tomography in detecting angle closure," *Acta Ophthalmol.* **90**(8), e621–e625 (2012).
21. M. Datiles et al., "Clinical evaluation of cataracts," *Duane's Clin. Ophthalmol.* **1**, 1–20 (1992).
22. C. Wu, R. A. Petersen, and D. K. VanderVeen, "RetCam imaging for retinopathy of prematurity screening," *J. Am. Assoc. Pediatr. Ophthalmol. Strabismus* **10**(2), 107–111 (2006).
23. S. A. Perera et al., "Use of EyeCam for imaging the anterior chamber angle," *Invest. Ophthalmol. Visual Sci.* **51**(6), 2993–2997 (2010).
24. M. Baskaran et al., "Angle assessment by EyeCam, goniophotography, and gonioscopy," *J. Glaucoma* **21**(7), 493–497 (2012).
25. V. K. Shinoj et al., "Note: A gel based imaging technique of the iridocorneal angle for evaluation of angle-closure glaucoma," *Rev. Sci. Instrum.* **85**(6), 066105 (2014).
26. ICNIRP, "Guidelines on limits of exposure to broad-band incoherent optical radiation (0.38 to 3 μm)," *Health Phys.* **73**(3), 539–554 (1997).
27. J. Ruiz-Ederra et al., "The pig eye as a novel model of glaucoma," *Exp. Eye Res.* **81**(5), 561–569 (2005).
28. C. Faber et al., "Orthotopic porcine corneal xenotransplantation using a human graft," *Acta Ophthalmol.* **87**(8), 917–919 (2009).
29. H.-T. Wong et al., "High-definition optical coherence tomography imaging of the iridocorneal angle of the eye," *Arch. Ophthalmol.* **127**(3), 256–260 (2009).
30. L. V. M. Brandão and M. C. Grieshaber, "Update on minimally invasive glaucoma surgery (MIGS) and new implants," *J. Ophthalmol.* **2013**, 705915 (2013).

31. R. S. Smith, D. Korb, and S. W. John, "A goniolens for clinical monitoring of the mouse iridocorneal angle and optic nerve," *Mol. Vis.* **8**, 26–31 (2002).

Vengalathunadakal K. Shinoj is currently engaged at the Centre for Optical and Laser Engineering (COLE), Nanyang Technological University (NTU), Singapore, as a research fellow. He was awarded a PhD degree from NTU, Singapore, in 2012. His research focuses on design and development of an improved imaging probe for ocular imaging targeting angle-closure glaucoma diagnosis. His research findings have been published in many internationally recognized peer-reviewed journals and presented in various prestigious international conferences.

Vadakke Matham Murukeshan has been with the School of Mechanical and Aerospace Engineering, Nanyang Technological University (NTU), Singapore, since 1997. He leads a research group that focuses on nanoscale optics, biomedical optics, and optical metrology. He has published over 250 international journal and conference proceedings papers, 6 book chapters, 6 patents, and 8 innovation disclosures. Currently, he is the deputy director of the Center for Optical and Laser Engineering (COLE) of NTU, Singapore.

Mani Baskaran is a senior clinical research fellow at SERI and assistant professor at the Office of Clinical Sciences, Duke-NUS Graduate Medical School, Singapore. His current research interests include imaging, diagnosis, and management of angle closure in Asia; and developing novel devices, software algorithms in anterior segment imaging with engineering faculty across, Singapore. He has published more than 110 international publications, 8 book chapters, and 6 copatents in the field of glaucoma.

Tin Aung is a senior consultant and head of glaucoma service at the, Singapore National Eye Centre, deputy director of the Singapore Eye Research Institute, and a professor in the Department of Ophthalmology at the National University of Singapore. He obtained his MBBS and master's degrees in medicine from the National University of Singapore. He obtained the fellowships of the Royal College of Surgeons of Edinburgh and the Royal College of Ophthalmologists in 1997 and a PhD degree in molecular genetics from University College London, UK, in 2004.